

U. S. DEPARTMENT OF THE INTERIOR
U. S. GEOLOGICAL SURVEY

**Laboratory Measurements of the Radiofrequency
Electrical and Magnetic Properties of
Soils from near Yuma, Arizona**

by

Gary R. Olhoeft¹ and Dennis E. Capron¹

Open File Report 93-701

This report is preliminary and has not been reviewed for conformity with U.S. Geological Survey editorial standards and nomenclature.

Use of brand names and model numbers in this report is for the sake of description only, and does not constitute endorsement by the U.S. Geological Survey.

¹U.S. Geological Survey, Box 25046 DFC MS964, Denver, CO 80225-0046

1993

Introduction

As part of a test of airborne ground penetrating radar systems, soil samples were collected and measured in the laboratory to determine their properties of importance to the subsurface propagation of electromagnetic energy over the frequency range from 1 to 1,000 MHz. The measured electrical and magnetic properties data along with models parameterizing the data are presented in this report. Surface and airborne ground penetrating radar results and a description of the overall test are presented in other reports.

Electrical Properties

The electrical properties that control electromagnetic propagation through a material are the complex dielectric permittivity and the DC (direct current) electrical conductivity (or its reciprocal: electrical resistivity). The electrical conductivity describes the ability of electric charge to be transported through the material. The dielectric permittivity describes the ability of opposite electric charges within the material to be separated by a distance (polarized). At high frequencies, the DC electrical conductivity is a fixed, frequency-independent, real number. The dielectric permittivity is a frequency dependent complex quantity. The dielectric permittivity is presented here as the relative permittivity (dielectric permittivity of the material divided by the permittivity of vacuum or free space, $\epsilon_o = 8.854 \times 10^{-12}$ Farad/meter).

To parameterize the data, the electrical properties are described by the Cole-Cole model (Cole and Cole, 1941), all relative to the free space permittivity:

$$\epsilon_r' - i \epsilon_r'' = \epsilon_\infty + (\epsilon_L - \epsilon_\infty) / (1 + (i \omega \tau_\epsilon)^\alpha_\epsilon)$$

with the electric loss tangent given as:

$$\tan \delta_\epsilon = \epsilon_r'' / \epsilon_r' + \sigma / \omega \epsilon_r'$$

where ϵ_r' = real part of the relative complex dielectric permittivity
 ϵ_r'' = imaginary part of the relative complex dielectric permittivity
 ϵ_L = low frequency limit of permittivity
 ϵ_∞ = high frequency limit of permittivity
 $\omega = 2 \pi f$ = radian frequency [f is frequency in 10^6 Hz]
 $i = \sqrt{-1}$
 τ_ϵ = time constant of relaxation [10^{-6} seconds]
 α_ϵ = Cole-Cole relaxation breadth distribution parameter
 (= 0 for infinitely broad, = 1 for single relaxation)
 σ = DC conductivity [Siemens/m].

Magnetic Properties

The magnetic property that controls electromagnetic propagation through a material is the complex magnetic permeability. The magnetic permeability is commonly assumed to be that of free space, $\mu_o = 4 \pi \times 10^{-7}$ Henry/meter, and a real, fixed parameter, independent of frequency. However, in a few of these soil samples, the magnetic permeability was found to be significantly higher than that for free space, complex and frequency dependent, describing the lossy magnetic polarization of the material.

To parameterize the data, the magnetic properties are also described by the Cole-Cole model (Olhoeft, 1972), all relative to the free space permeability:

$$\mu_r' - i \mu_r'' = \mu_\infty + (\mu_\ell - \mu_\infty) / (1 + (i \omega \tau_\mu)^\alpha)^\mu$$

with the magnetic loss tangent given as:

$$\tan \delta_\mu = \mu_r'' / \mu_r'$$

where μ_r' = real part of the relative complex magnetic permeability

μ_r'' = imaginary part of the relative complex magnetic permeability

μ_ℓ = low frequency limit of permeability

μ_∞ = high frequency limit of permeability

$\omega = 2 \pi f$ = radian frequency [f is frequency in 10^6 Hz]

$i = \sqrt{-1}$

τ_μ = time constant of relaxation [10^{-6} seconds]

α_μ = Cole-Cole relaxation breadth distribution parameter
(= 0 for infinitely broad, = 1 for single relaxation)

Laboratory Measurements

Samples were collected in the field by Lincoln Laboratory, U.S. Geological Survey, and the Swedish Carabas team personnel. The samples collected by the USGS (Figures 2 through 158) are all located on the map in Figure 1. The locations of the other samples are less certain.

Samples were weighed in their collection bottles before and after vacuum drying (with the weight of the empty bottle subtracted) to determine the natural water content. Samples from the subsurface were measured dry and at various water contents (by adding distilled water). Samples were placed into gold-plated, solid-coin-silver, General Radio GR-900 precision coaxial air lines, 3 cm long, for measurement with a Hewlett Packard 8753 network analyzer, using full 12-port transmission-reflection-through, open-short-load calibrations (using updated procedures similar to Kutrubes (1986)). Forward and reverse measurements were made using the reflection and transmission from one end of the sample holder (forward) and then again from the other end (reverse). Sample holder air lines were weighed empty, with dry sample, and at various added water amounts to determine sample dry bulk density and weight percent water contents.

In each figure, the upper left plot is the relative dielectric permittivity, the lower left plot is the electric loss tangent, the upper right plot is the relative magnetic permeability, and the lower right plot is the magnetic loss tangent, each versus log frequency. Each plot shows the forward and reverse measurements (the jagged lines) and a smooth curve showing the fit of the model parameters. The unchanging line with a minimum near 100 MHz in both loss tangent plots represents the minimum resolvable losses for the sample holder and measurement system. Also labelled on the plots are the dry bulk density (upper left), water content (lower right), and dielectric and magnetic Cole-Cole model parameters (lower plots). The text label at the bottom of each figure is whatever was written on the field sample container. Some samples were subsampled to test measurement repeatability and sample heterogeneity (for examples, Figures 4-34), and subsamples were designated #1, #2, and so forth. At the highest measured frequencies, sample holder resonance sometimes appears (exhibited by a rapidly increasing permittivity with increasing frequency) and should be ignored.

The forward and reverse measurements are good indicators of the errors in the measurement process and the heterogeneity of the sample. In an ideal, homogeneous, isotropic sample with a perfect measurement apparatus, the two curves should be identical. When the two curves are separated by the same distance over the frequency range of measurement, cumulative instrument and computational error are represented by that separation. Divergence of the curves with increasing frequency is an indication of heterogeneity in the sample (e.g., the sample holder is not uniformly packed with soil or is unevenly water-wet throughout).

Discussion

The soil samples exhibited natural water contents from a fraction of one percent to several percent by weight. All samples were disturbed by the sampling acquisition process and were measured at dry bulk densities probably lower than in situ. However, the disturbance of digging and burying test targets for the ground penetrating radars probably represents an equivalent amount of soil density reduction in the replaced soil above the targets. In situ undisturbed electrical properties are probably higher in permittivity and loss than shown in these measurements.

Most of the soils measured appear to be representative of low water content sandy soils that could be found almost anywhere in the world (Kutrubes, 1986; Olhoeft, 1987). All exhibited strongly frequency dependent dielectric properties when wet, even with fractional-weight-percent water contents. However, some soil samples exhibited properties indicative of clay minerals with much stronger frequency dependence and correspondingly higher losses. A few soil samples exhibited extremely unusual and highly lossy magnetic properties. Some lossy magnetic soils had magnetic losses higher than electrical losses, which were easily explained in terms of high iron content from a mineral like magnetite. A second type of lossy magnetic soils were like no other previously known soils and require further investigation. Frequency dependent dielectric permittivity and magnetic permeability result in varying velocity of electromagnetic propagation with frequency (dispersion).

The data presented in Figures 2 through 158 are from the USGS sampling which traversed the site from north to south (Figure 1). The remaining data in Figure 159 through 208 are from the Lincoln Laboratory and Carabas Team soil sampling.

Figures 2 through 43 show measurements on the samples collected near -500 meters, site Hood, where the trucks were buried. Figures 2, 3, 4, 34 and 39 show the electromagnetic properties in their natural water content state as a function of depth. The remaining figures show the results with artificially varying water content. Note how the electrical resistivity and losses vary by nearly two orders of magnitude with less than a factor of 6 variation in water content from the surface to 50 cm depth. Either salts or clay minerals must be present in these samples to account for the rapid change in electrical properties with changing water content (Olhoeft, 1987). The magnetic properties are normal and essentially those of free space.

Figures 44 through 49 show measurements on the samples collected near +500 meters, site Sheridan, where the dipole array was located. The properties are those of normal sand, showing lower losses than site Hood at -500 meters. The magnetic properties are normal and essentially those of free space.

Figures 50 and 51 show measurements on the samples collected near +1050 meters, site Jackson, where the semilog periodic array was located. The water content is very low here, yielding very low loss from normal sands. The magnetic properties are normal and essentially those of free space.

Figure 52 through 57 show measurements on the samples collected near +1680 meters, site Moseby, where the repeaters were located. The water content is very low here, yielding very low loss from normal sands. The magnetic properties are normal and essentially those of free space.

Figures 58 through 95 show measurements on the samples collected near +2040 meters, site Butler, where the plastic and steel pipes are buried. The water content varies widely at this site, but the electrical properties are still mostly those of low loss sand. Despite the presence of magnetite sands at this site, the relative magnetic permeability is still low (< 1.2), and magnetic losses do not exceed electrical losses (for example, Figure 88). The magnetic properties could be safely assumed to be essentially those of free space.

Figures 96 through 101 show measurements on the samples collected near +2270 meters, site Stuart, where the repeaters were buried. The water content is very low here, yielding very low loss from normal sands. The magnetic properties are normal and essentially those of free space.

Figures 102 through 121 show measurements on the samples collected near +2500-2640 meters, site Custer, where the dipoles are buried. The water content is highly variable at this site, causing very low loss at the surface but very high losses at about 50 cm depth. At Custer subsite D, an anomalous magnetic behavior was observed, yielding magnetic losses an order of magnitude higher than dry electrical losses (Figure 119) with a high magnetic permeability. No known natural material has been previously observed to behave this way nor exhibit these properties, though we have since observed similar behavior in anomalous soil samples from Idaho.

Figures 122 through 127 show measurements on the samples collected near +3000 meters, site McClellan, where the long wire is buried. The water content is highly variable at this site, causing very low loss at the surface but very high losses at about 50 cm depth. The anomalous magnetic behavior was again observed, yielding magnetic losses an order of magnitude higher than dry electrical losses with a high magnetic permeability. These samples (Figures 126 and 127) also exhibited magnetic losses high enough to compete with high-water-content electrical losses. There is no known explanation for this behavior.

Figures 128 through 133 show measurements on the samples collected near +3120 meters, site Beauregard, where repeaters were buried. The water content is highly variable at this site, causing very low loss at the surface but very high losses at about 50 cm depth. The anomalous magnetic behavior was again observed (Figure 132) though not high enough at this site to compete with the electrical properties in the wet soils.

Figures 134 through 140 show measurements on the samples collected near +3200 meters, site Douglas, where the dipoles are buried. The water content is highly variable at this site, causing very low loss at the surface but very high losses at about 50 cm depth. The anomalous magnetic behavior was again observed, yielding magnetic losses an order of magnitude higher than dry electrical losses with a high magnetic permeability. These samples (Figures 137 and 140) also exhibited magnetic losses high enough to compete with high-water-content electrical losses. There is no known explanation for this behavior.

Figures 141 through 149 show measurements on the samples collected near +3400 meters, site Stanton (also called Mudd in the surveying data files), where the mines are buried. Despite highly variable water contents, the samples all exhibit very low losses, typical of dry sandy materials. There are slight indications of possible magnetic losses (Figures 146 to 149), but none are significant in comparison to the electrical losses.

Figures 150 through 158 show measurements on the samples collected near +3450 meters, site Stanton, where the mines are buried. The water content is highly variable at this site, causing very low loss at the surface and higher losses at about 50 cm depth. The anomalous magnetic behavior was again observed (Figures 157 and 158) though not high enough at this site to compete with the electrical properties in the wet soils.

The remaining soil sample results in Figures 159 through 208 are not as well

located (the data in Figures 183 through 208 are located on the grid points shown in the plot labels), but essentially show similar behavior. The anomalous magnetic loss appears again in Figures 164 and 165.

In Figures 171, 176, 183 and 204 another type of magnetic loss appears. This appears to be caused by the presence of iron metal or iron-bearing minerals. This second type of magnetic behavior can be simulated with mixtures of iron and silica powder (Figures 184 through 194). The soil sample in Figure 183, for example, is very similar to the simulant in Figure 187, suggesting about 30 percent iron-equivalent in the soil. Note also that the natural water content in the soil of Figure 183 produces electrical losses that are lower than the magnetic losses -- particularly above about 60 MHz. No simulant has yet been found for the first, more anomalous magnetic loss (as in Figure 119).

Summary

In general, the near surface soils are very low water content (fraction of one weight percent), high electrical resistivity (thousands of ohm-meters), low electromagnetic loss materials. Beginning from 20 to 50 cm depth throughout the site, there is a general increase in water content (up to several weight percent) with electrical resistivity dropping to tens of ohm-meters or less and dielectric permittivity rising. In general the losses are also higher at the North end of the site than at the South end. The anomalous magnetic loss becomes significant in the middle of the site.

In nearly all cases, the high frequency model parameters and Cole-Cole distribution parameters are well resolved in fits to the data. However, the time constants and the low frequency parameters are only minimum limiting values.

References

- Cole, K. S. and Cole, R. S., 1941, Dispersion and adsorption in dielectrics, I, alternating current characteristics: *J. Chem. Phys.*, v. 9, p. 341-351.
- Kutrubes, D. L., 1986, Dielectric permittivity measurements of soils saturated with hazardous fluids: MSc Thesis, Dept. of Geophysics, Colo. School of Mines, Golden, CO, 300p.
- Olhoeft, G. R., 1972, Time dependent magnetization and magnetic loss tangents: MSc Thesis, Dept. of Electrical Engineering, Massachusetts Institute of Technology, Cambridge, MA, 94p.
- Olhoeft, G. R., 1987, Electrical properties from 10^{-3} to 10^{+9} Hz -- physics and chemistry: in *Proc. of the 2nd Int'l. Symp. on the Physics and Chemistry of Porous Media*, Schlumberger-Doll, Ridgefield, CT, October, 1986, *Am. Inst. Phys., Conf. Proc.* 154, J. R. Banavar, J. Koplik and K. W. Winkler, eds., NY, AIP, p. 281-298.

Acknowledgement

This work was funded by the U.S. Department of Defense. J. E. Lucius and M. H. Powers assisted with sample collection. M. H. Powers created the map in Figure 1 from data supplied by D. H. Enggren at Lincoln Laboratory. The artificial mixtures in Figures 184 through 194 were supplied by Steven Ostro of the Jet Propulsion Laboratory.

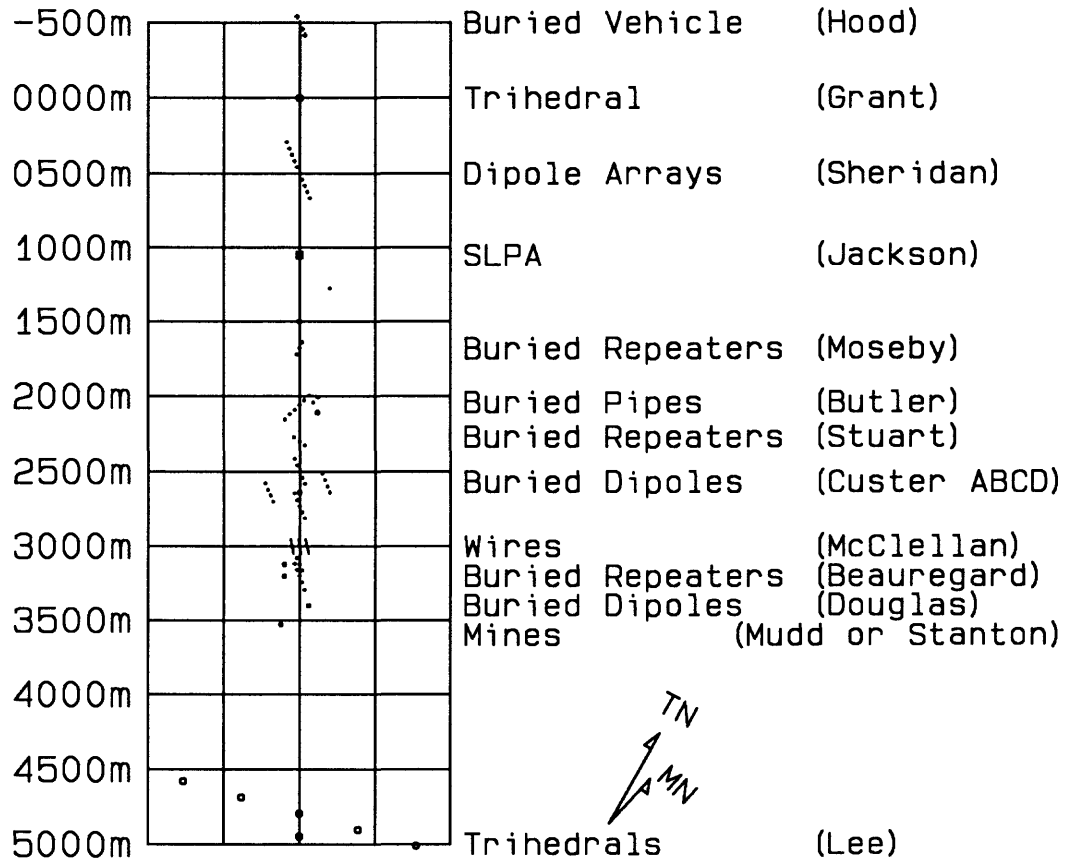


Figure 1 - Plan map of the test area. Numbers along the left axis are distances in meters along the length of the line. In each sample figure caption, those numbers are given to help locate the sample (where known).

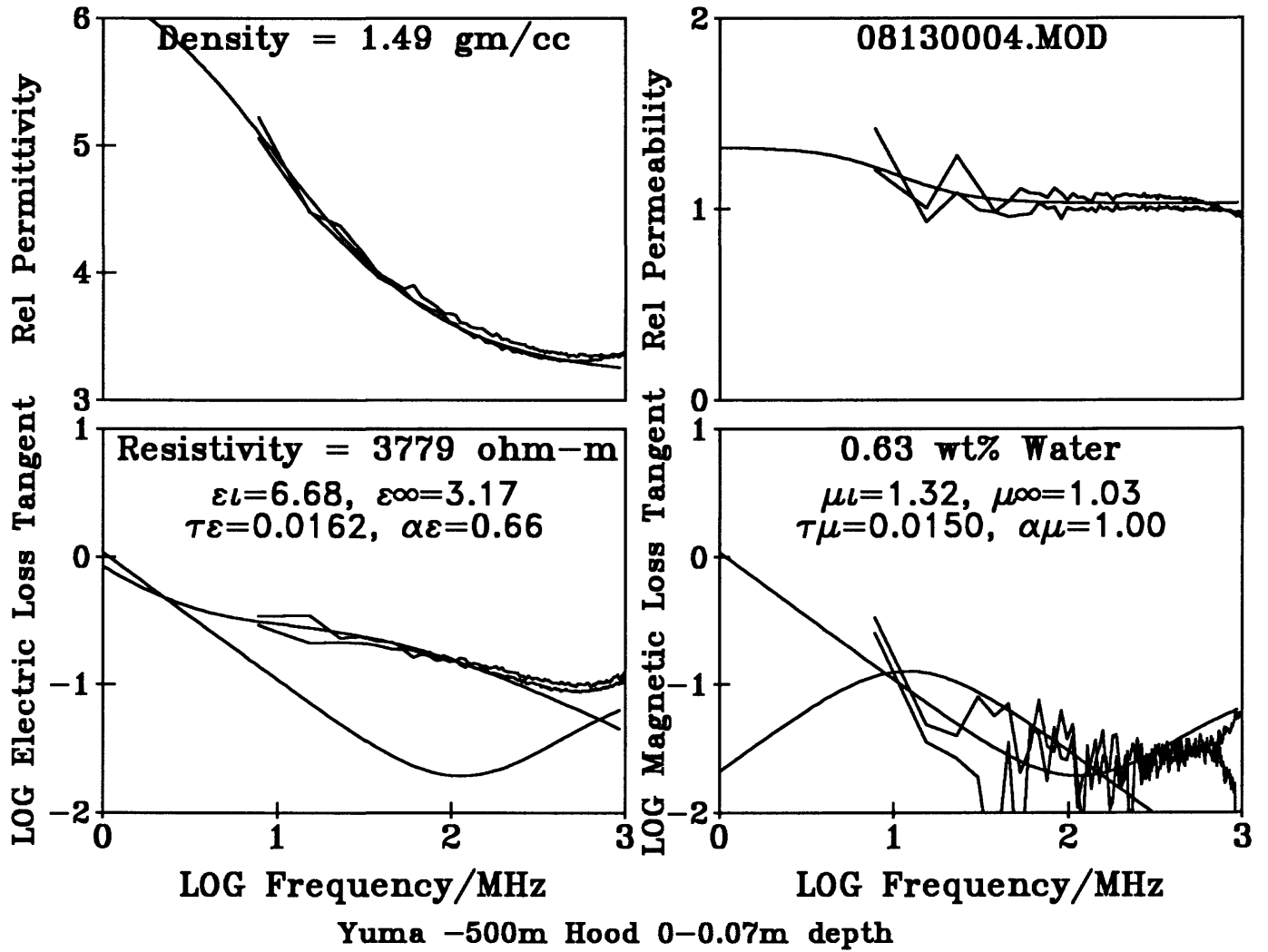


Figure 2 -
Natural state electromagnetic properties with water content preserved in sealed, taped,
sample bottle.

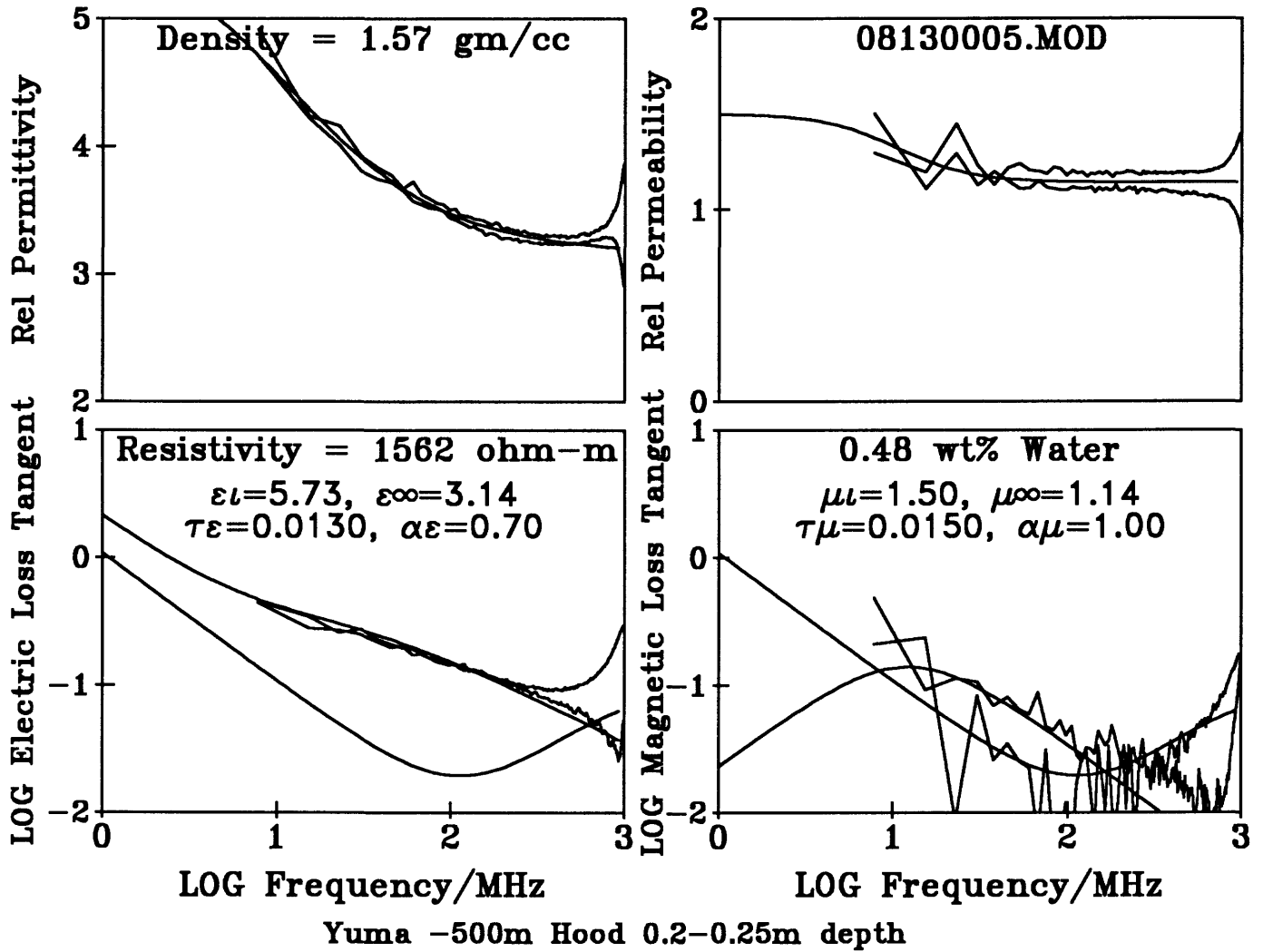


Figure 3 -
Natural state electromagnetic properties with water content preserved in sealed, taped,
sample bottle.

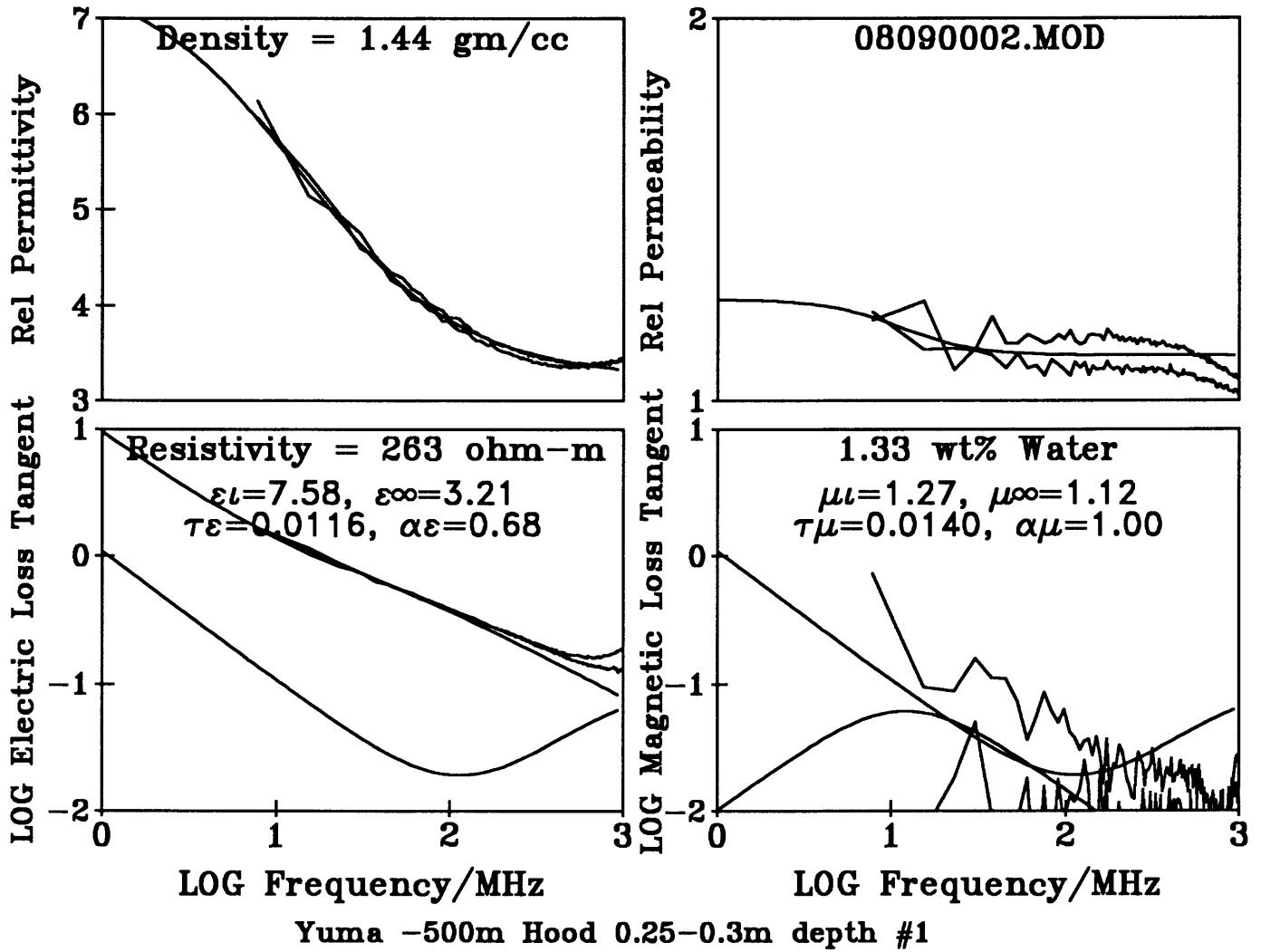


Figure 4 -
Natural state electromagnetic properties with water content preserved in sealed, taped,
sample bottle.

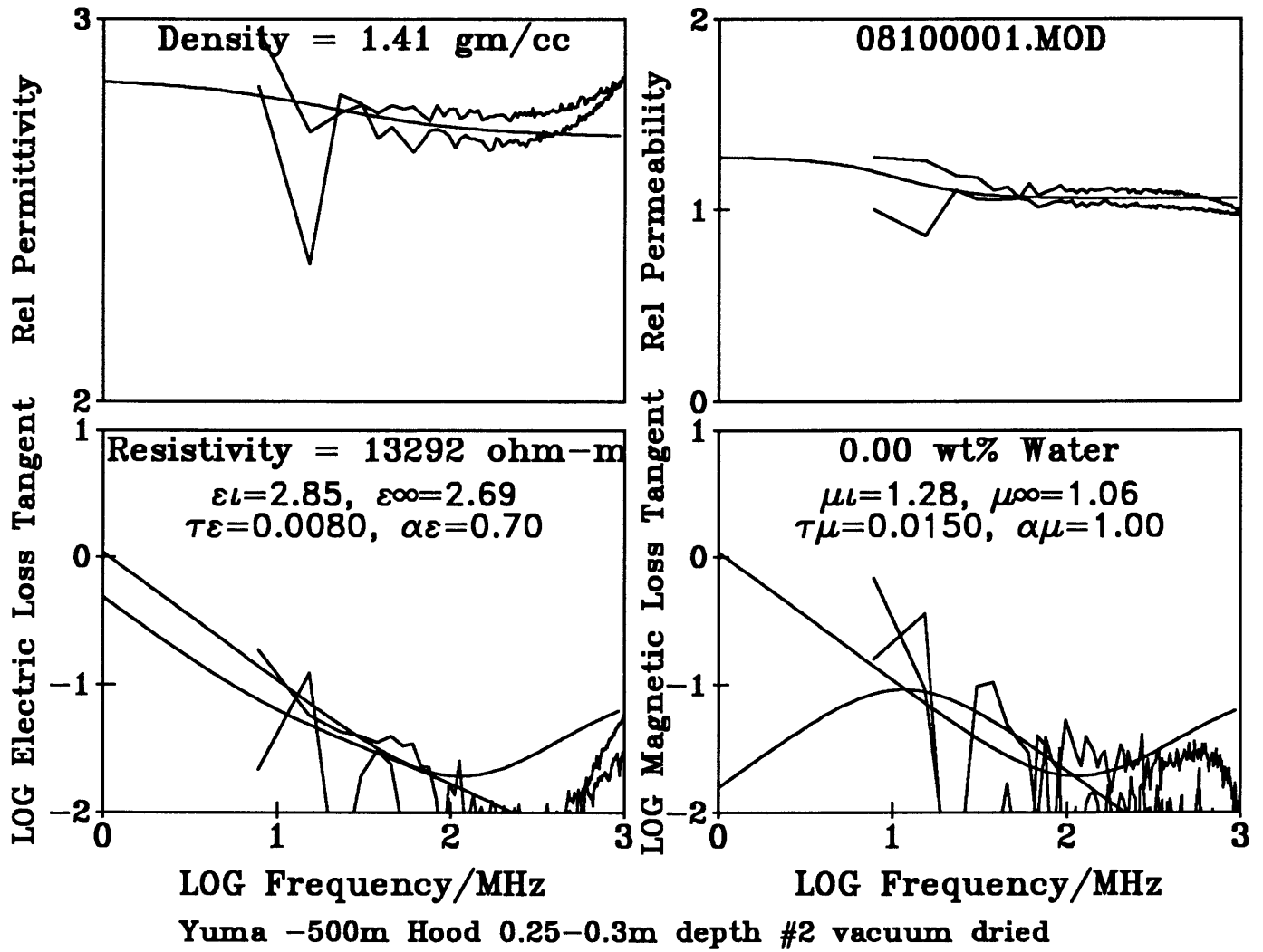


Figure 5 -

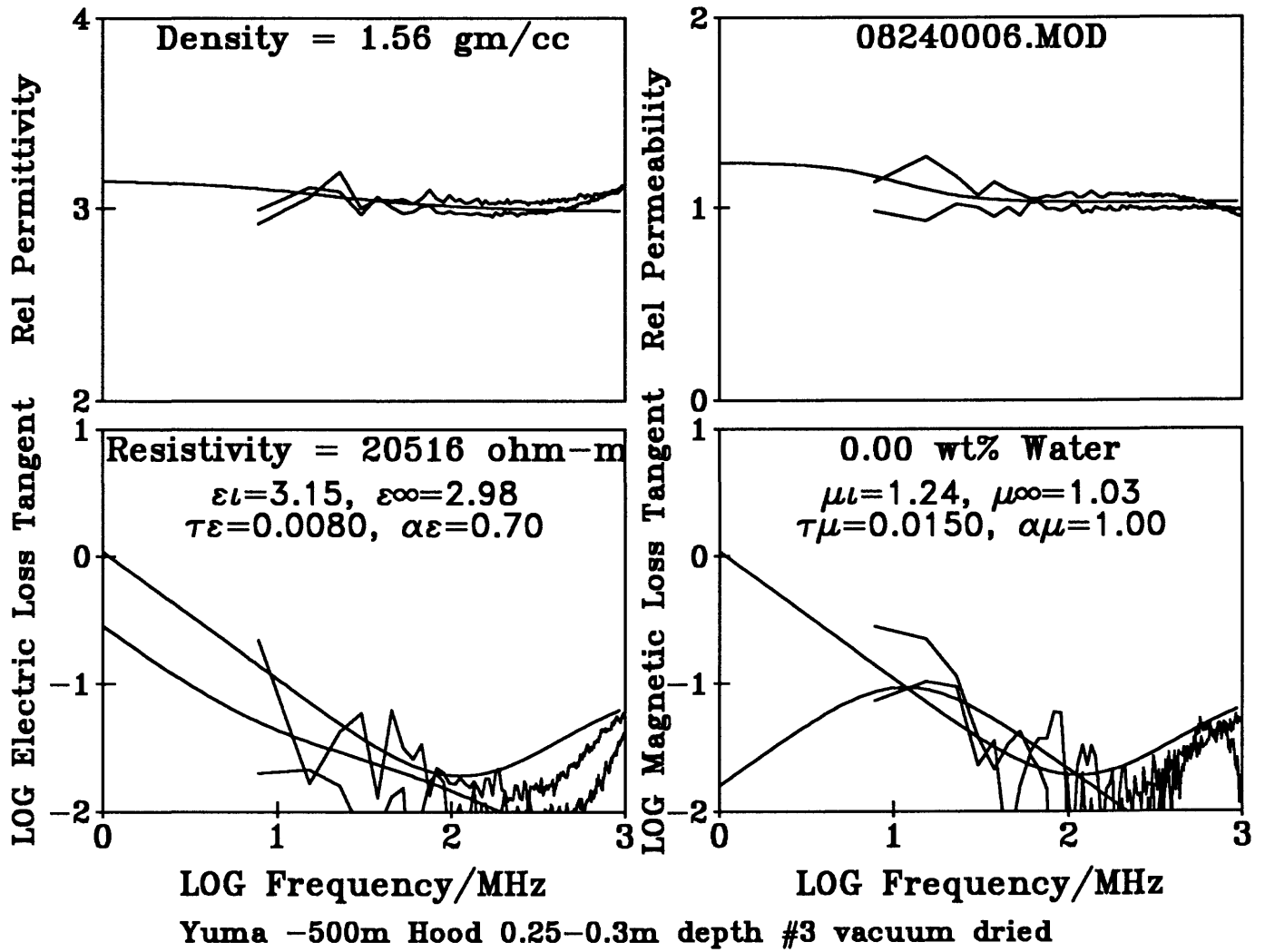


Figure 6 -

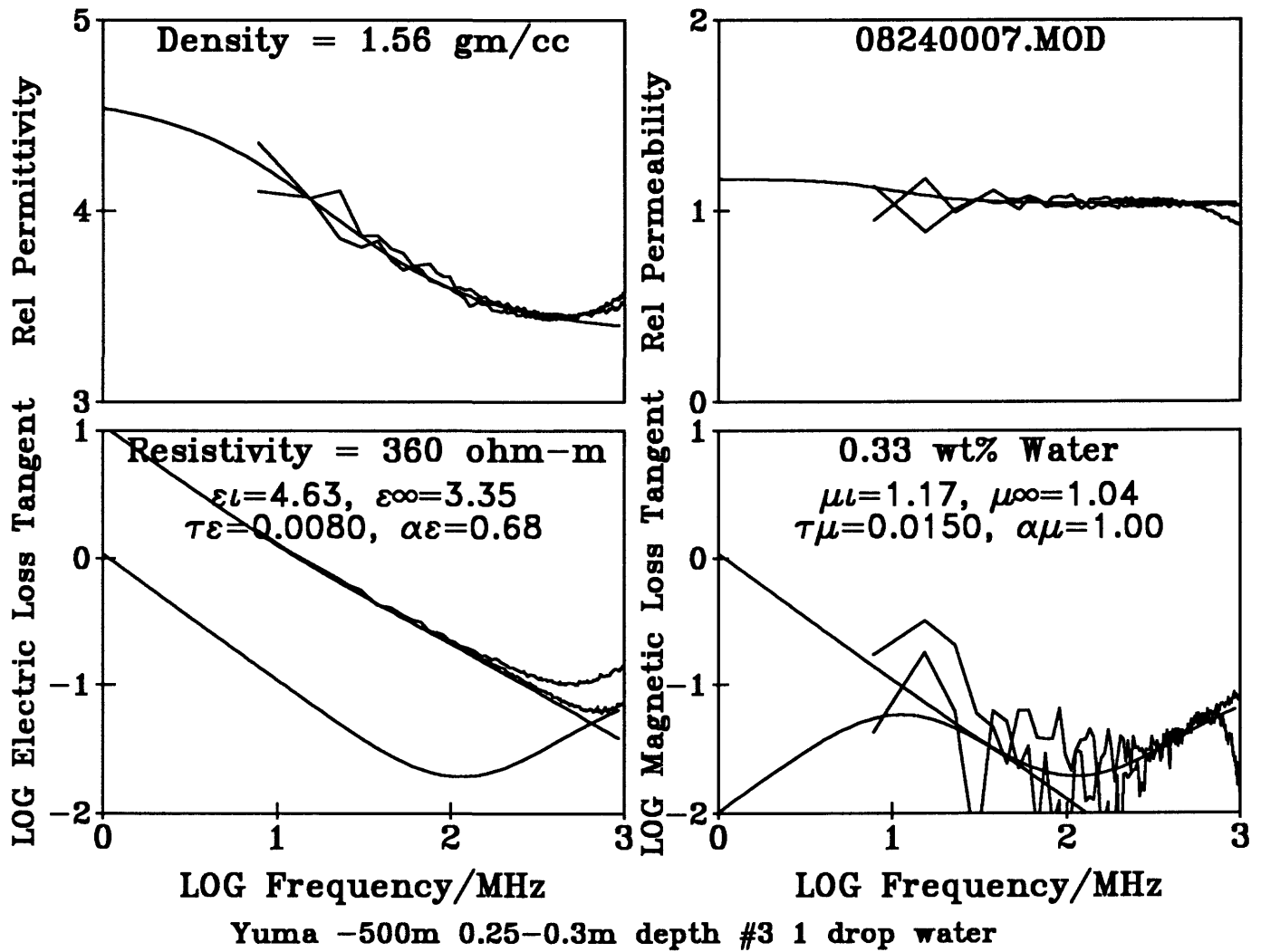
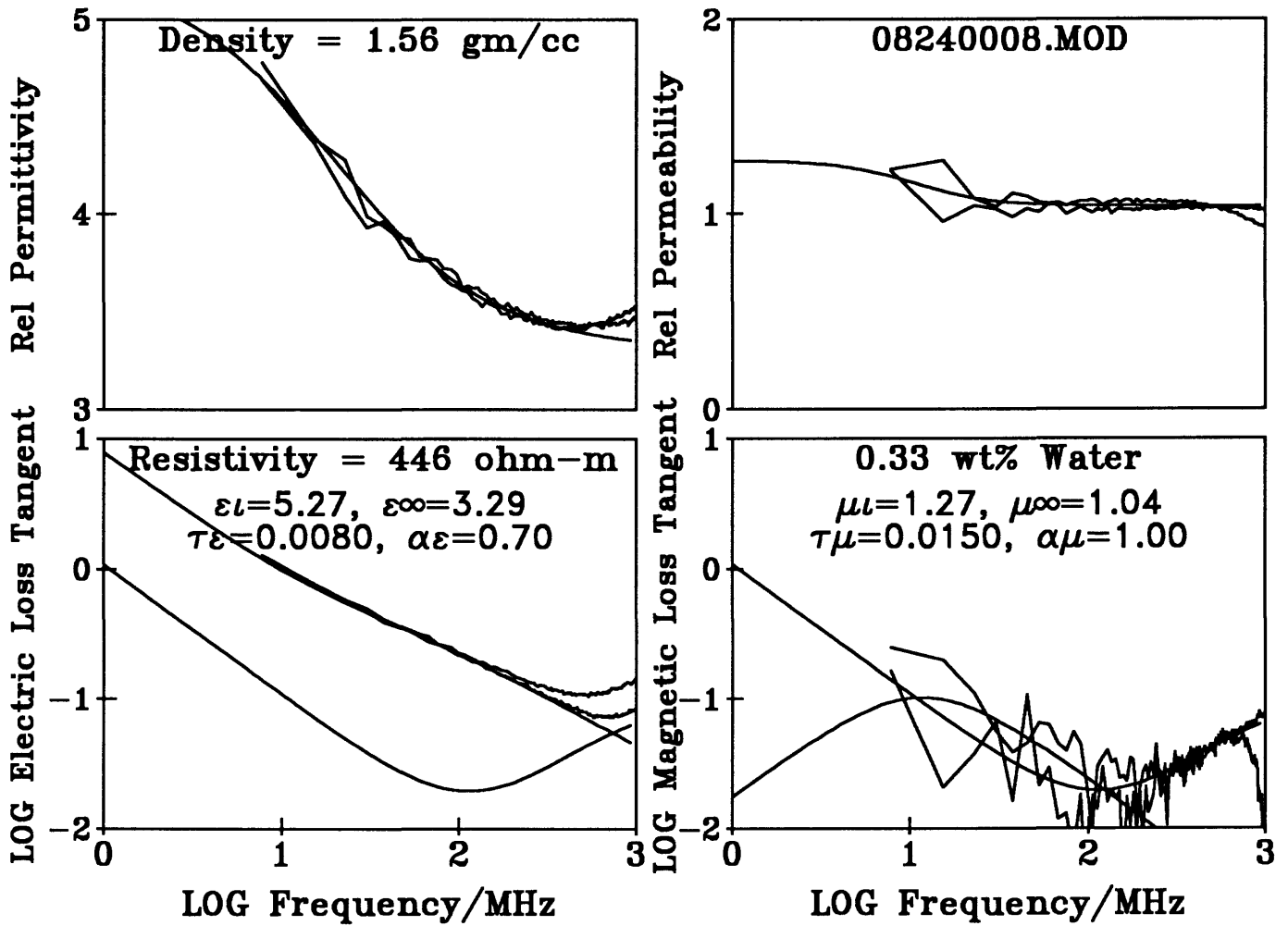


Figure 7 -



Yuma -500m Hood 0.25-0.3m depth #3 1 drop water + 30 min.

Figure 8 -

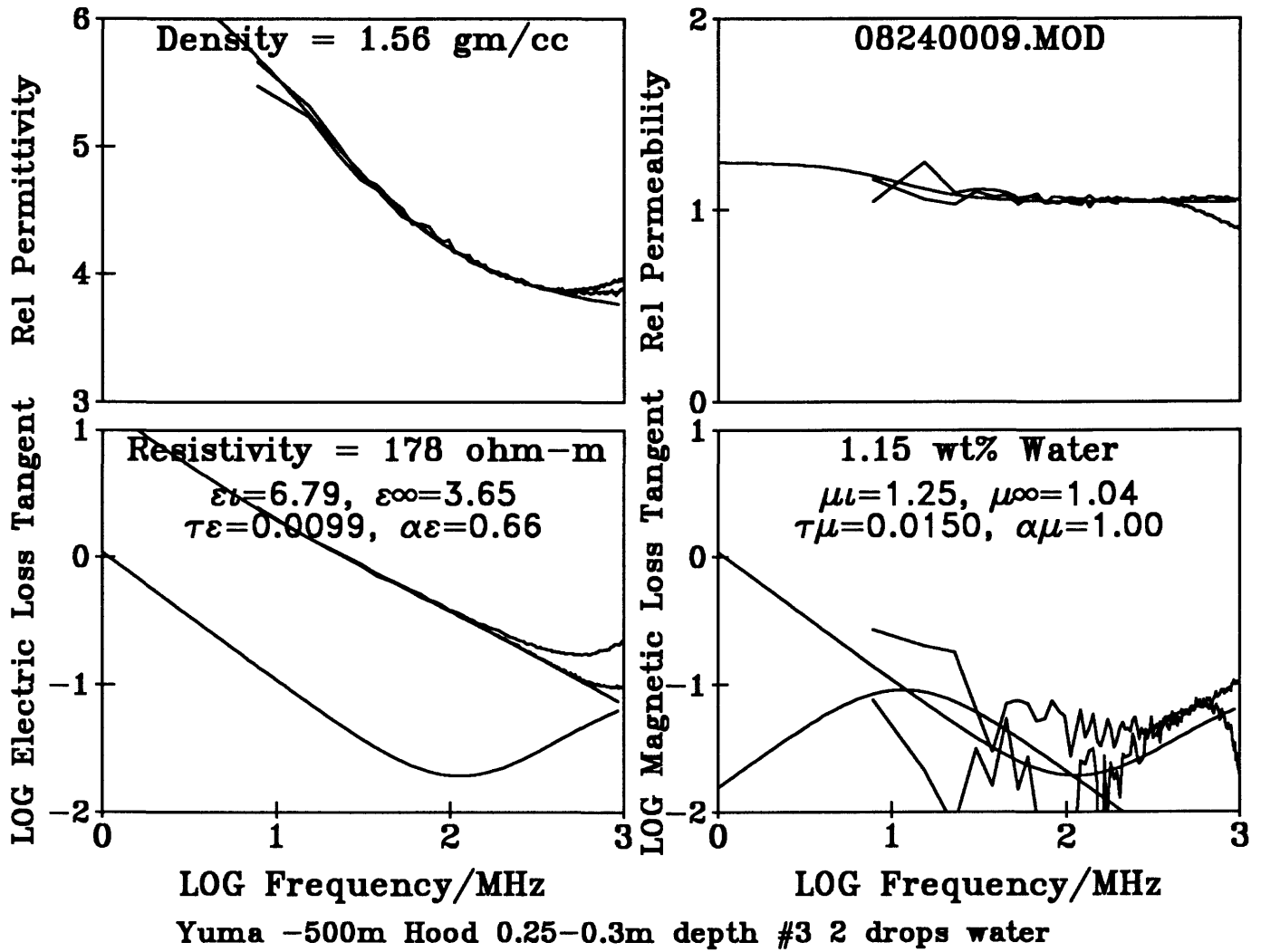
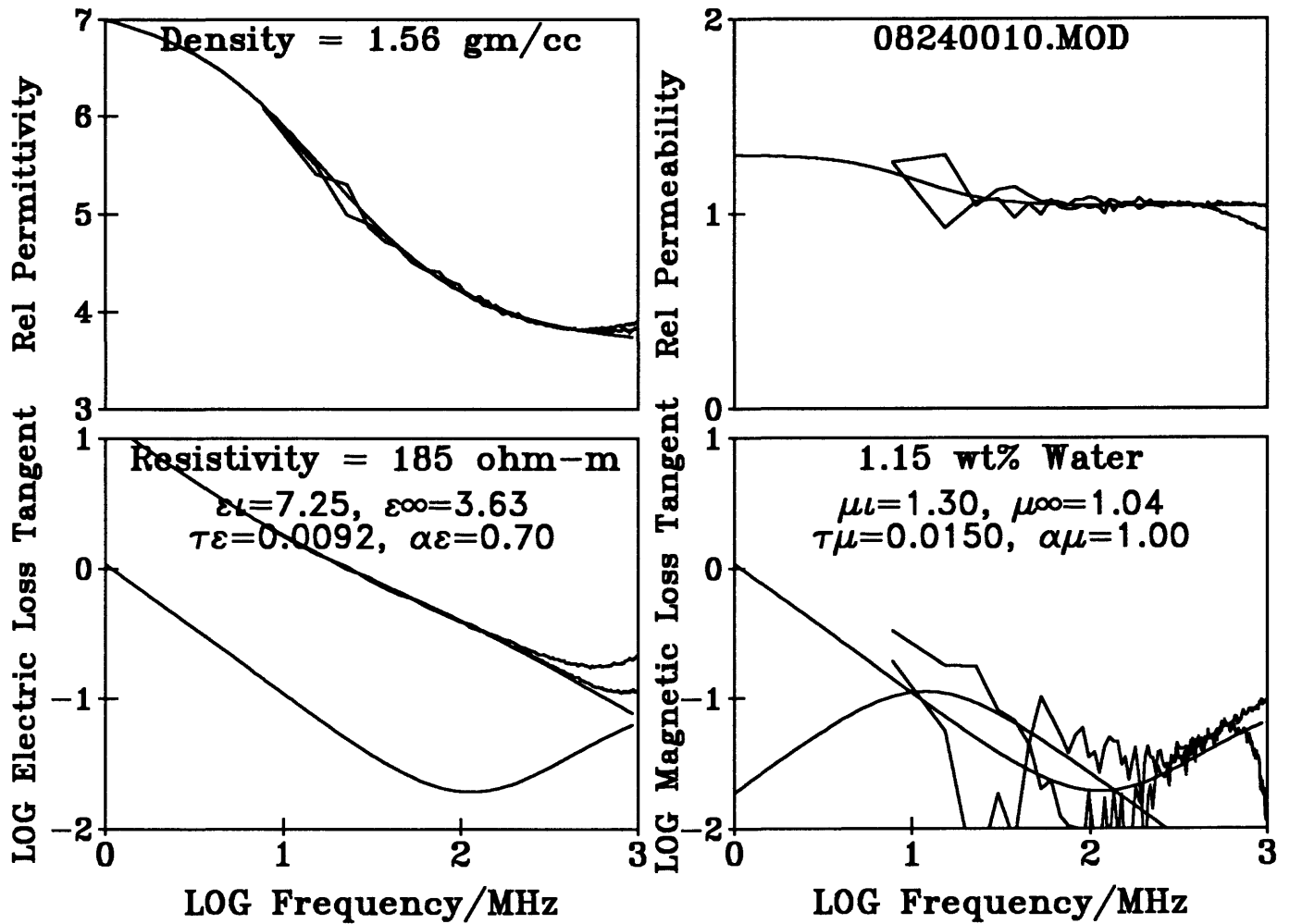


Figure 9 -



Yuma -500m Hood 0.25-0.3m depth #3 2 drops water + 30 min.

Figure 10 -

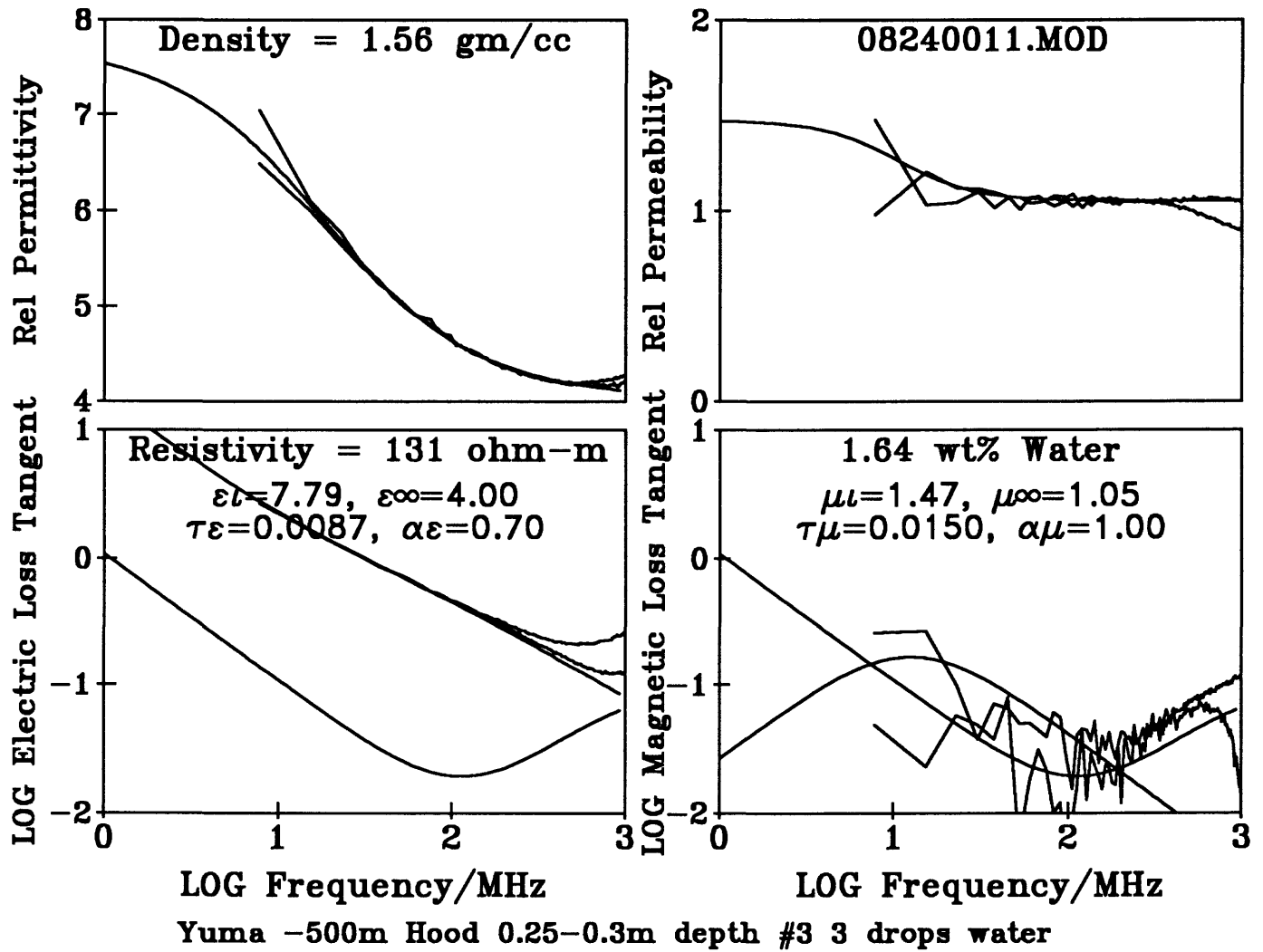
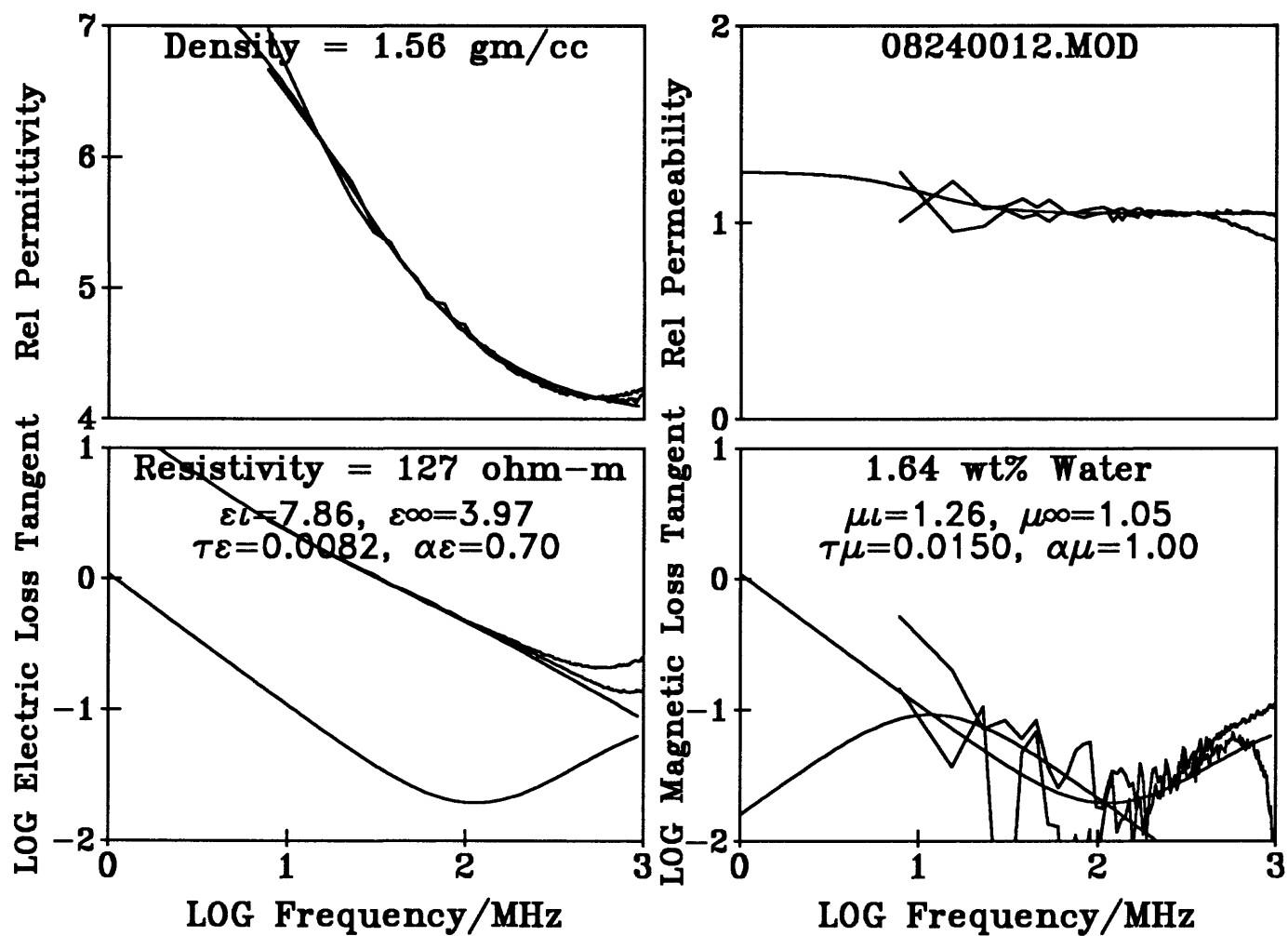


Figure 11 -



Yuma -500m Hood 0.25-0.3m depth #3 3 drops water + 30 min.

Figure 12 -

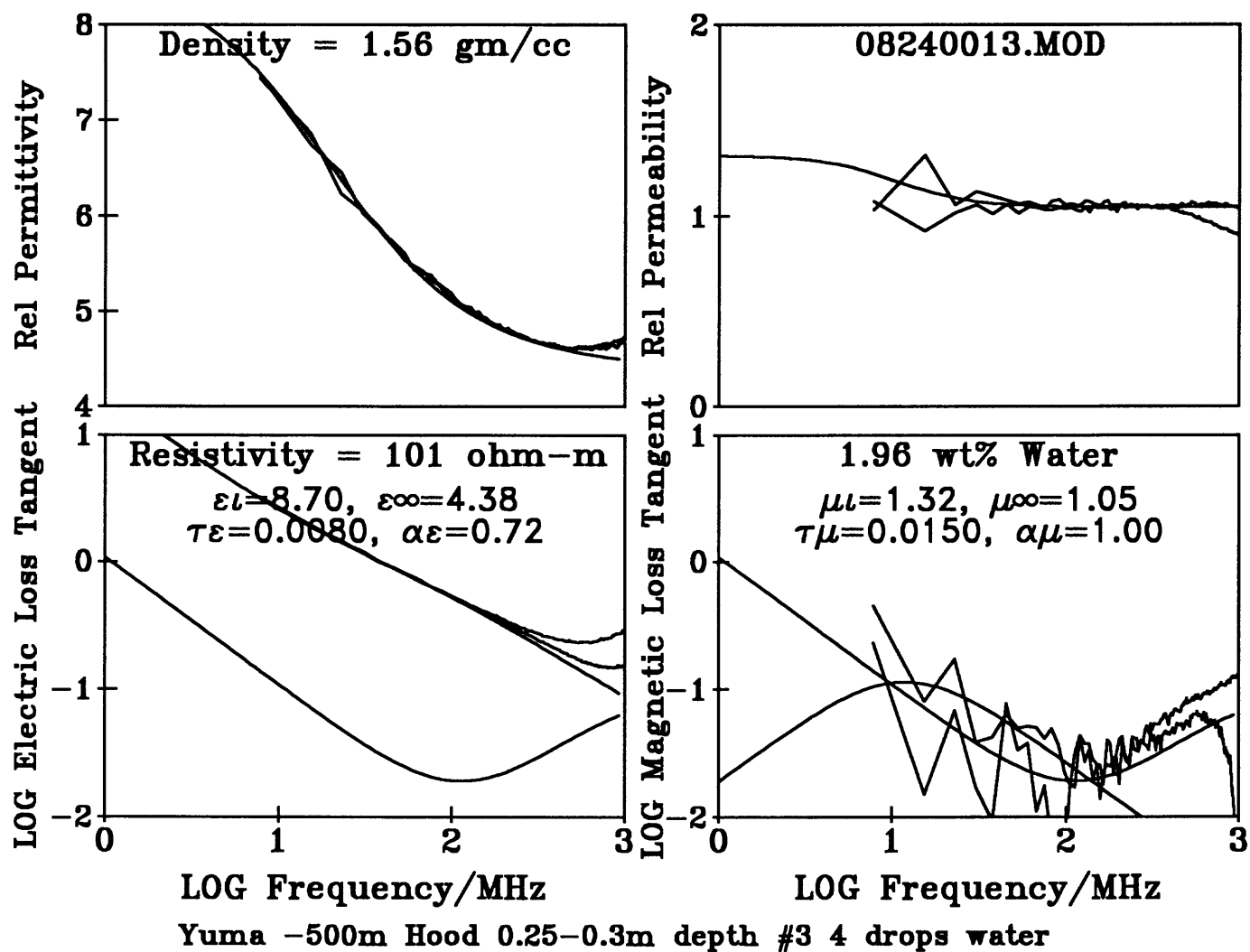
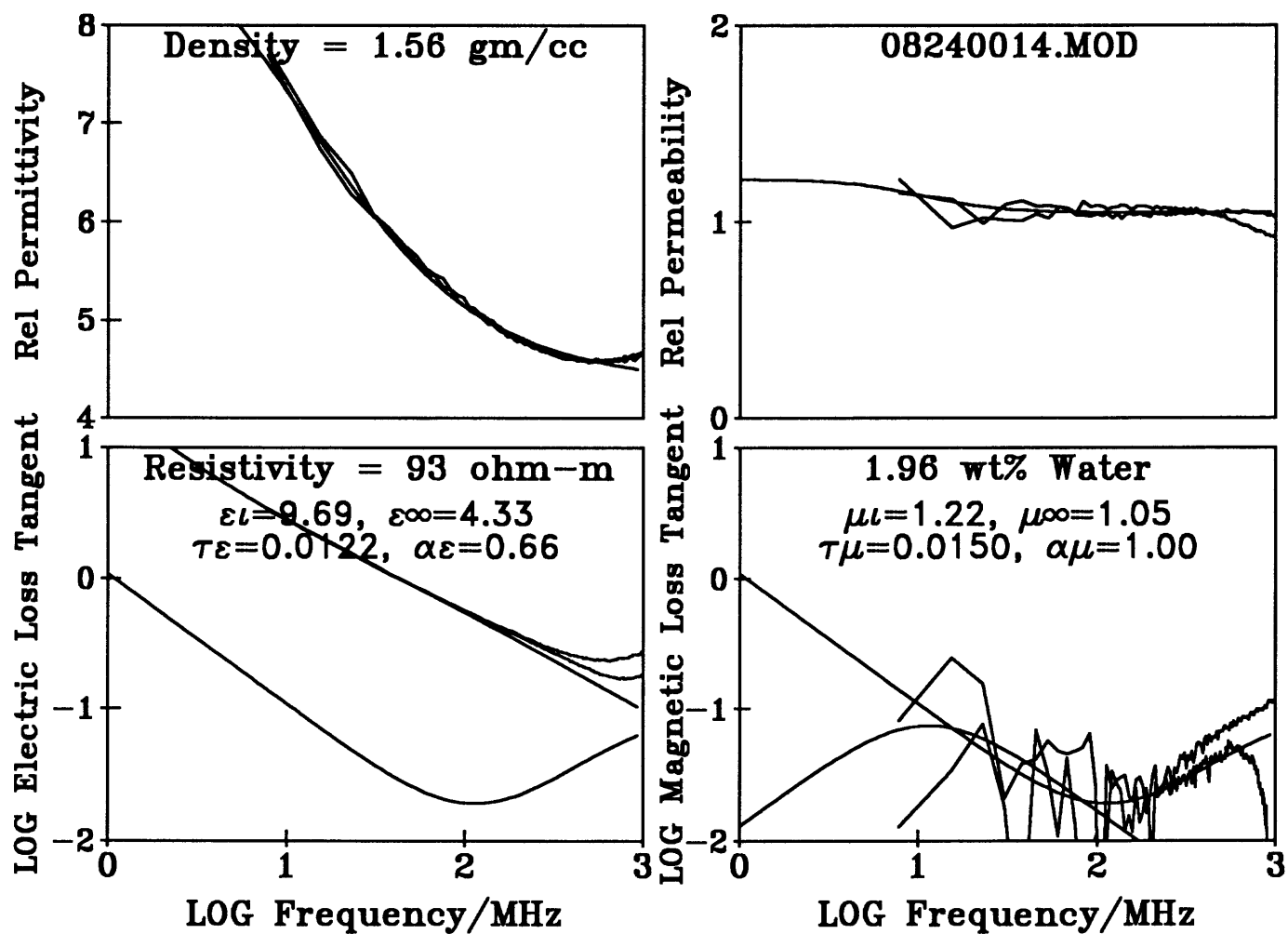


Figure 13 -



Yuma -500m Hood 0.25-0.3m depth #3 4 drops water + 30 min.

Figure 14 -

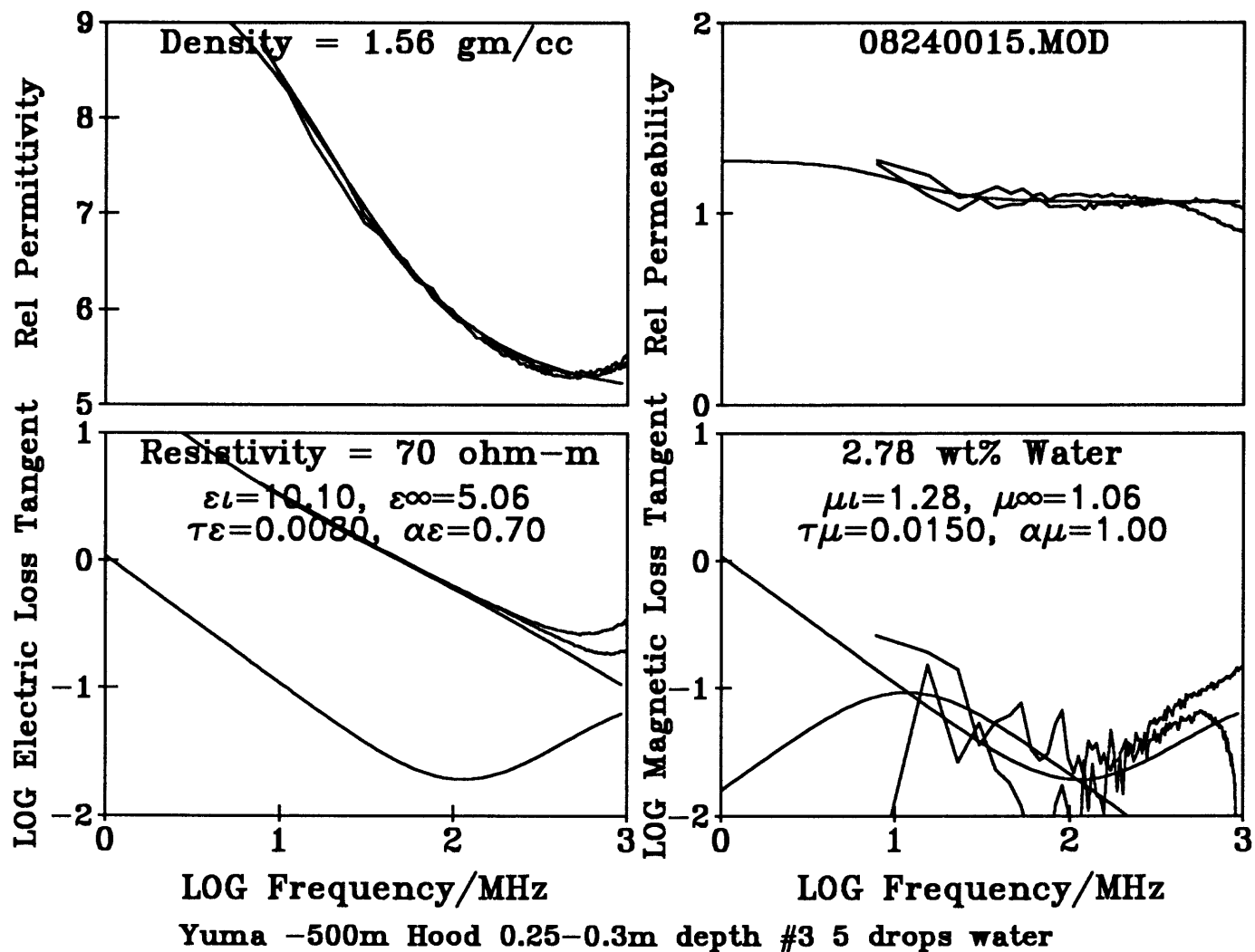
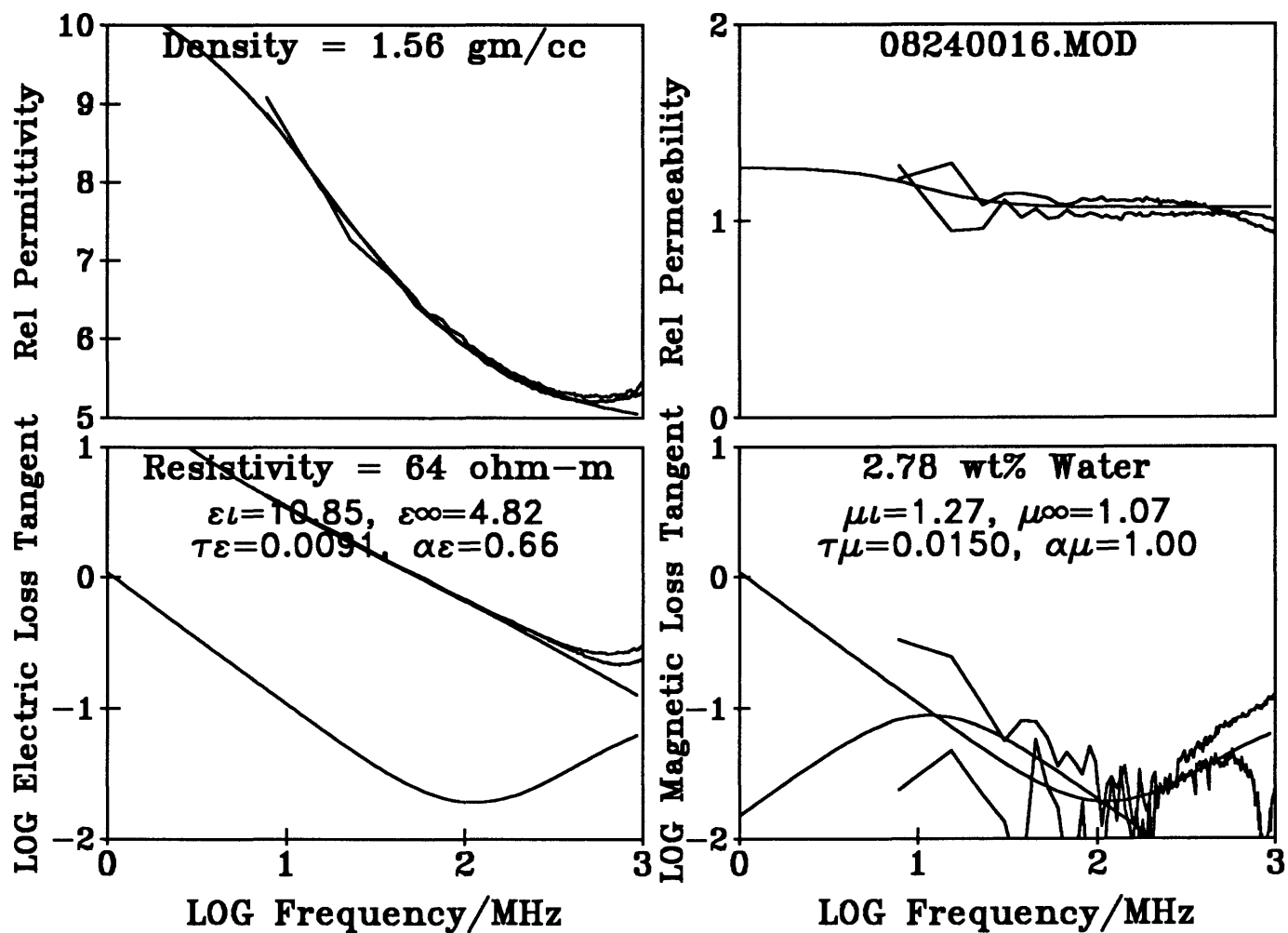


Figure 15 -



Yuma -500m Hood 0.25-0.3m depth #3 5 drops water + 30 min.

Figure 16 -

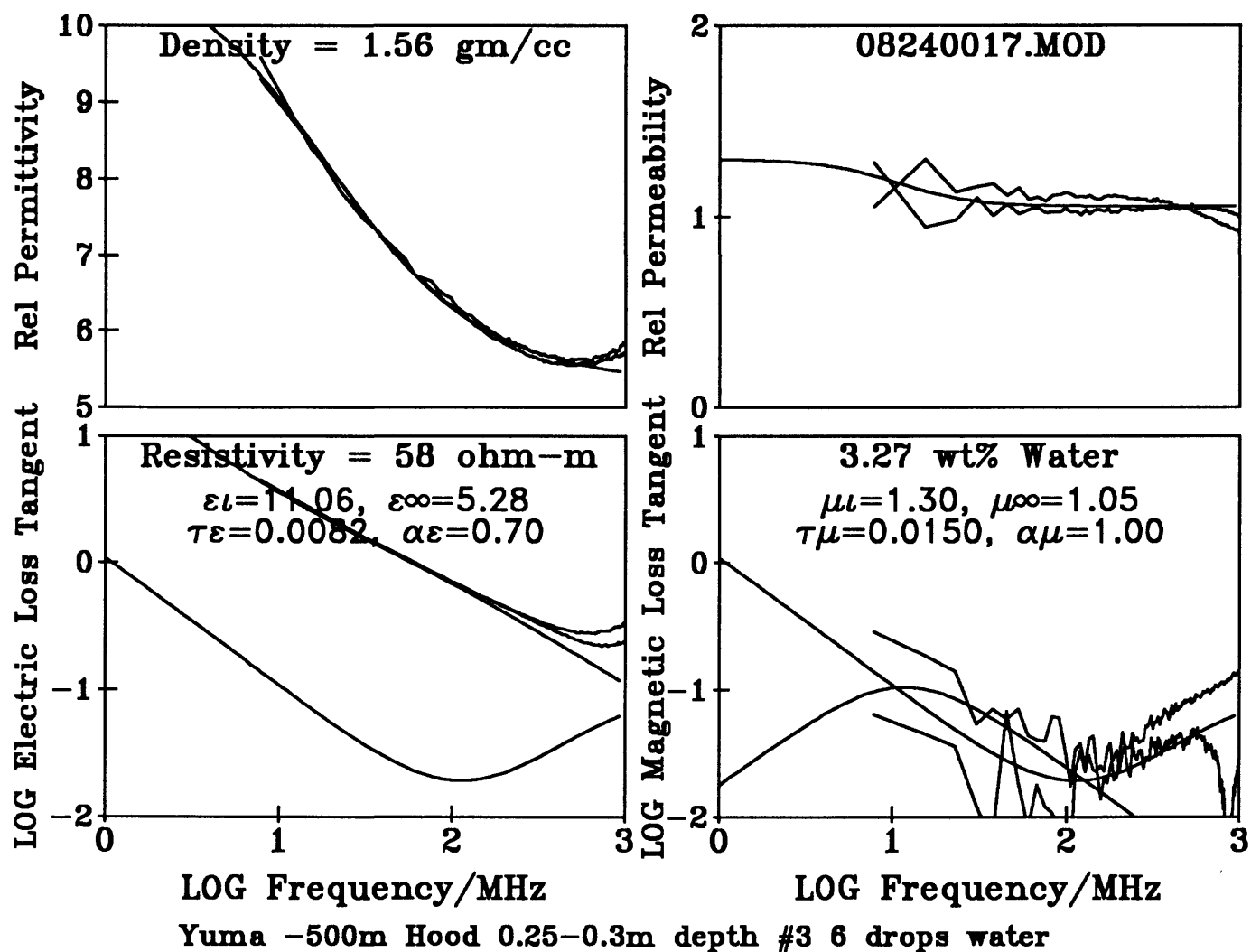


Figure 17 -

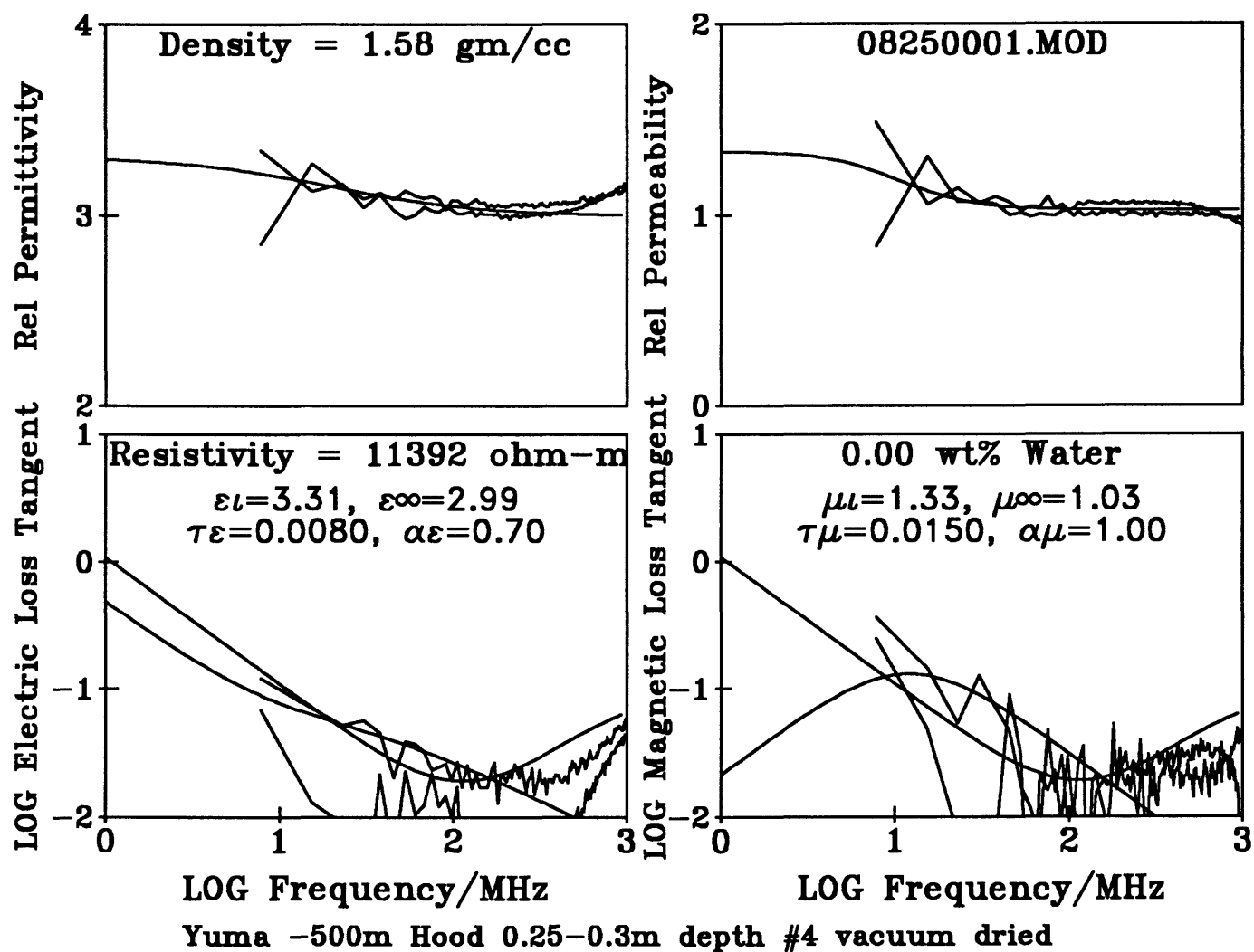


Figure 18 -

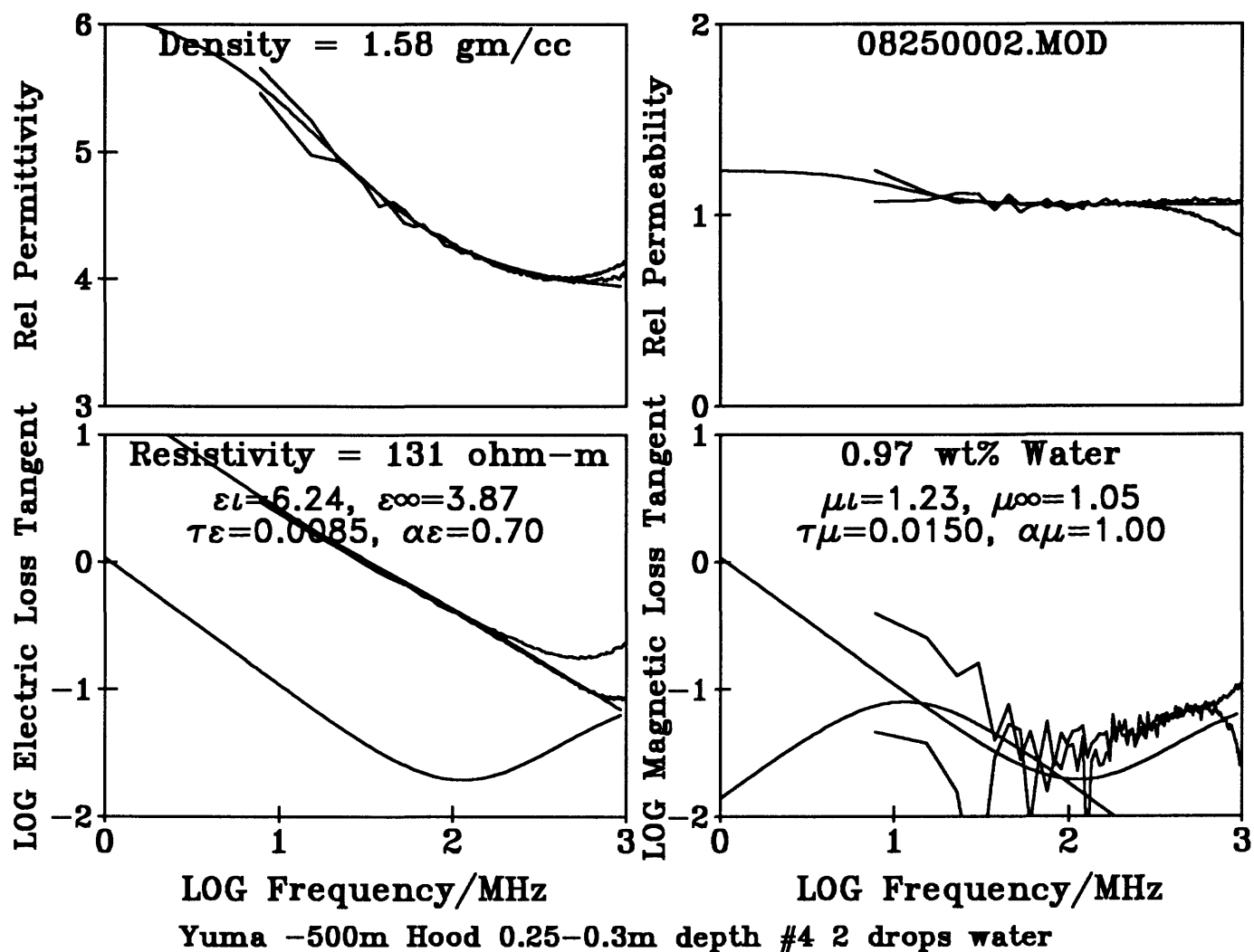


Figure 19 -

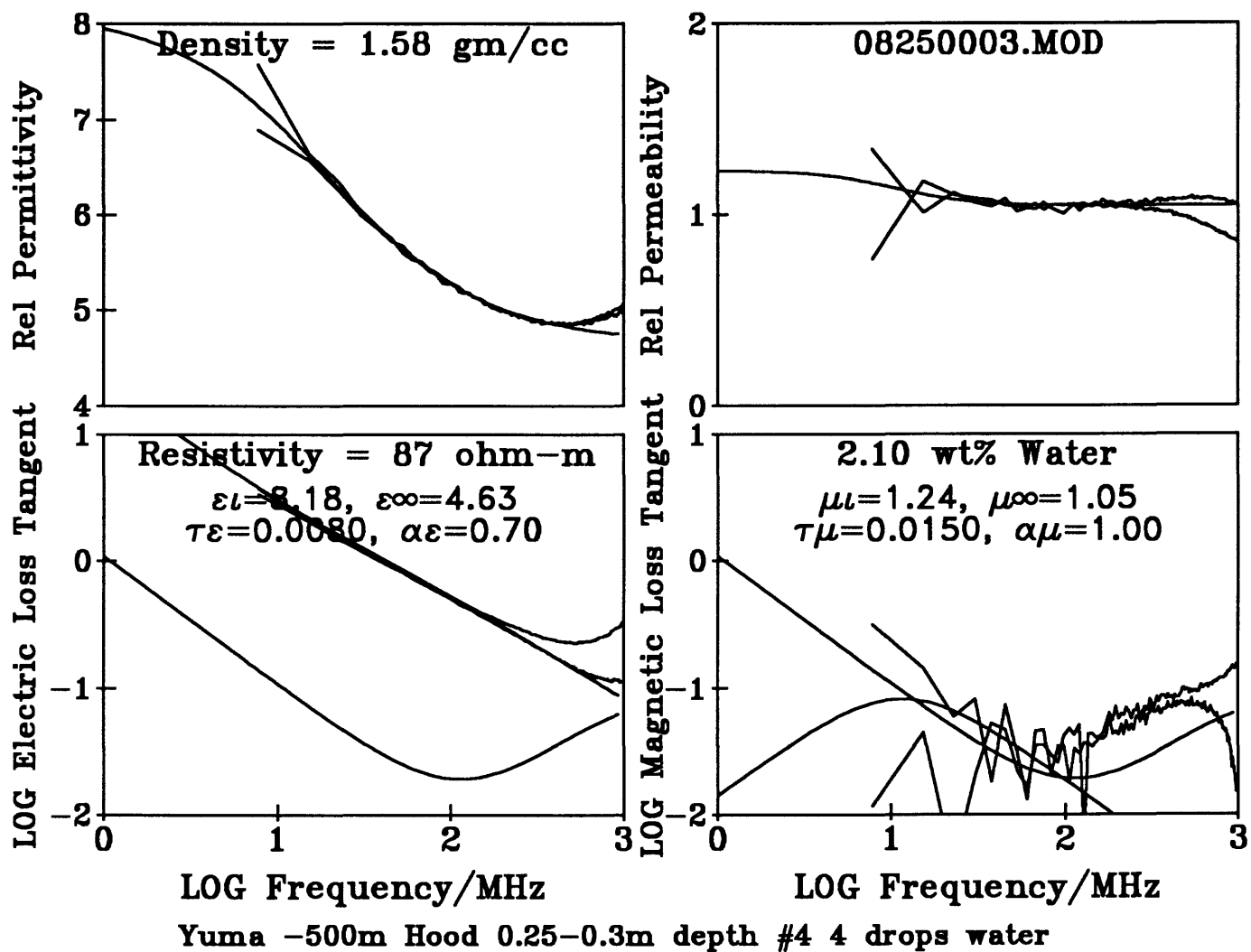


Figure 20 -

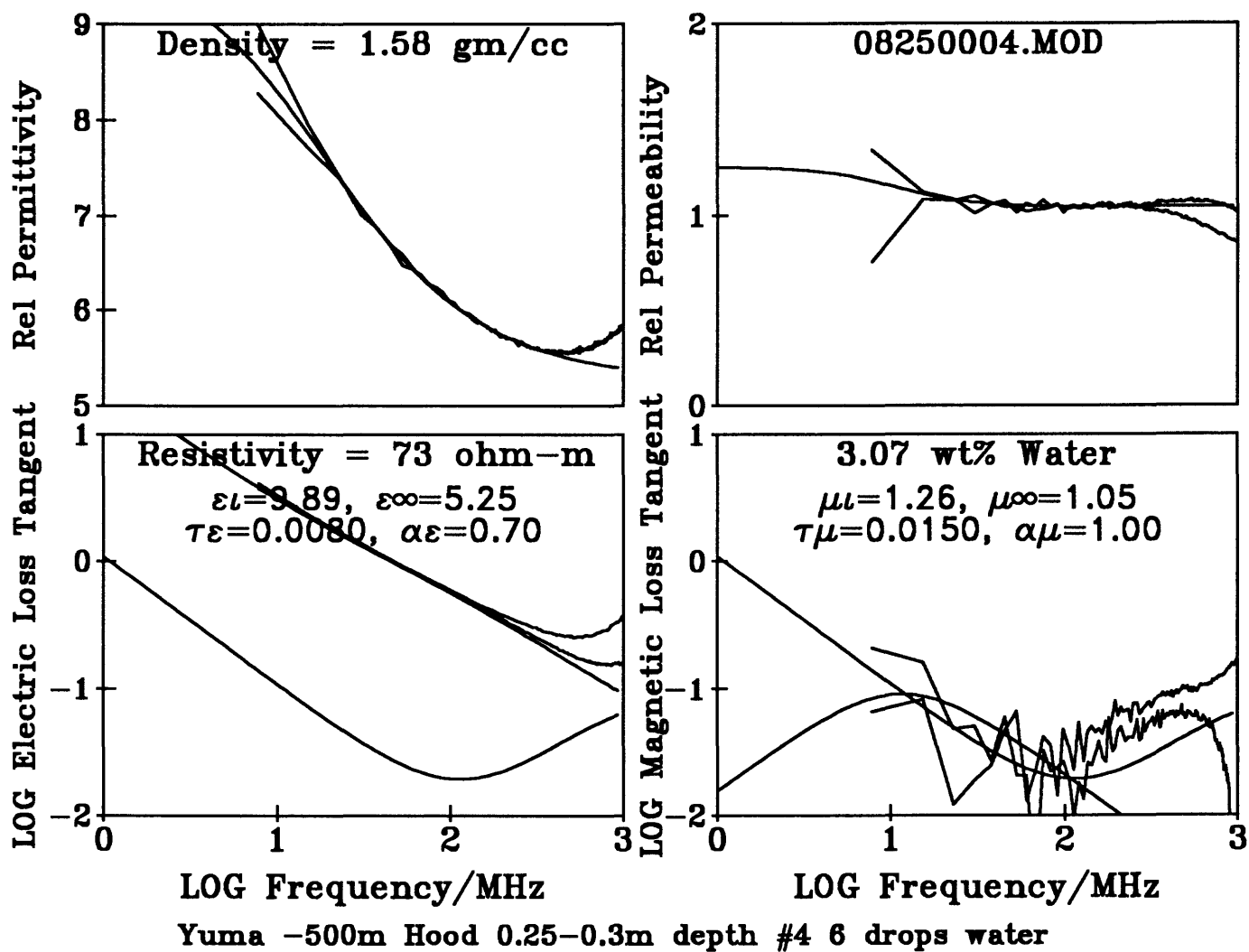


Figure 21 -

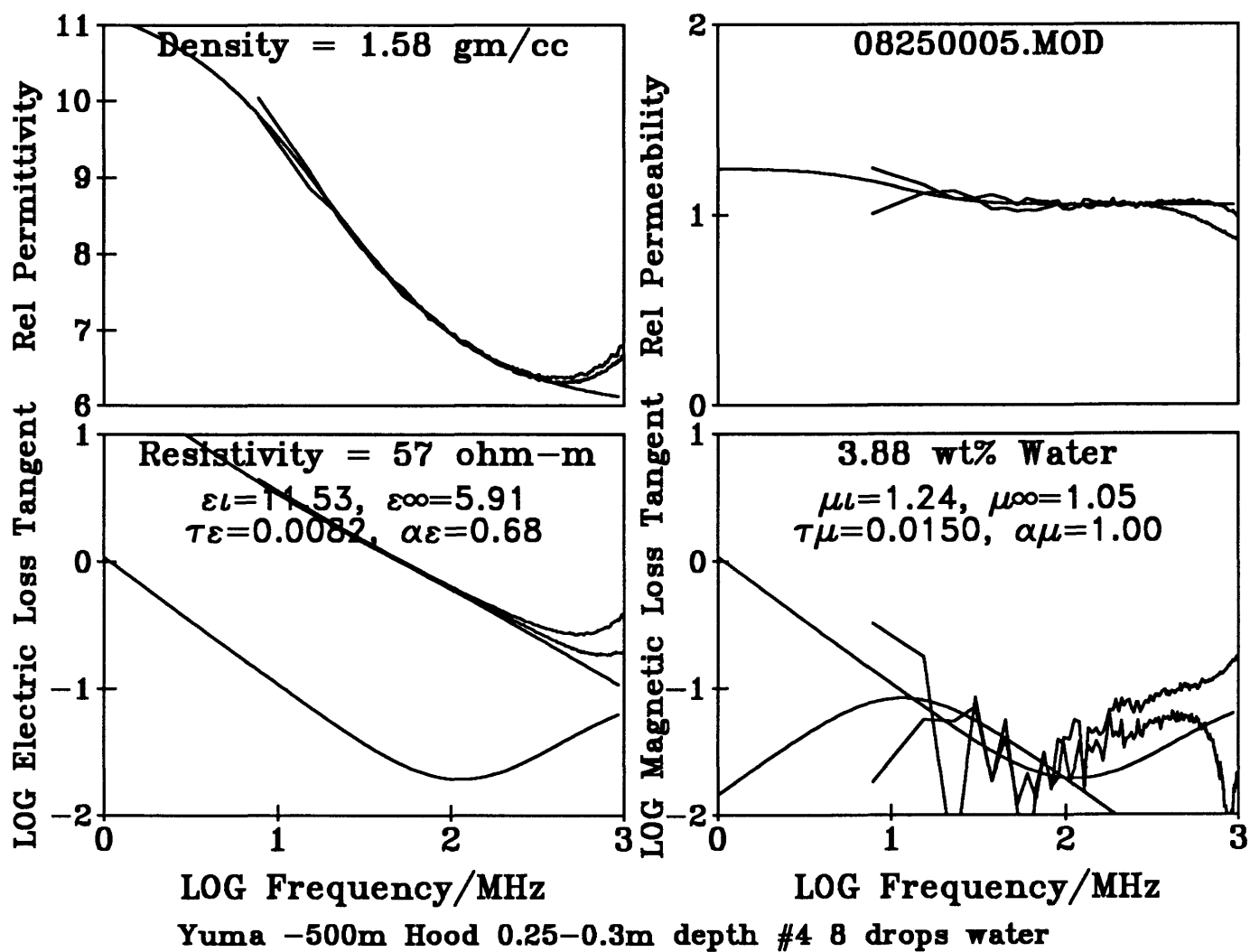


Figure 22 -

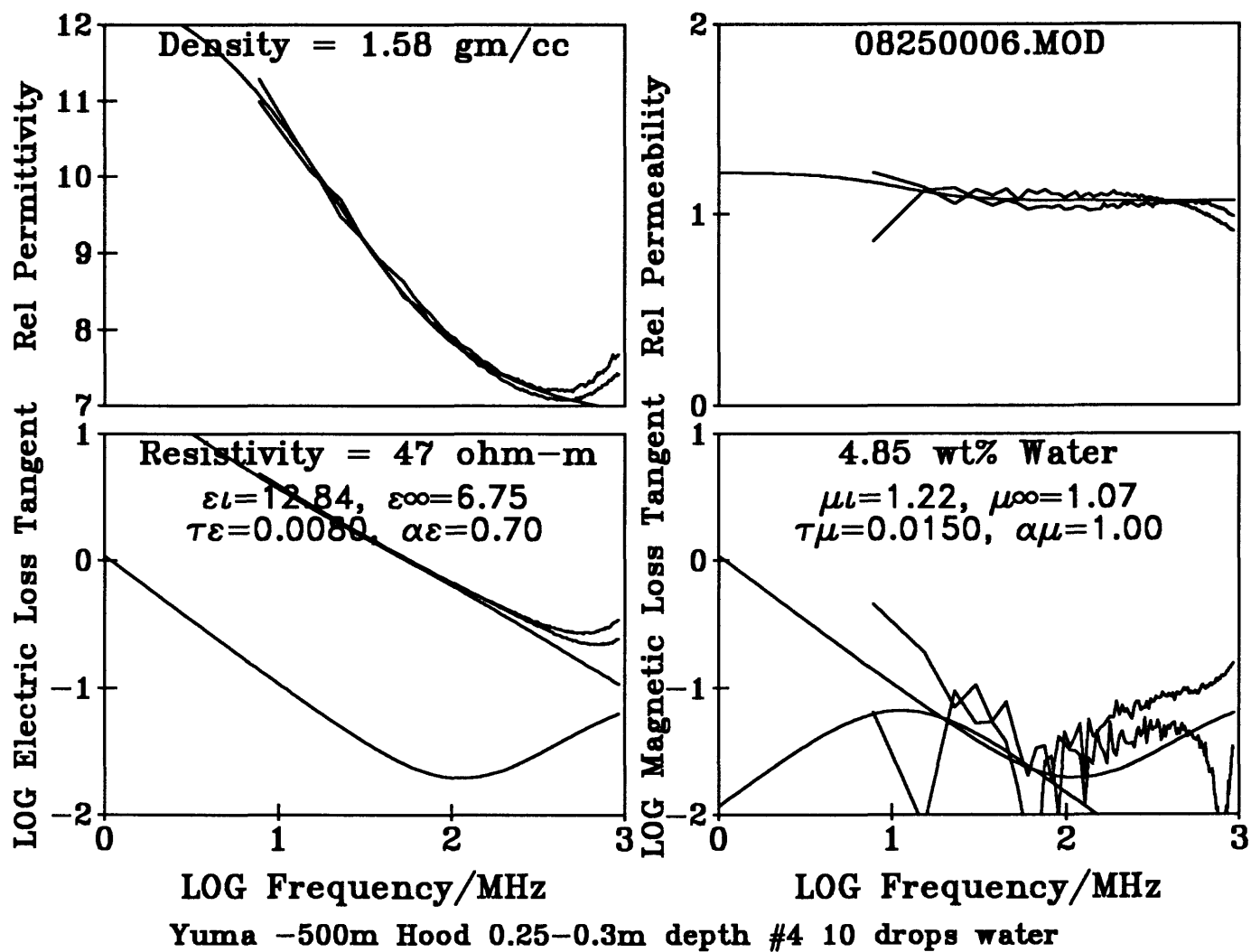


Figure 23 -

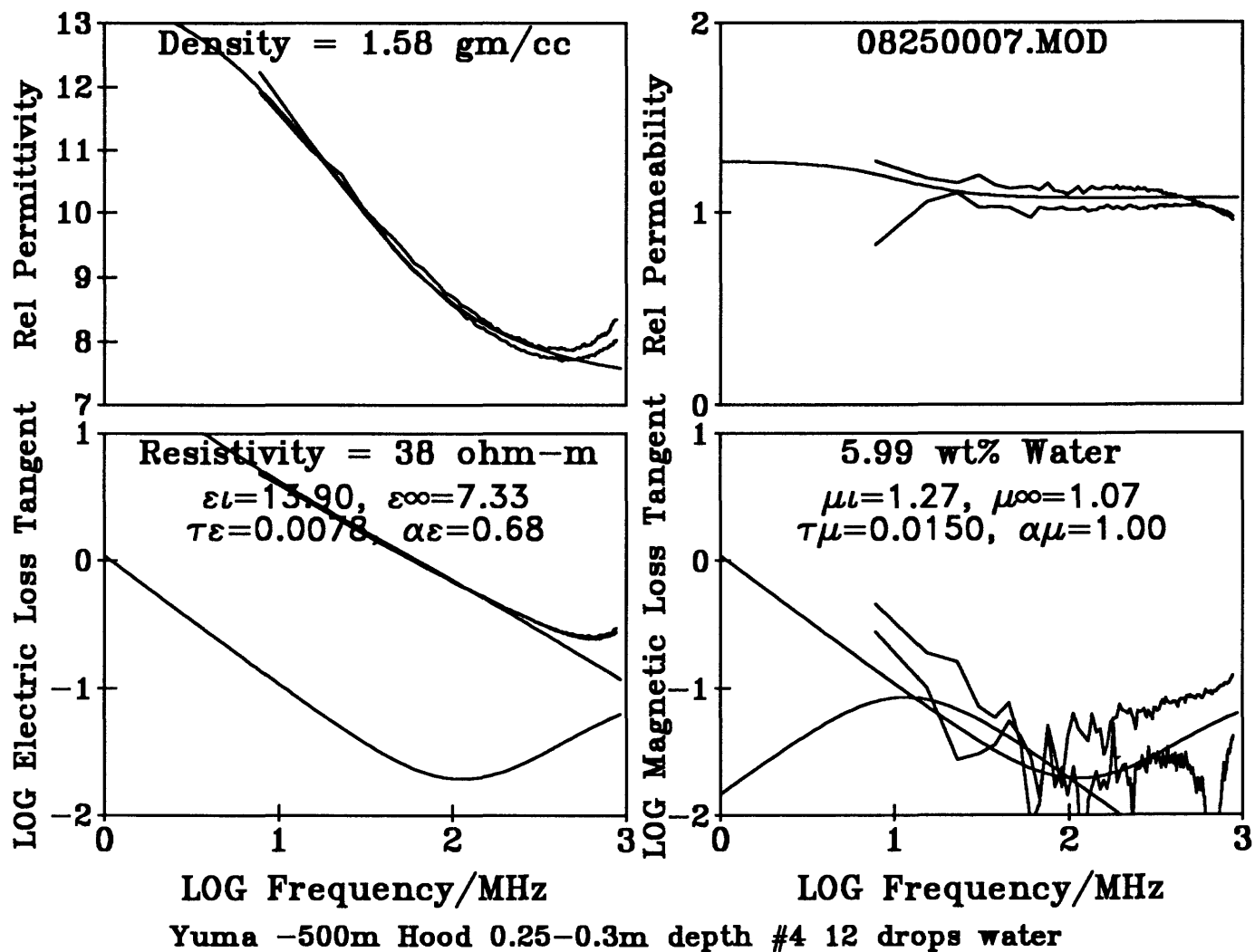


Figure 24 -

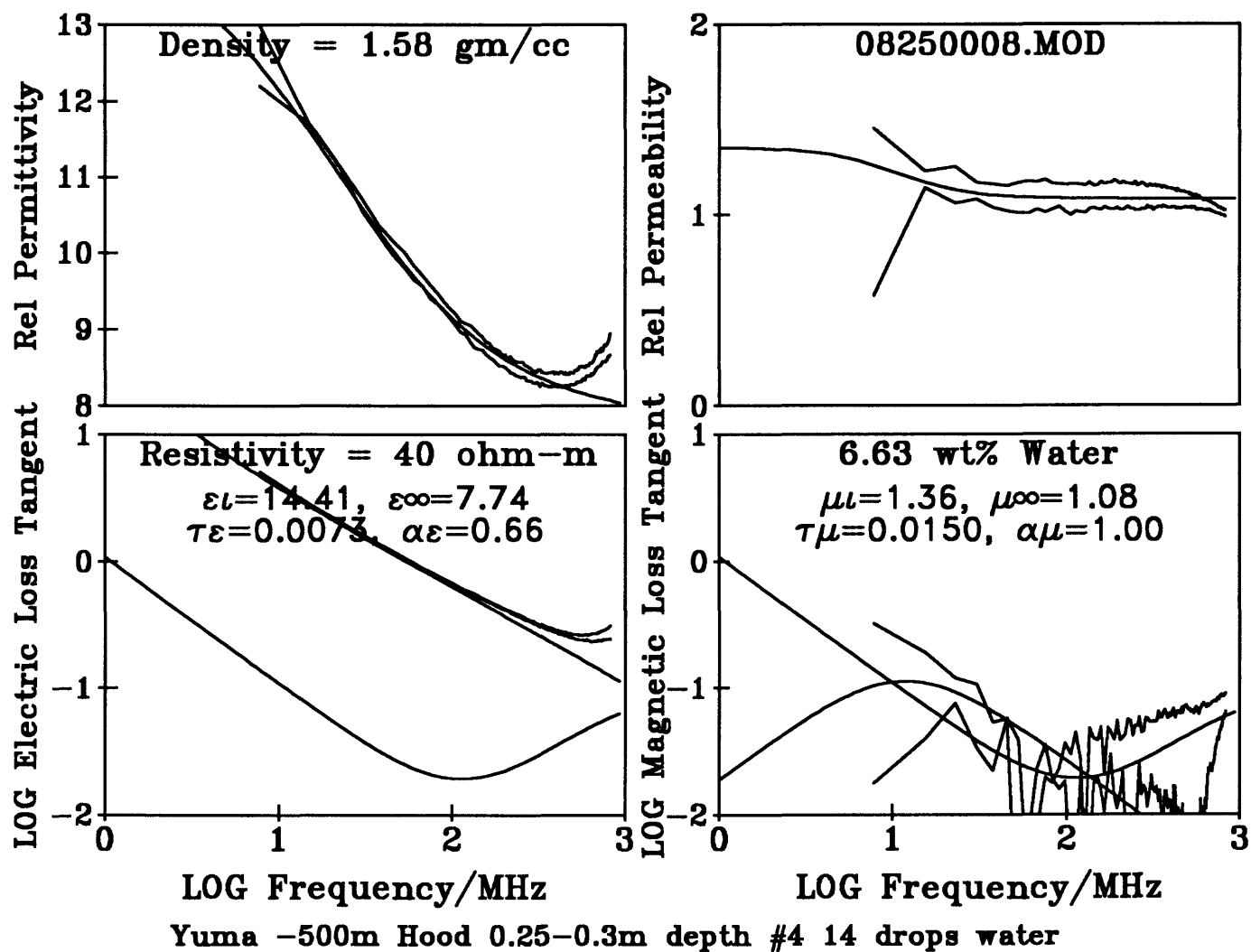


Figure 25 -

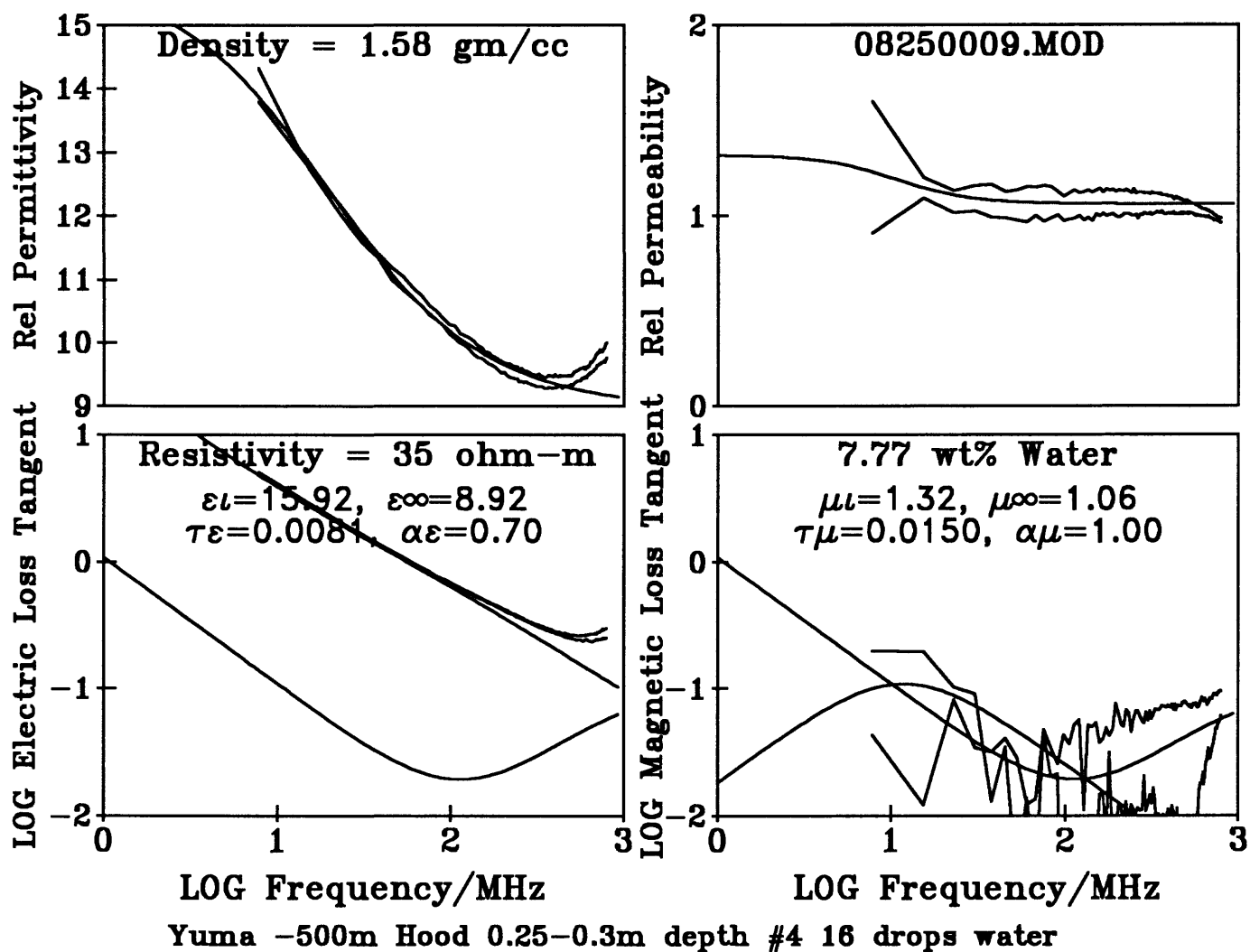


Figure 26 -

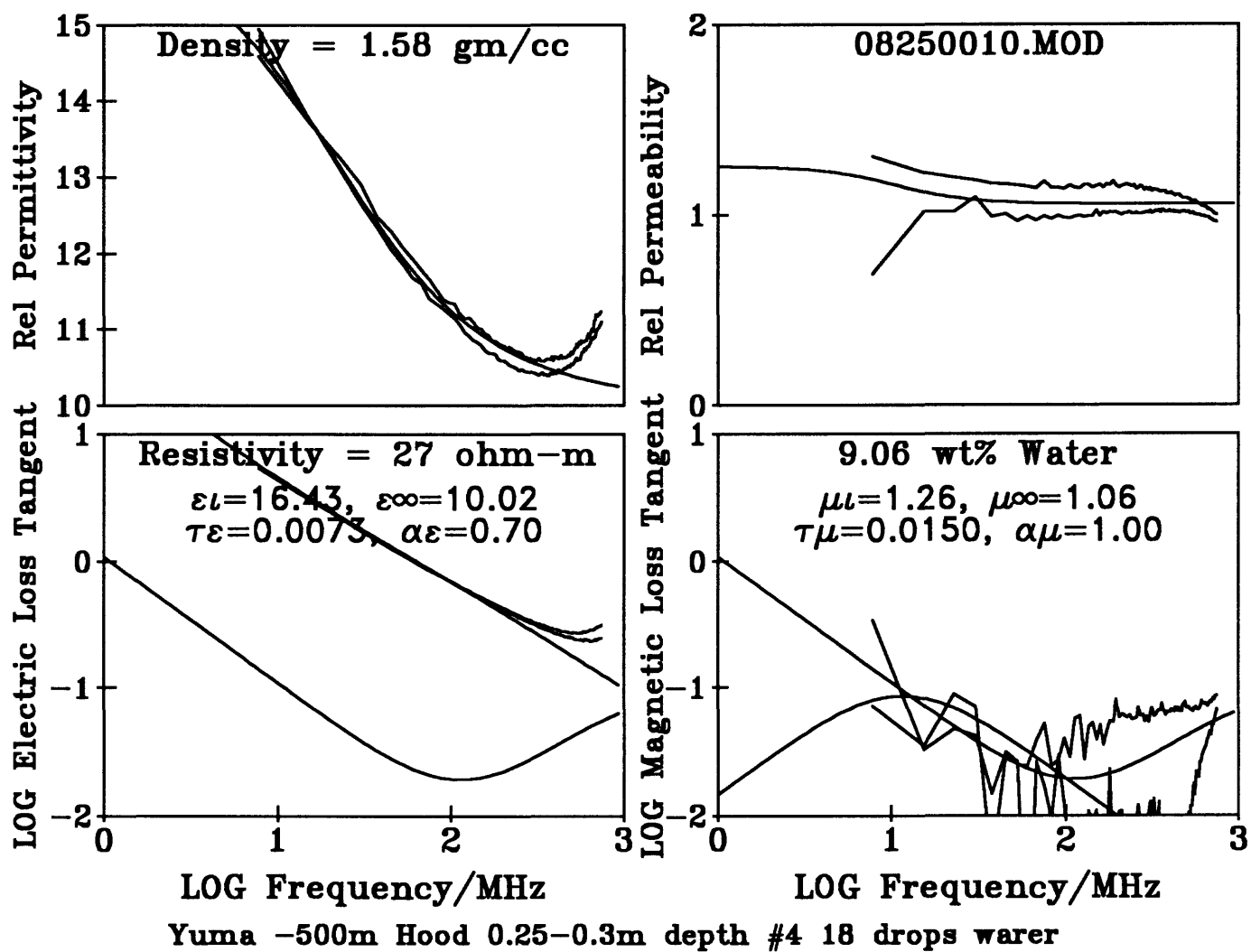


Figure 27 -

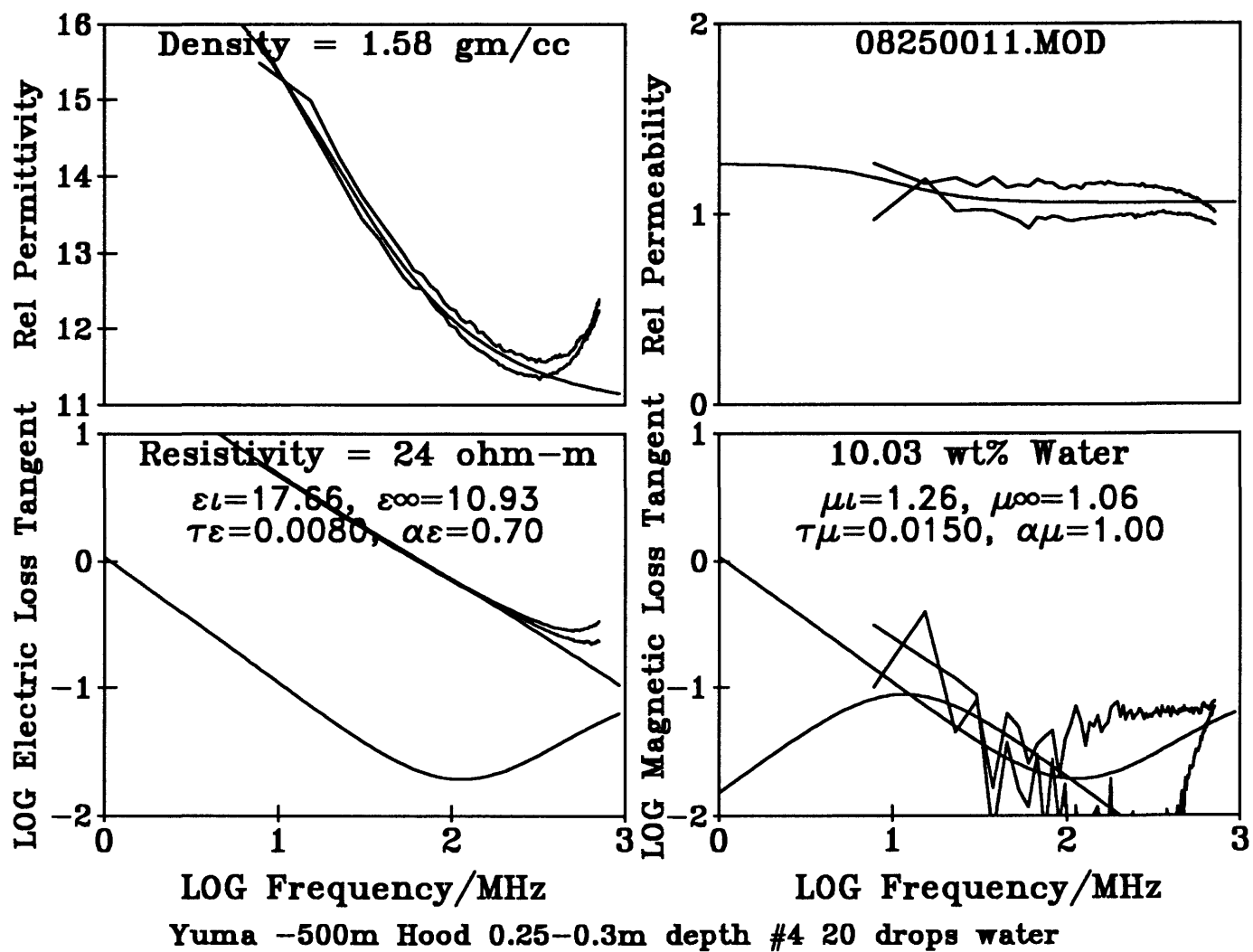


Figure 28 -

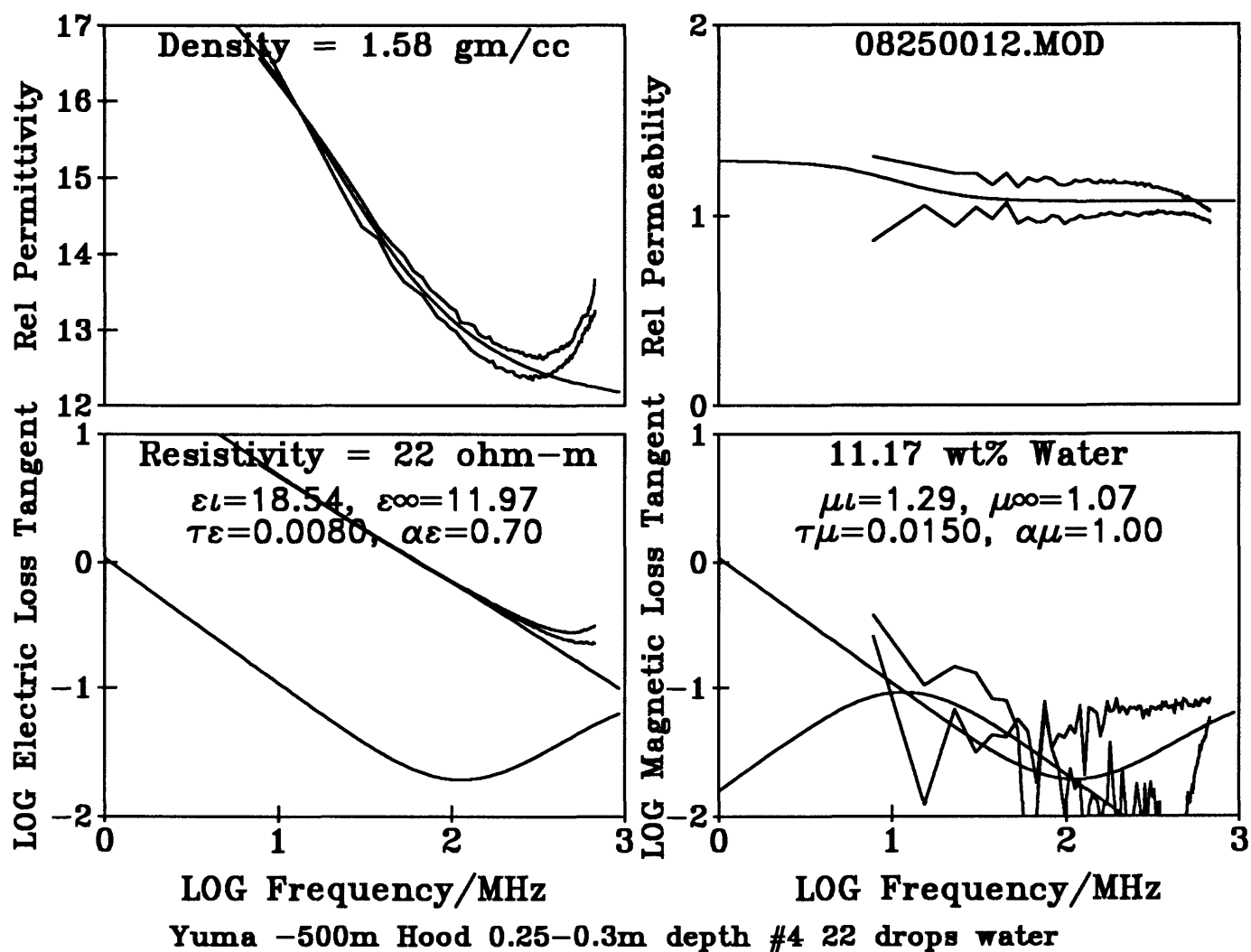


Figure 29 -

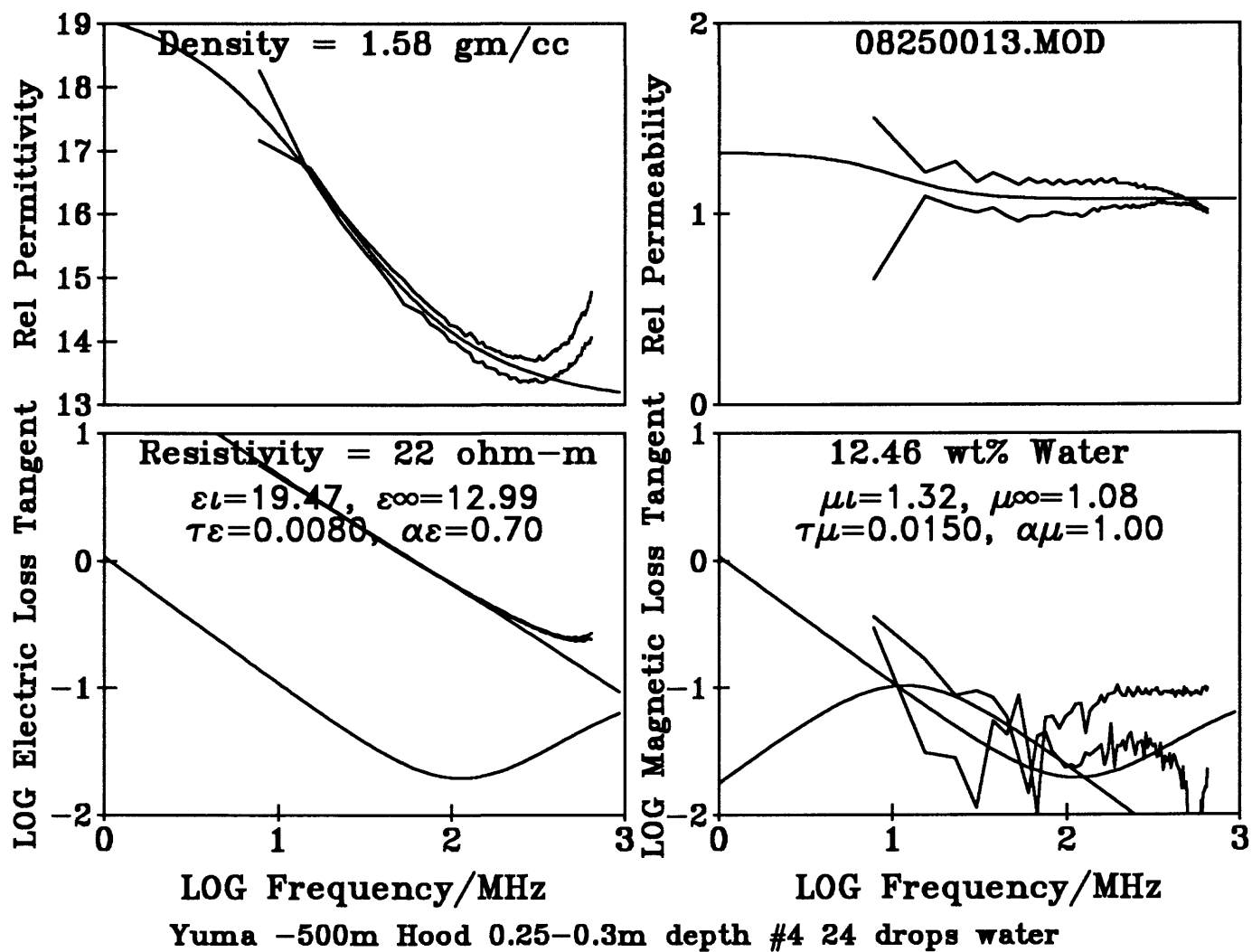


Figure 30 -

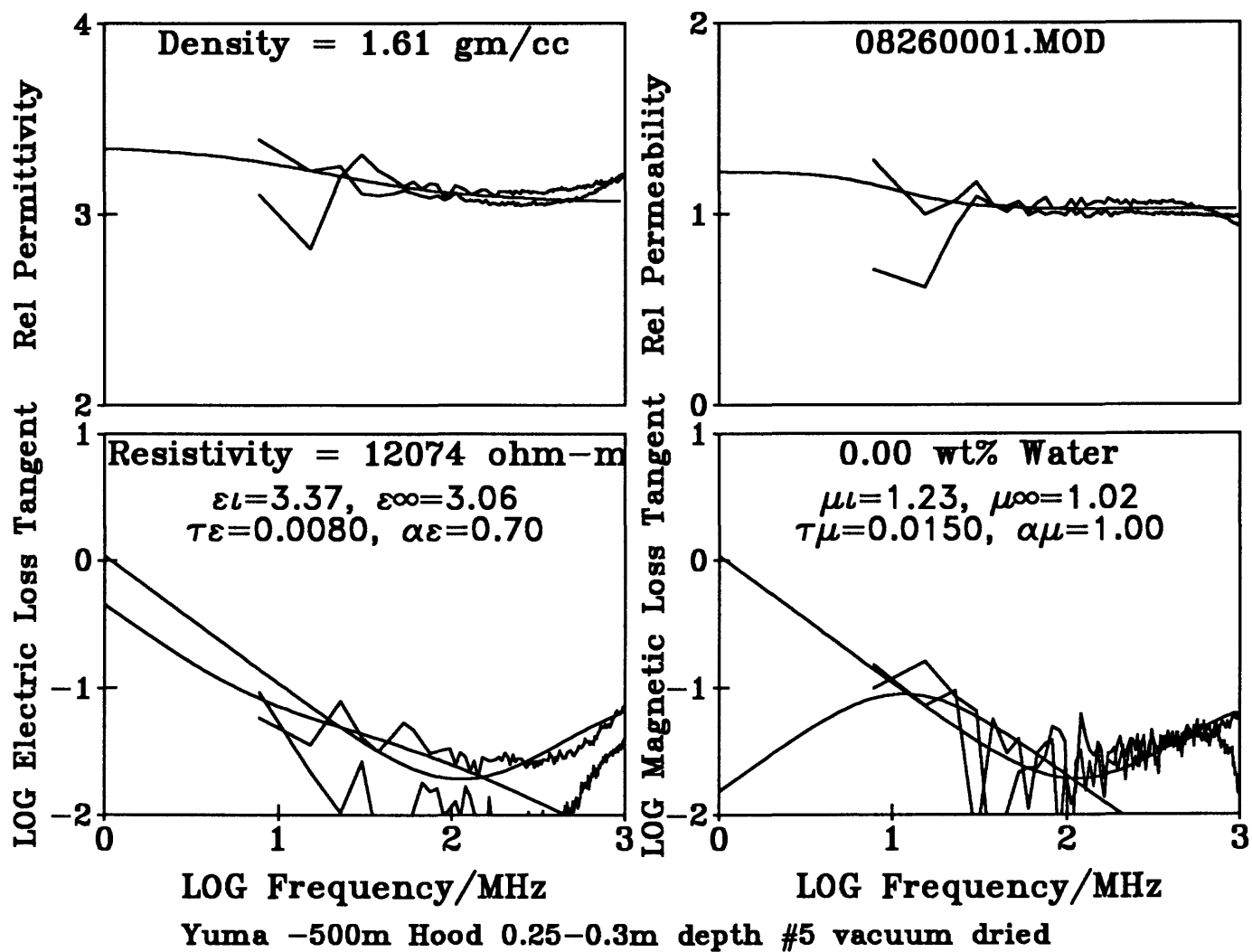


Figure 31 -

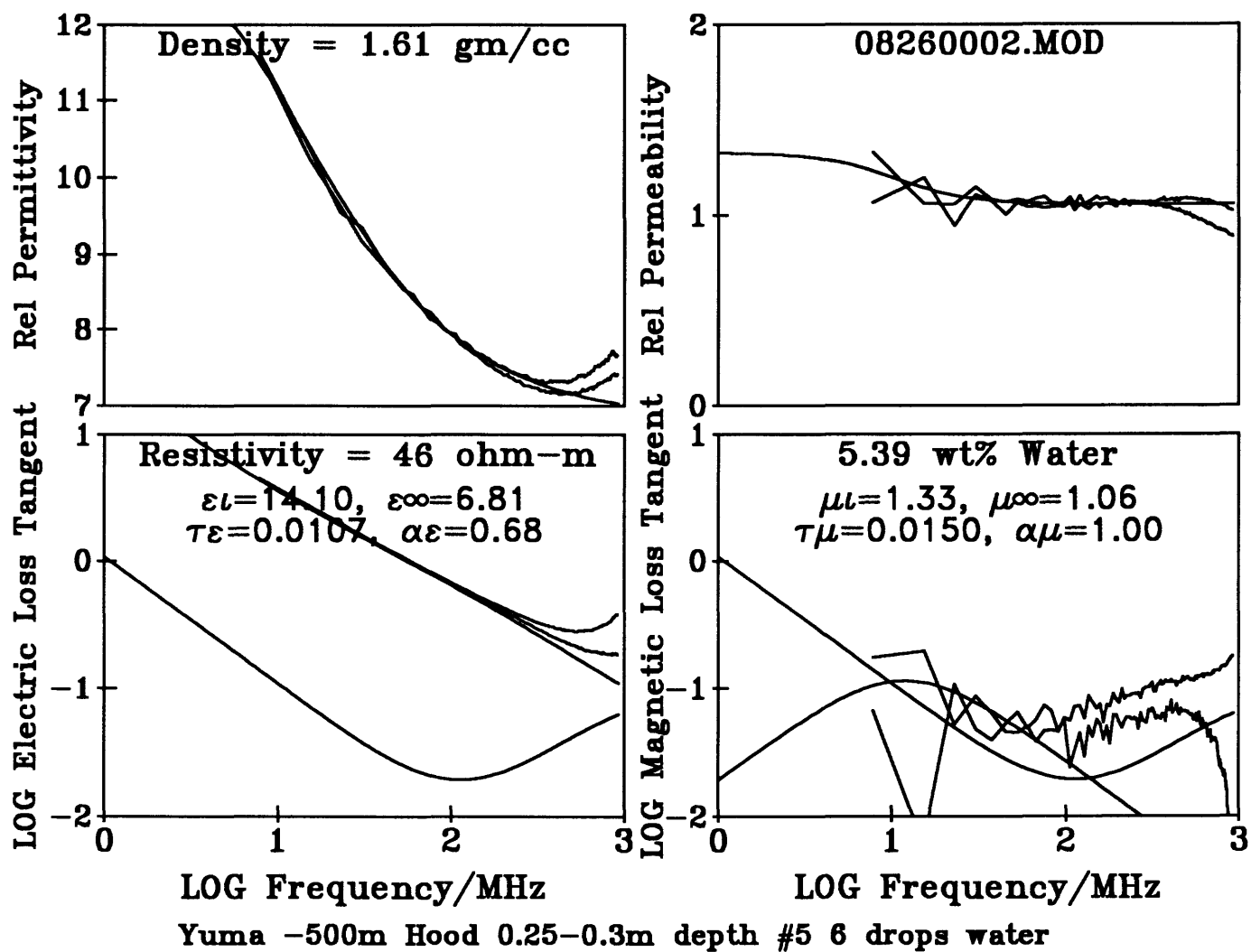


Figure 32 -

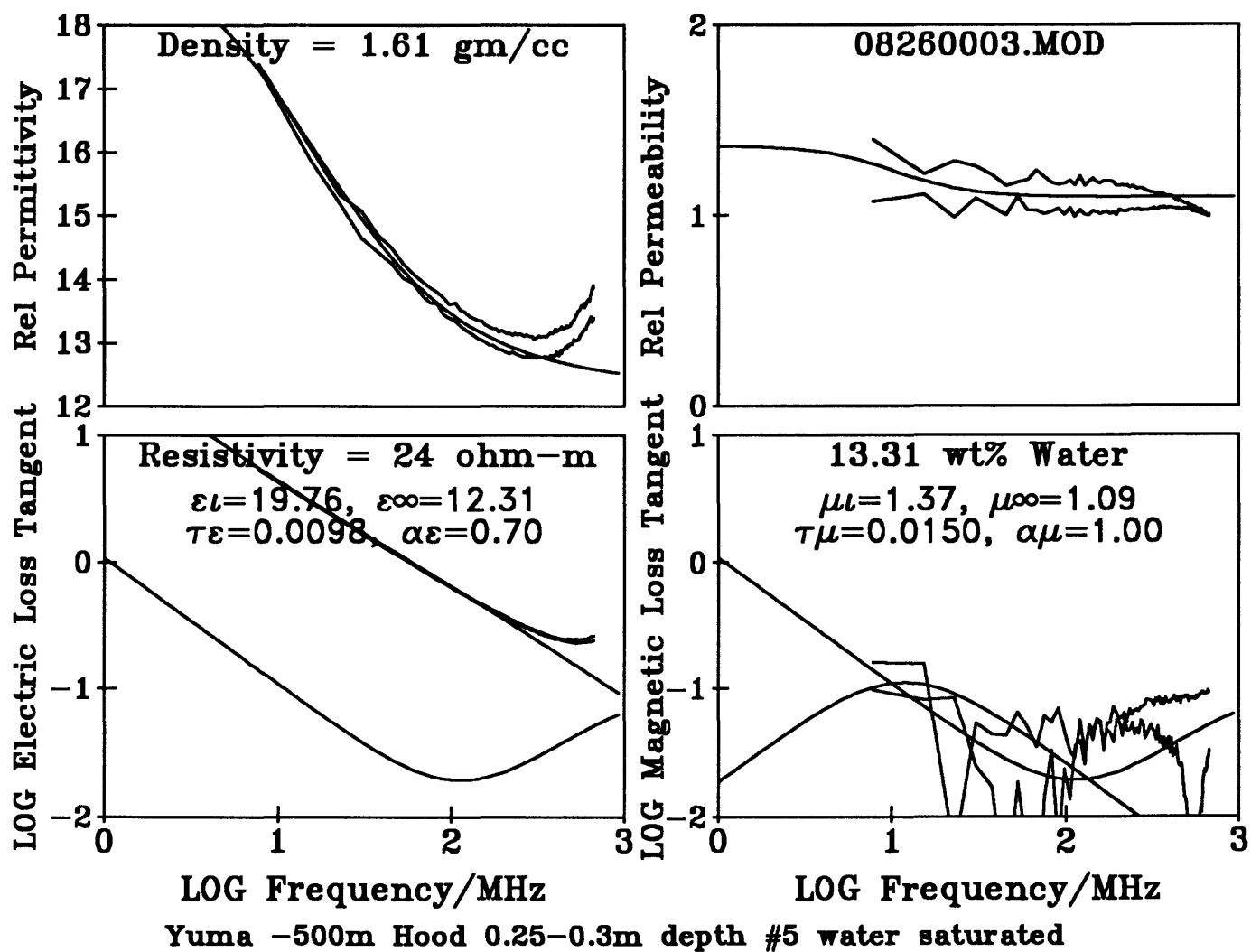


Figure 33 -

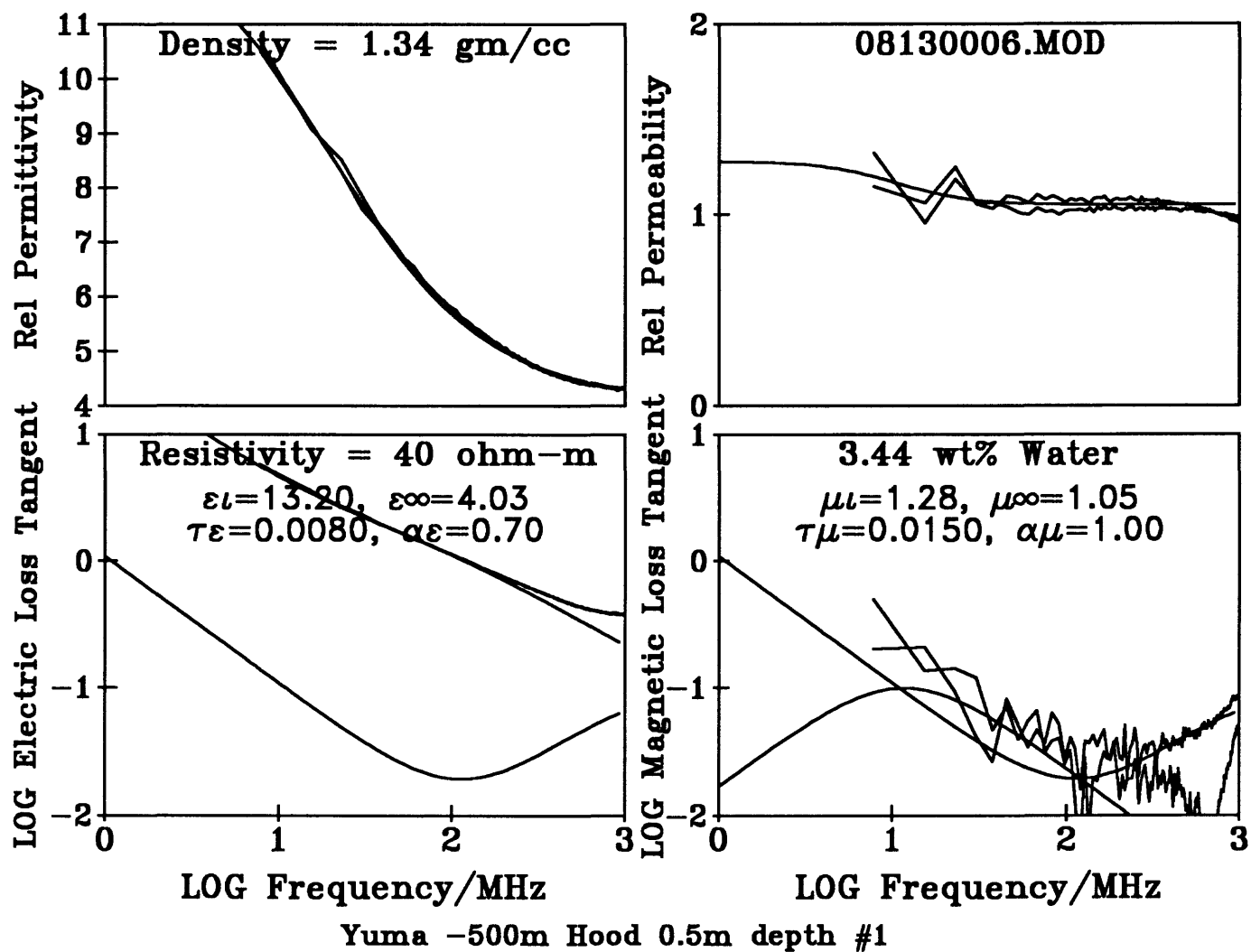


Figure 34 -
Natural state electromagnetic properties with water content preserved in sealed, taped,
sample bottle.

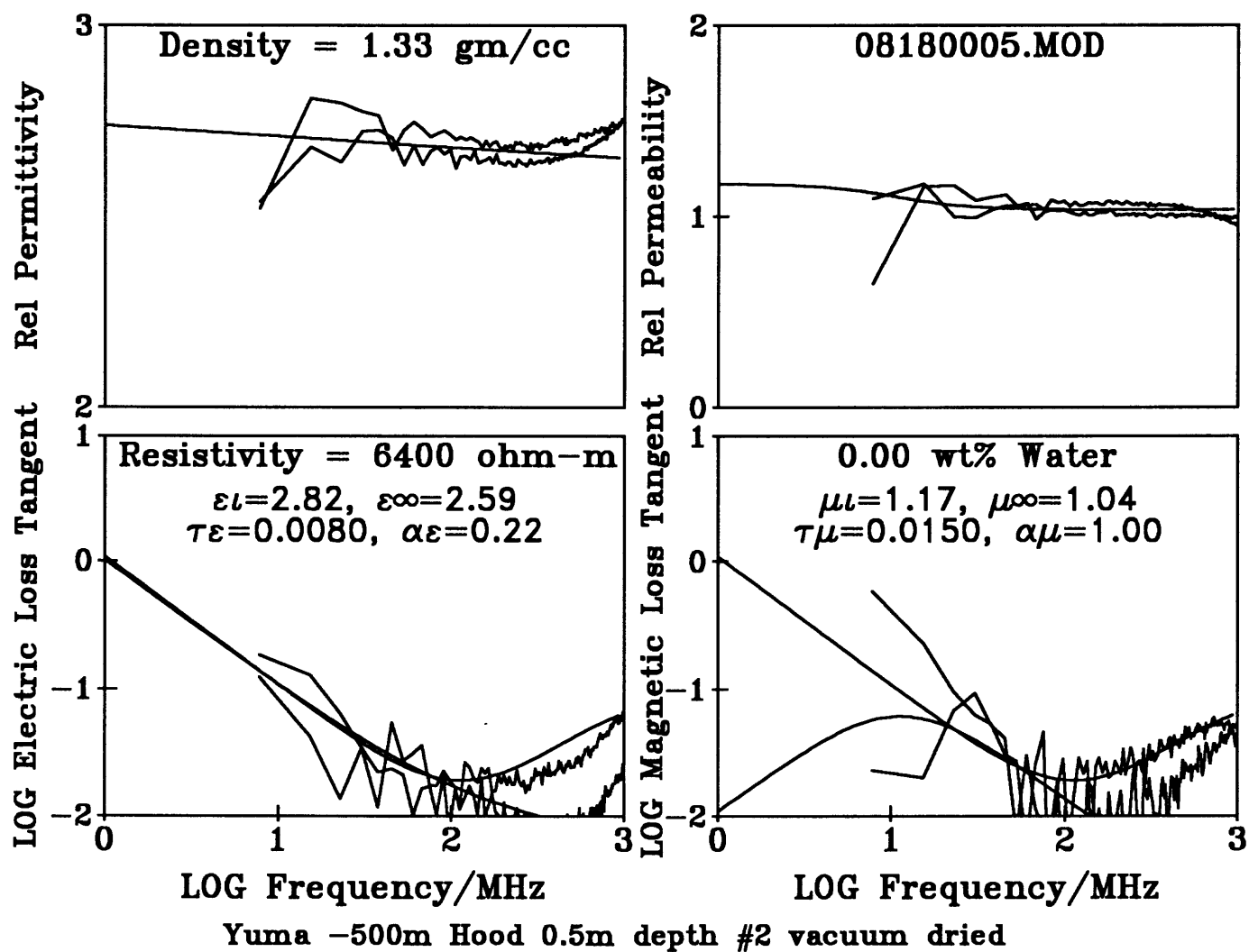


Figure 35 -

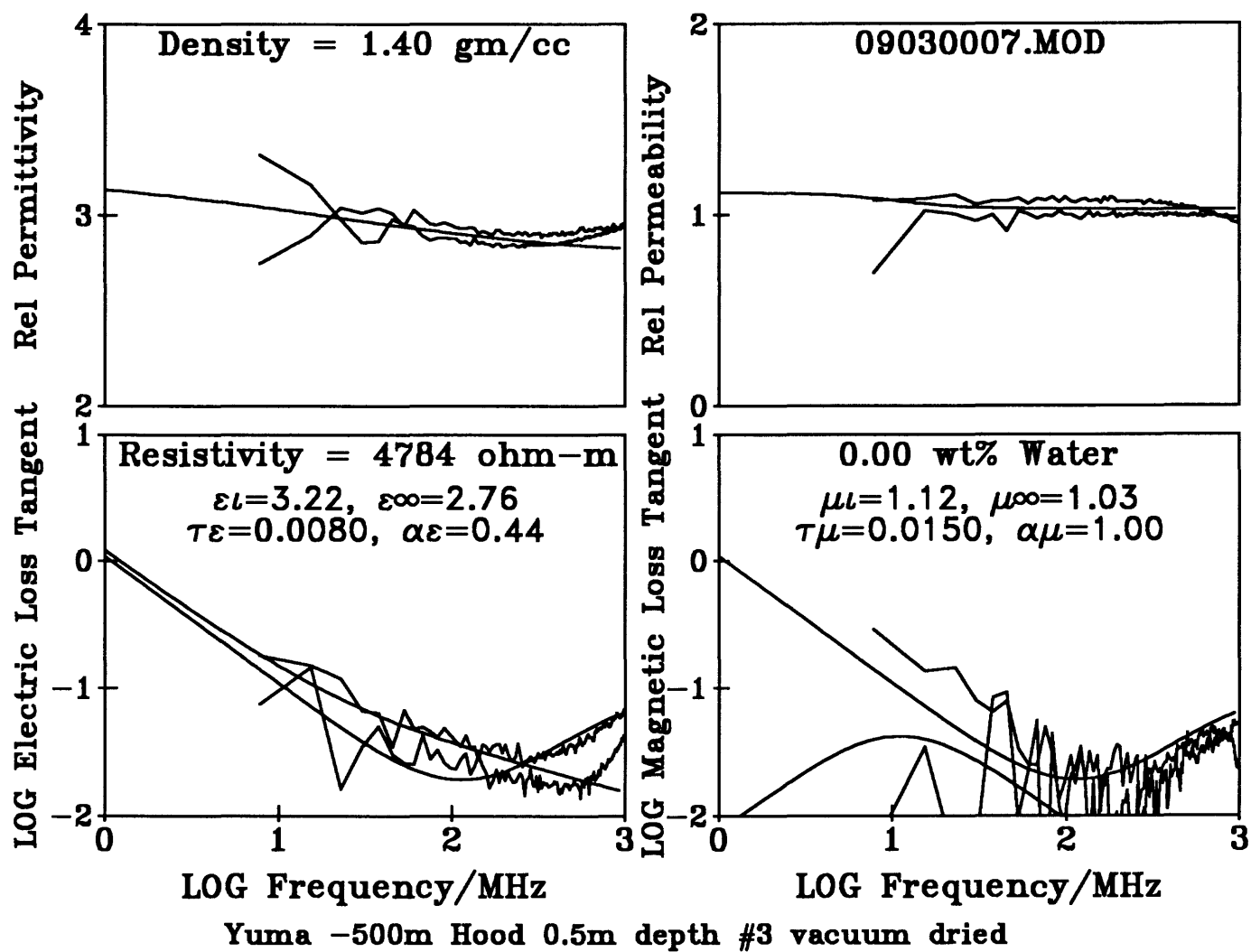


Figure 36 -

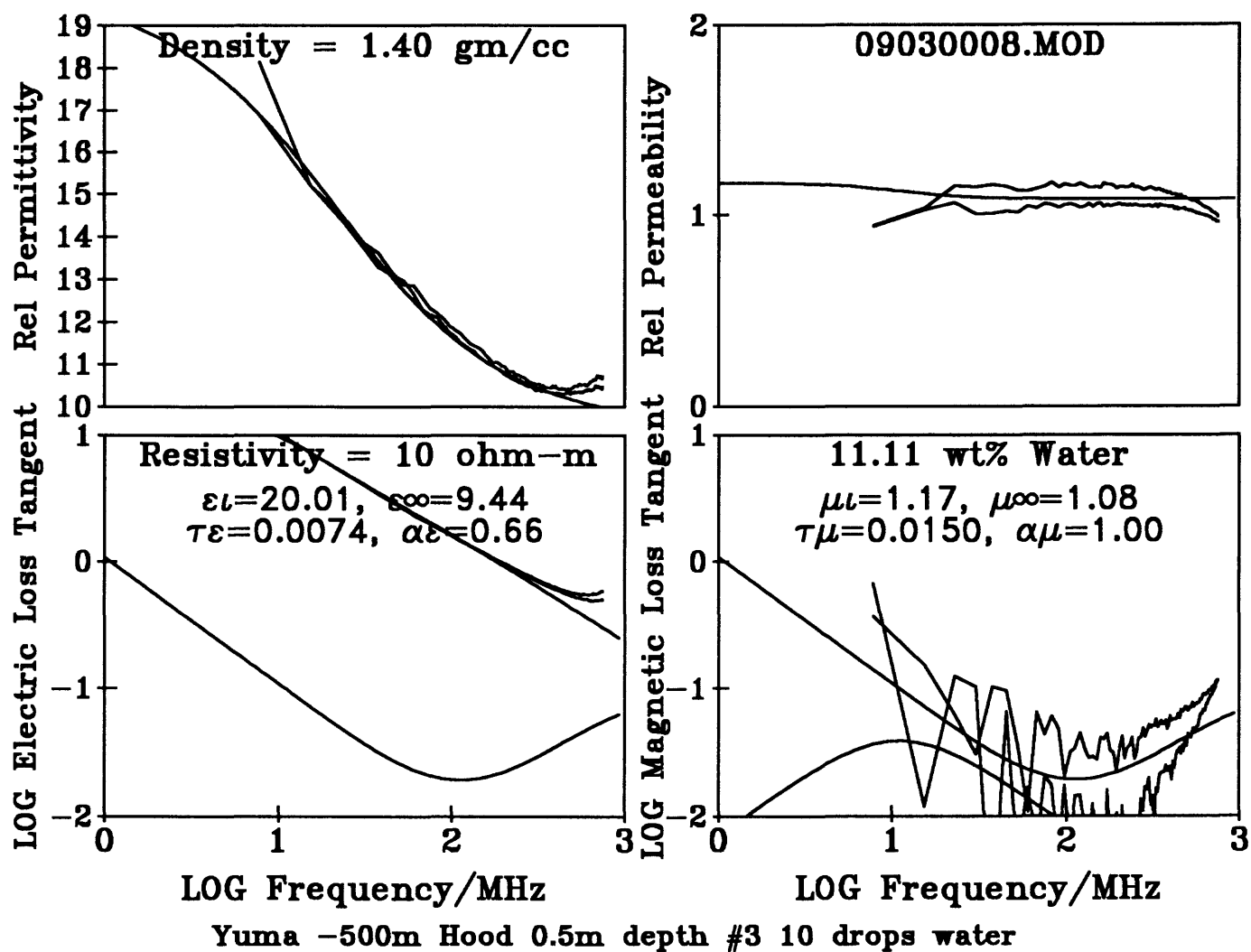


Figure 37 -

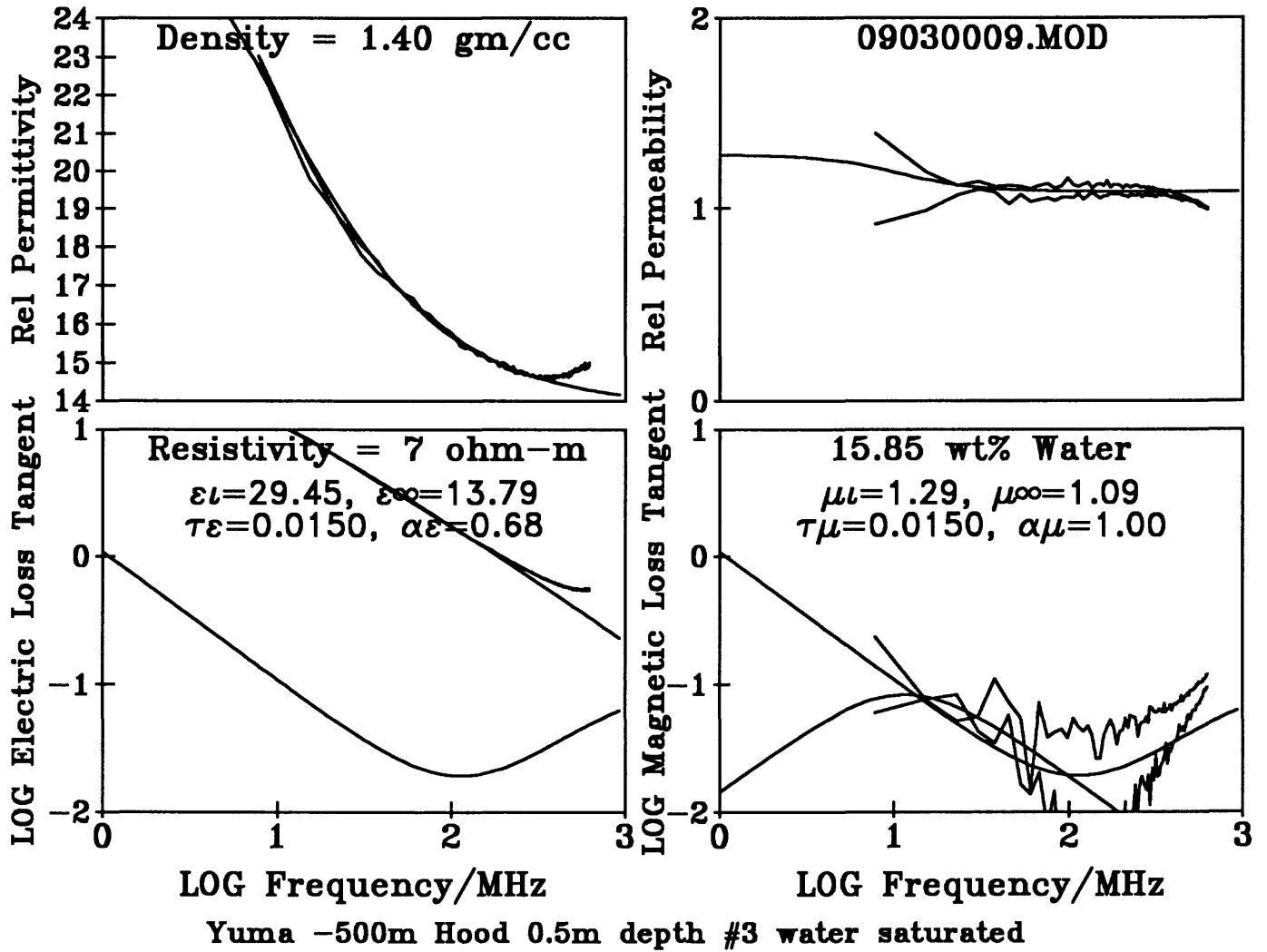


Figure 38 -

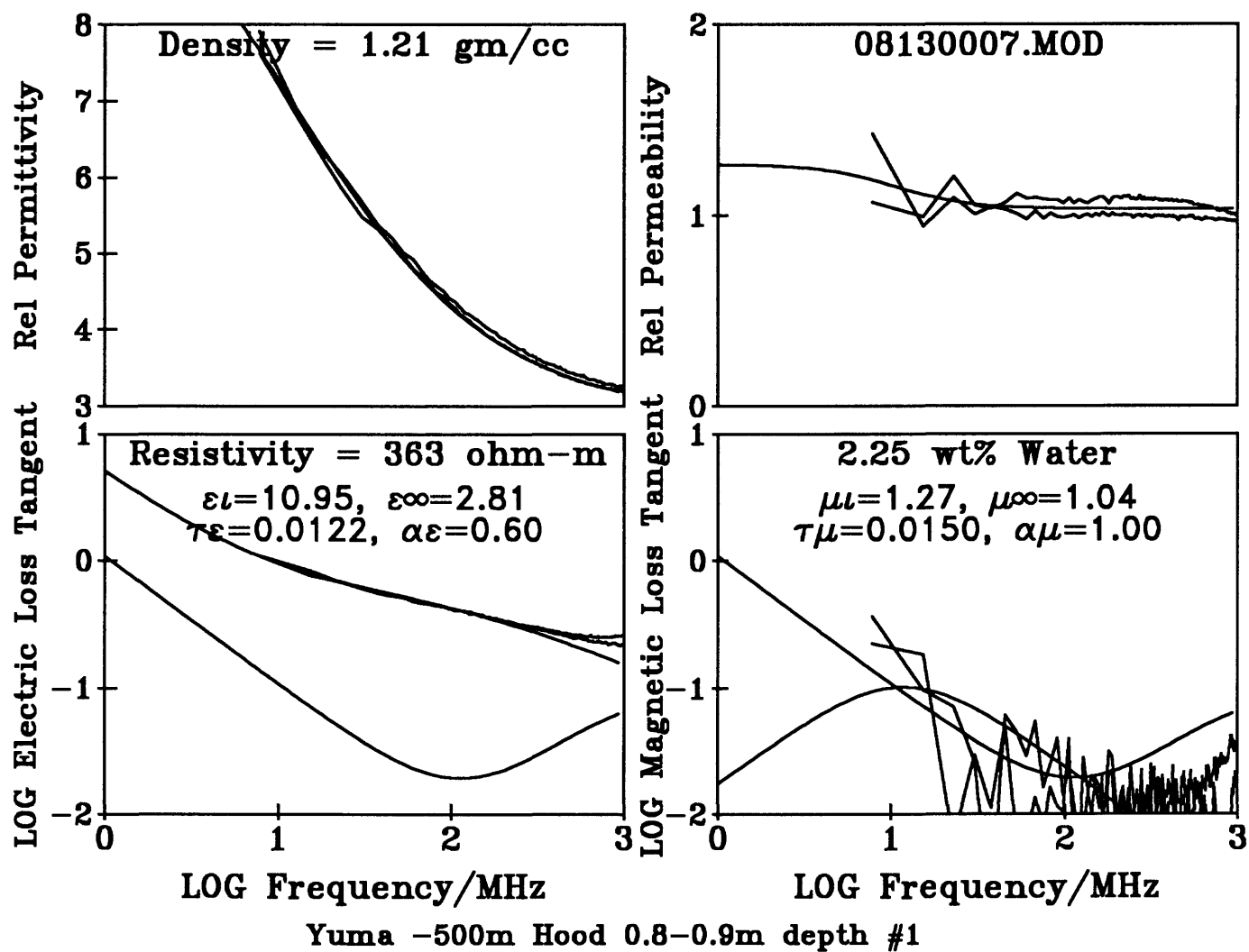


Figure 39 -
Natural state electromagnetic properties with water content preserved in sealed, taped, sample bottle.

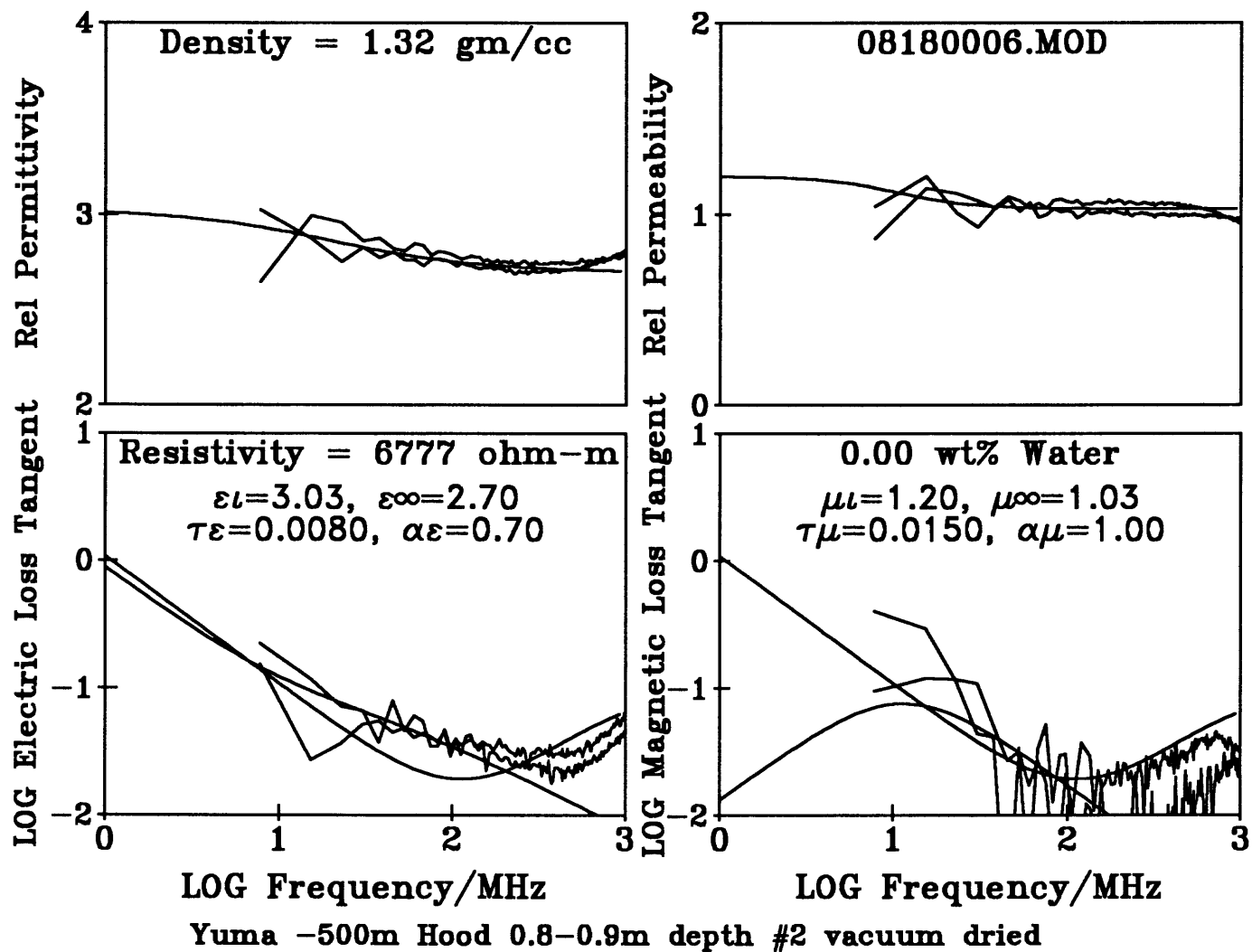


Figure 40 -

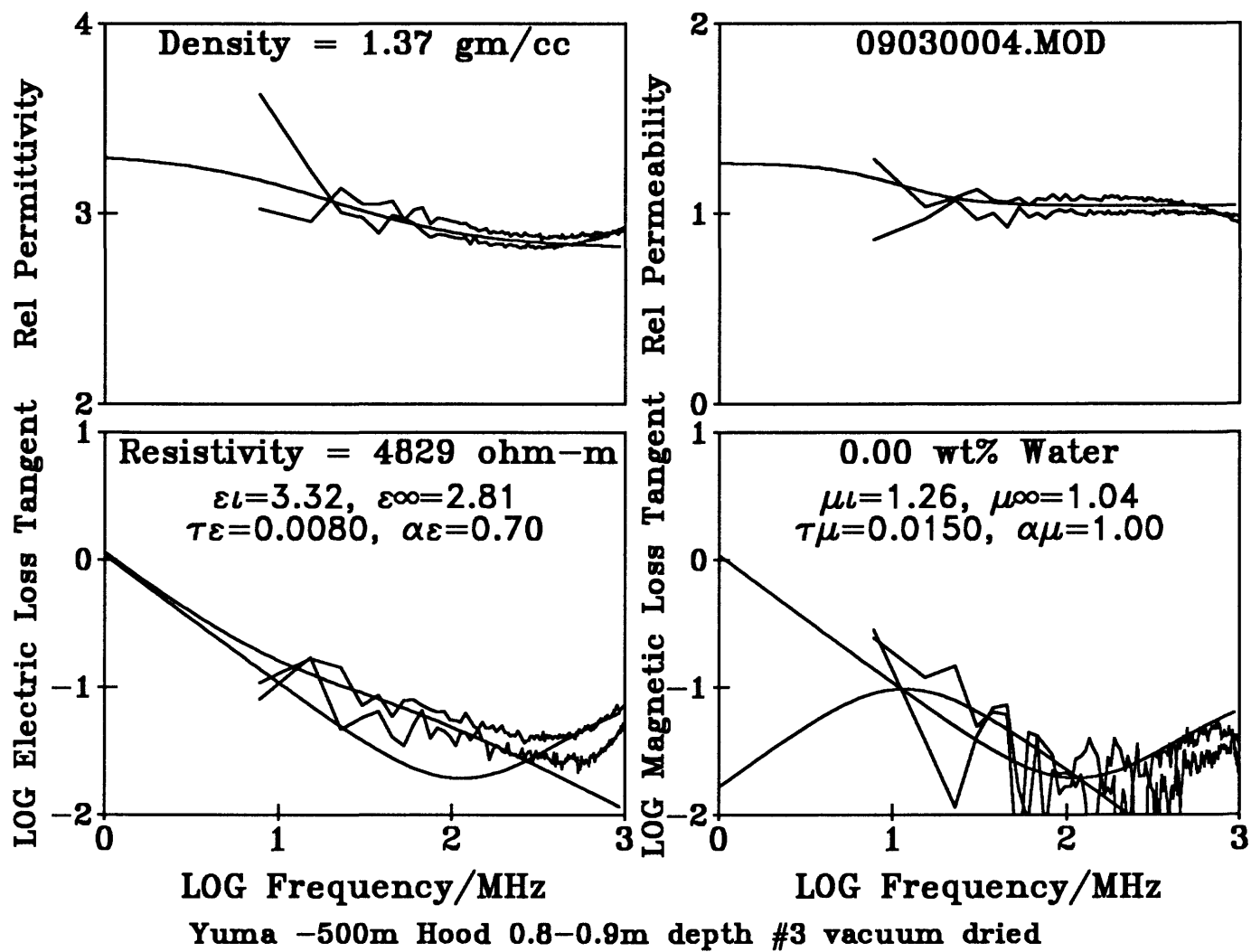


Figure 41 -

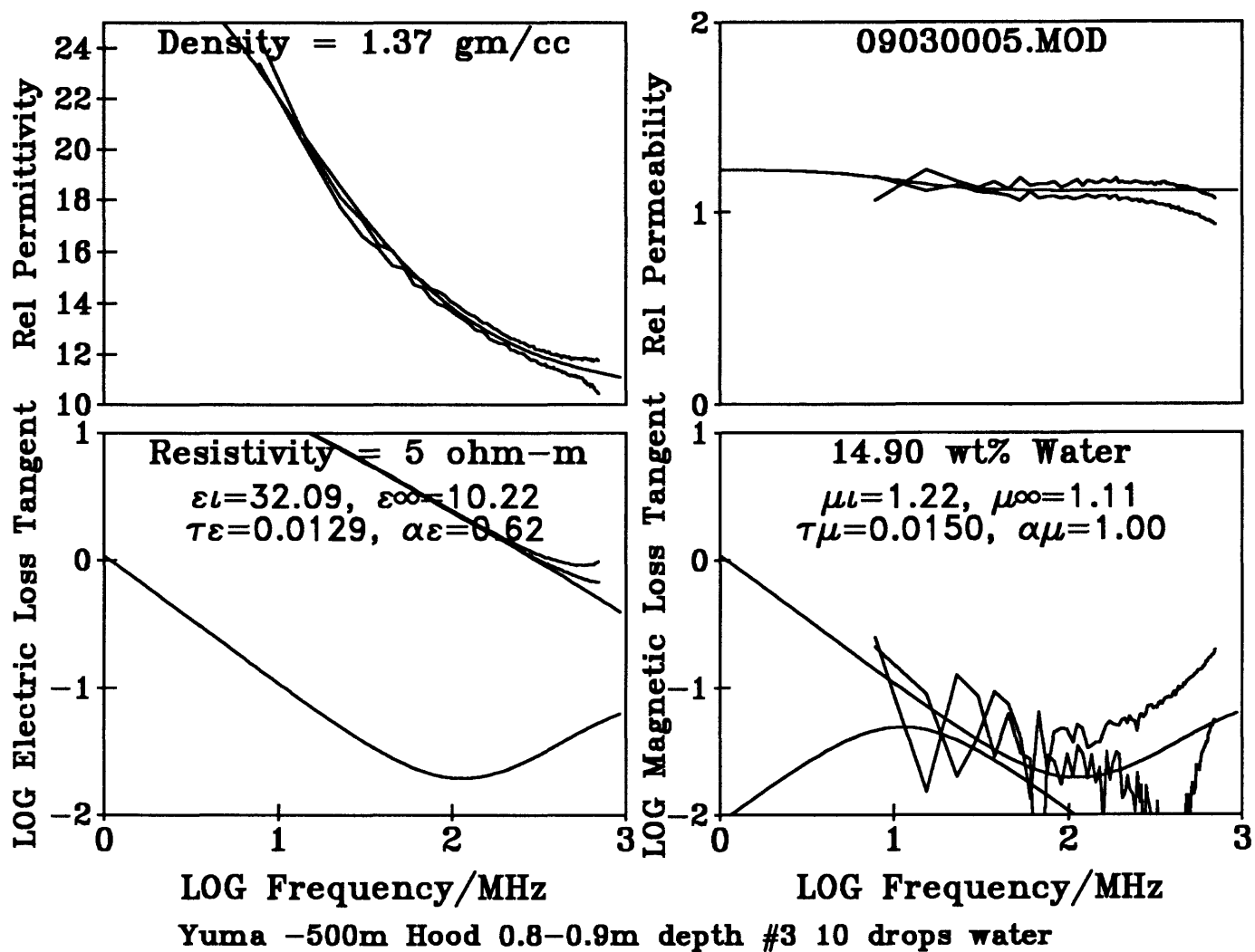


Figure 42 -

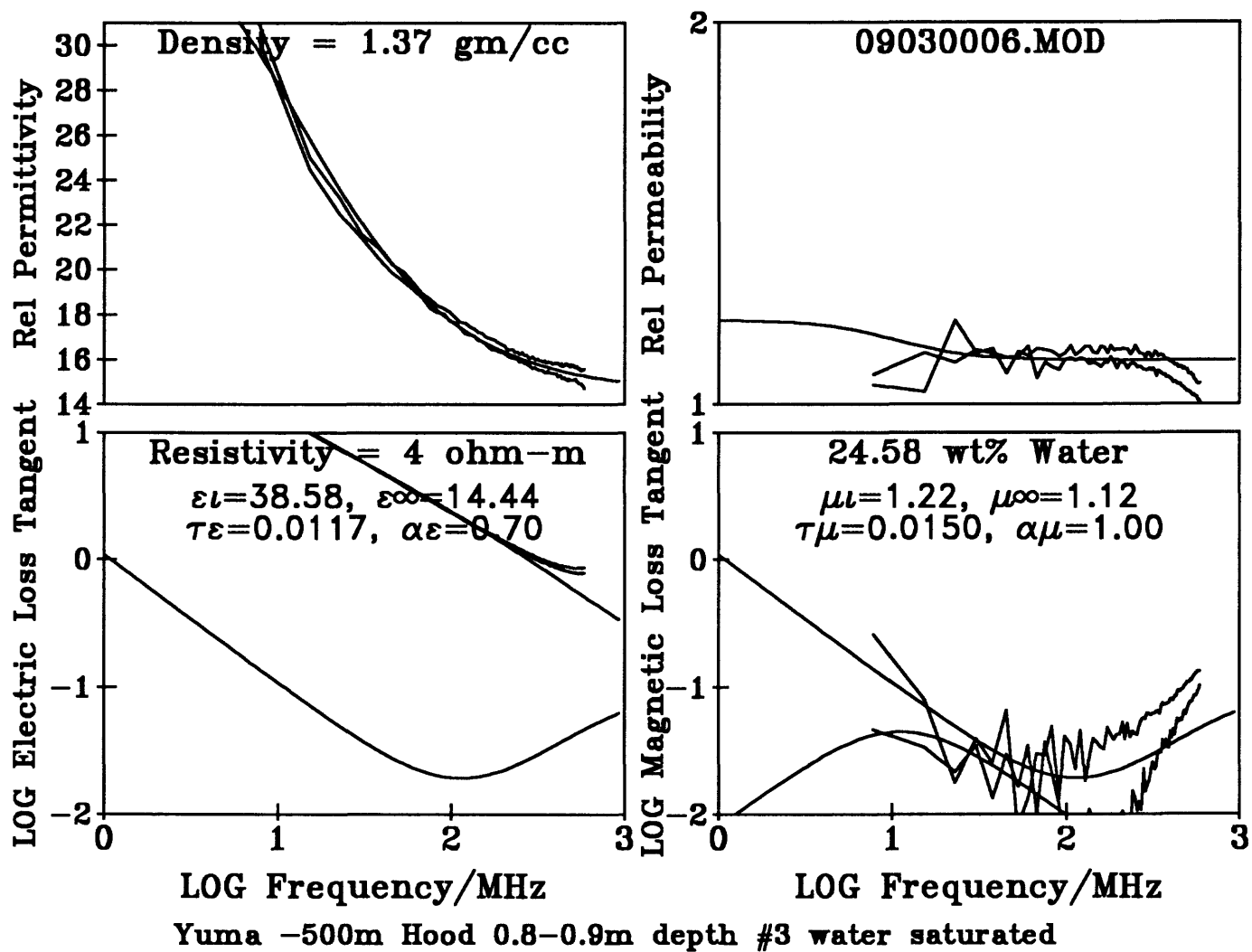


Figure 43 -

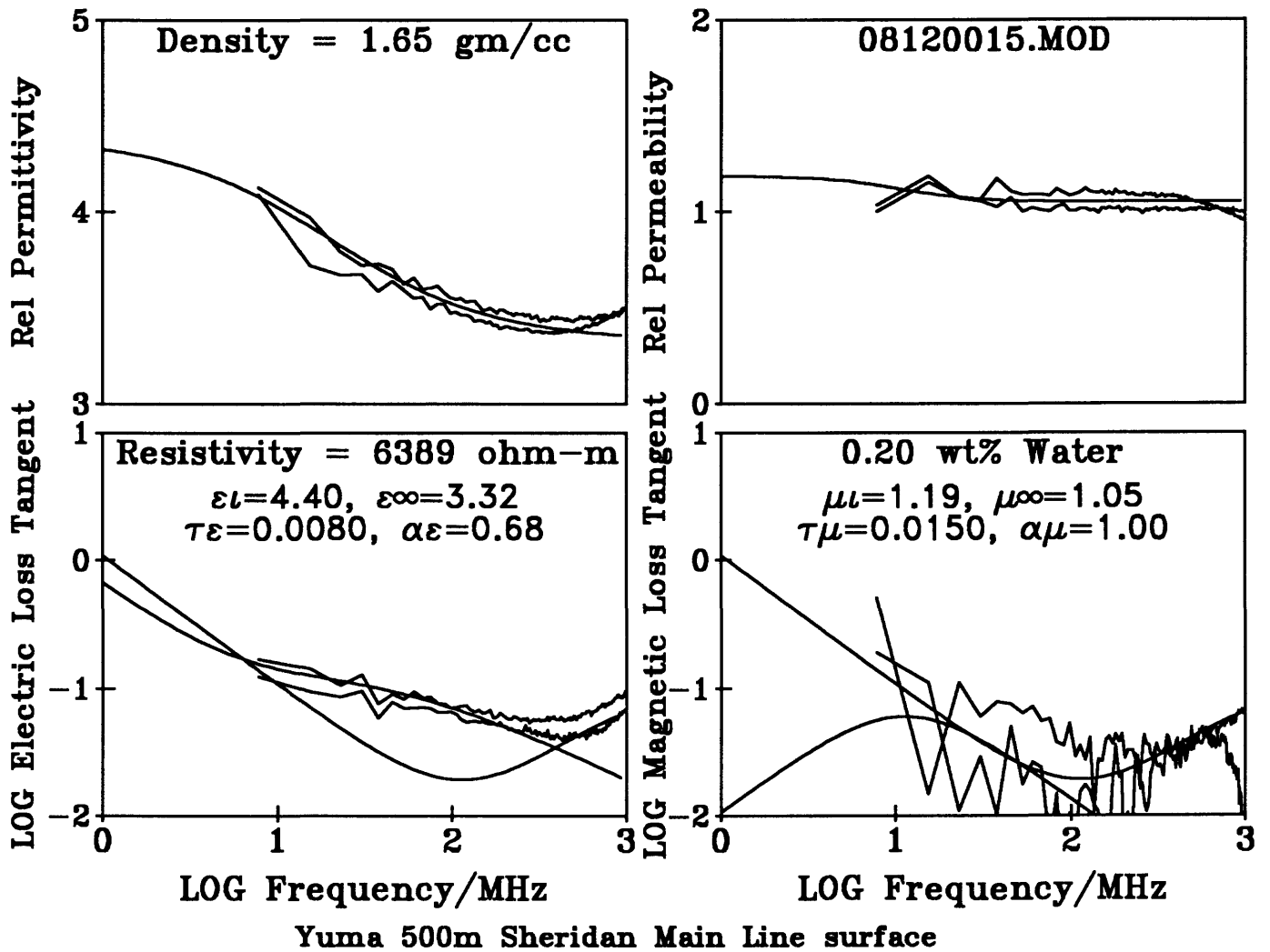


Figure 44 -
Natural state electromagnetic properties with water content preserved in sealed, taped,
sample bottle.

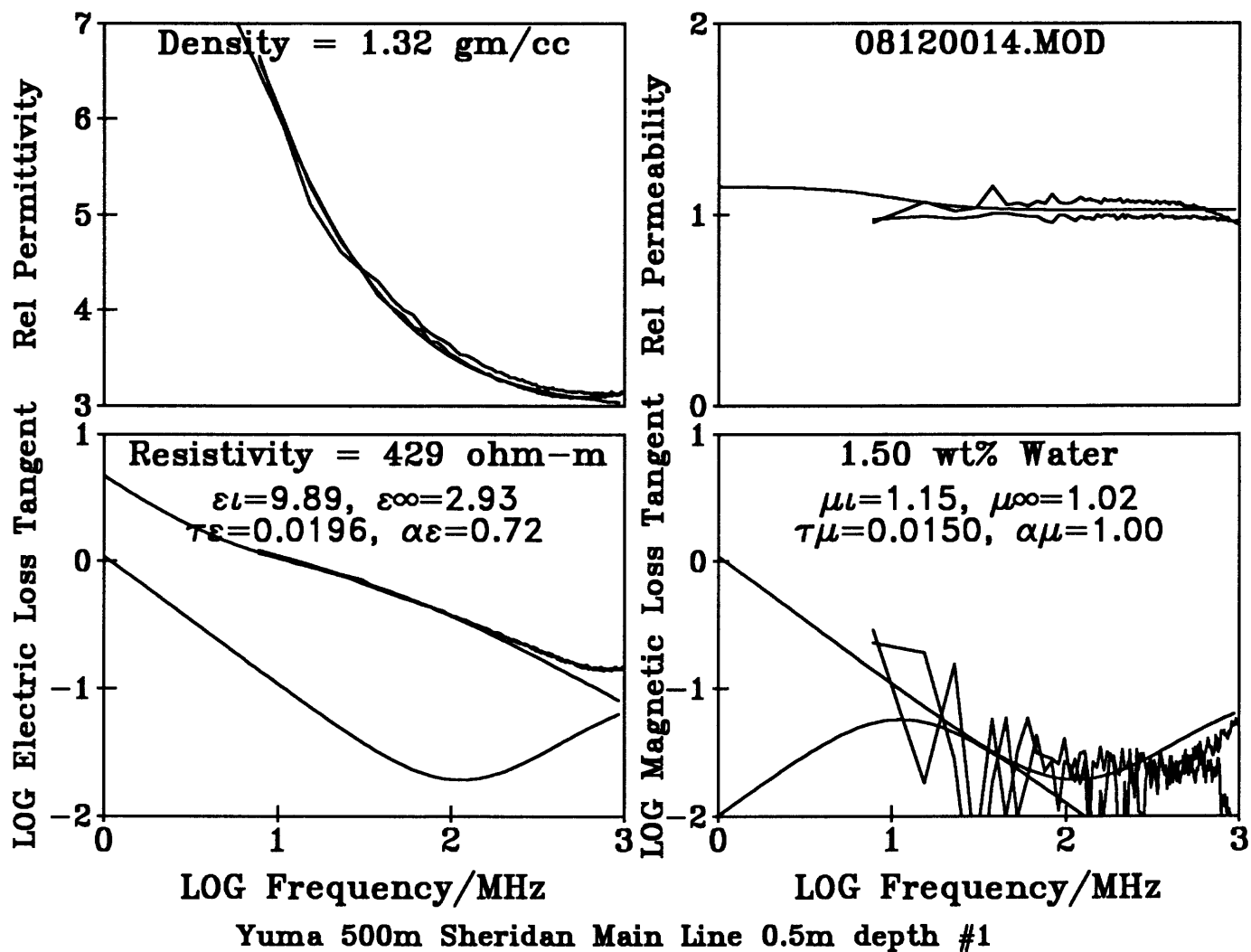


Figure 45 -
Natural state electromagnetic properties with water content preserved in sealed, taped,
sample bottle.

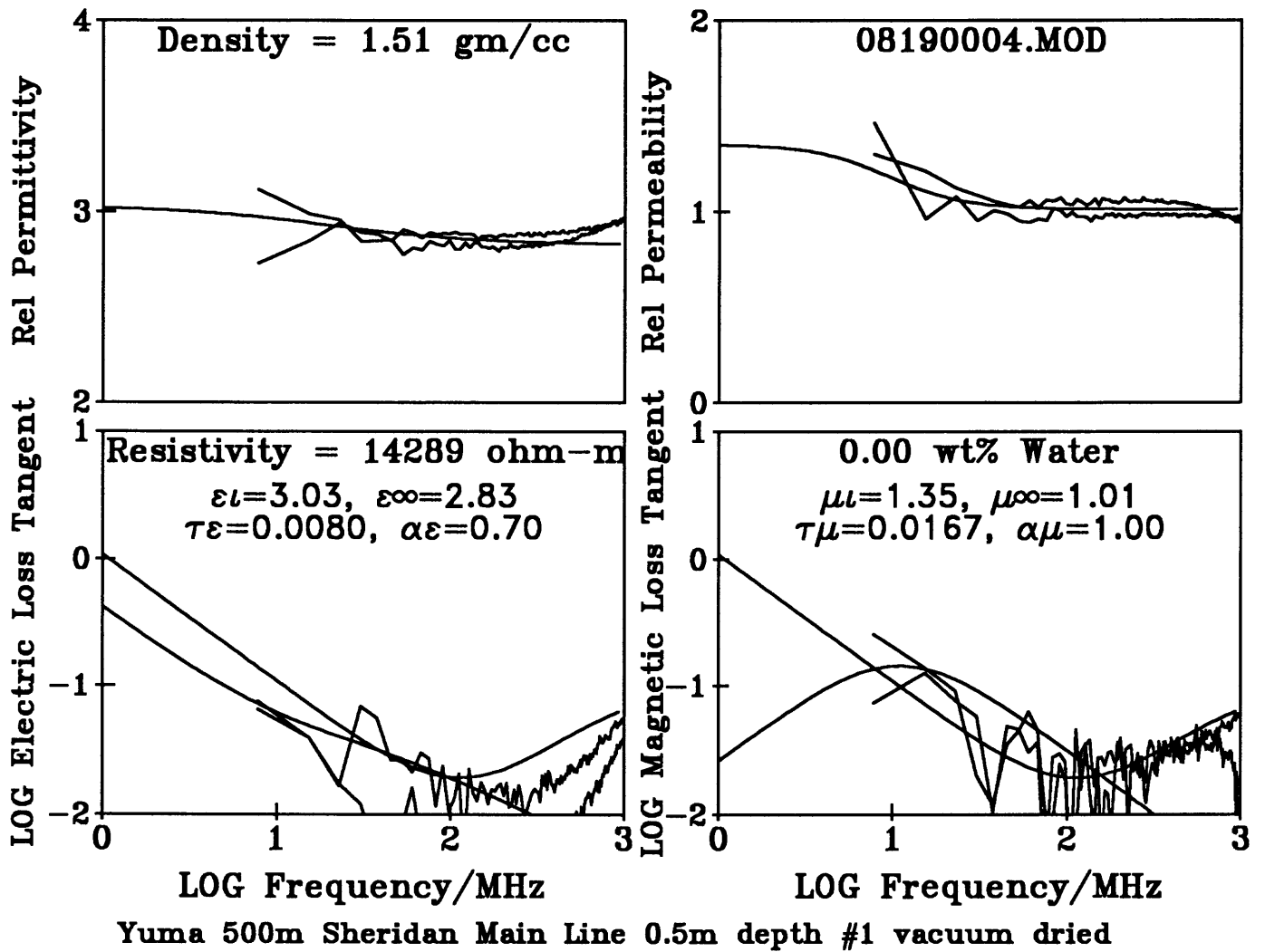


Figure 46 -

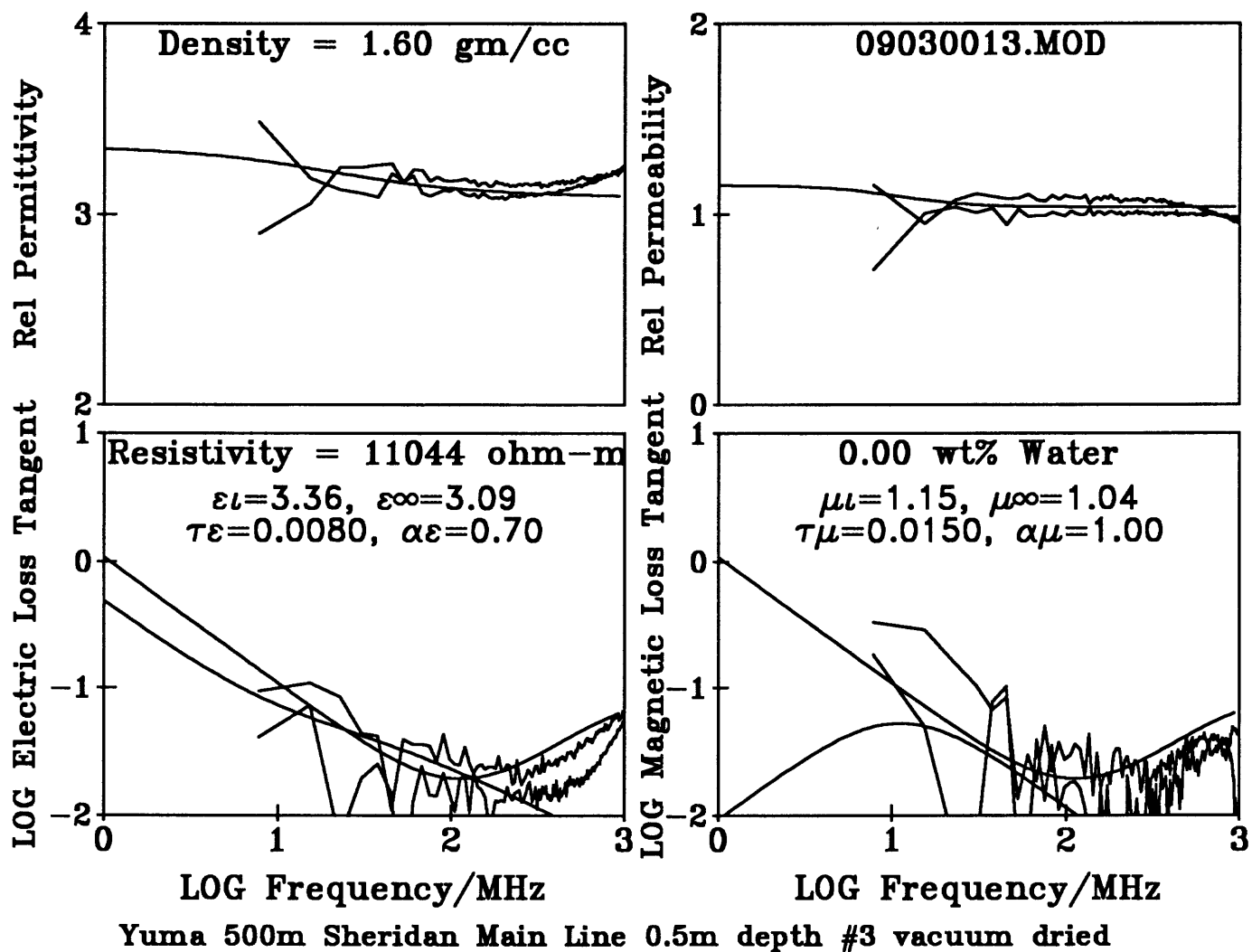


Figure 47 -

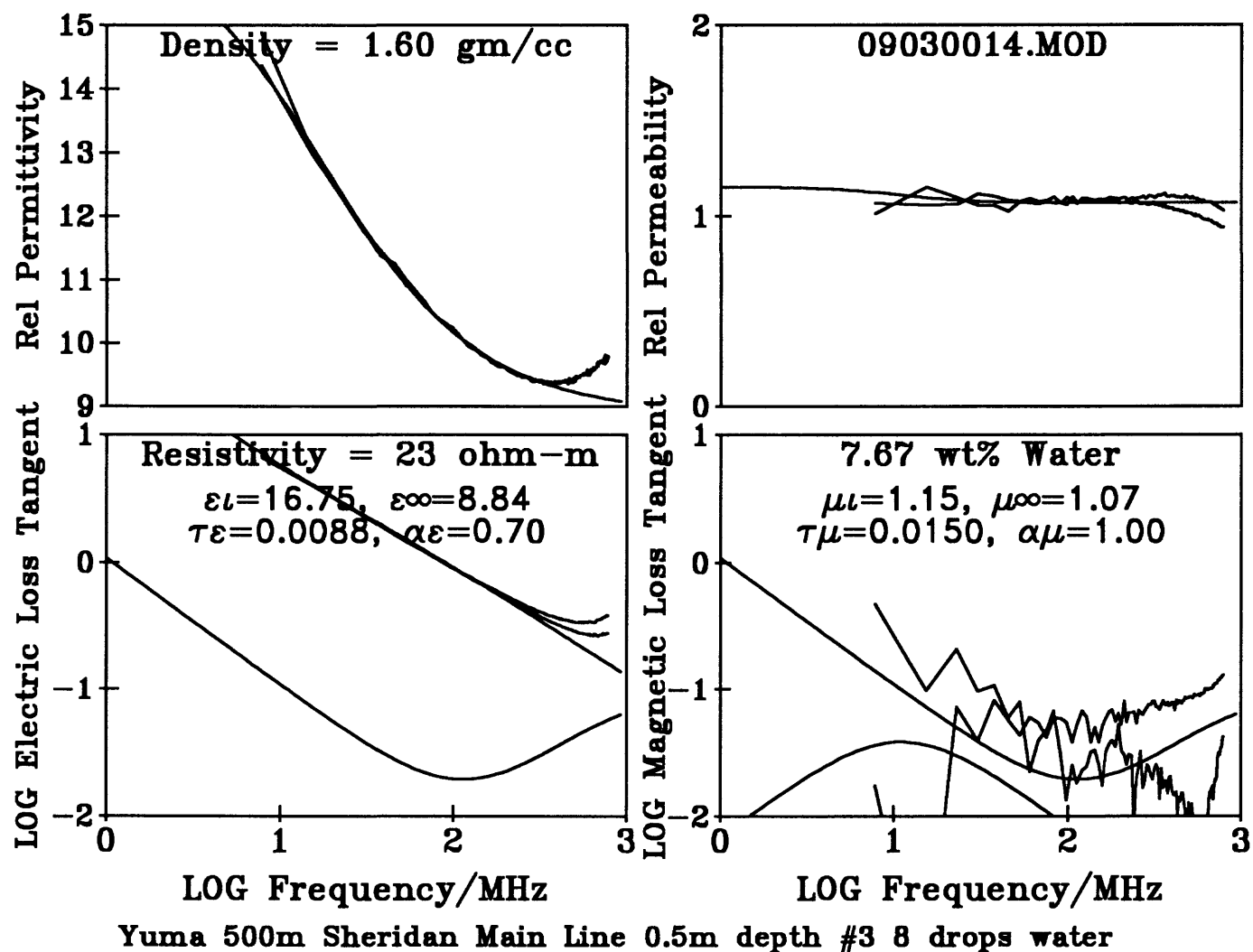
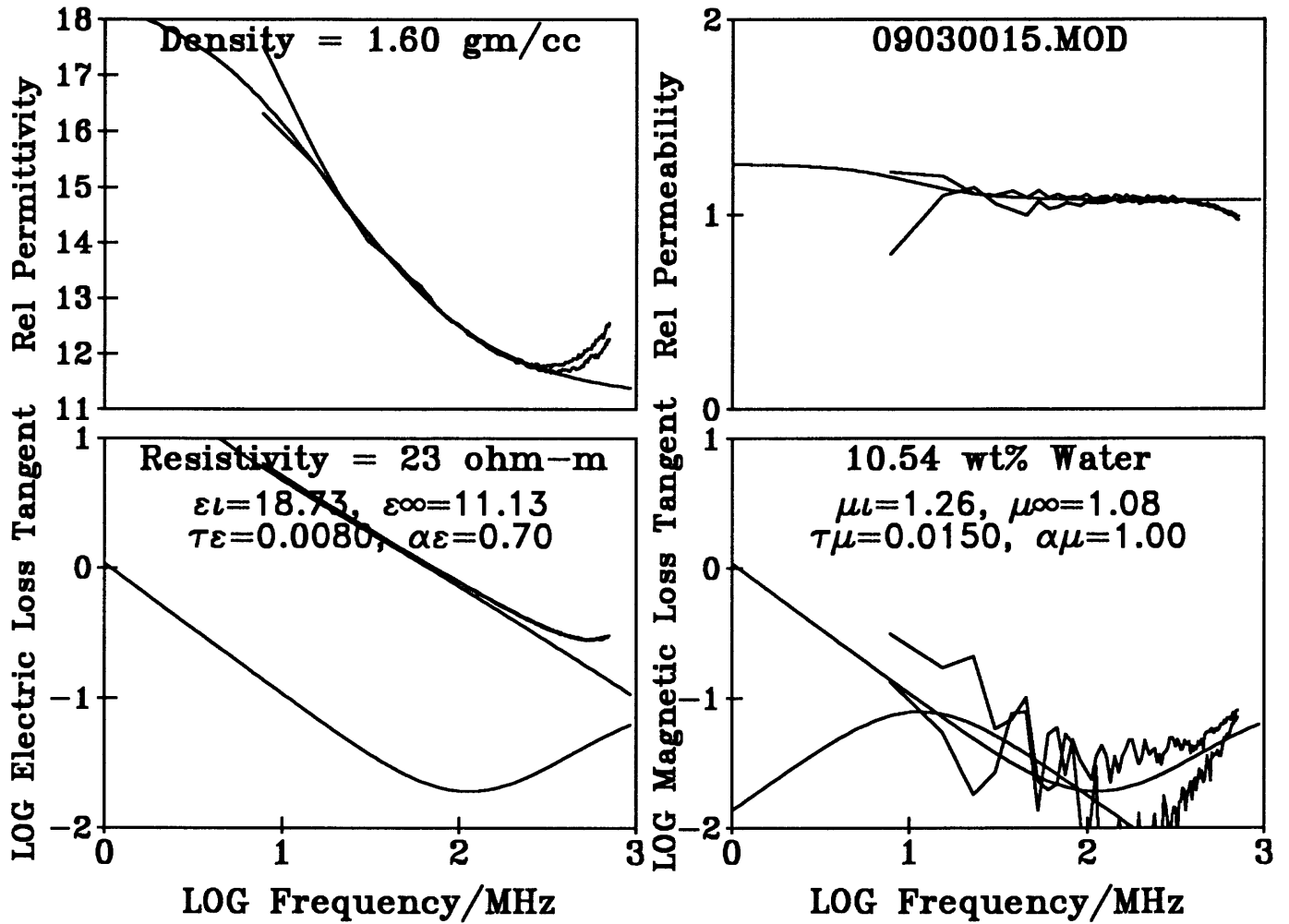


Figure 48 -



Yuma 500m Sheridan Main Line 0.5m depth #3 water saturated

Figure 49 -

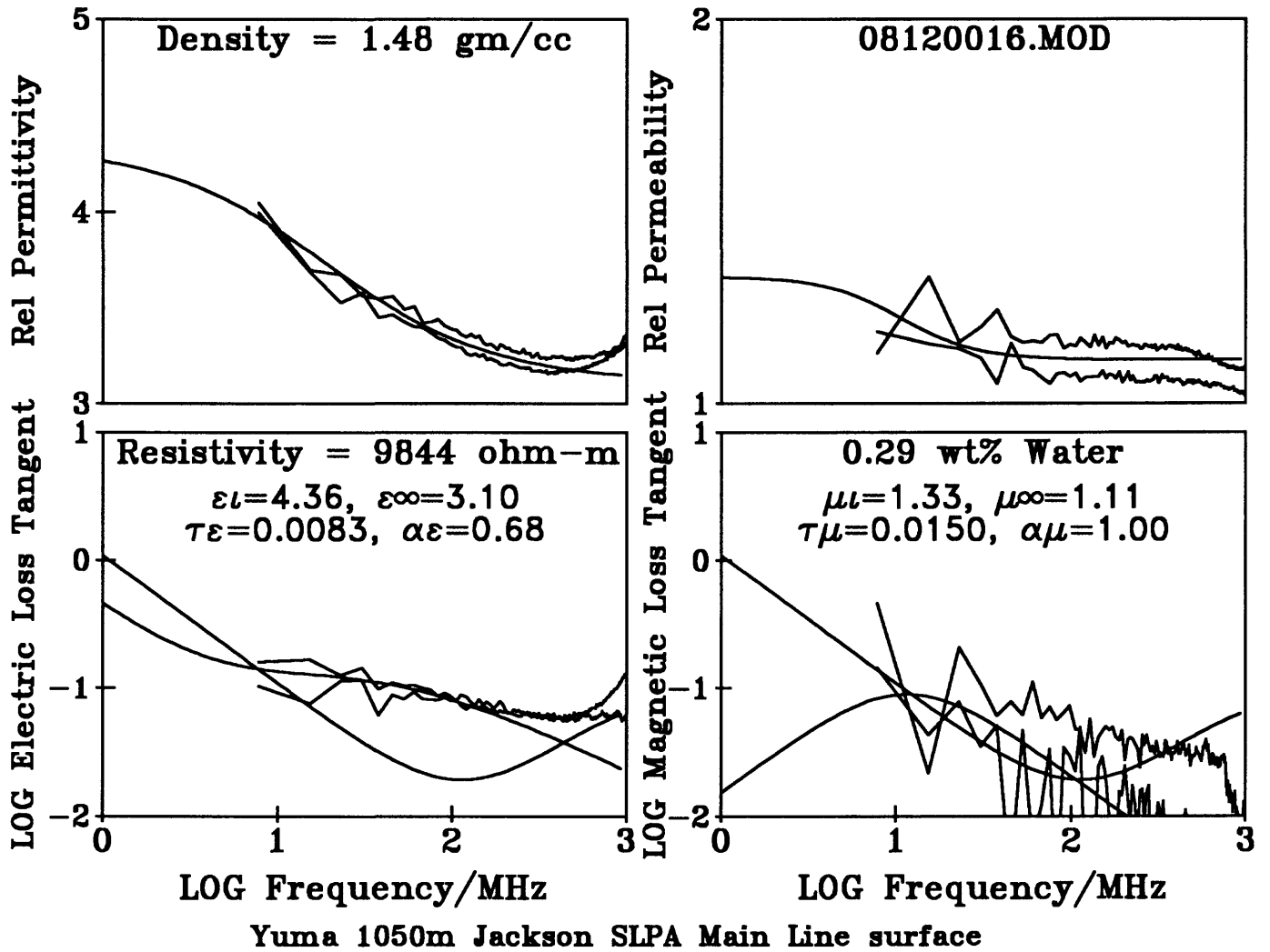


Figure 50 -
 Natural state electromagnetic properties with water content preserved in sealed, taped,
 sample bottle.

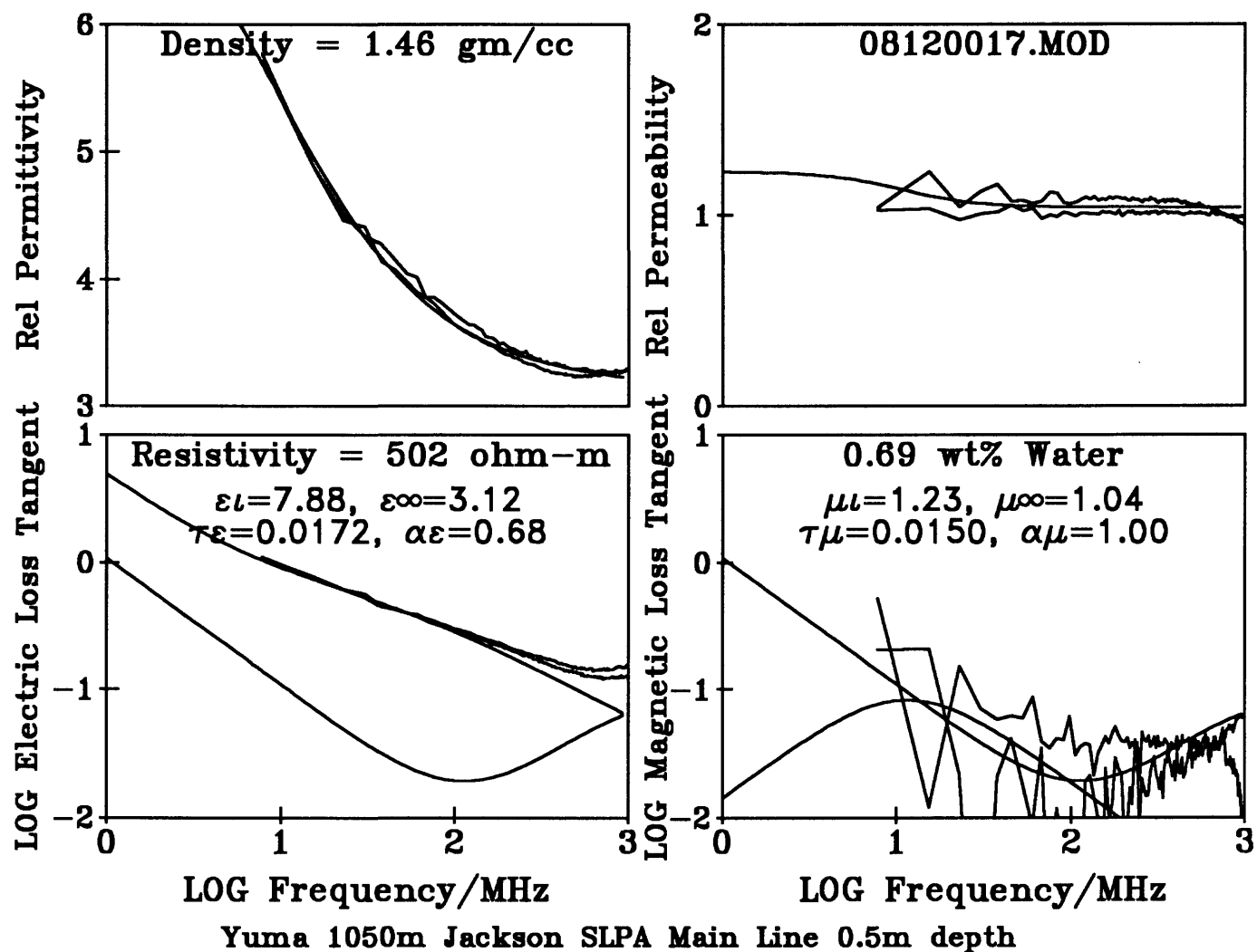


Figure 51 -
 Natural state electromagnetic properties with water content preserved in sealed, taped,
 sample bottle.

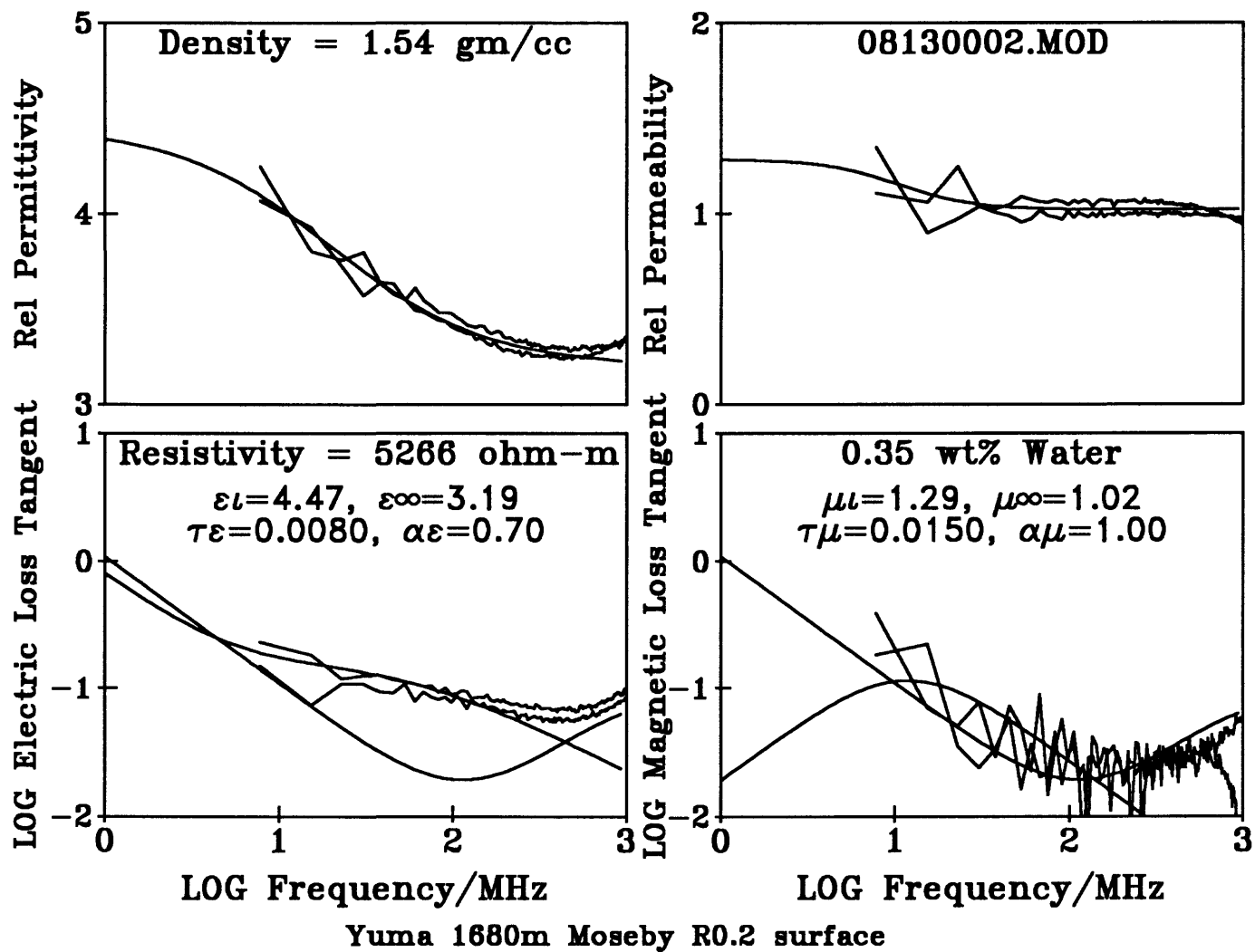


Figure 52 -
Natural state electromagnetic properties with water content preserved in sealed, taped,
sample bottle.

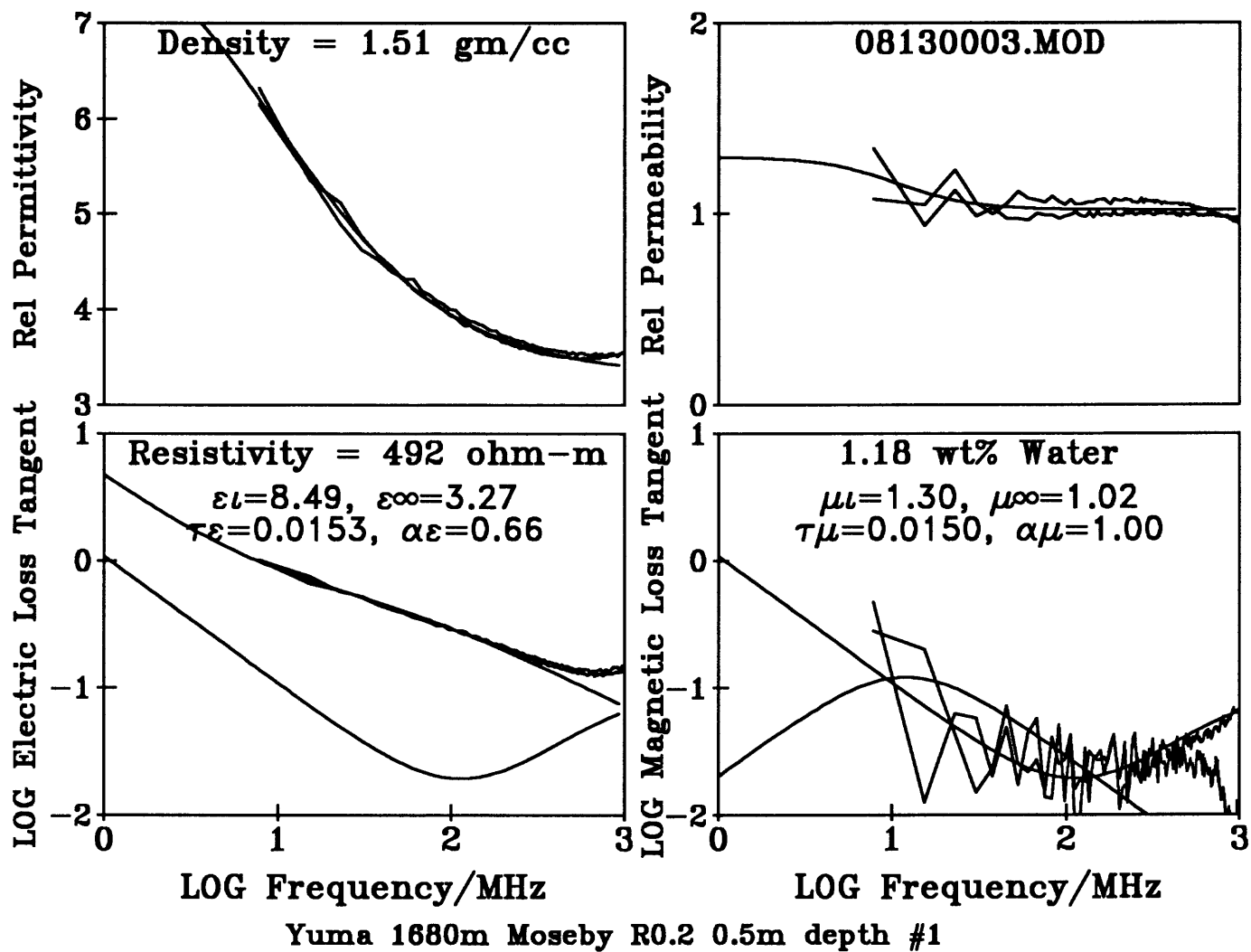


Figure 53 -
Natural state electromagnetic properties with water content preserved in sealed, taped,
sample bottle.

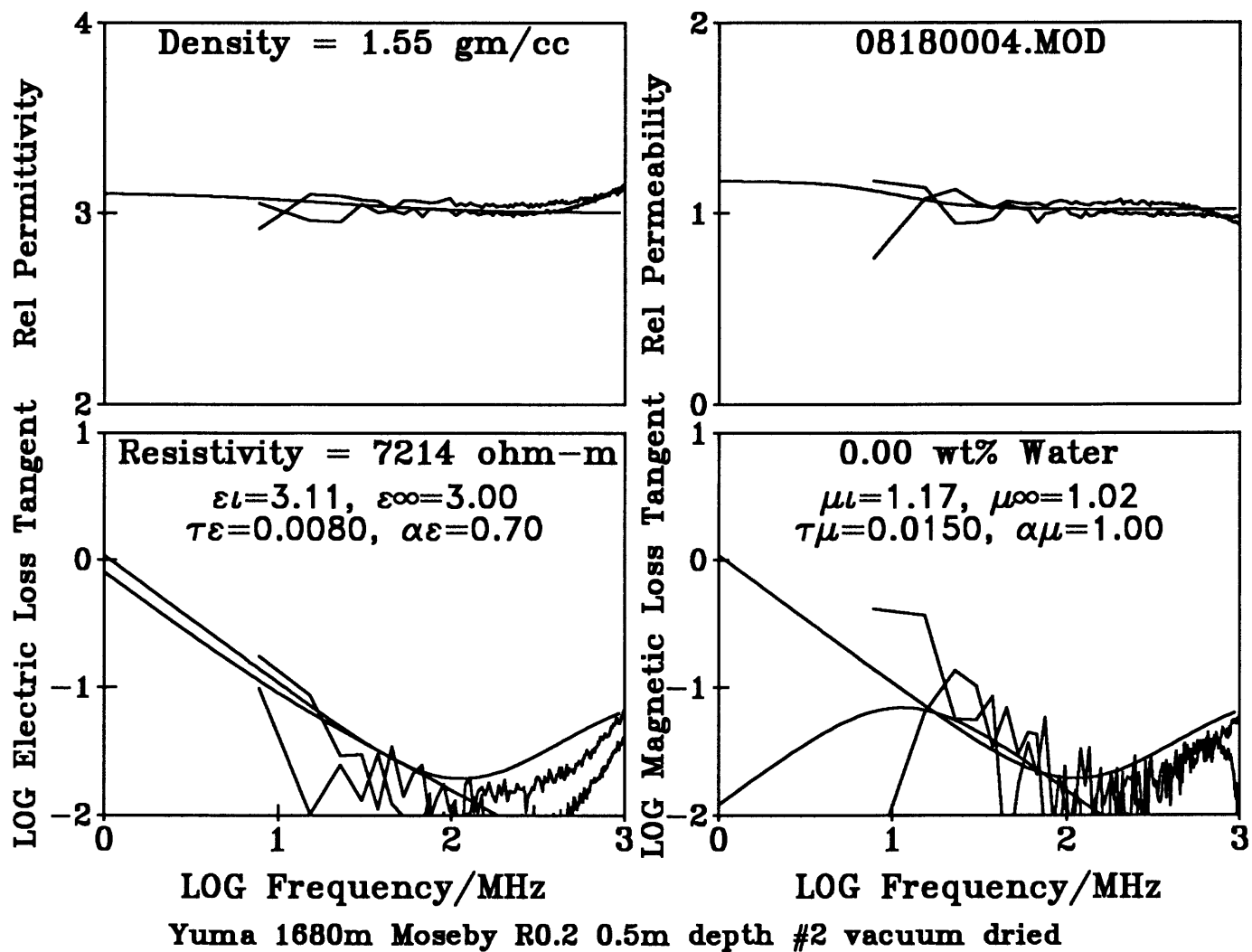


Figure 54 -

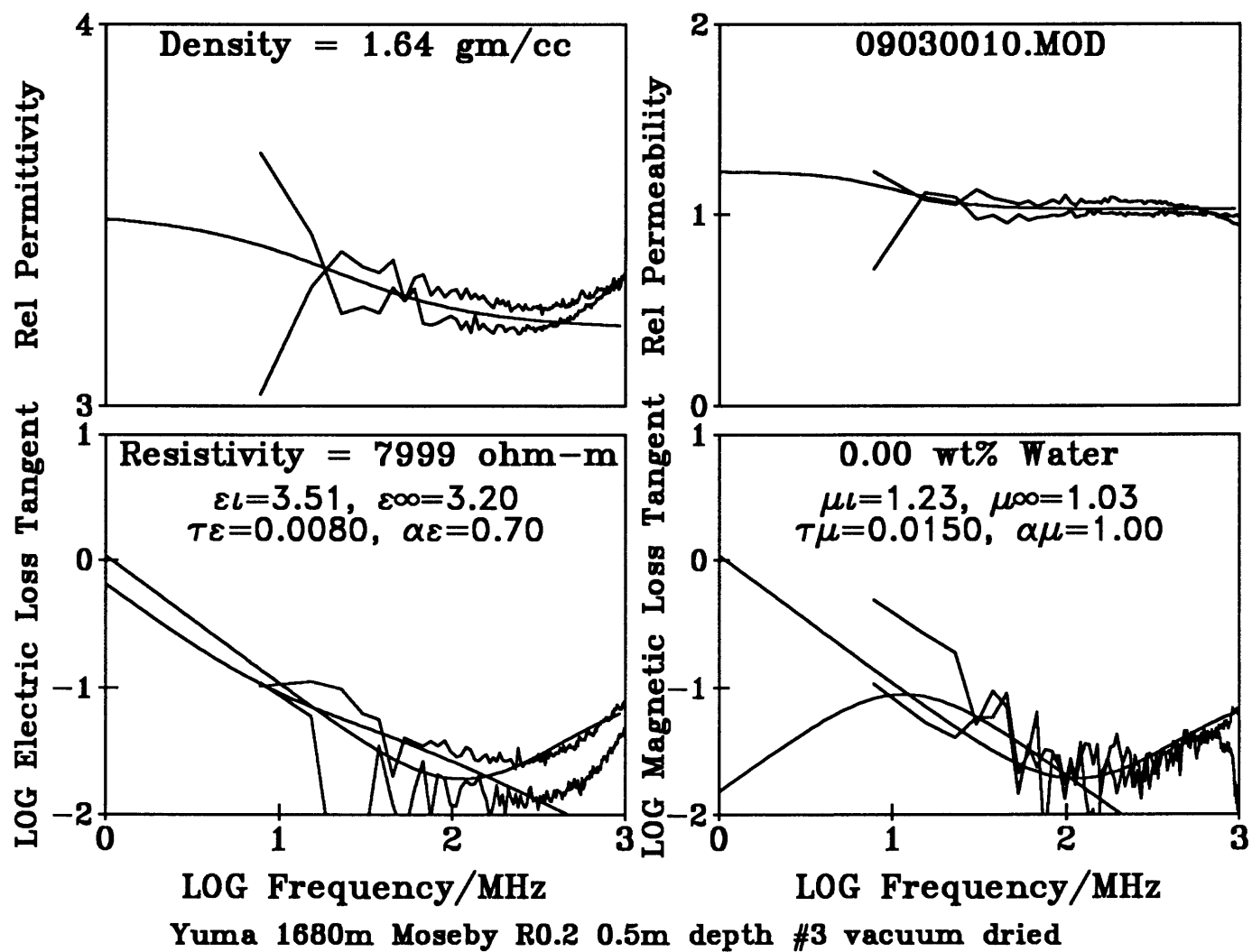


Figure 55 -

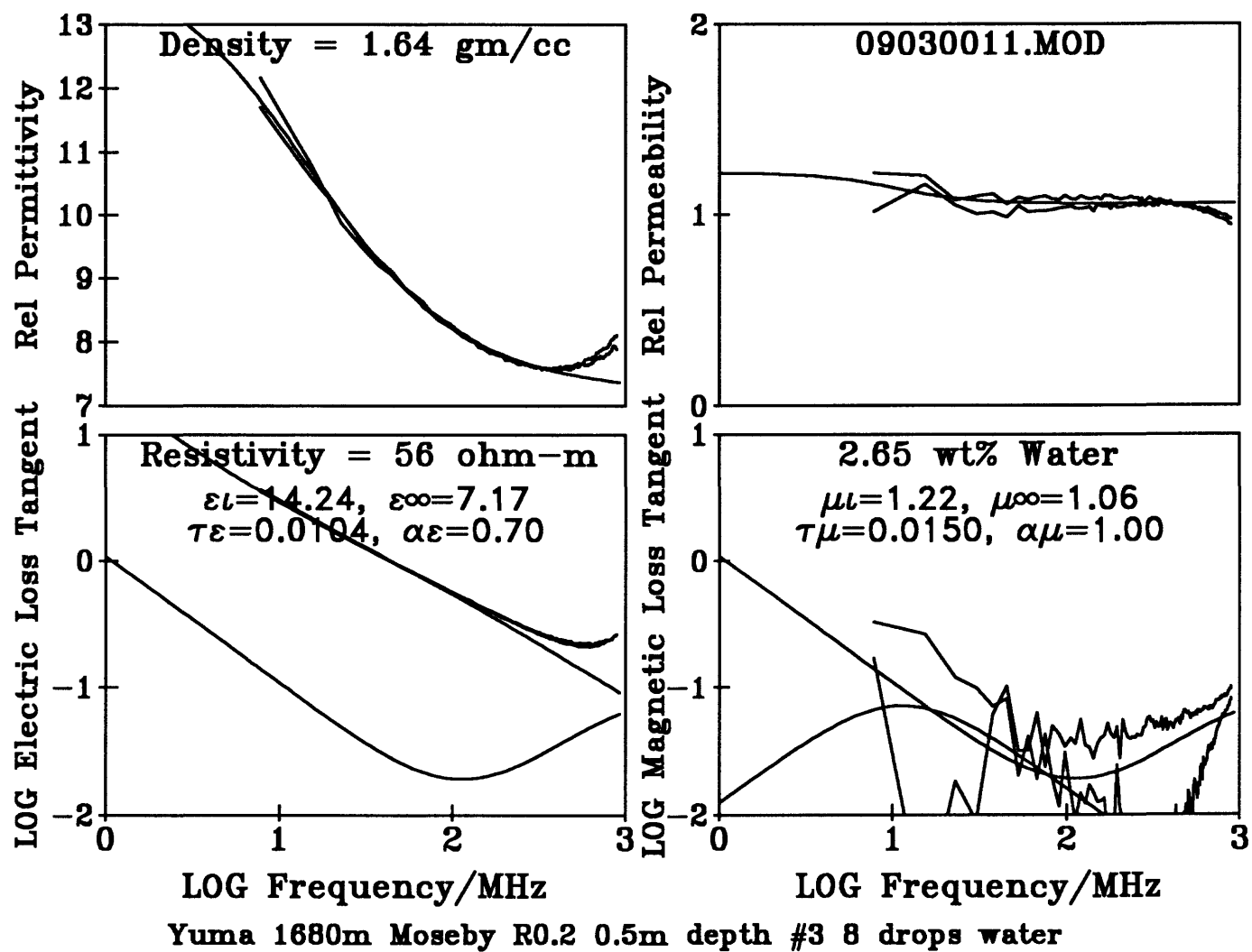


Figure 56 -

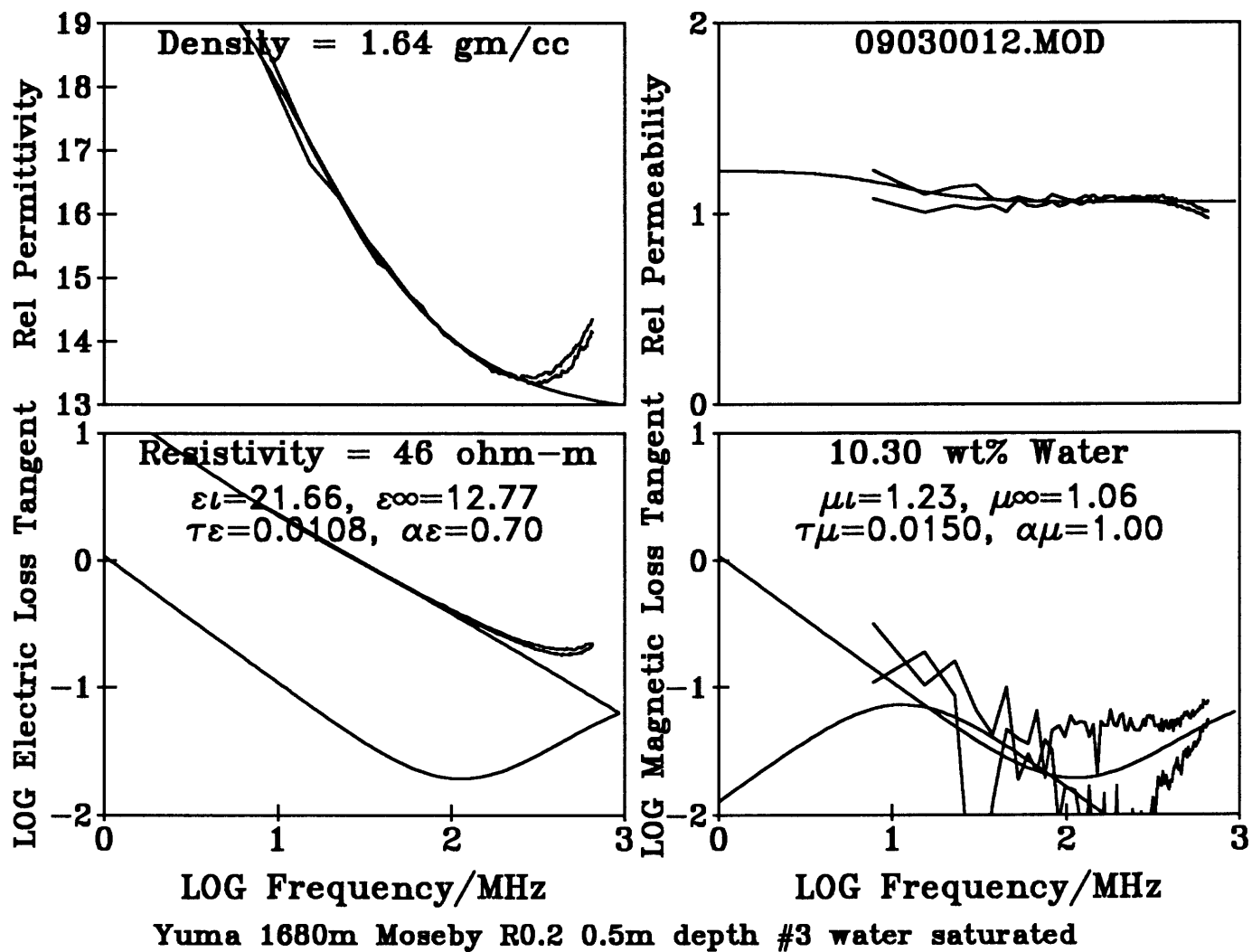


Figure 57 -

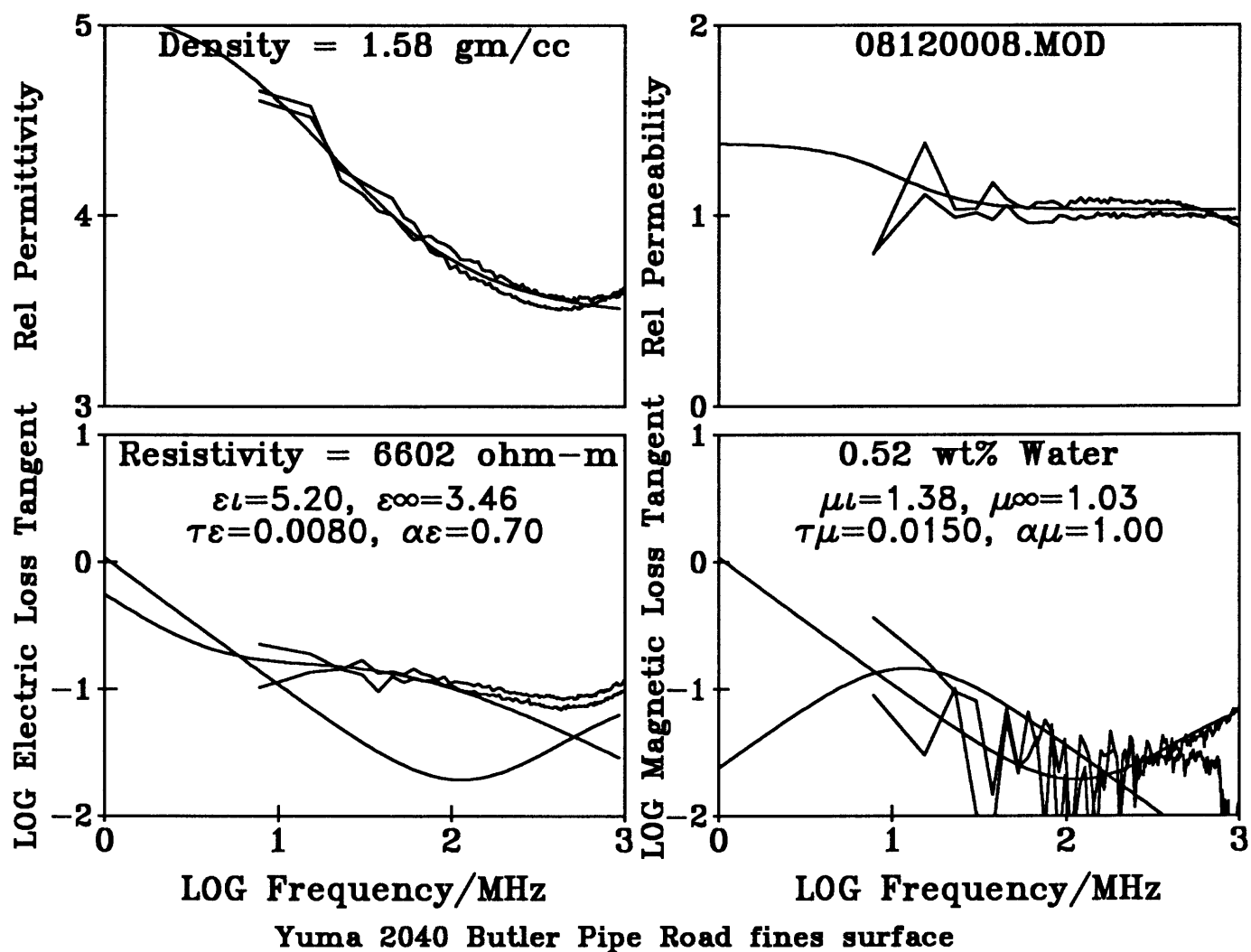


Figure 58 -
Natural state electromagnetic properties with water content preserved in sealed, taped,
sample bottle.

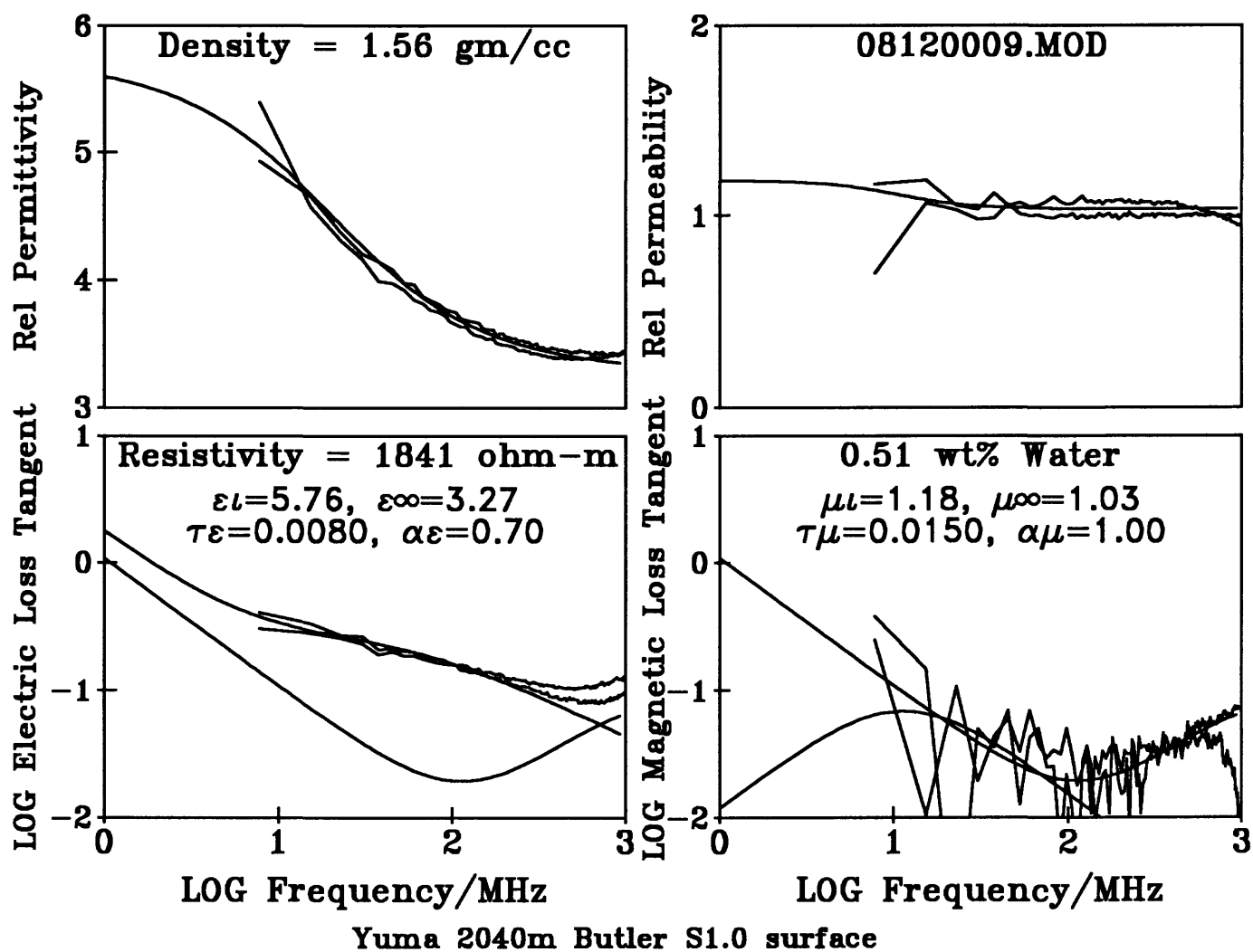


Figure 59 -
 Natural state electromagnetic properties with water content preserved in sealed, taped,
 sample bottle.

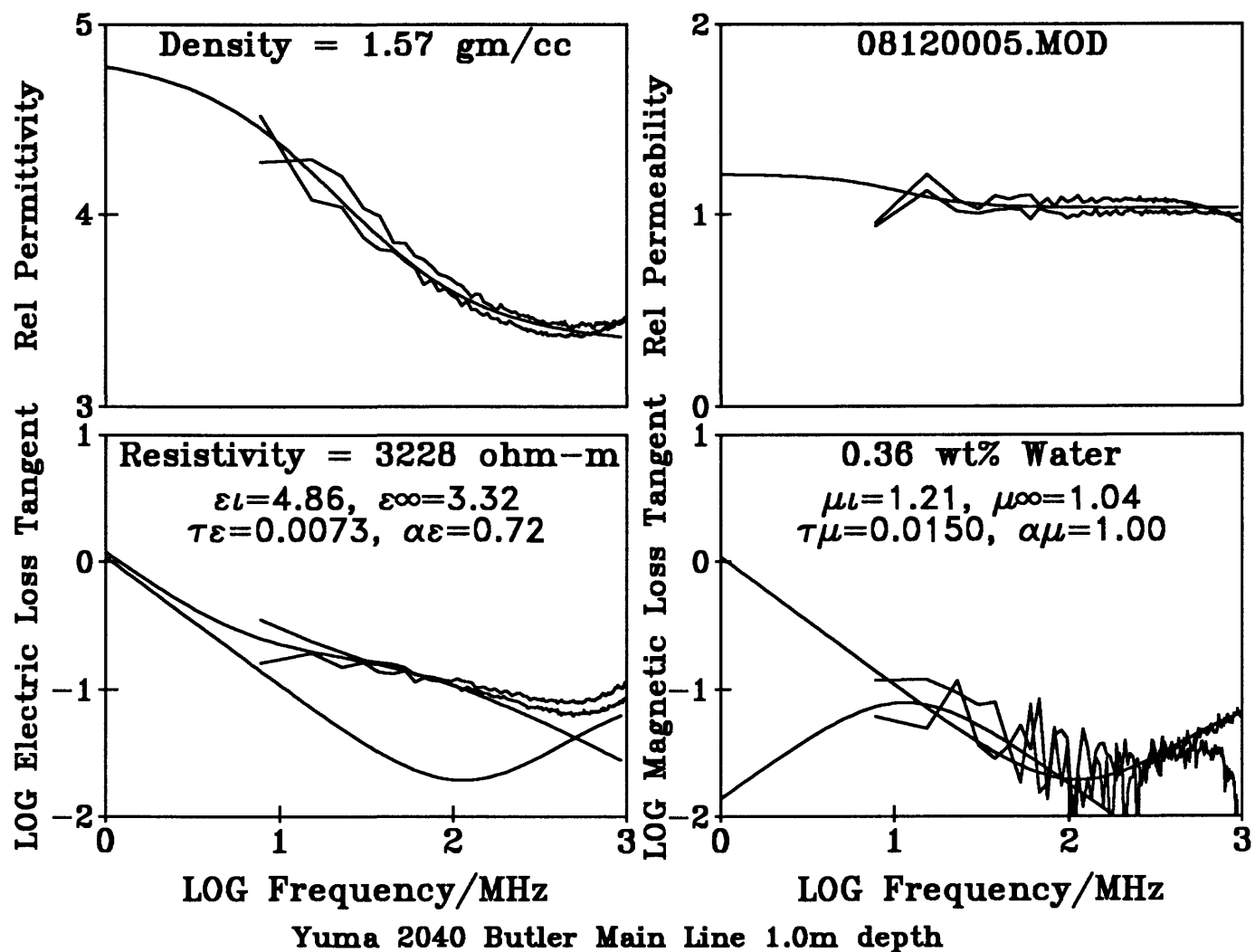


Figure 60 -
 Natural state electromagnetic properties with water content preserved in sealed, taped,
 sample bottle.

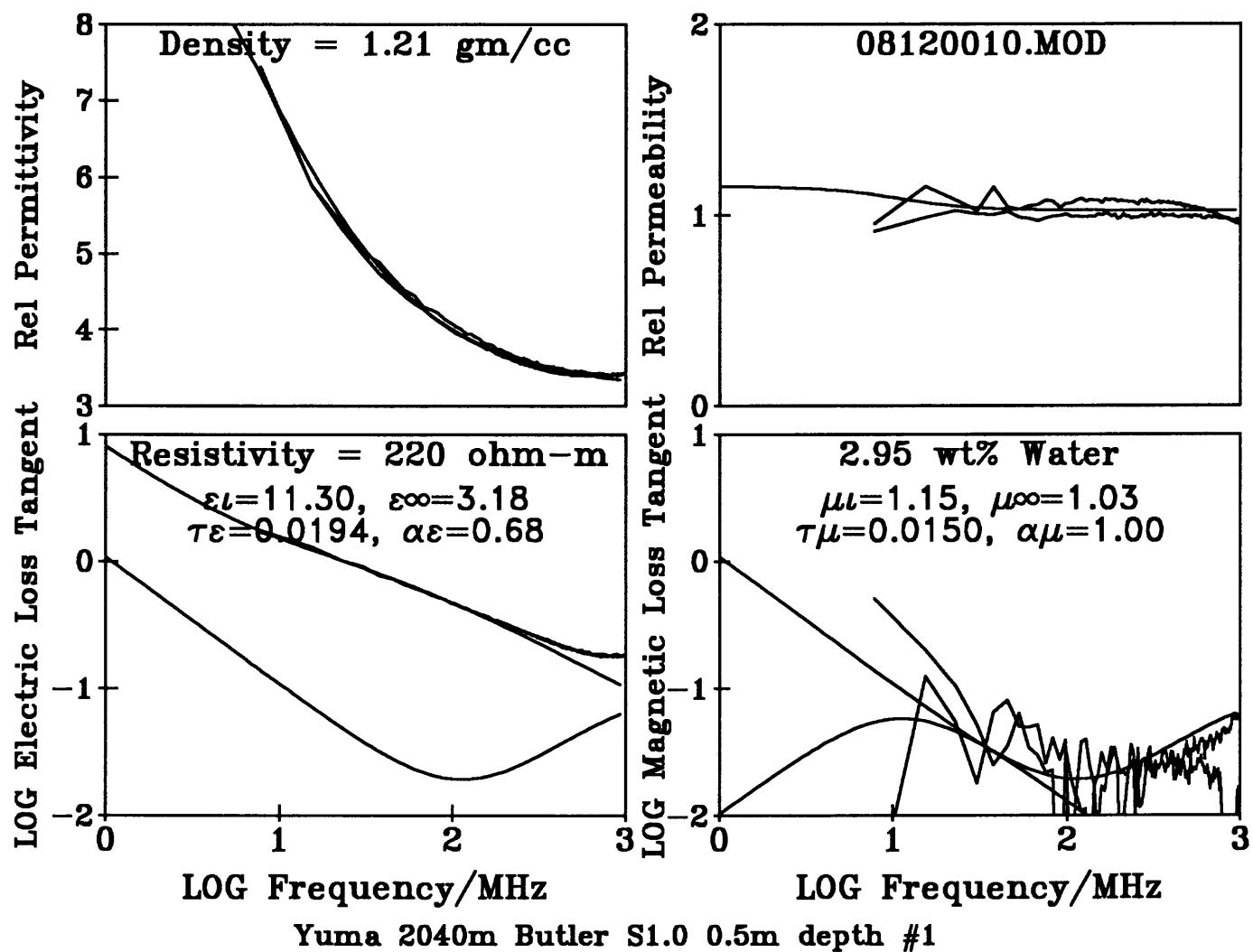


Figure 61 -
Natural state electromagnetic properties with water content preserved in sealed, taped,
sample bottle.

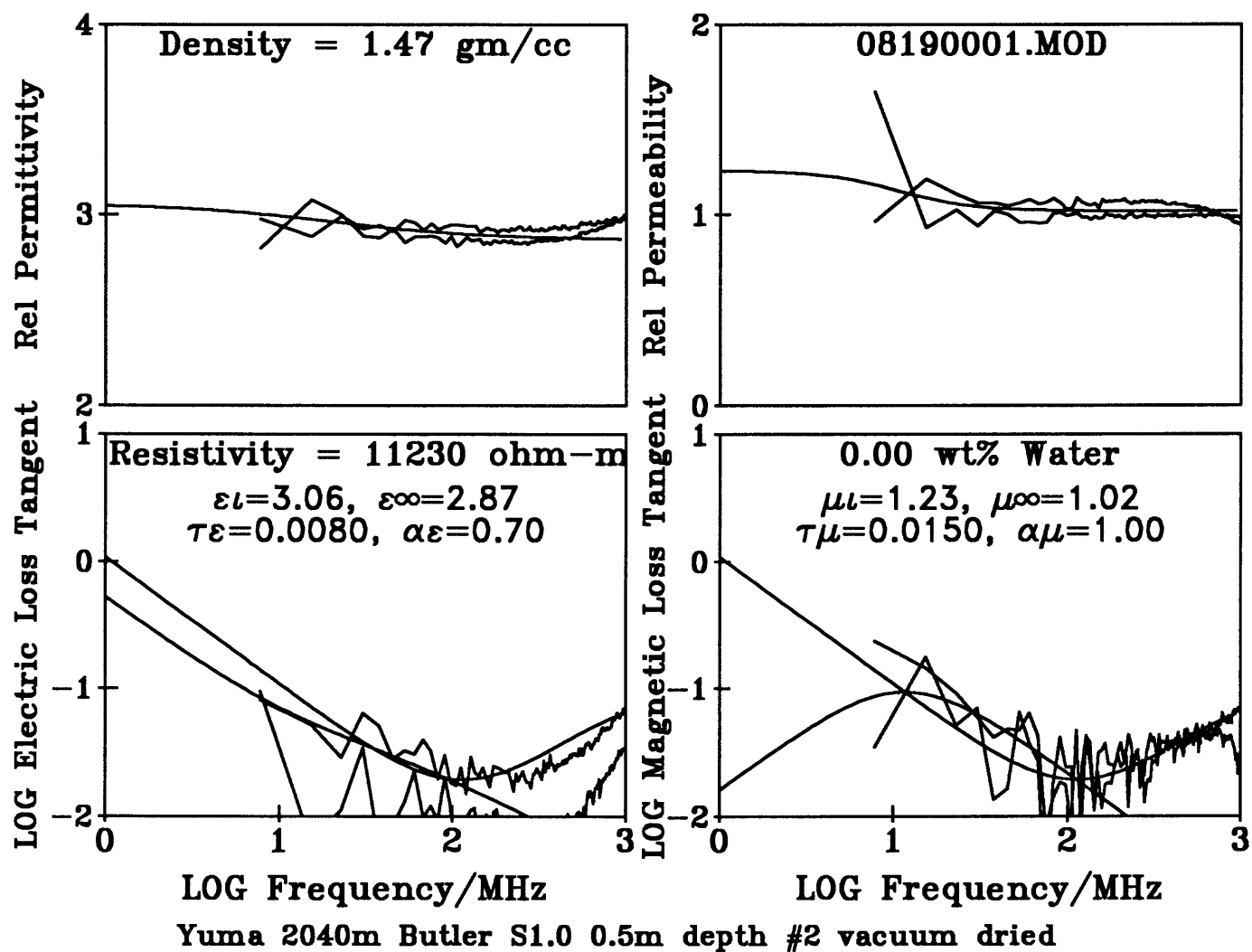


Figure 62 -

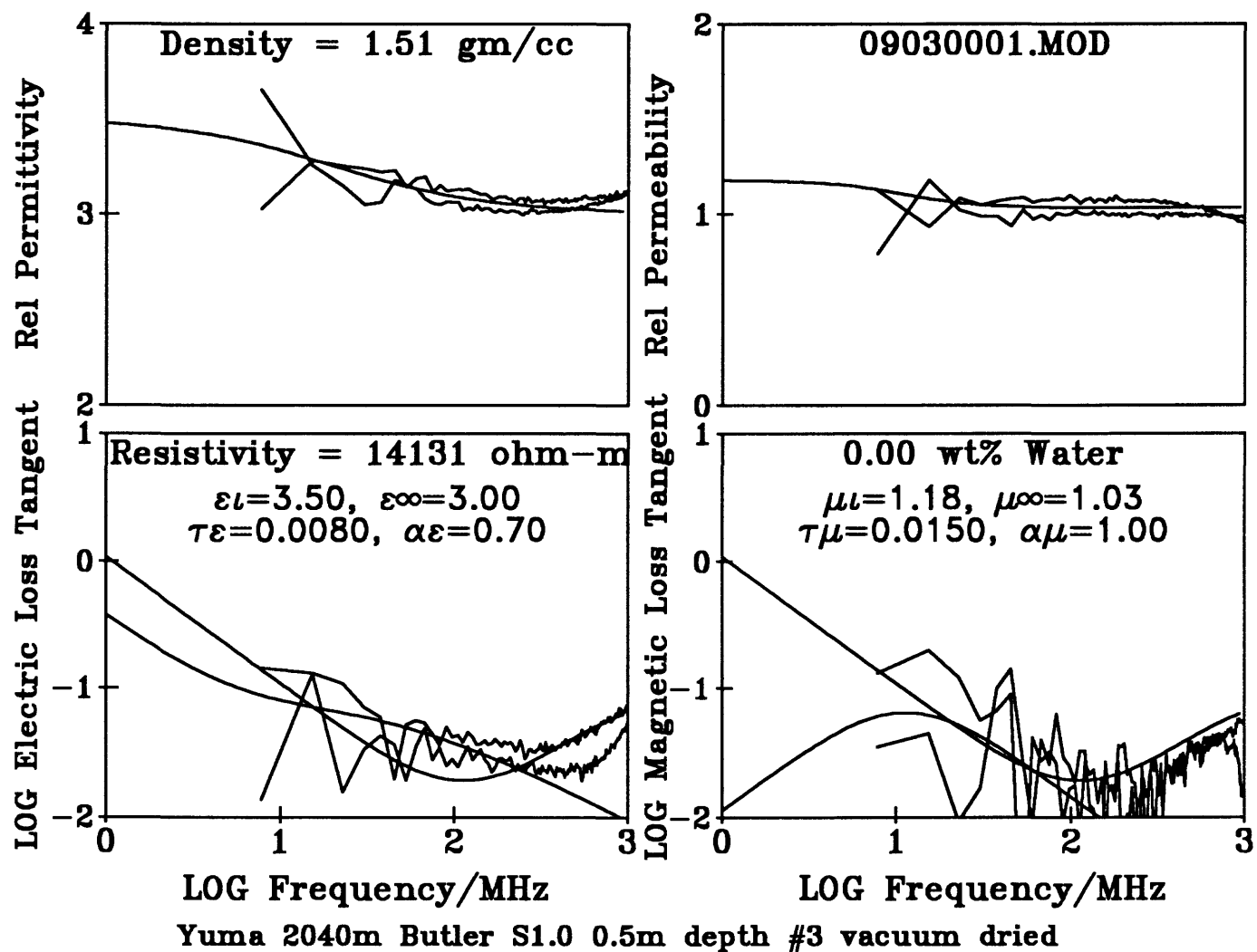


Figure 63 -

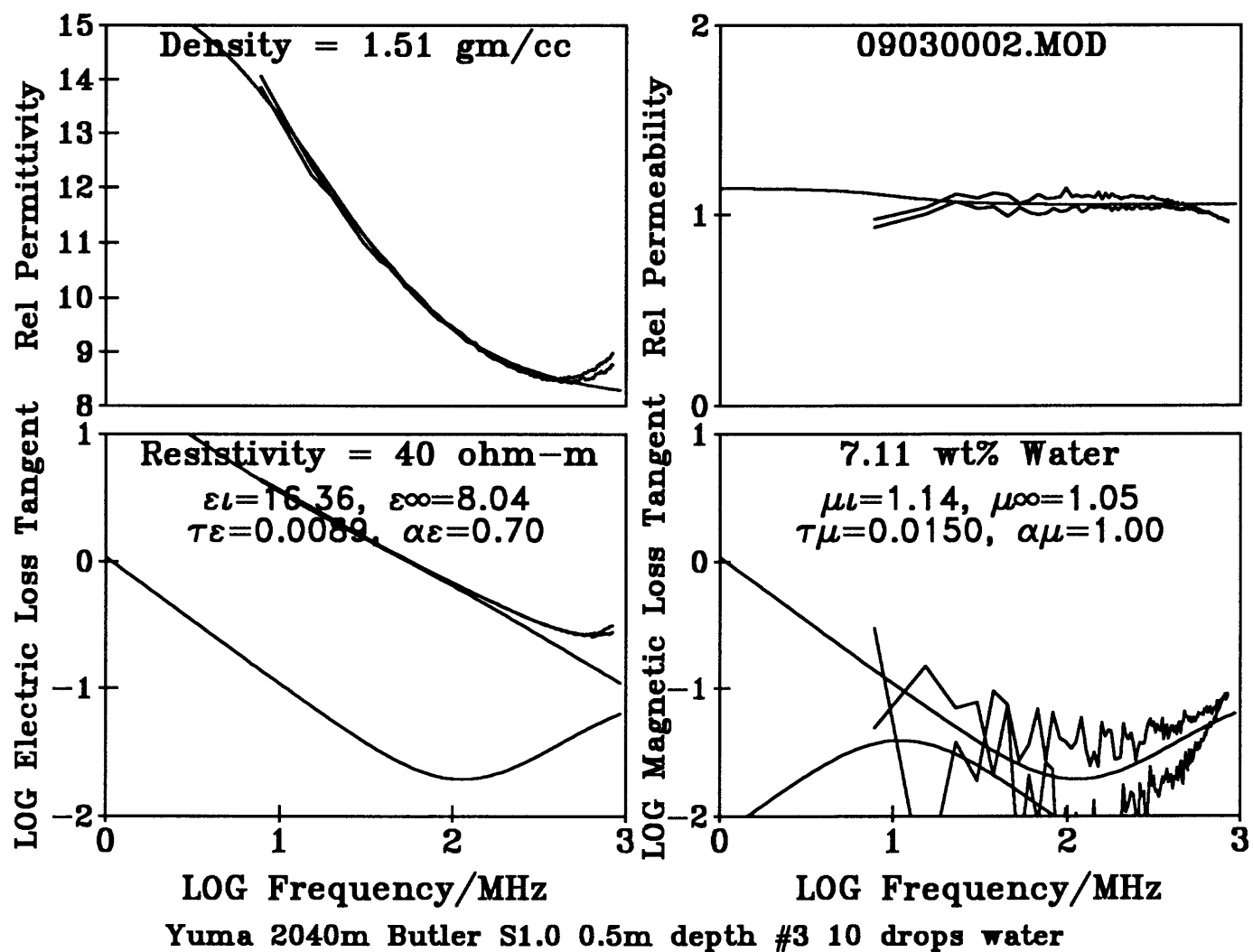


Figure 64 -

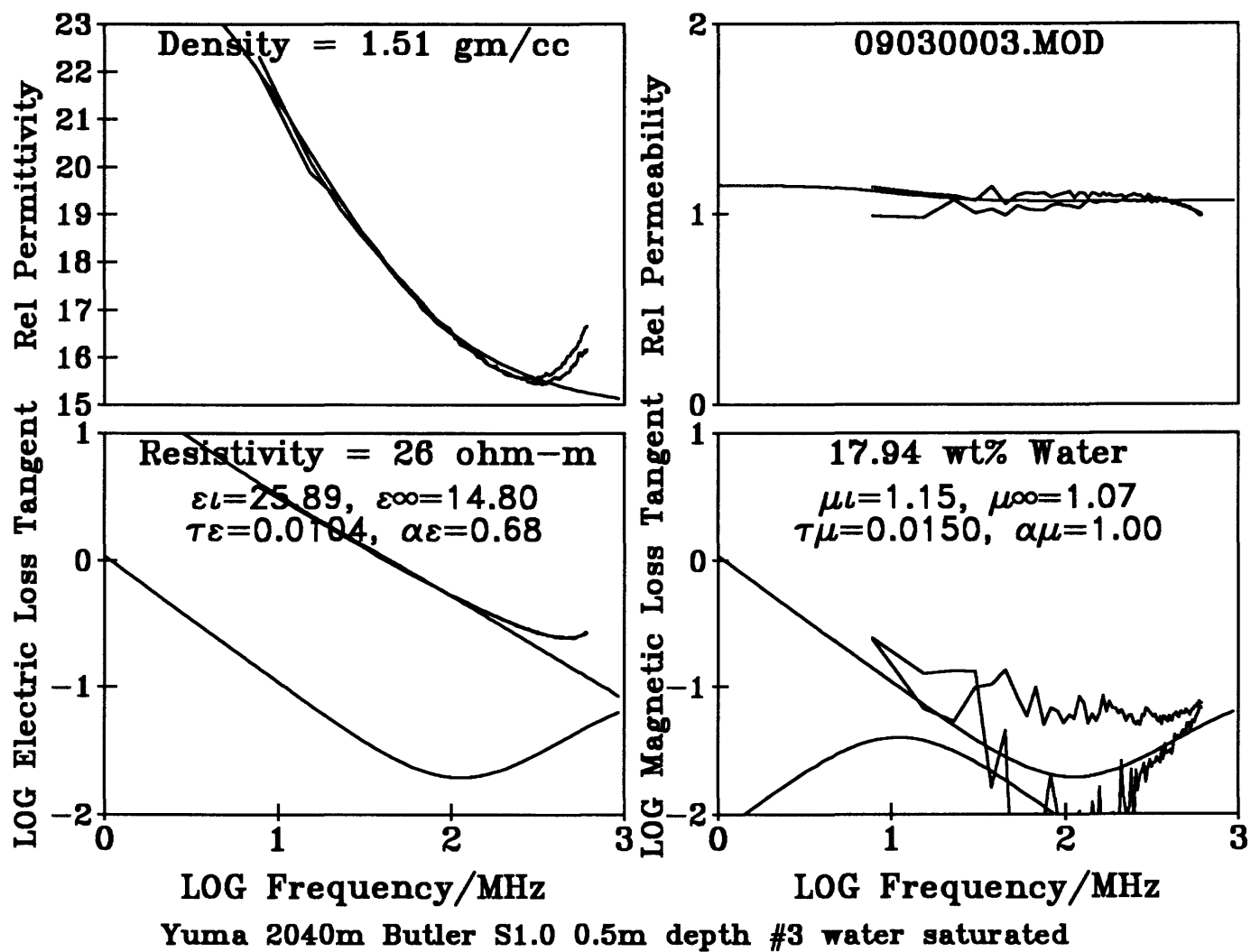


Figure 65 -

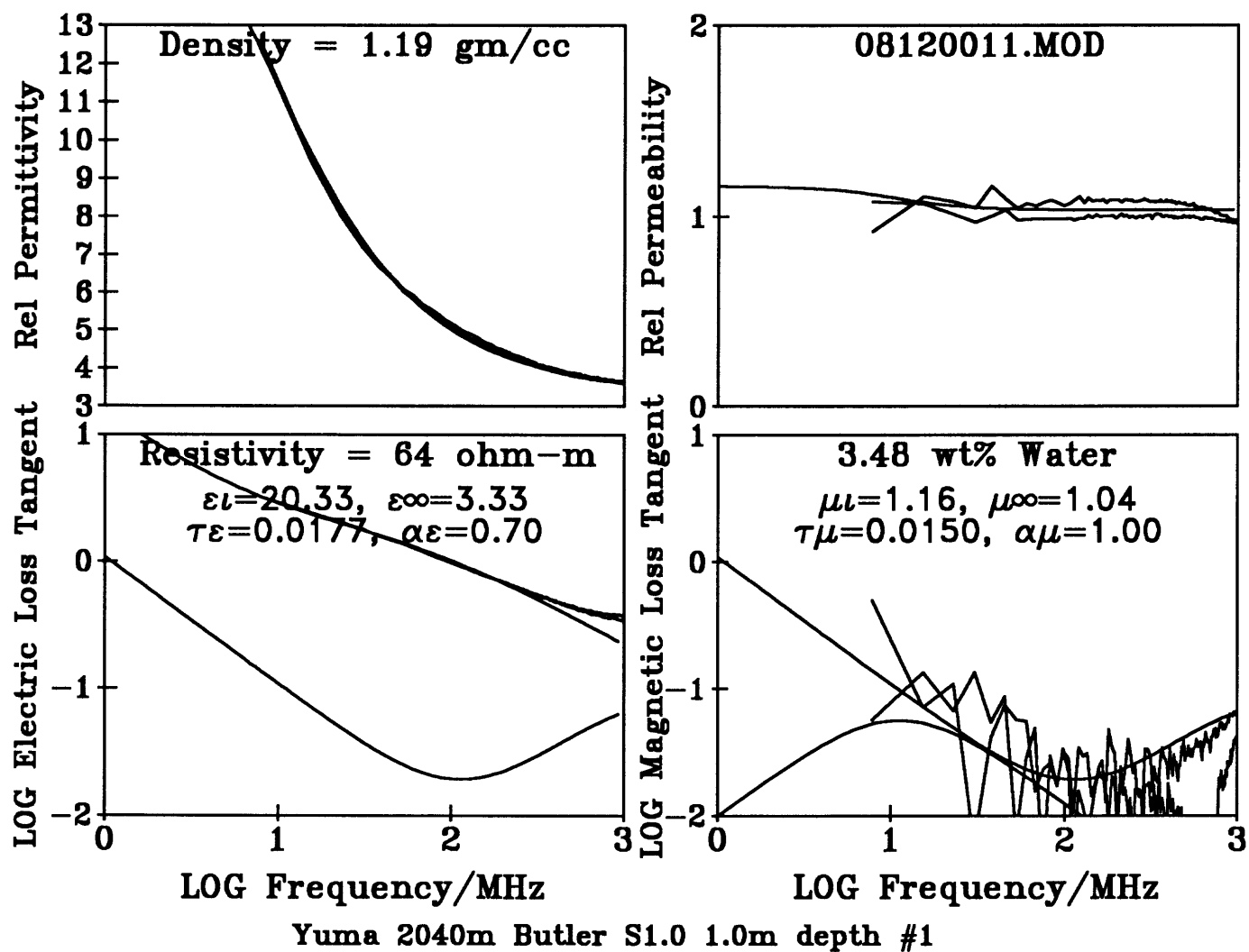


Figure 66 -
Natural state electromagnetic properties with water content preserved in sealed, taped,
sample bottle.

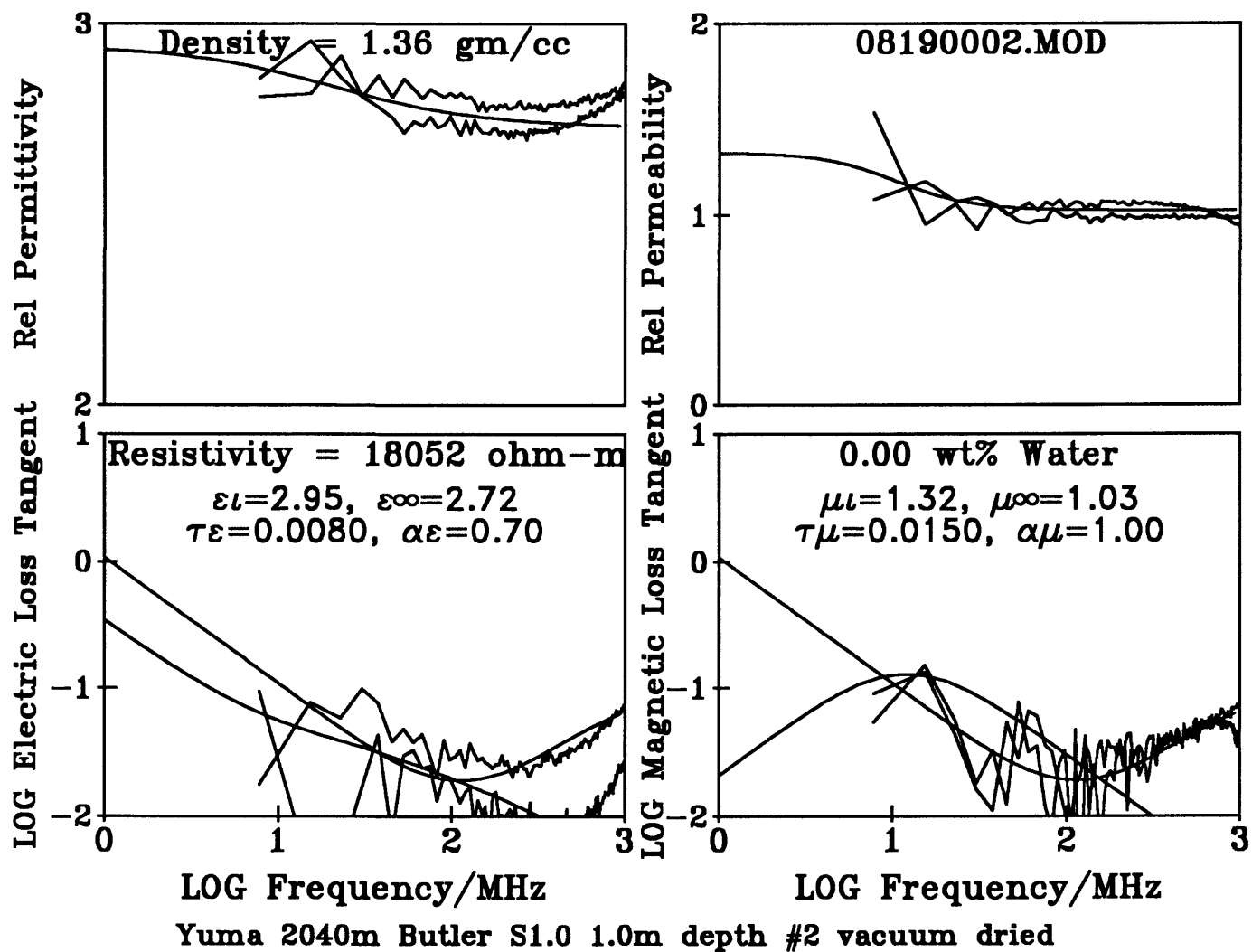


Figure 67 -

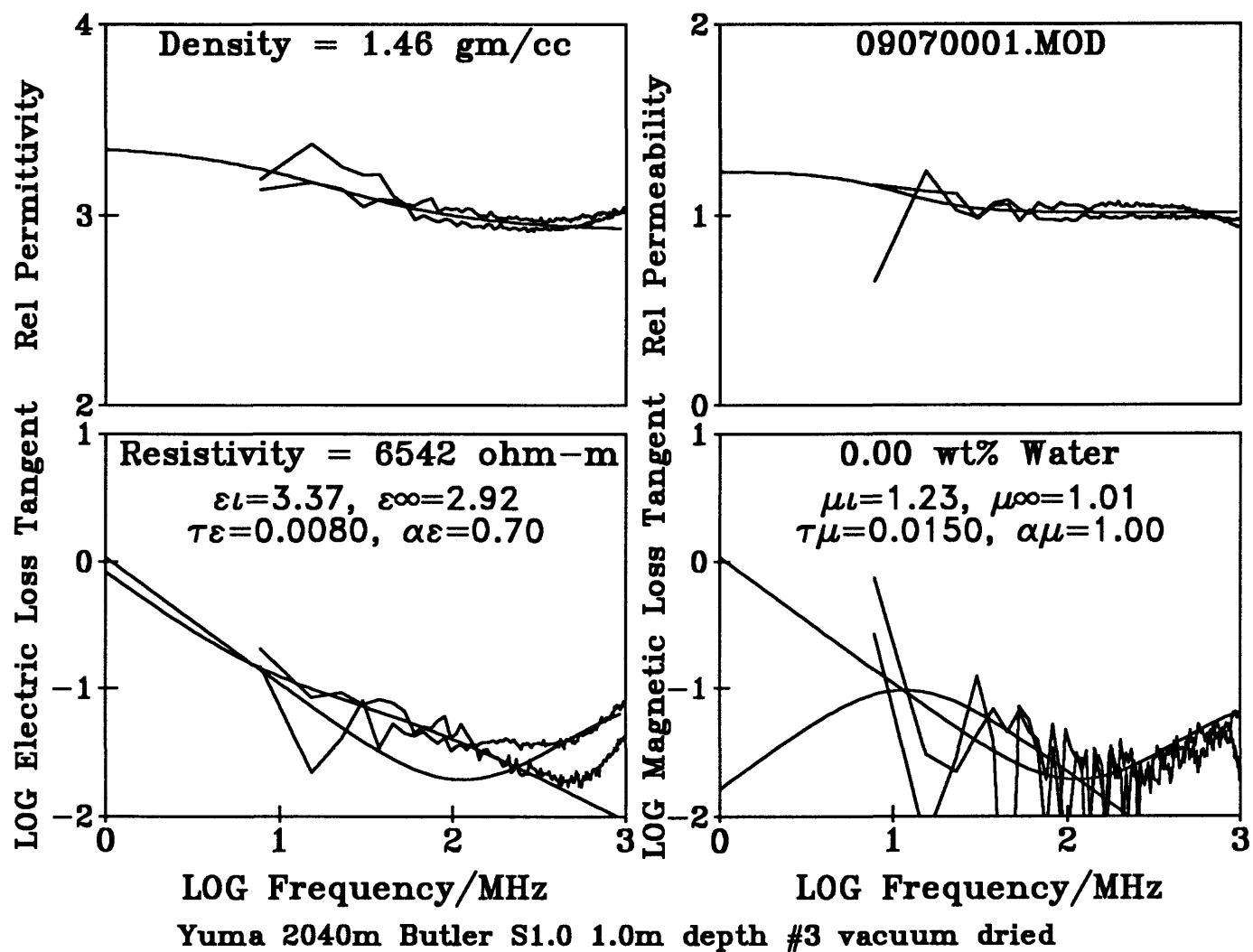


Figure 68 -

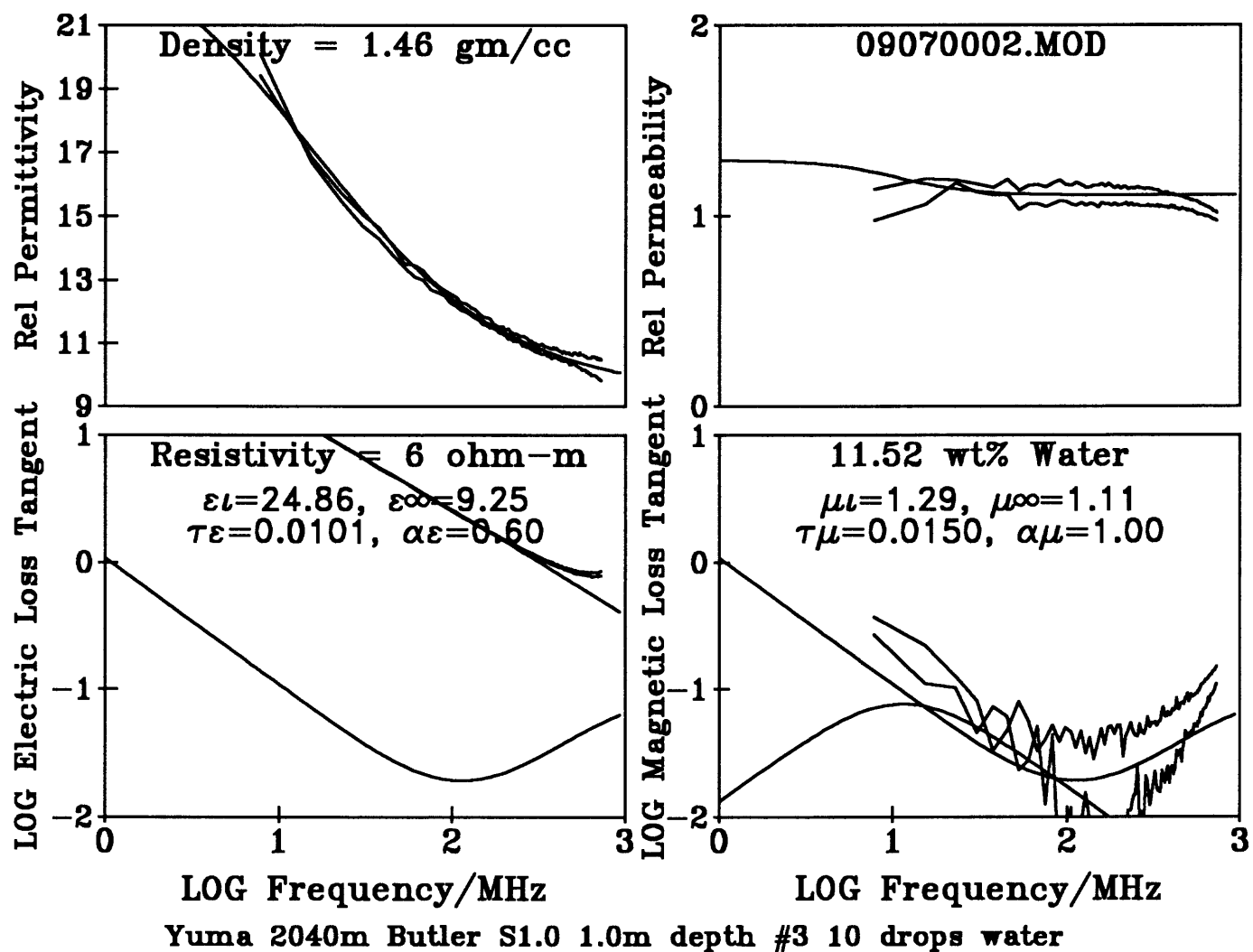


Figure 69 -

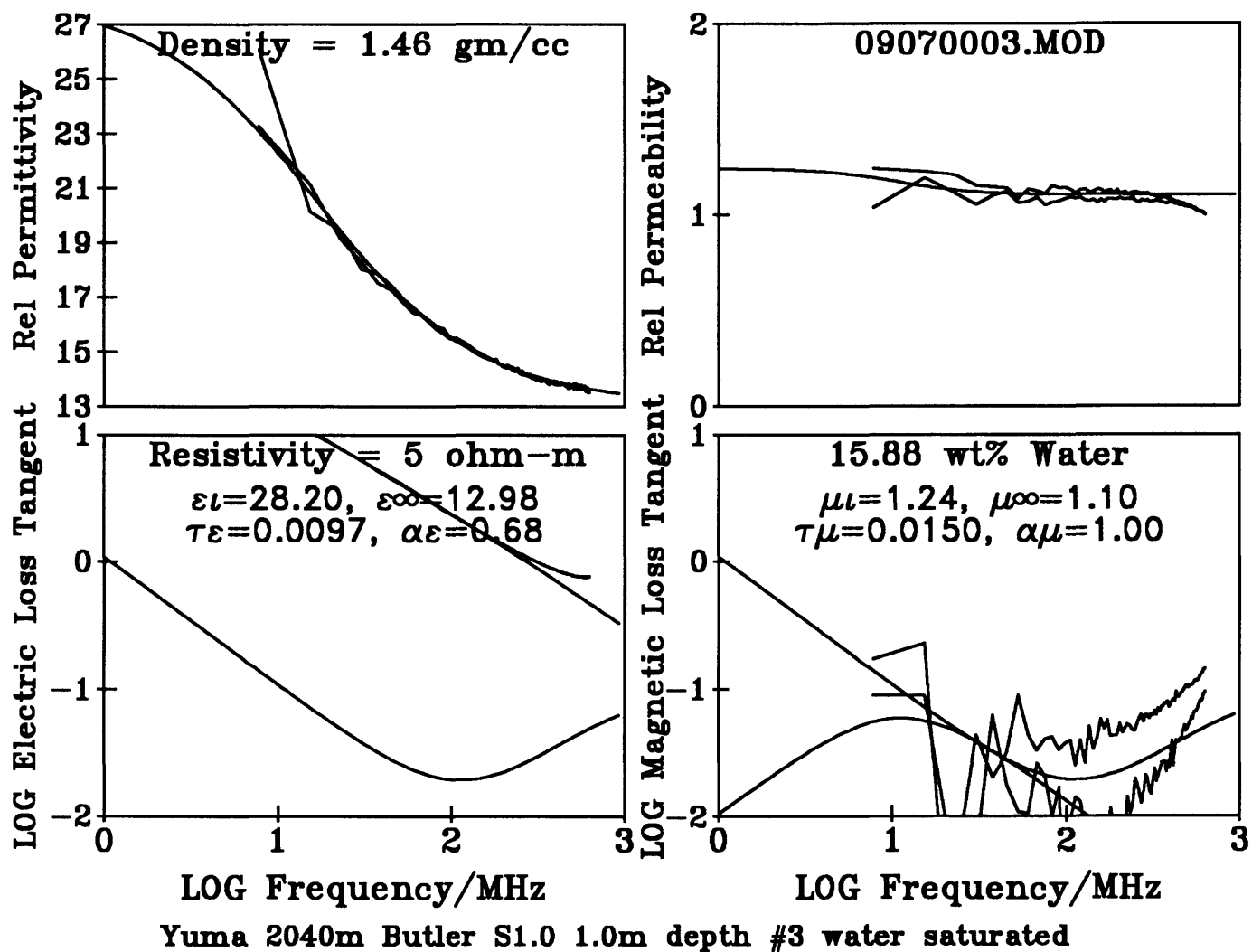


Figure 70 -

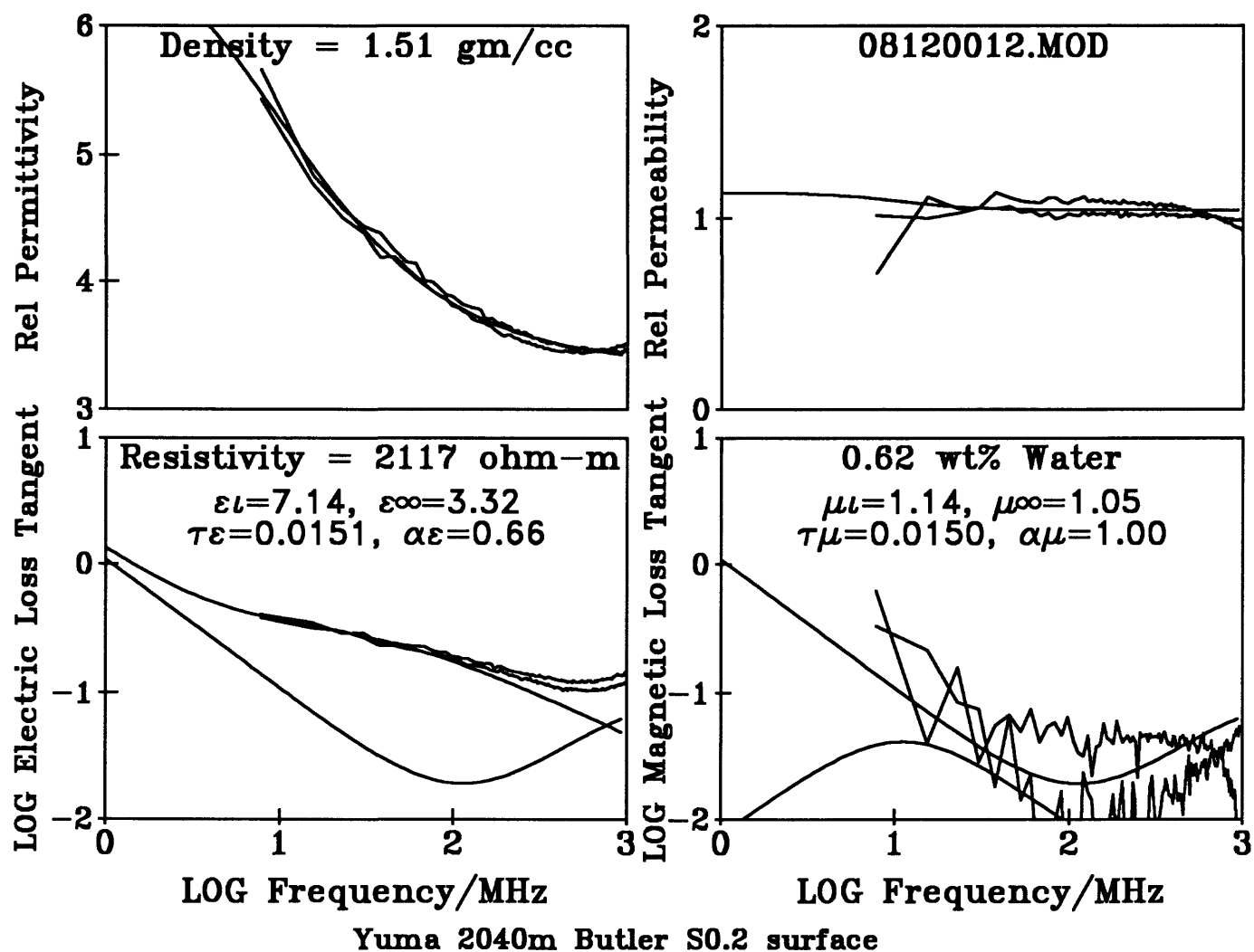


Figure 71 -
 Natural state electromagnetic properties with water content preserved in sealed, taped,
 sample bottle.

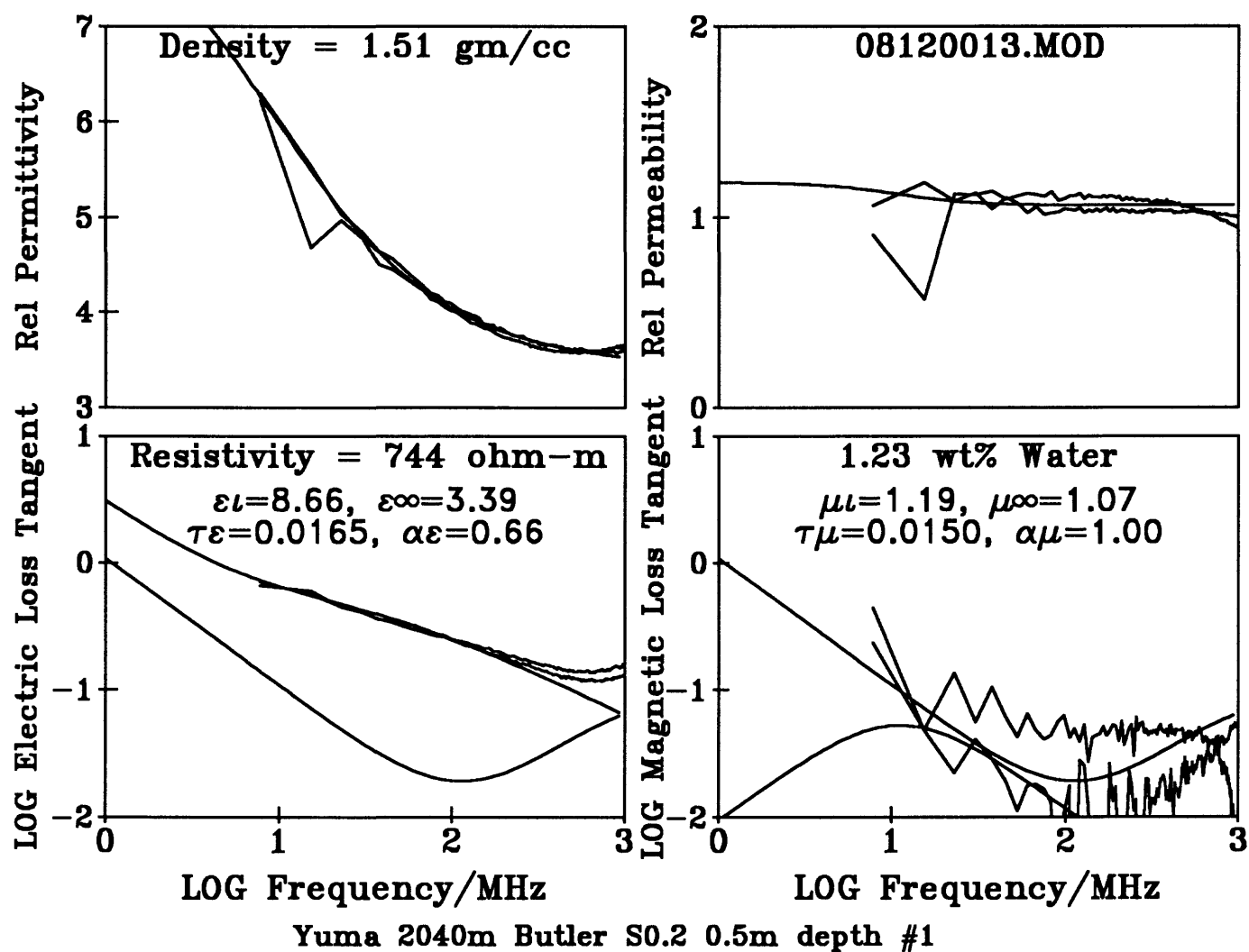


Figure 72 -
Natural state electromagnetic properties with water content preserved in sealed, taped, sample bottle.

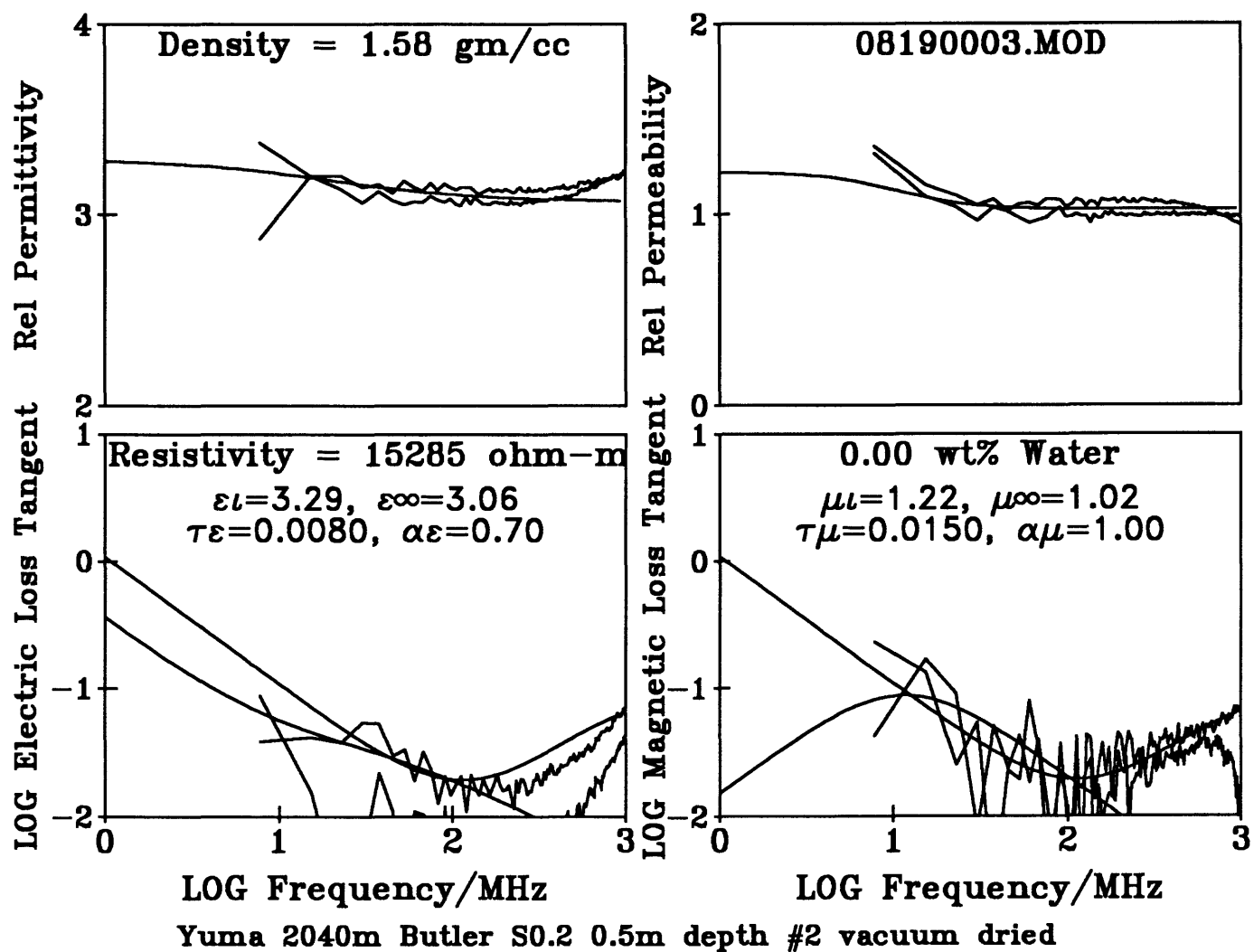


Figure 73 -

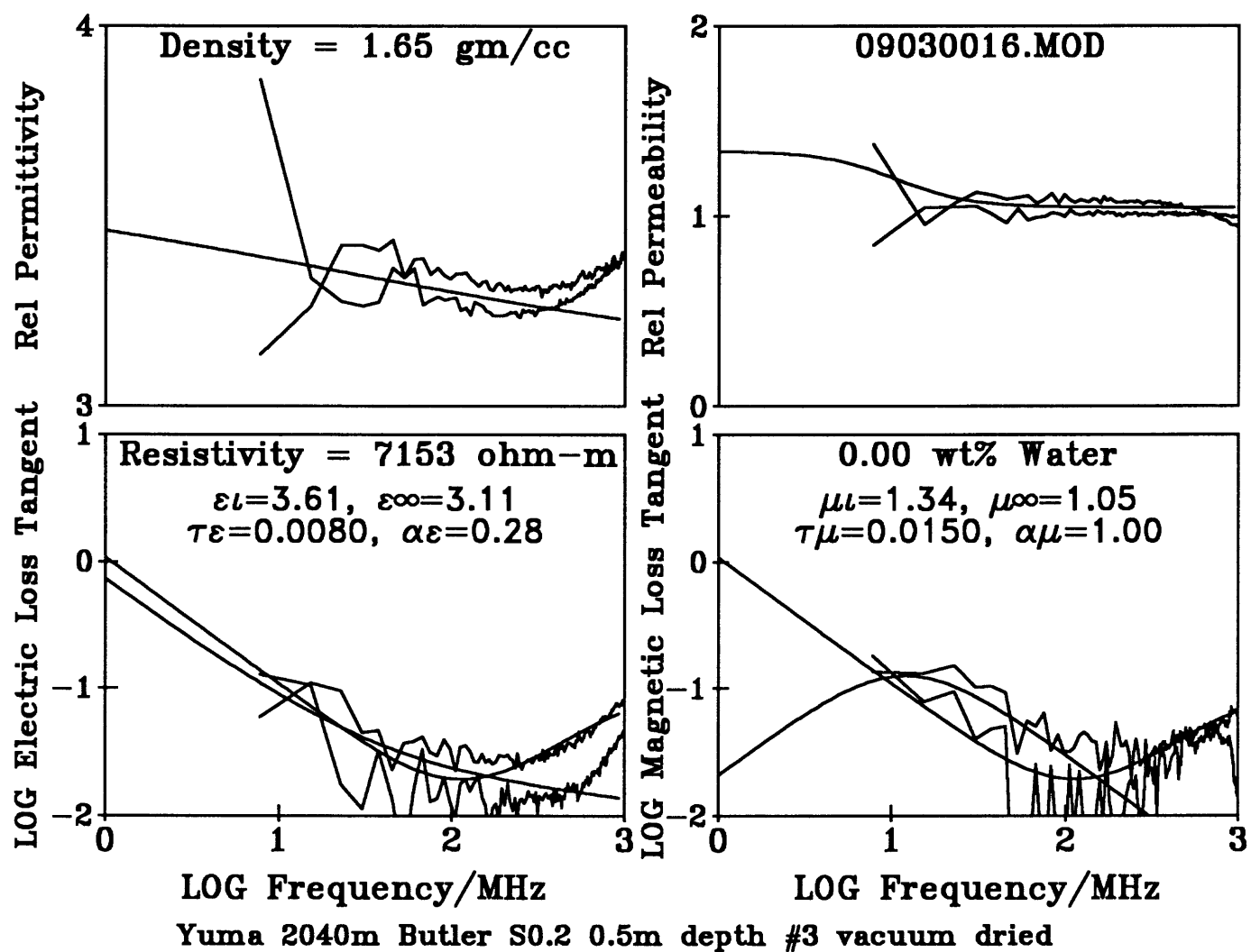


Figure 74 -

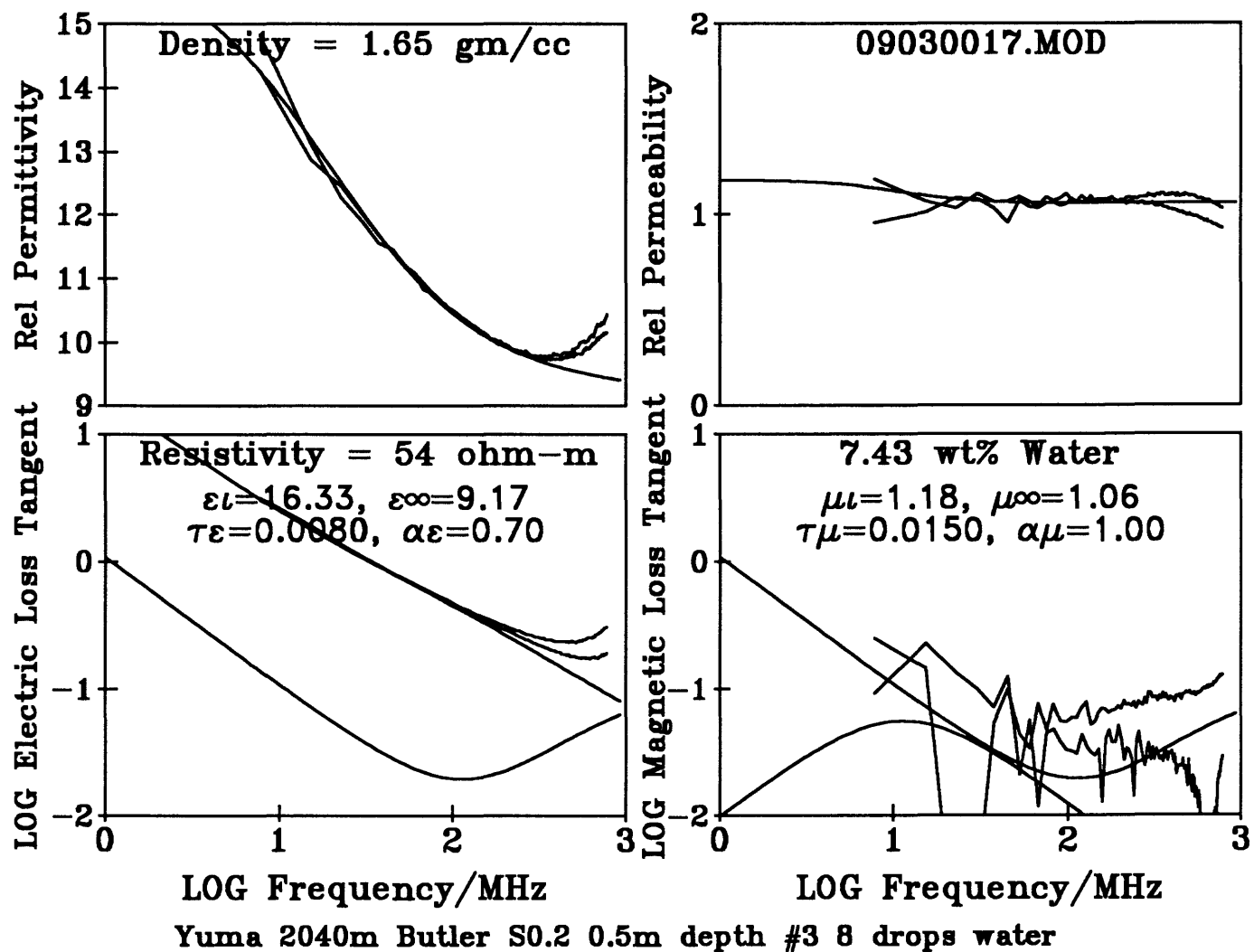


Figure 75 -

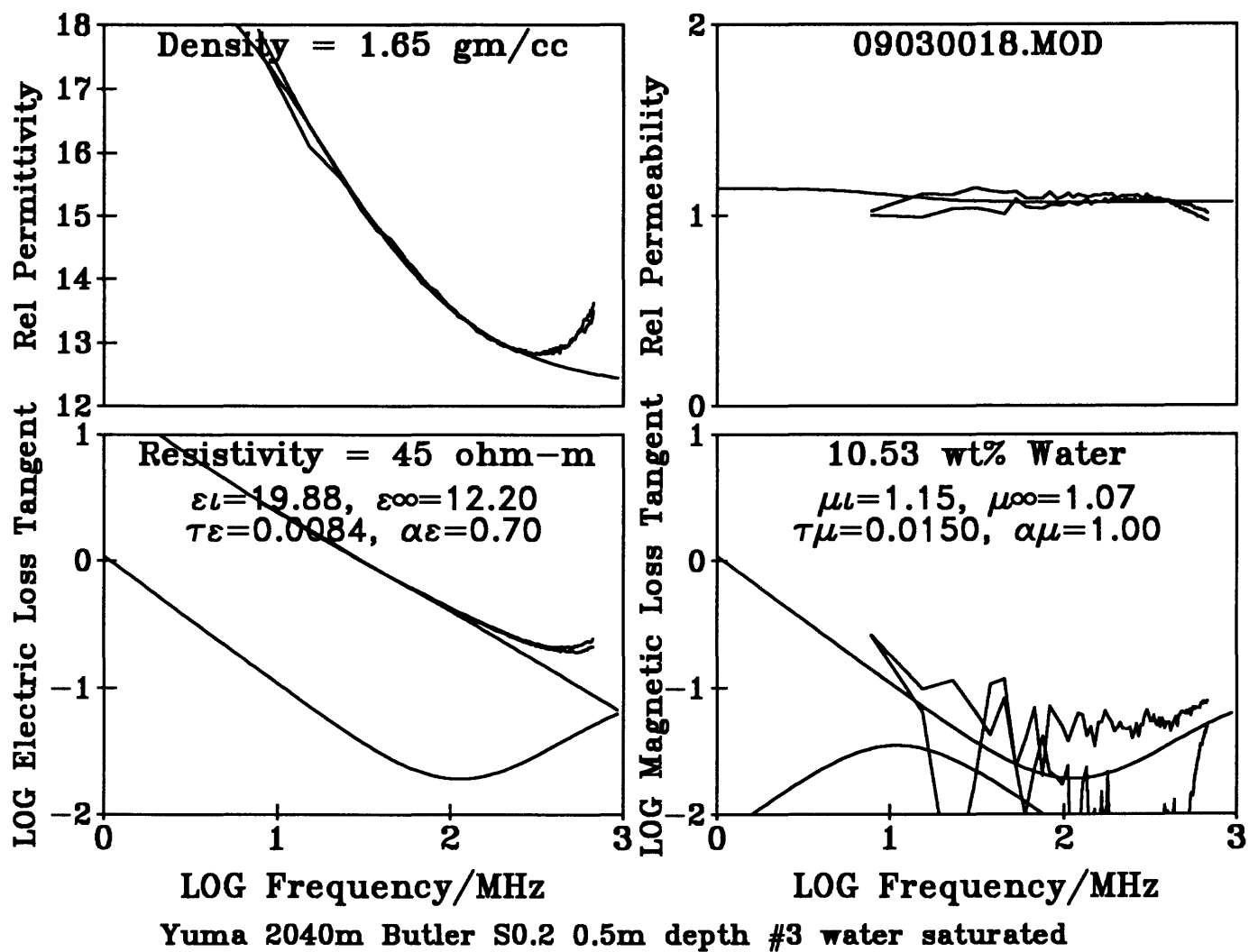


Figure 76 -

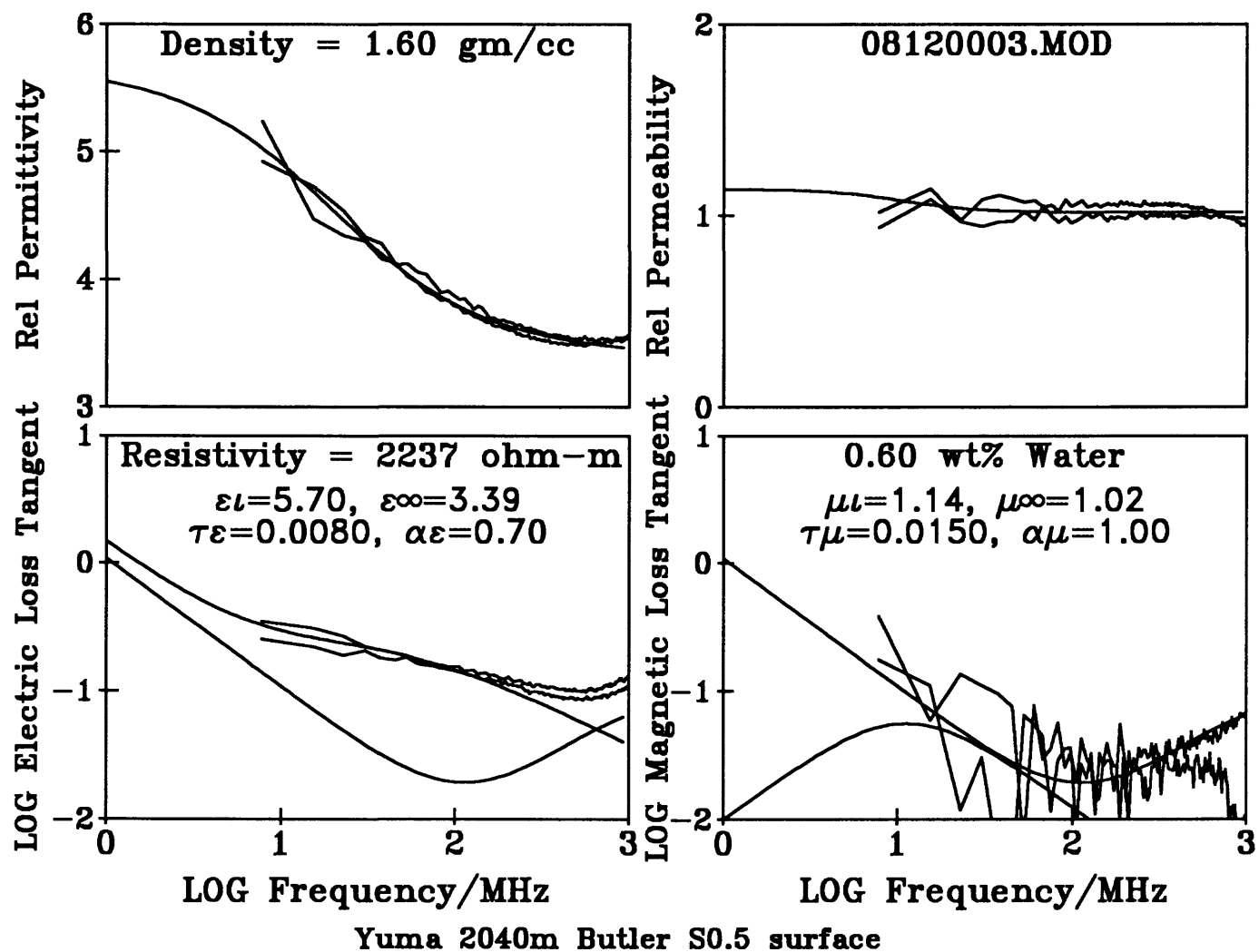


Figure 77 -
 Natural state electromagnetic properties with water content preserved in sealed, taped,
 sample bottle.

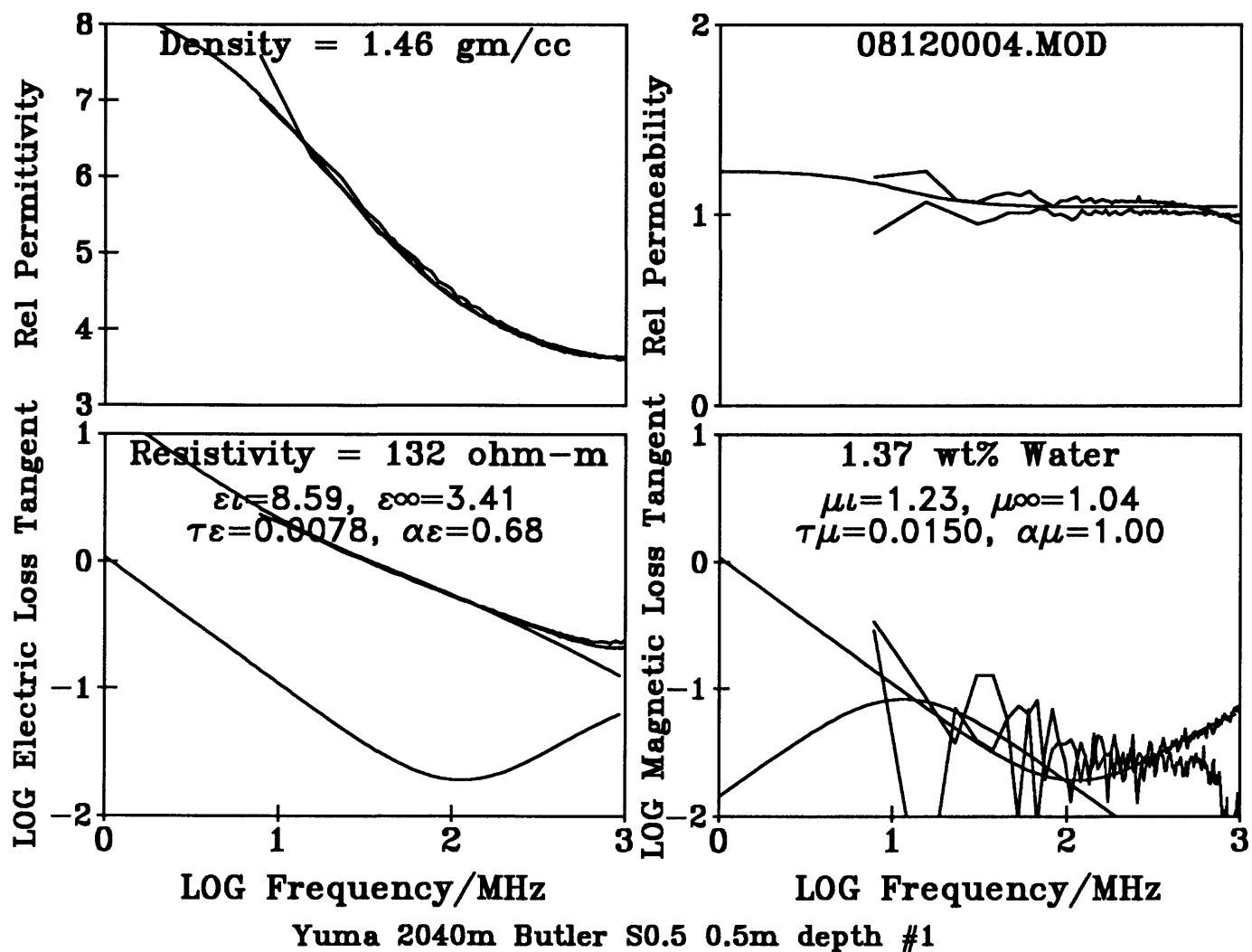


Figure 78 -
Natural state electromagnetic properties with water content preserved in sealed, taped, sample bottle.

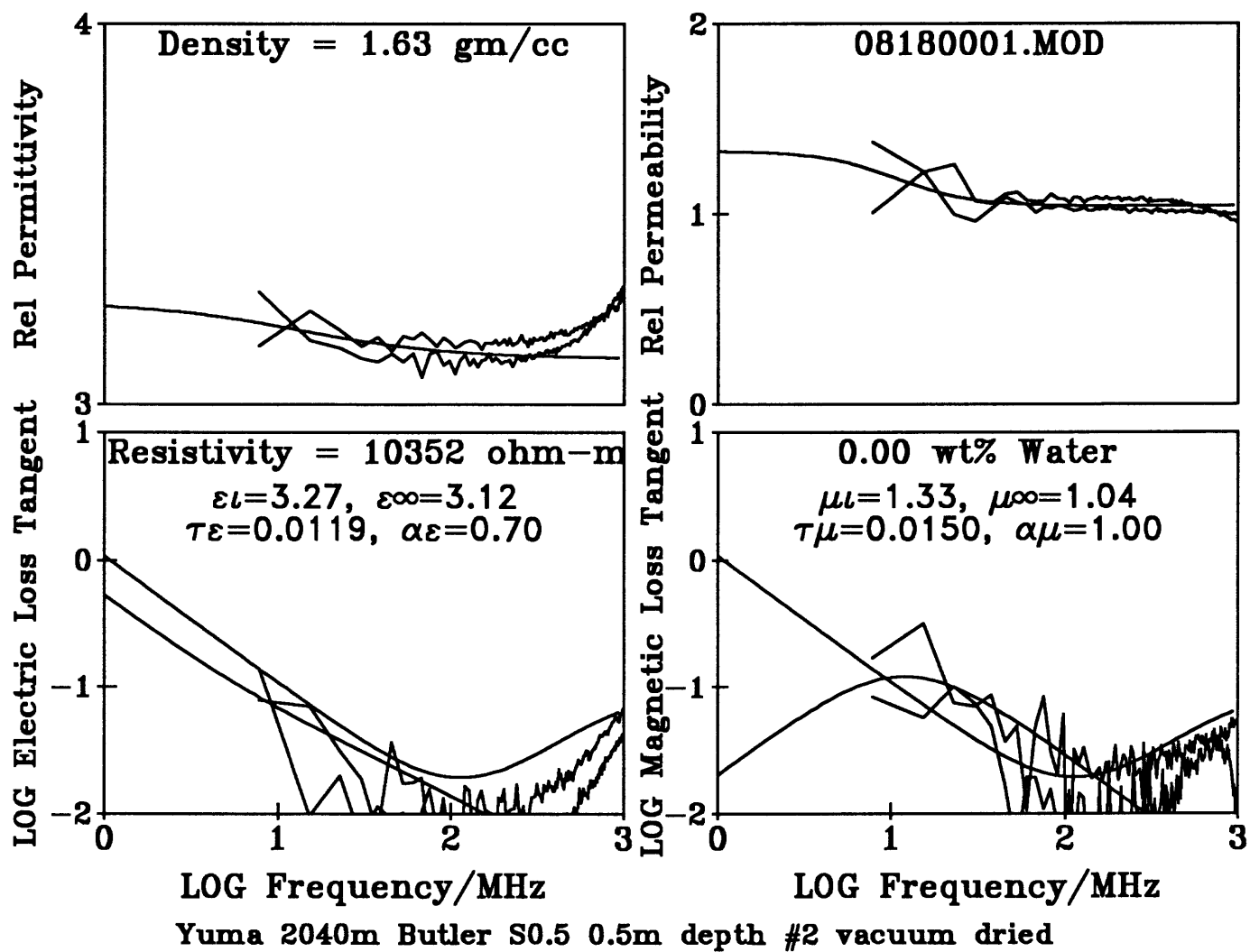


Figure 79 -

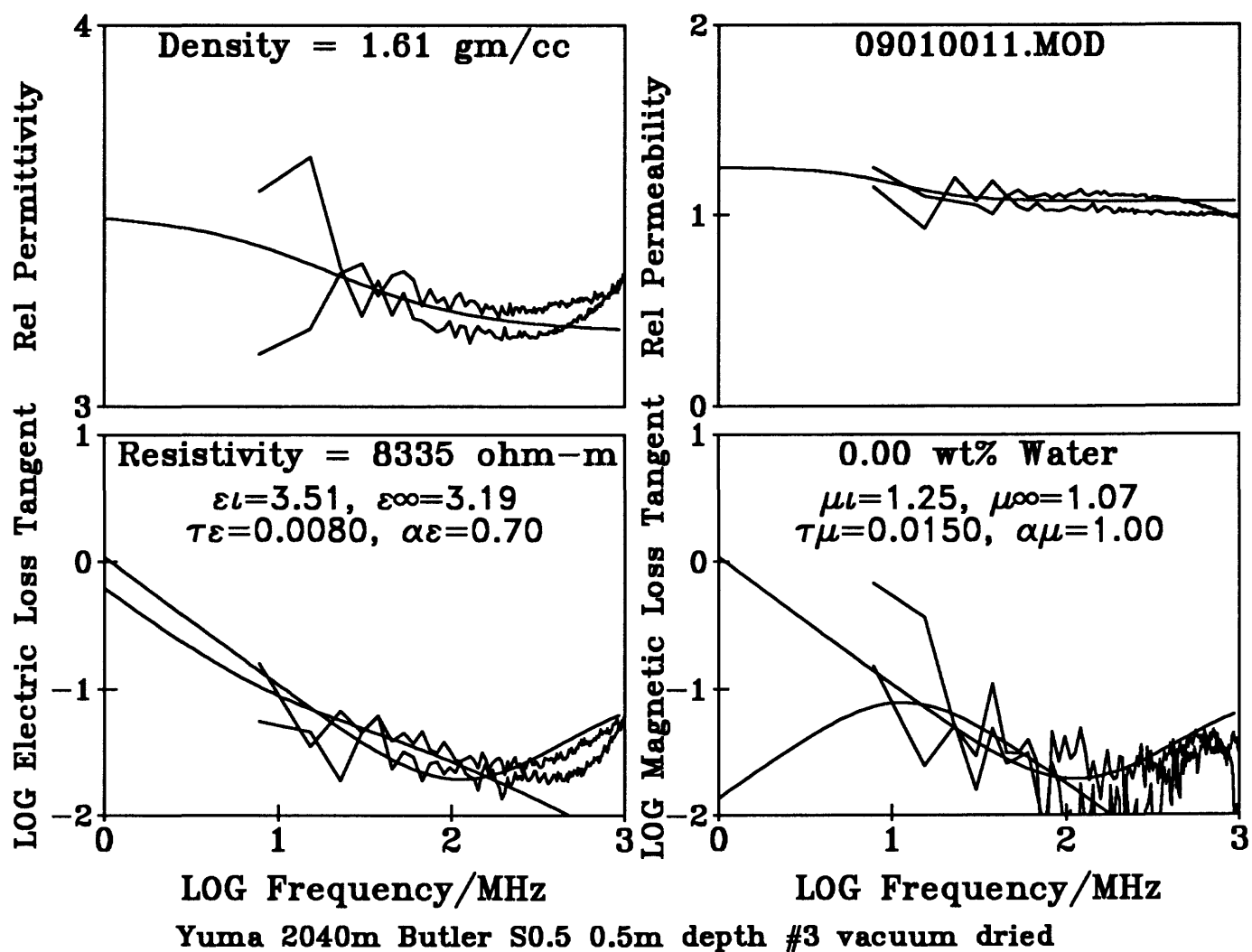


Figure 80 -

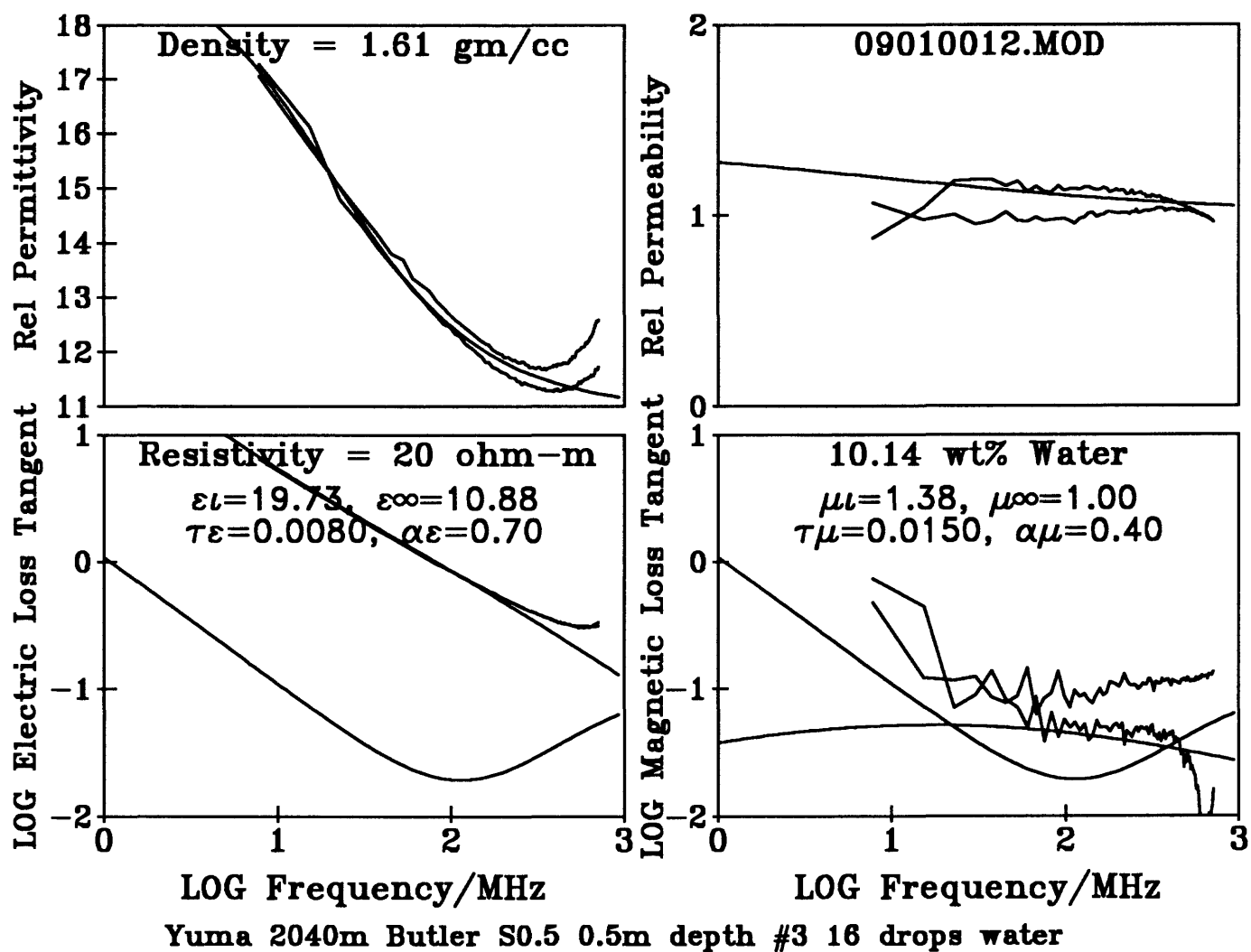


Figure 81 -

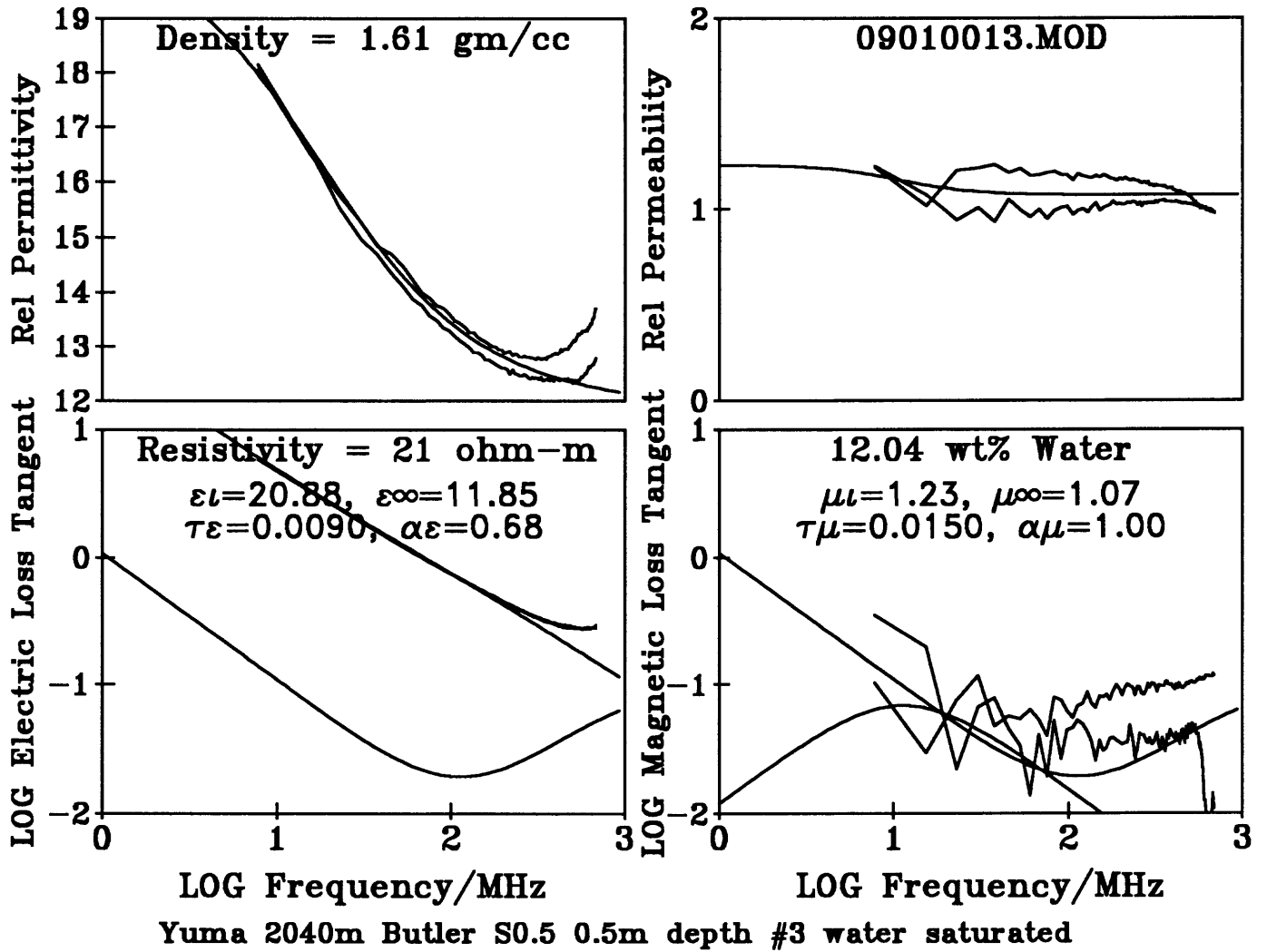


Figure 82 -

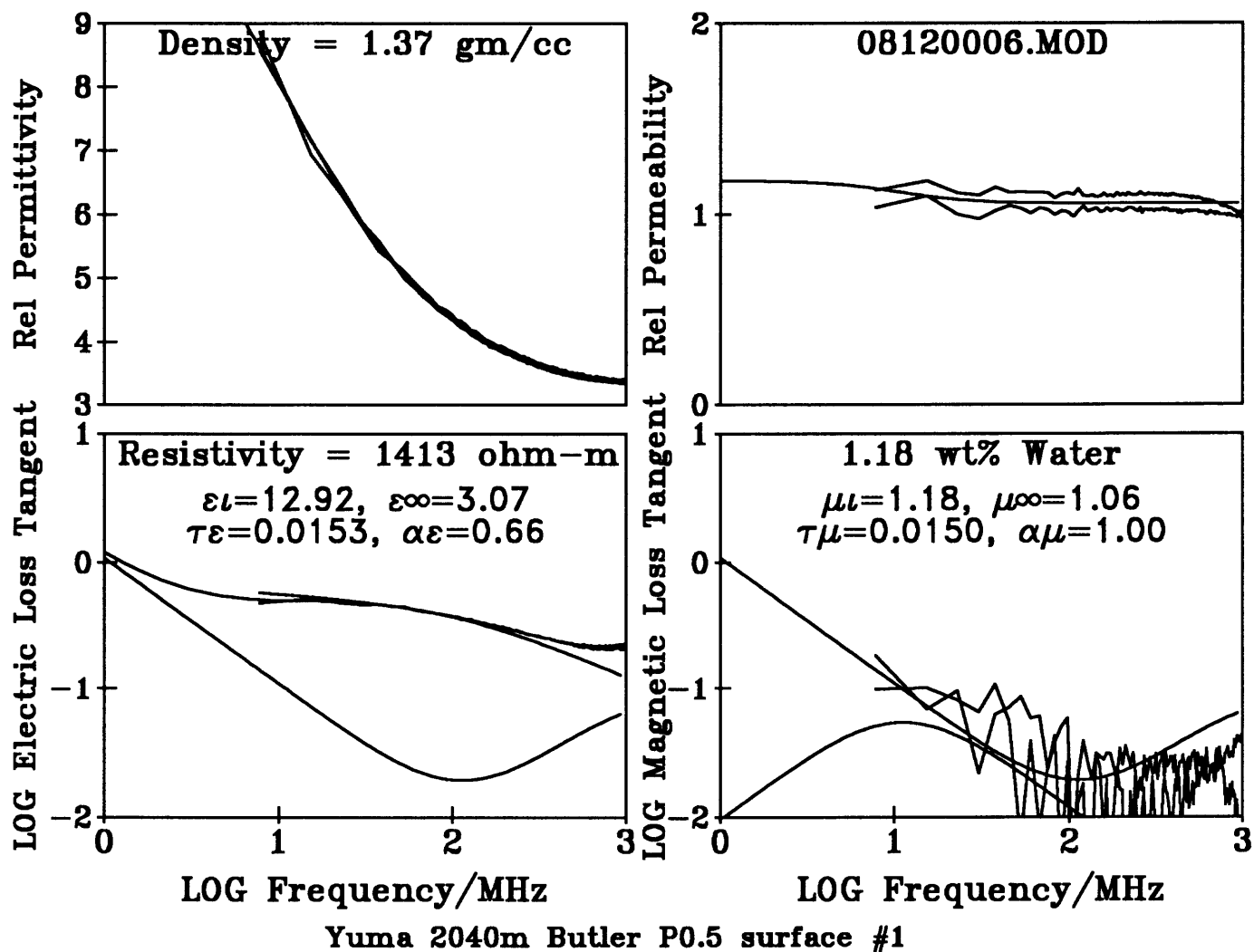


Figure 83 -
Natural state electromagnetic properties with water content preserved in sealed, taped,
sample bottle.

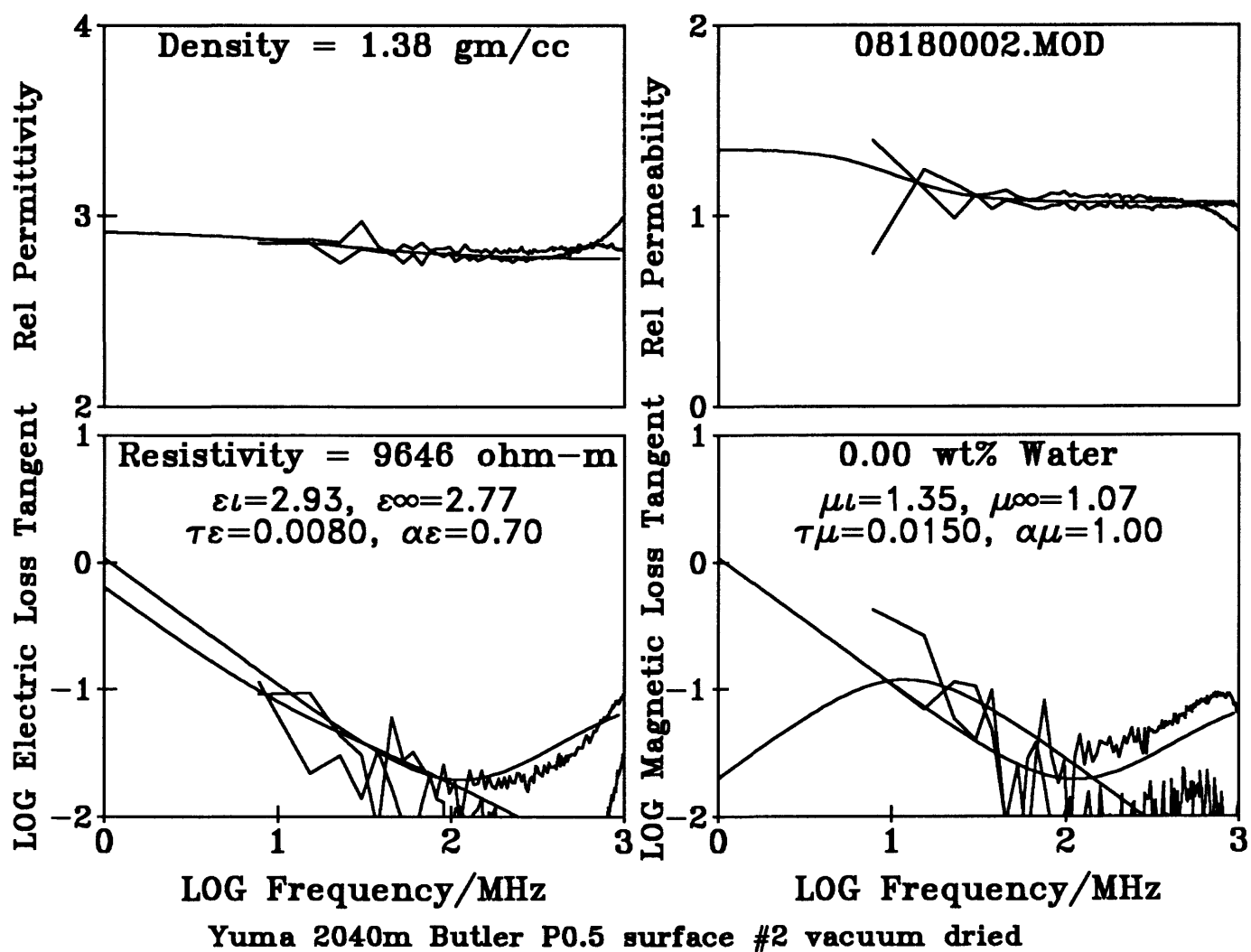


Figure 84 -

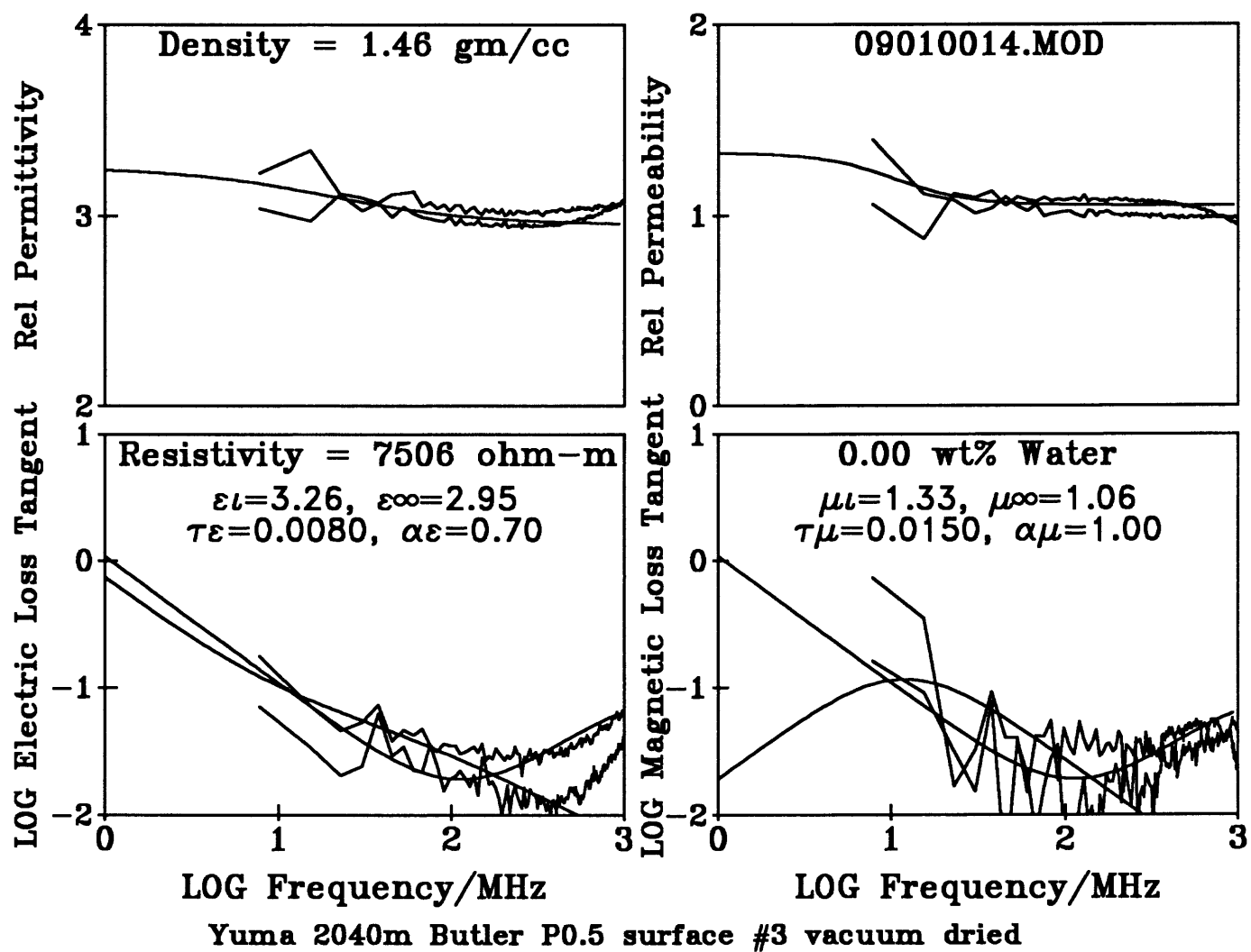


Figure 85 -

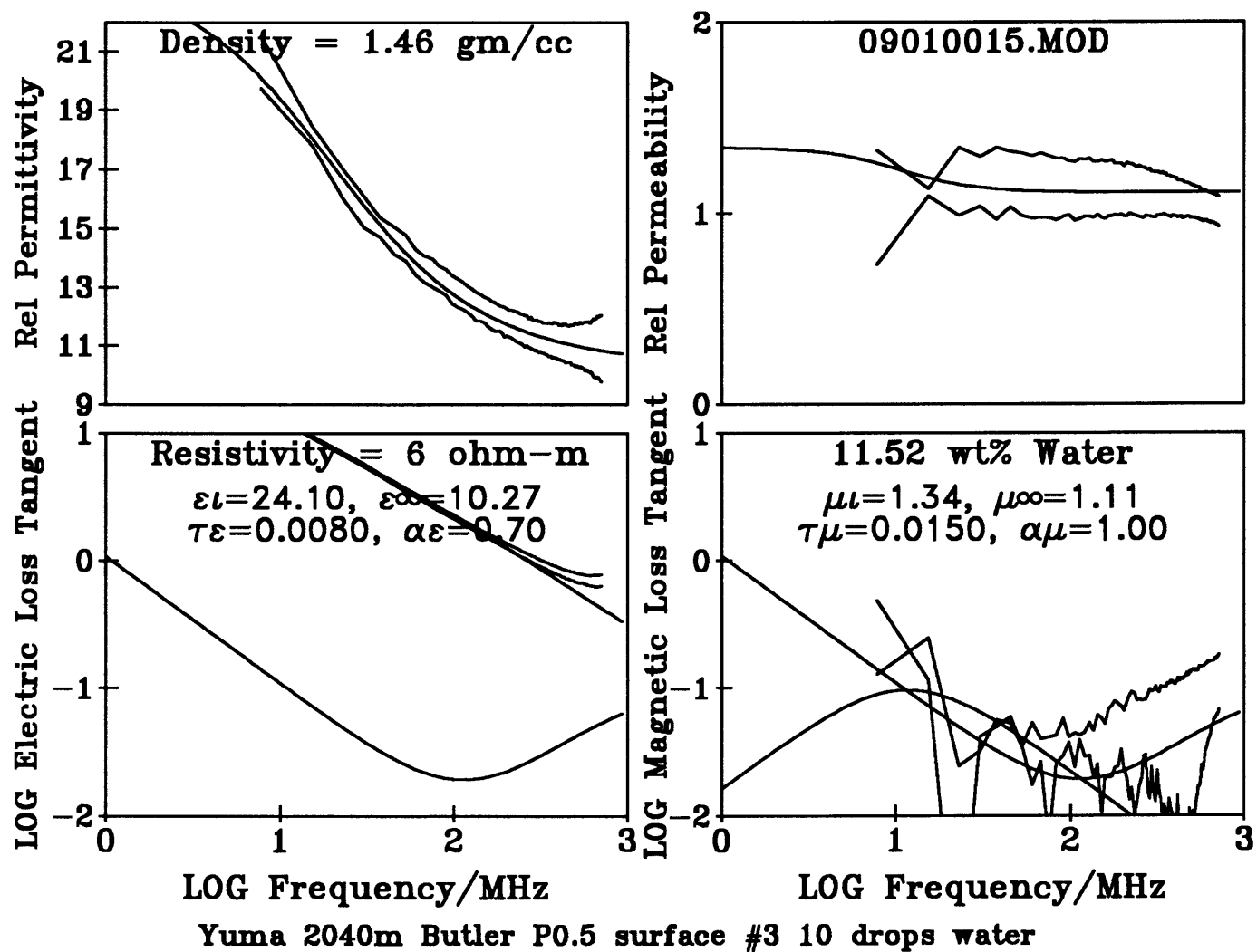


Figure 86 -

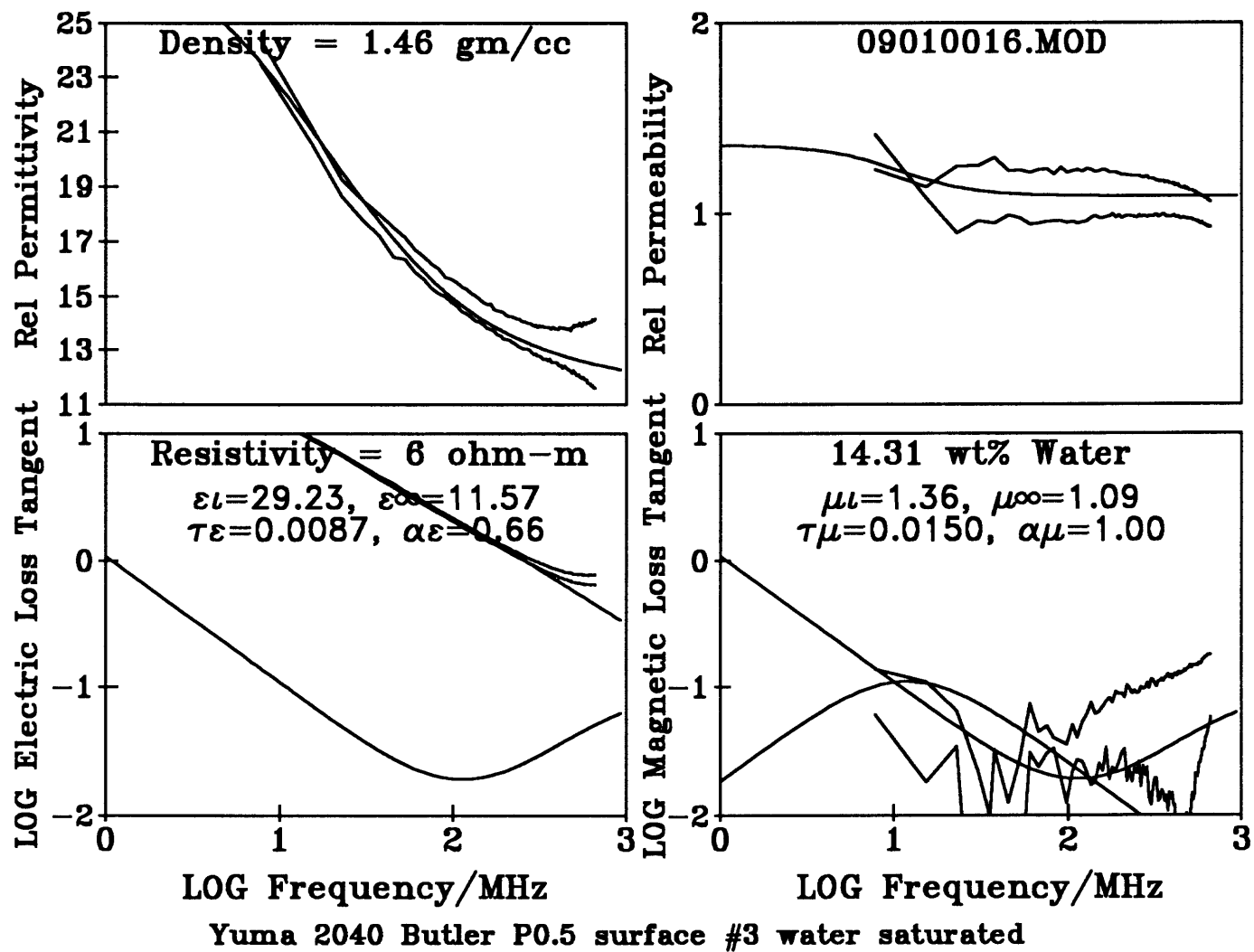
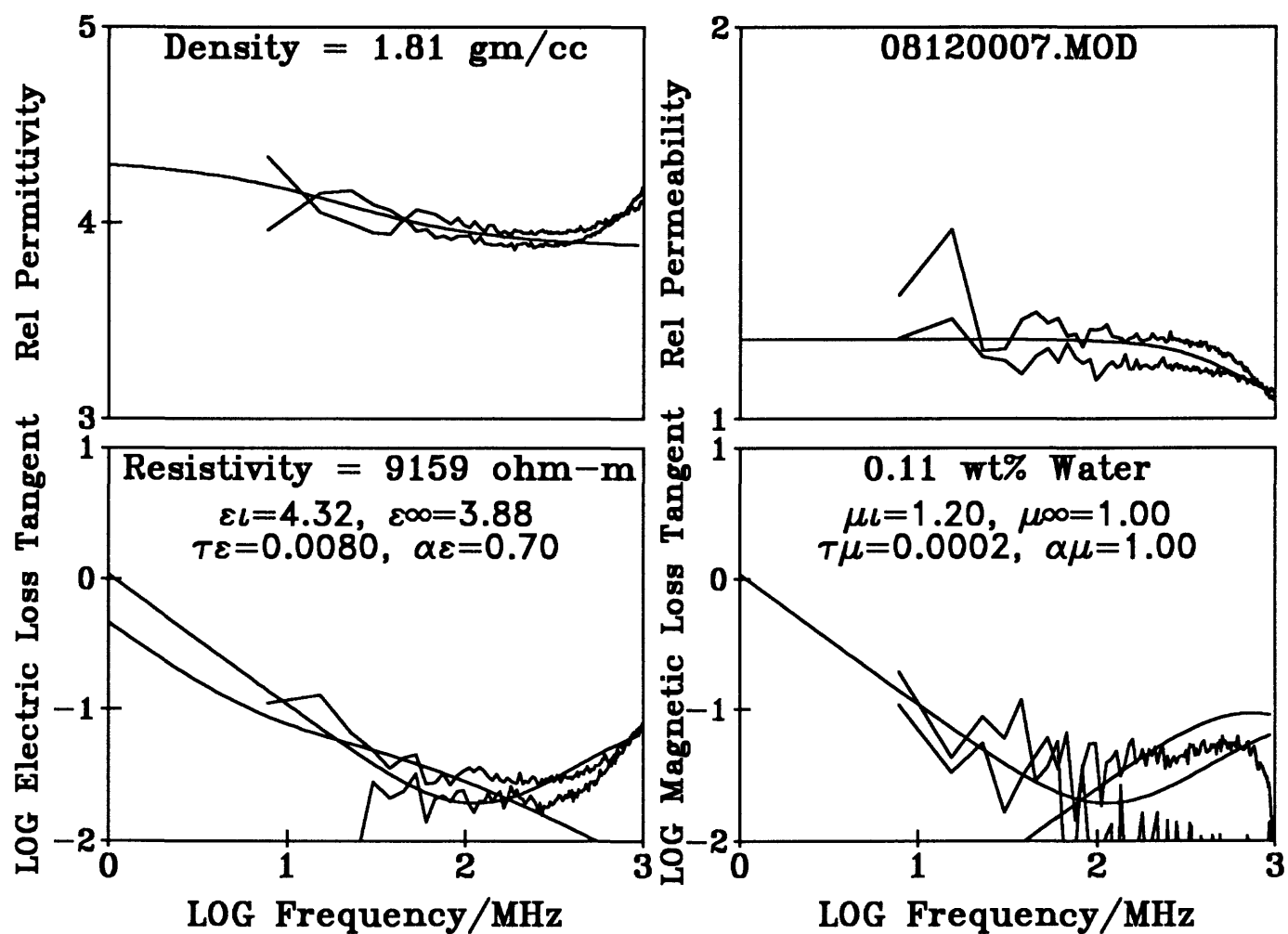
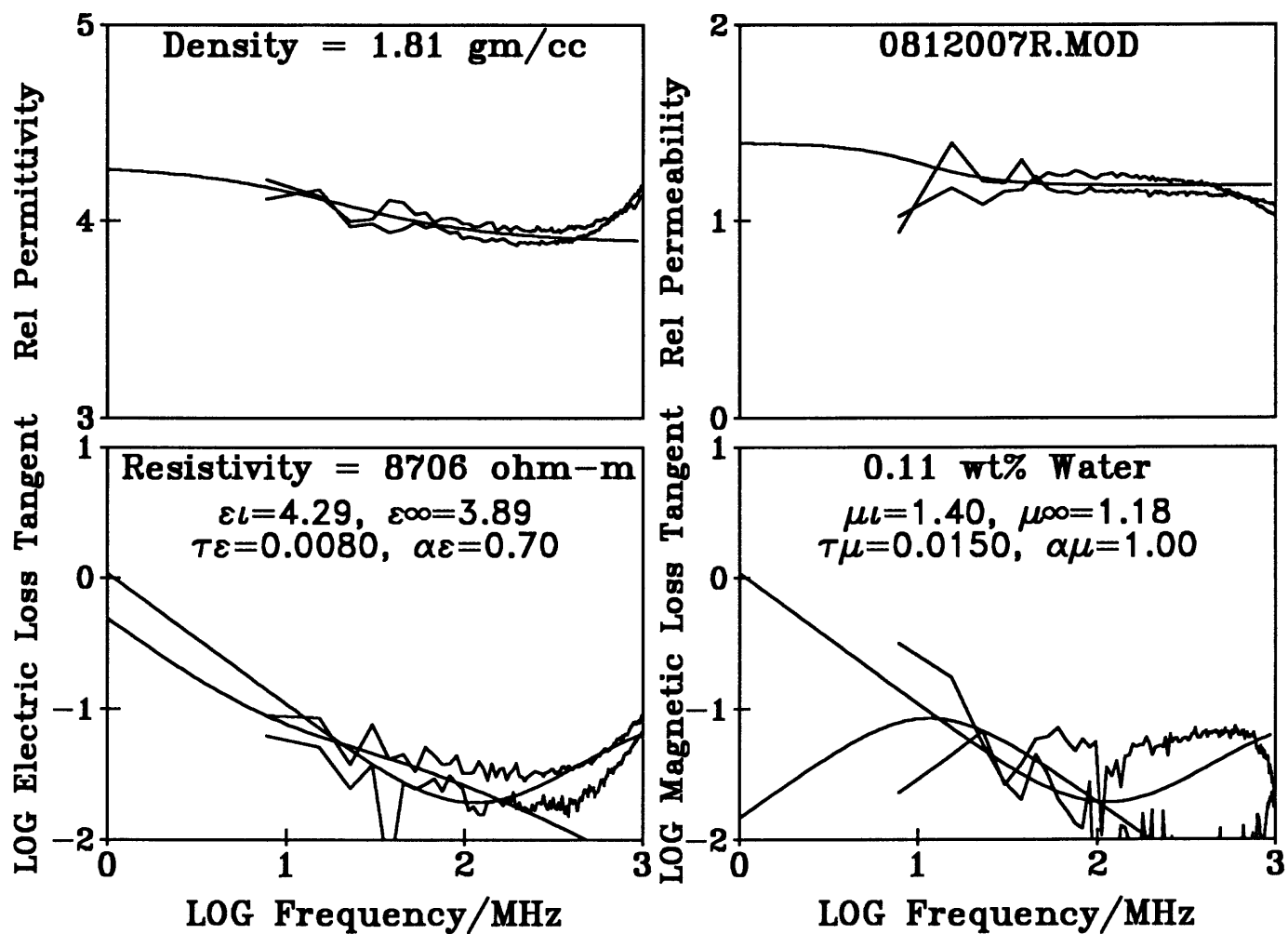


Figure 87 -



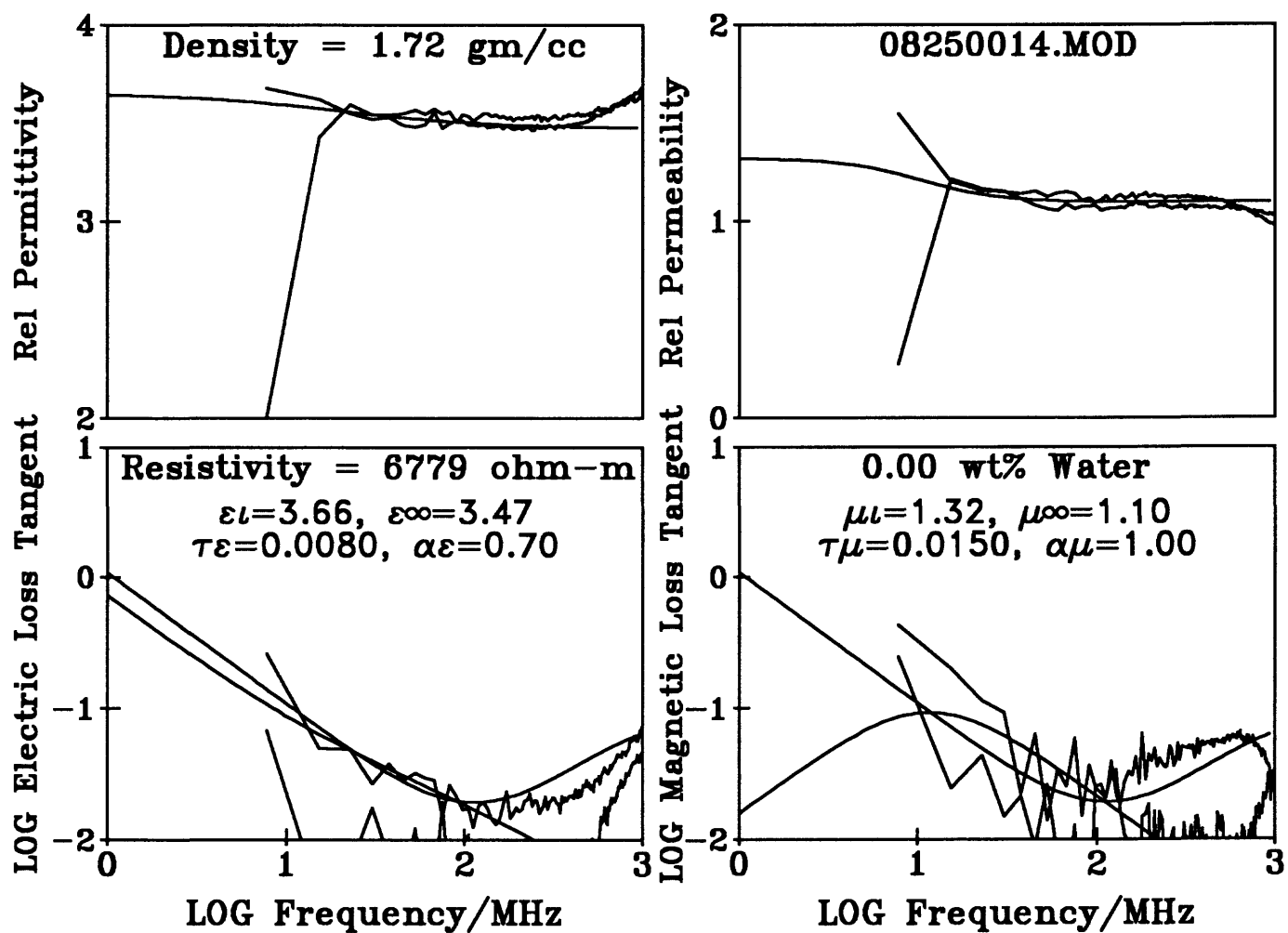
Yuma 2040m Butler Fe304 sand in stream channel north of S0.5 #1

Figure 88 -
Natural state electromagnetic properties with water content preserved in sealed, taped,
sample bottle.



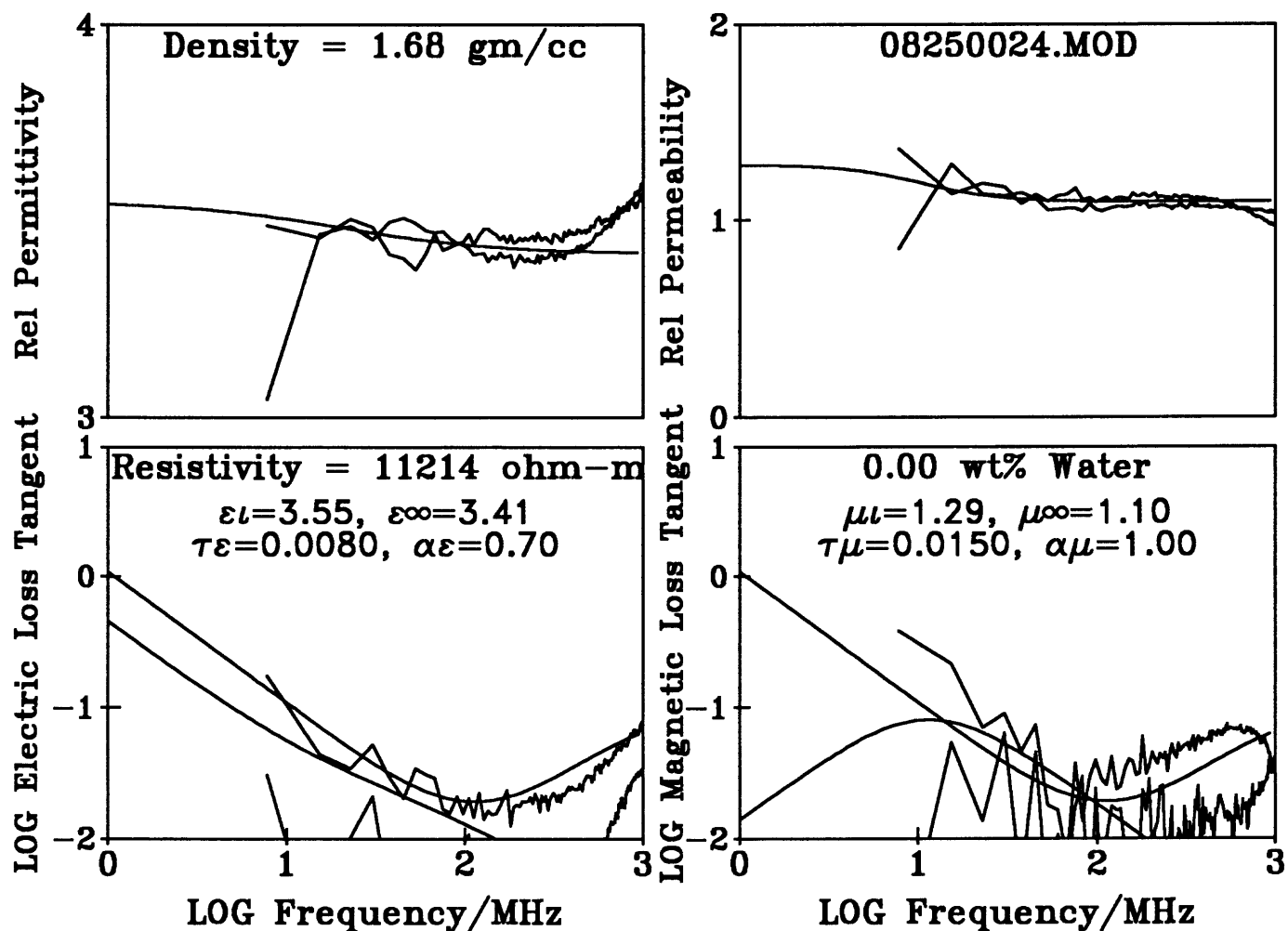
Yuma 2040m Butler Fe304 sand in stream channel north of S0.5 #2

Figure 89 -
Natural state electromagnetic properties with water content preserved in sealed, taped,
sample bottle.



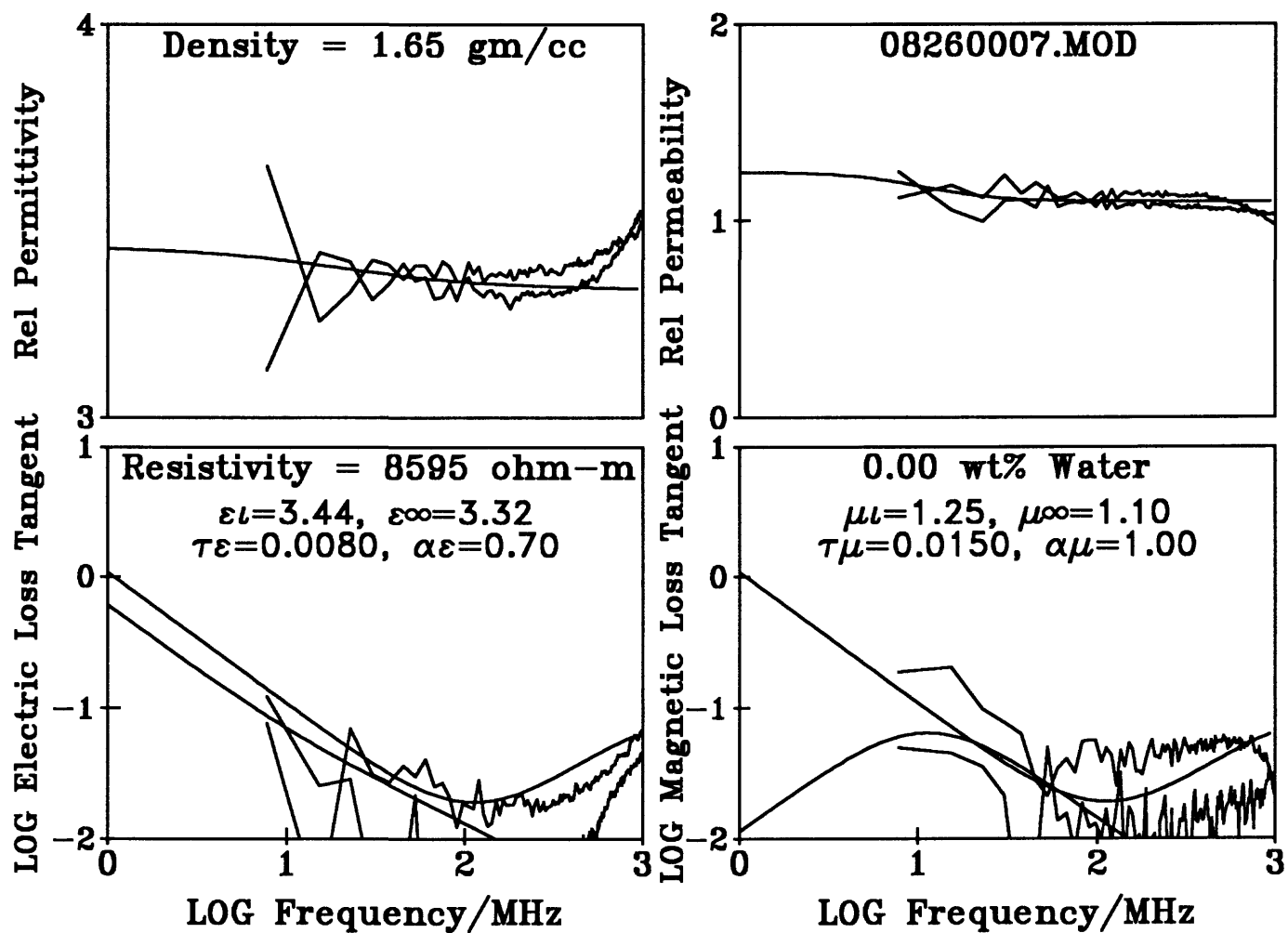
Yuma 2040m Butler Fe304 sand in stream channel N of S0.5 #3 vac. dried

Figure 90 -



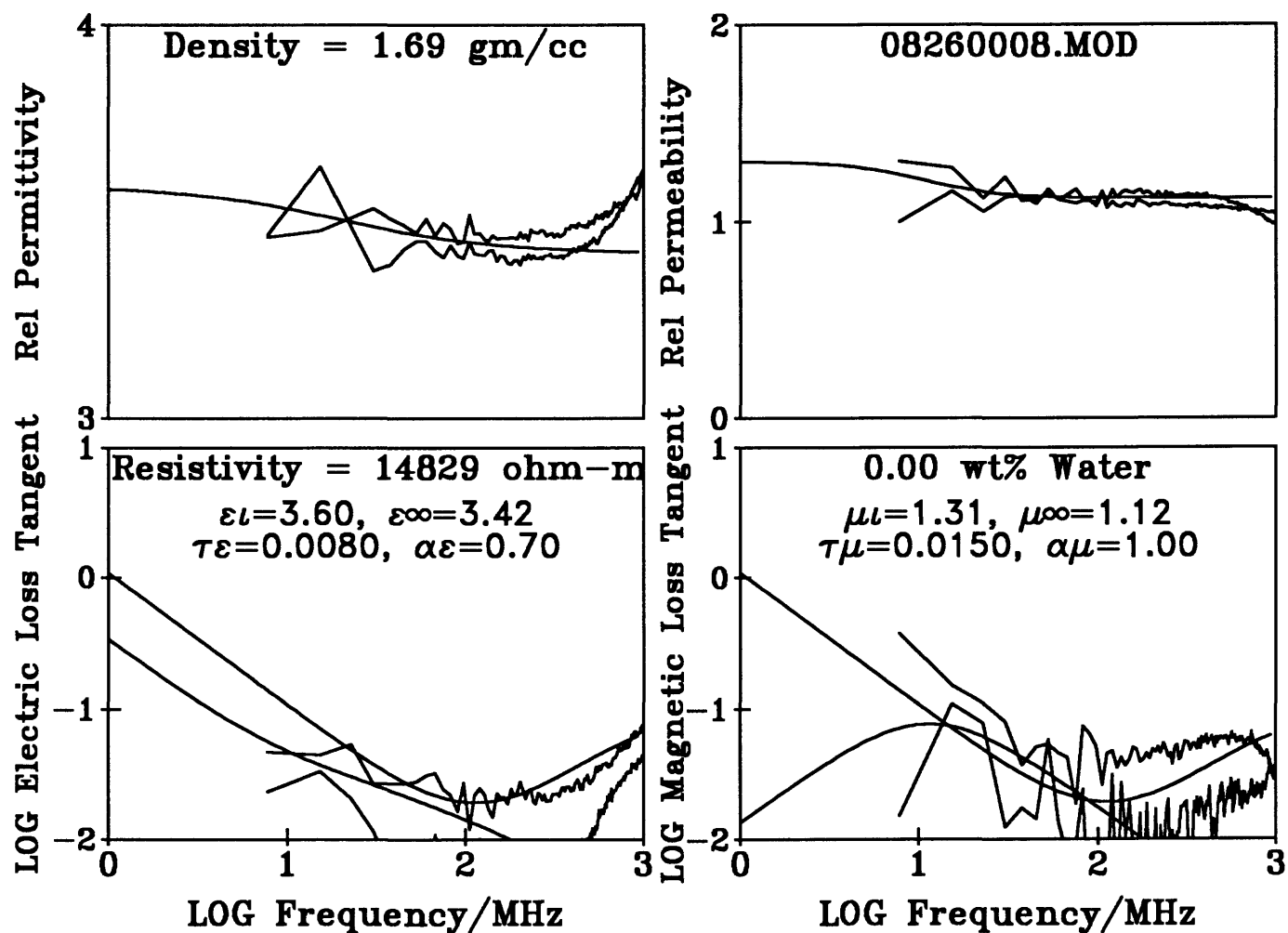
Yuma 2040m Butler Fe304 sand in stream channel N of S0.5 #4 vac. dried

Figure 91 -



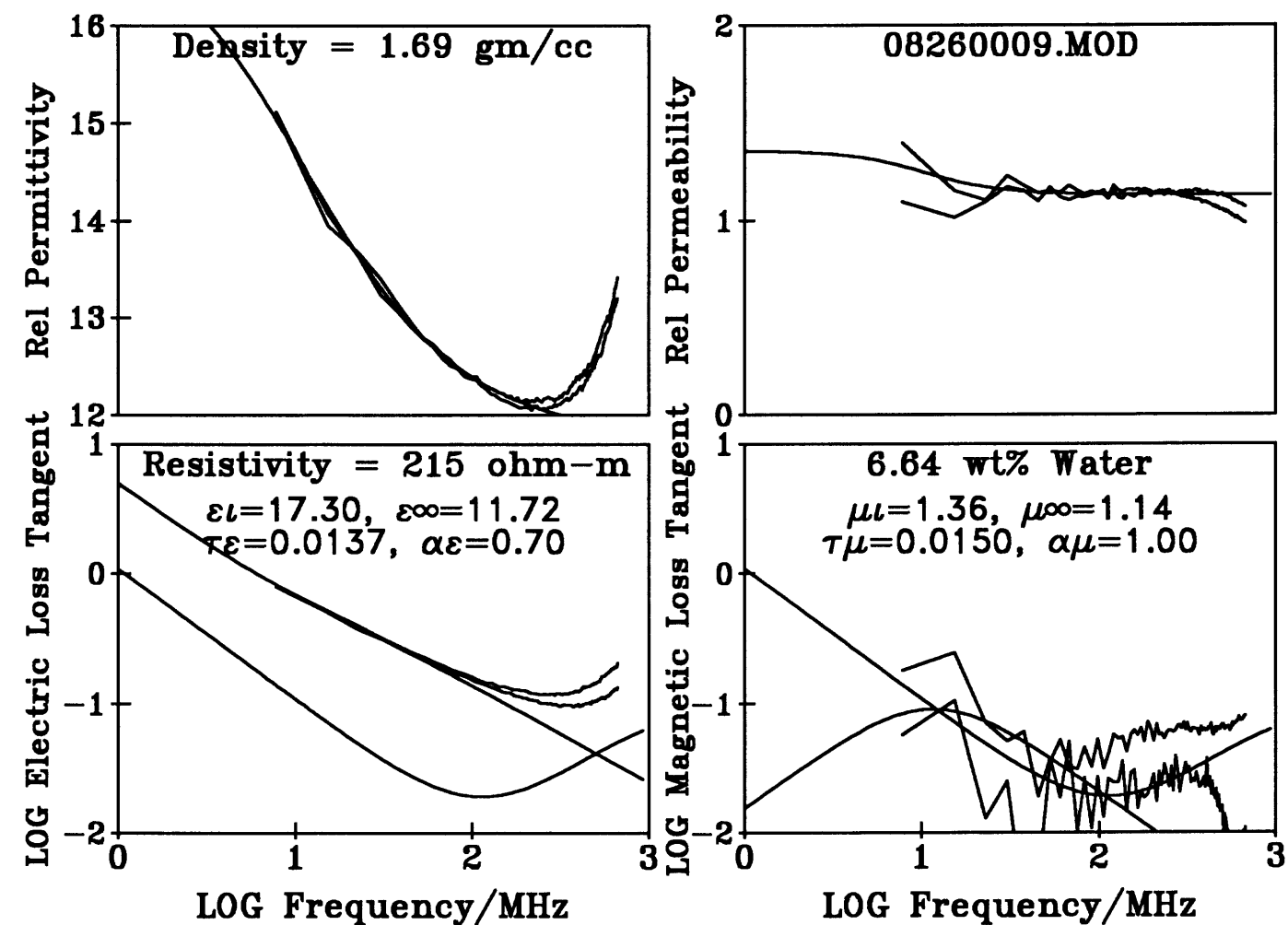
Yuma 2040m Butler Fe304 sand in stream channel N of S0.5 #5 vac. dried

Figure 92 - Vacuum dry



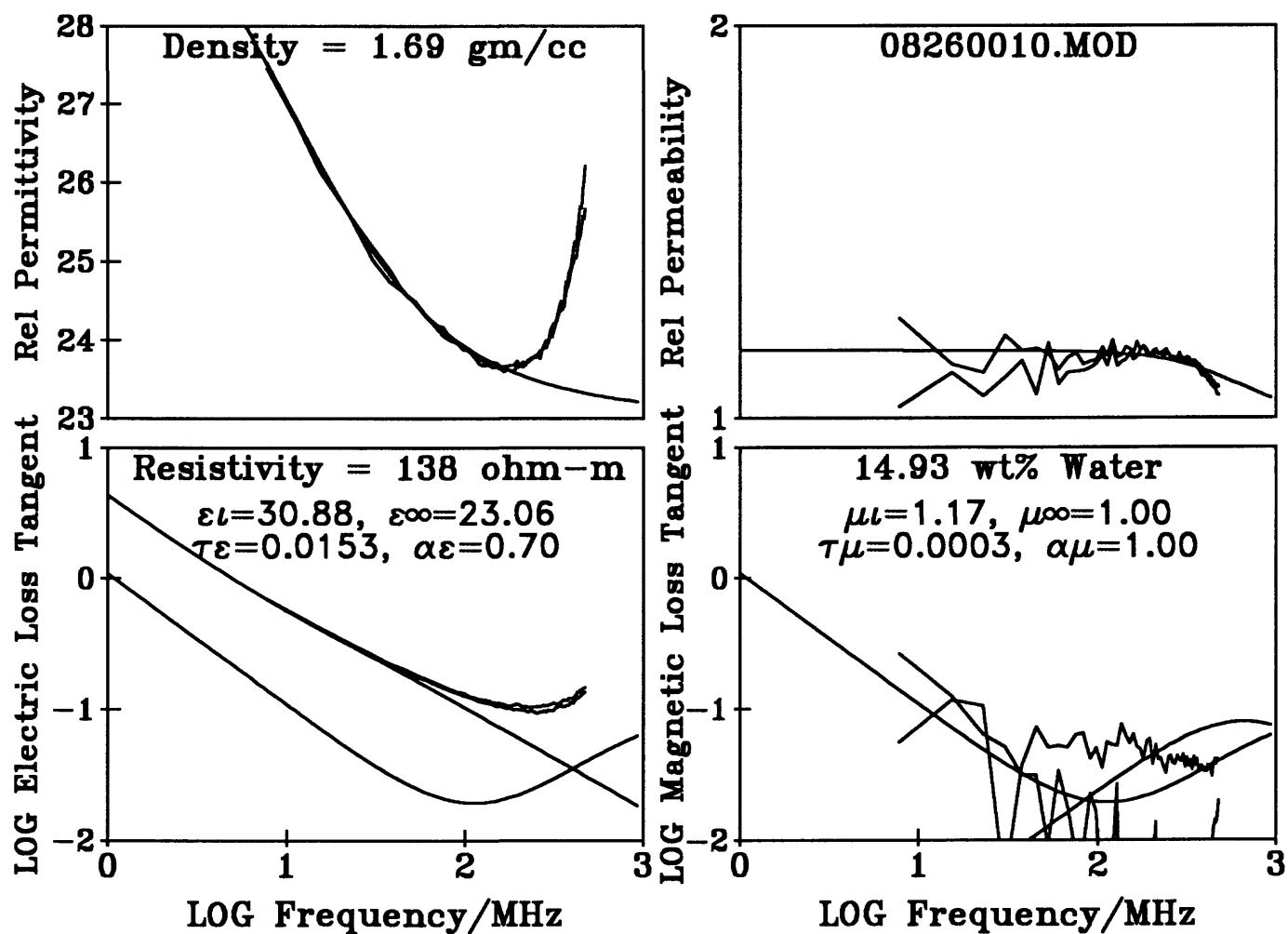
Yuma 2040m Butler Fe304 sand in stream channel N of S0.5 #6 vac. dried

Figure 93 -



Yuma 2040m Butler Fe304 stream channel sand N of S0.5 #6 9-drops water

Figure 94 -



Yuma 2040m Butler Fe304 sand in stream channel N of S0.5 #6 water sat.

Figure 95 -

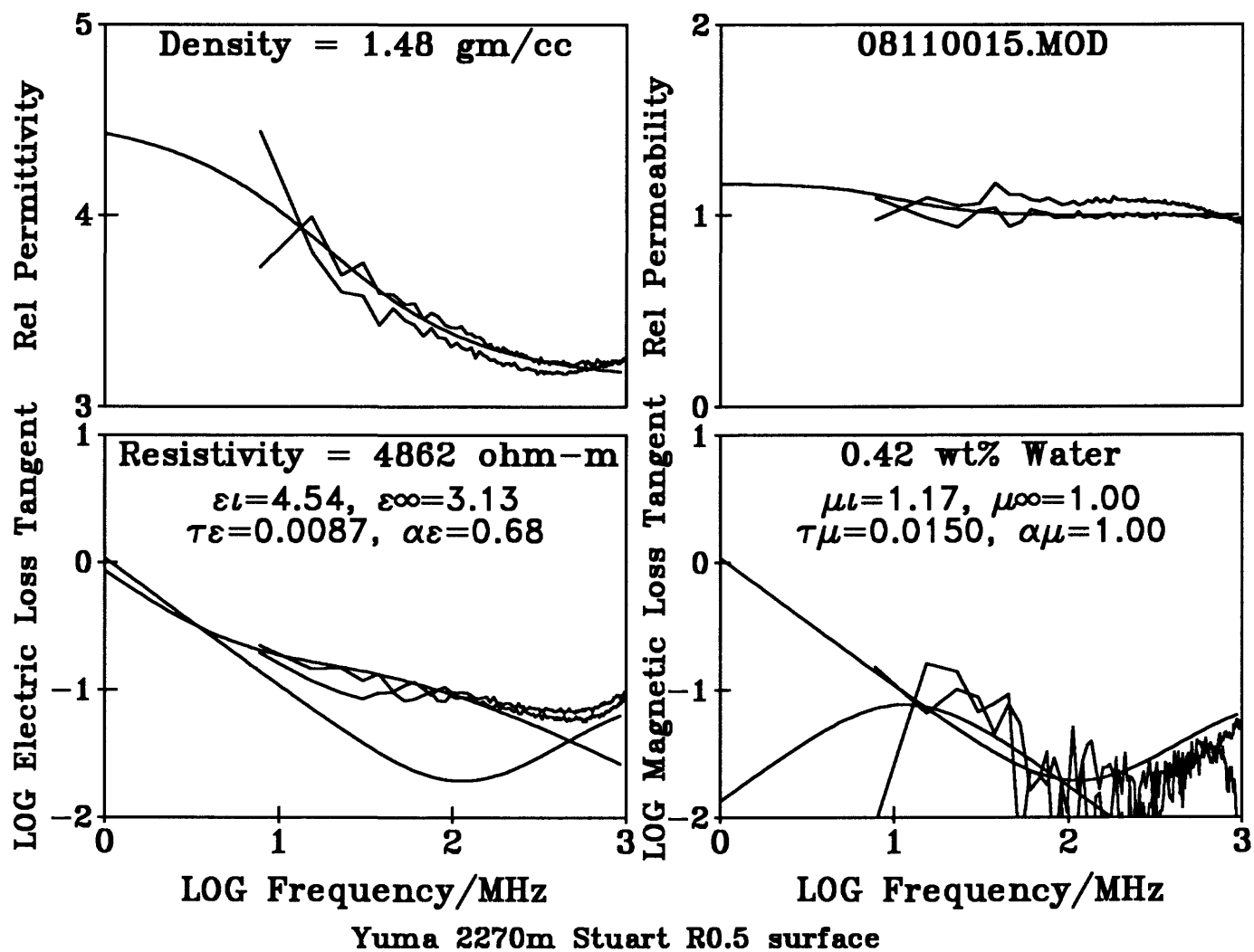


Figure 96 -
Natural state electromagnetic properties with water content preserved in sealed, taped, sample bottle.

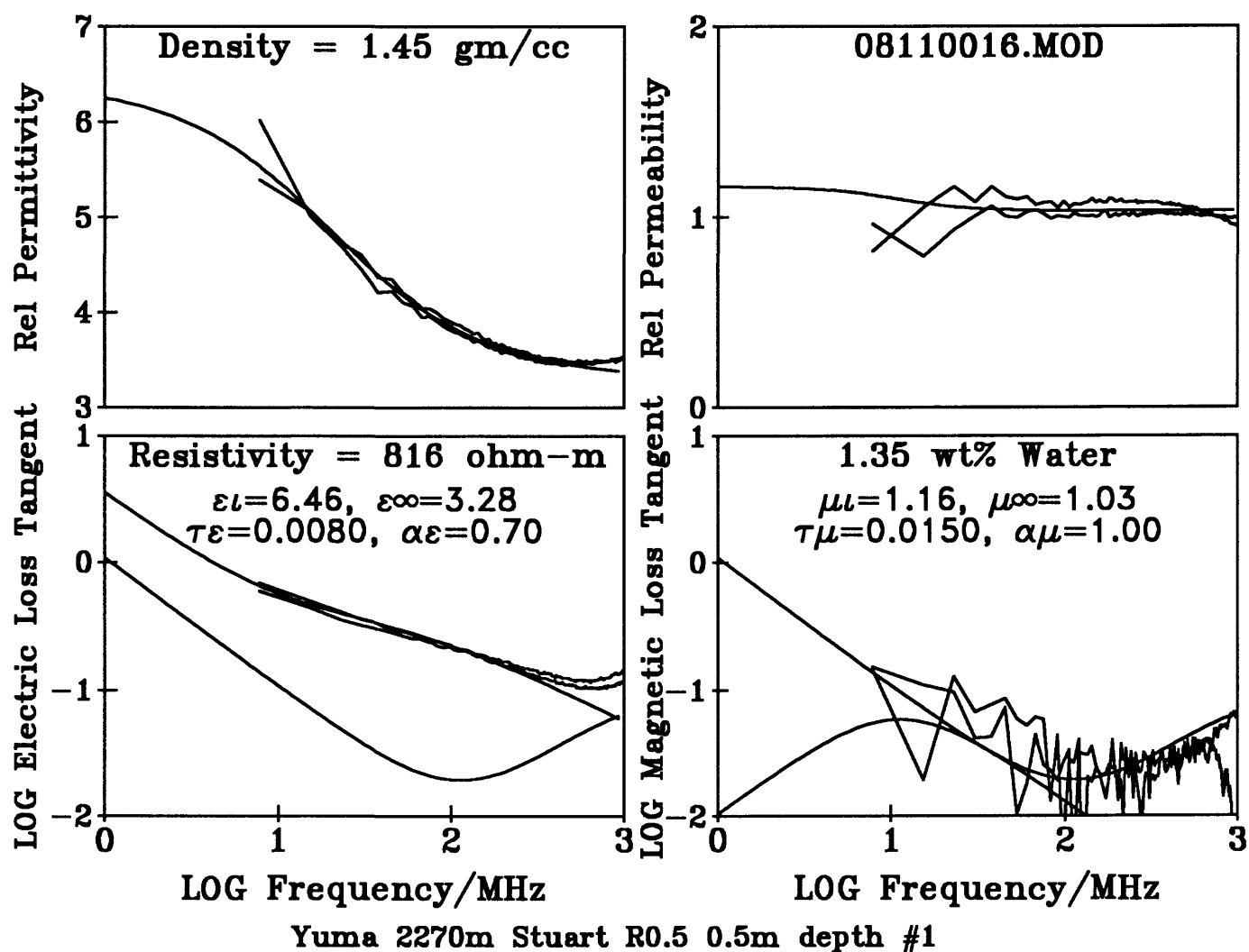


Figure 97 -
Natural state electromagnetic properties with water content preserved in sealed, taped, sample bottle.

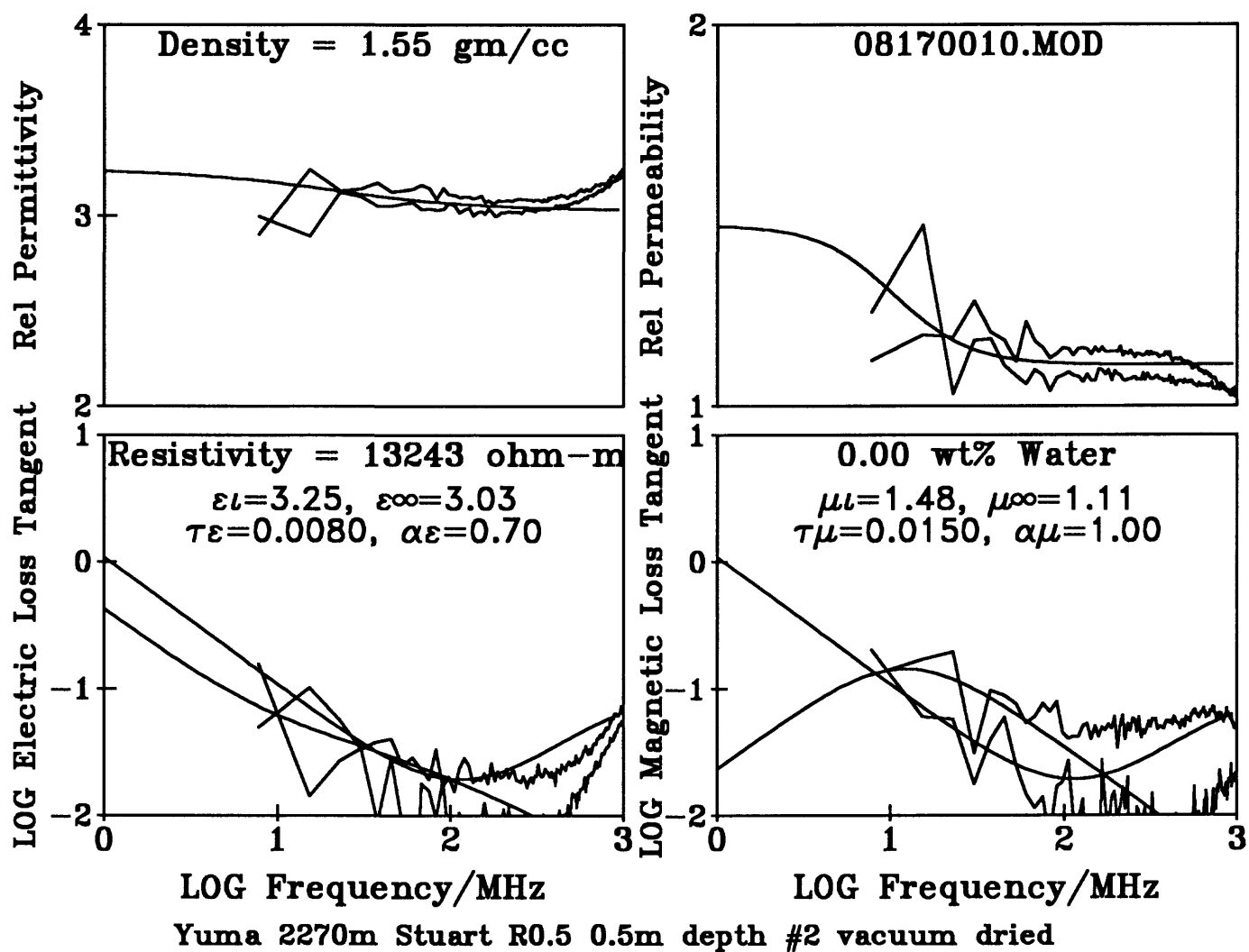


Figure 98 -

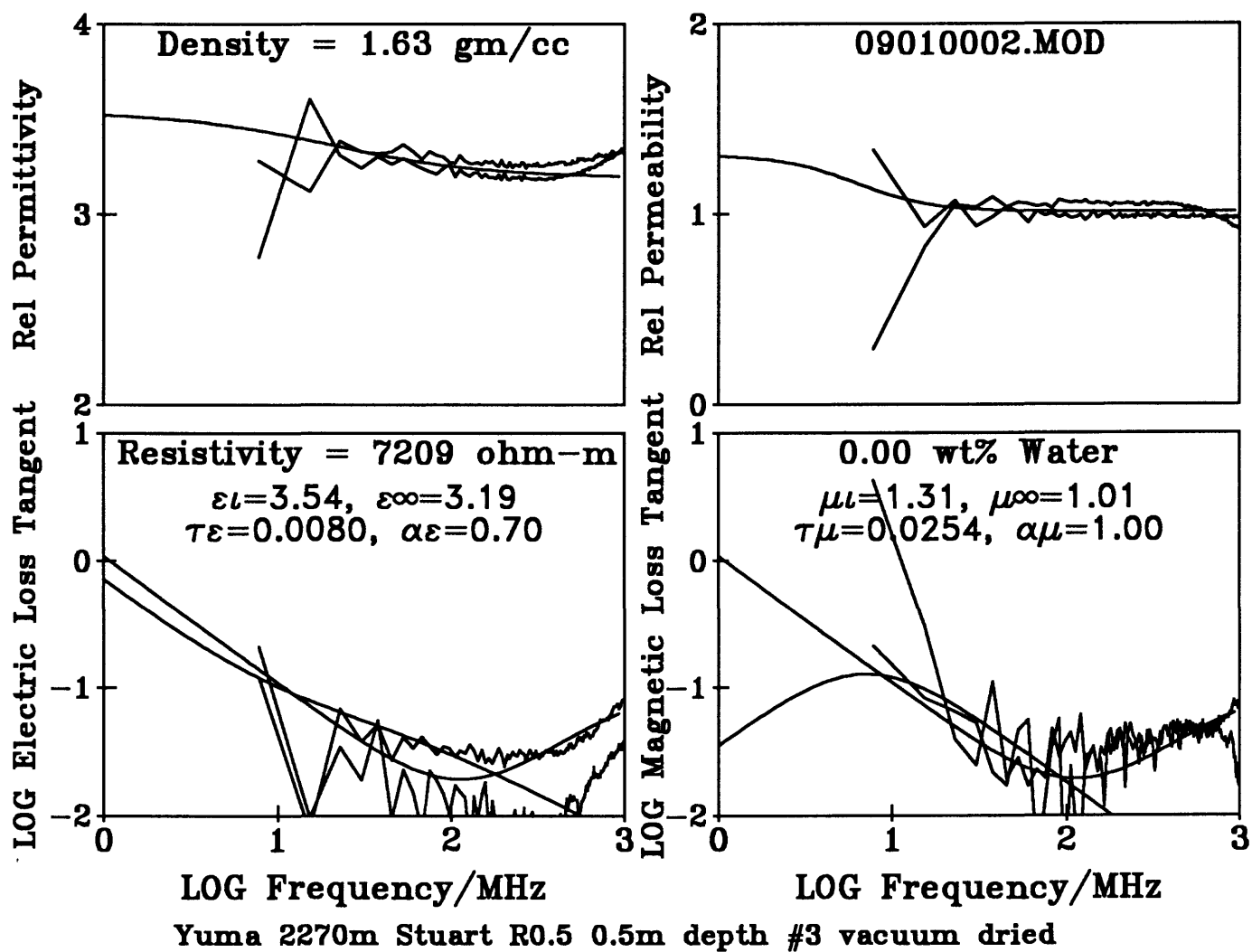


Figure 99 -

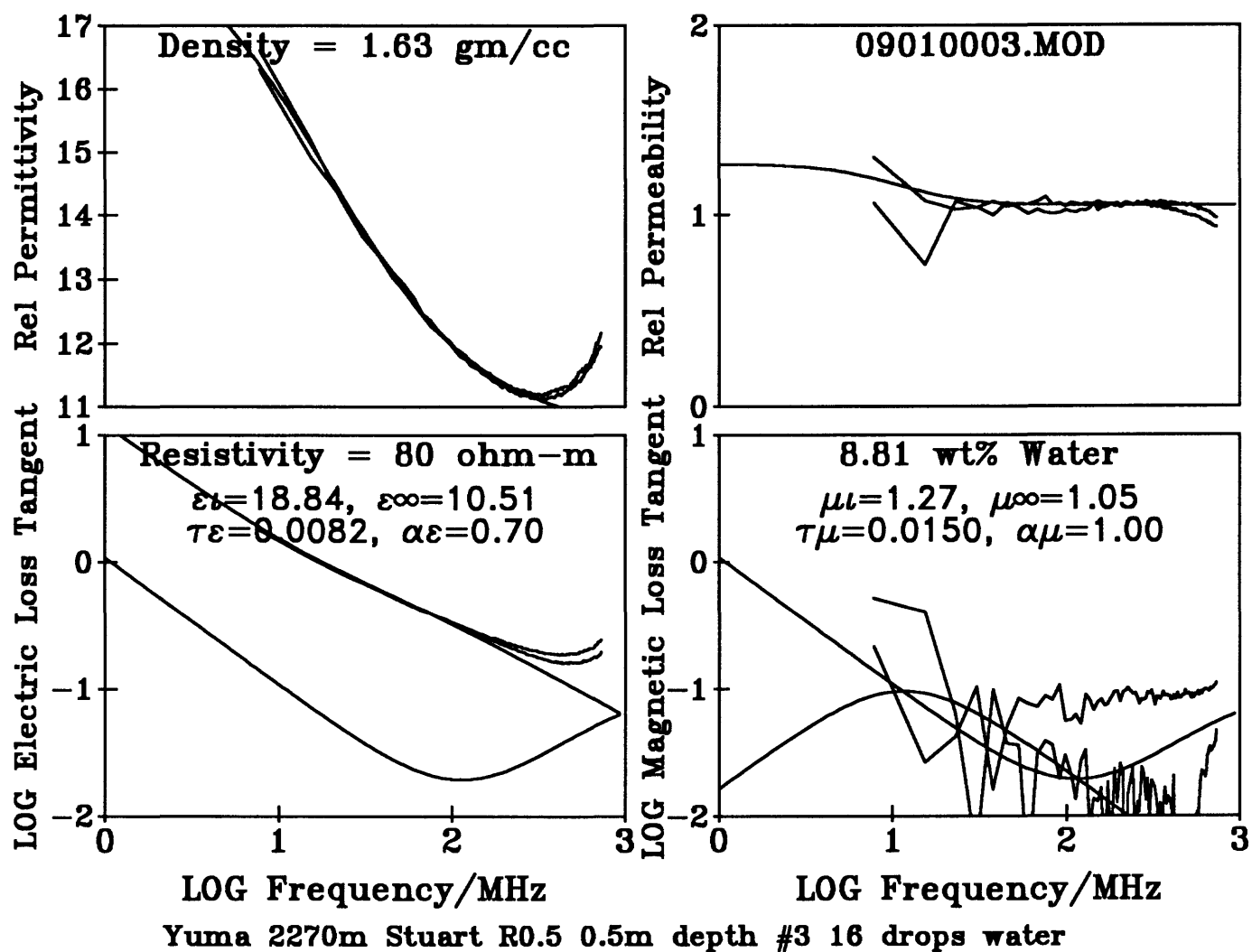


Figure 100 -

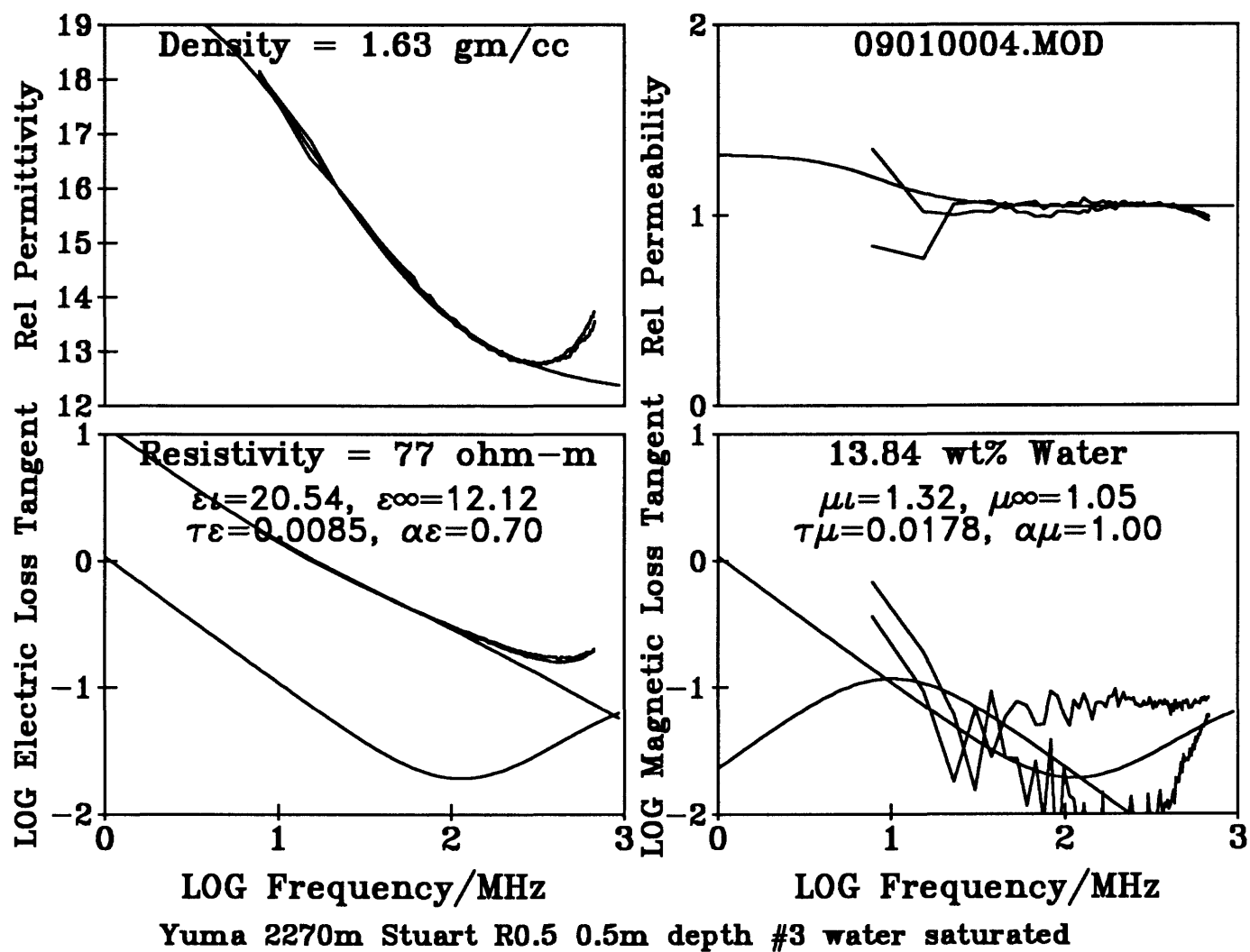


Figure 101 -

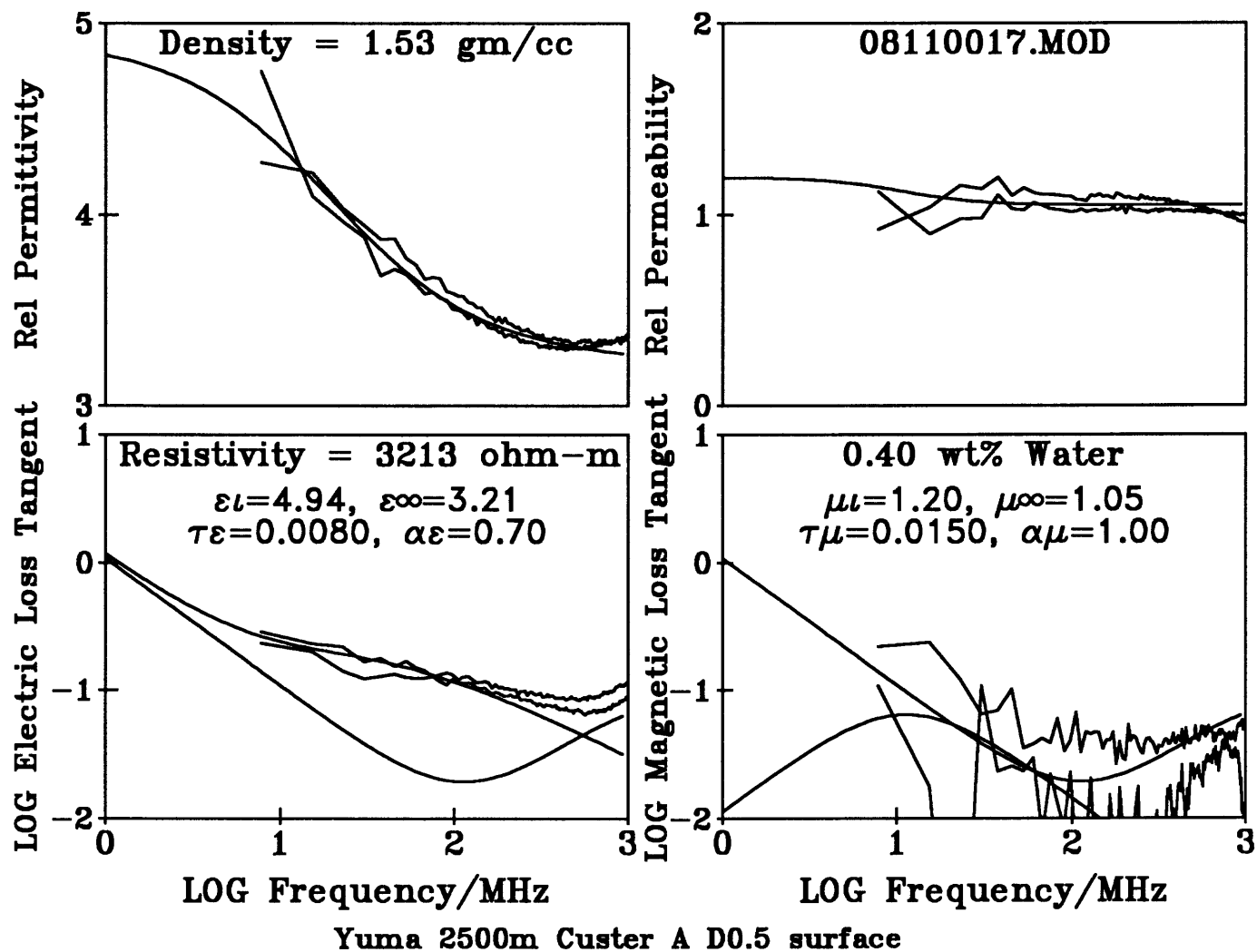


Figure 102 -
Natural state electromagnetic properties with water content preserved in sealed, taped,
sample bottle.

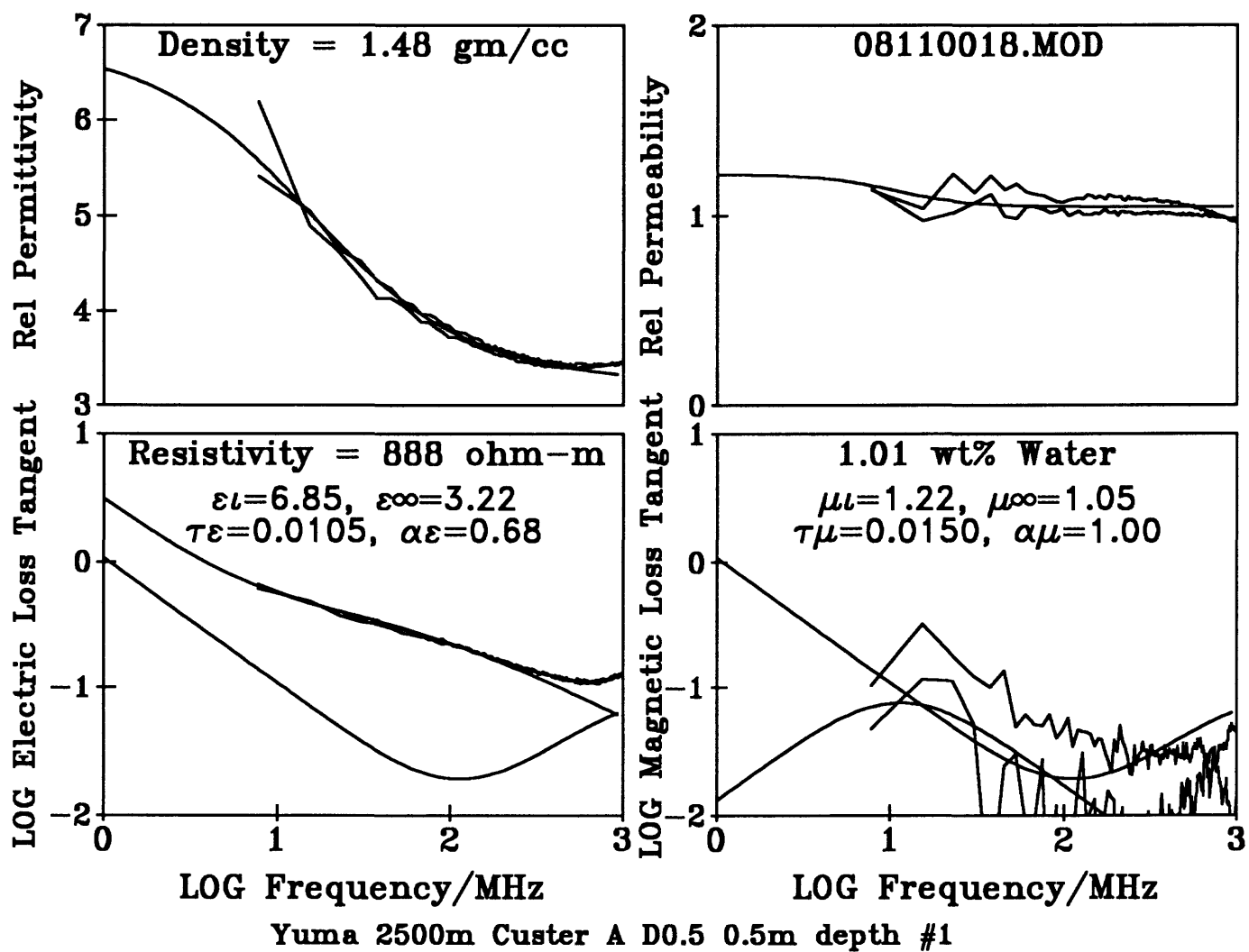


Figure 103 -
Natural state electromagnetic properties with water content preserved in sealed, taped,
sample bottle.

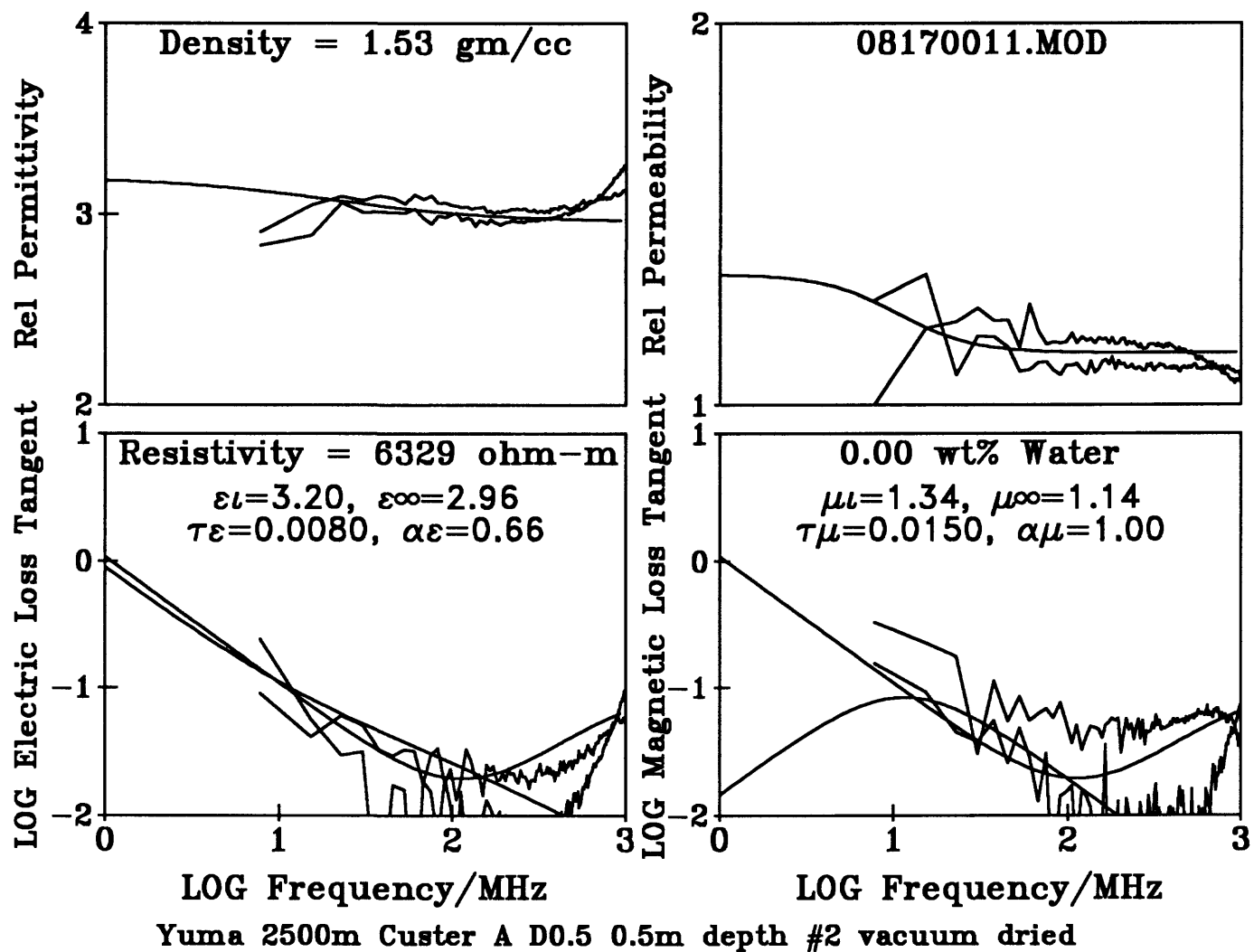


Figure 104 -

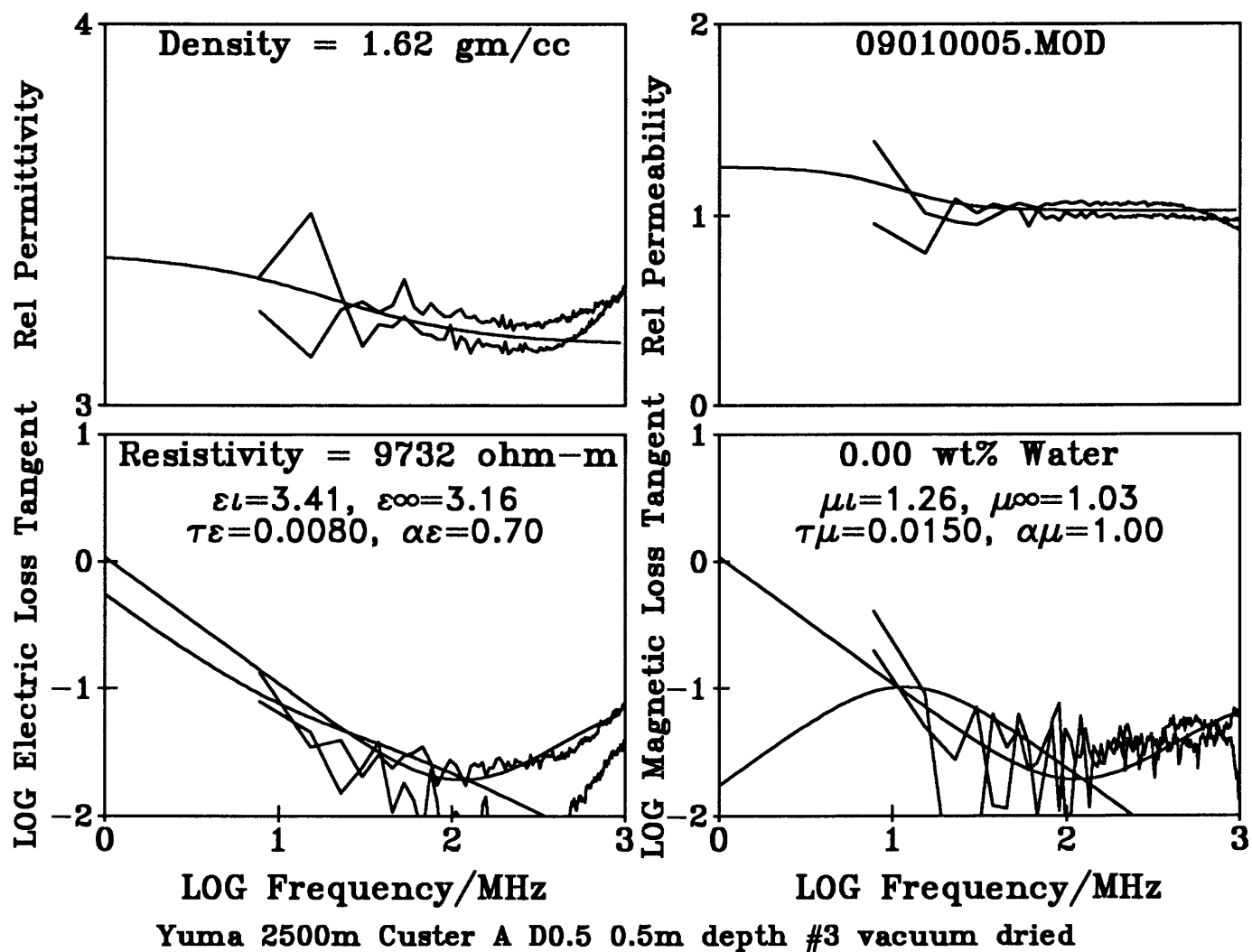


Figure 105 -

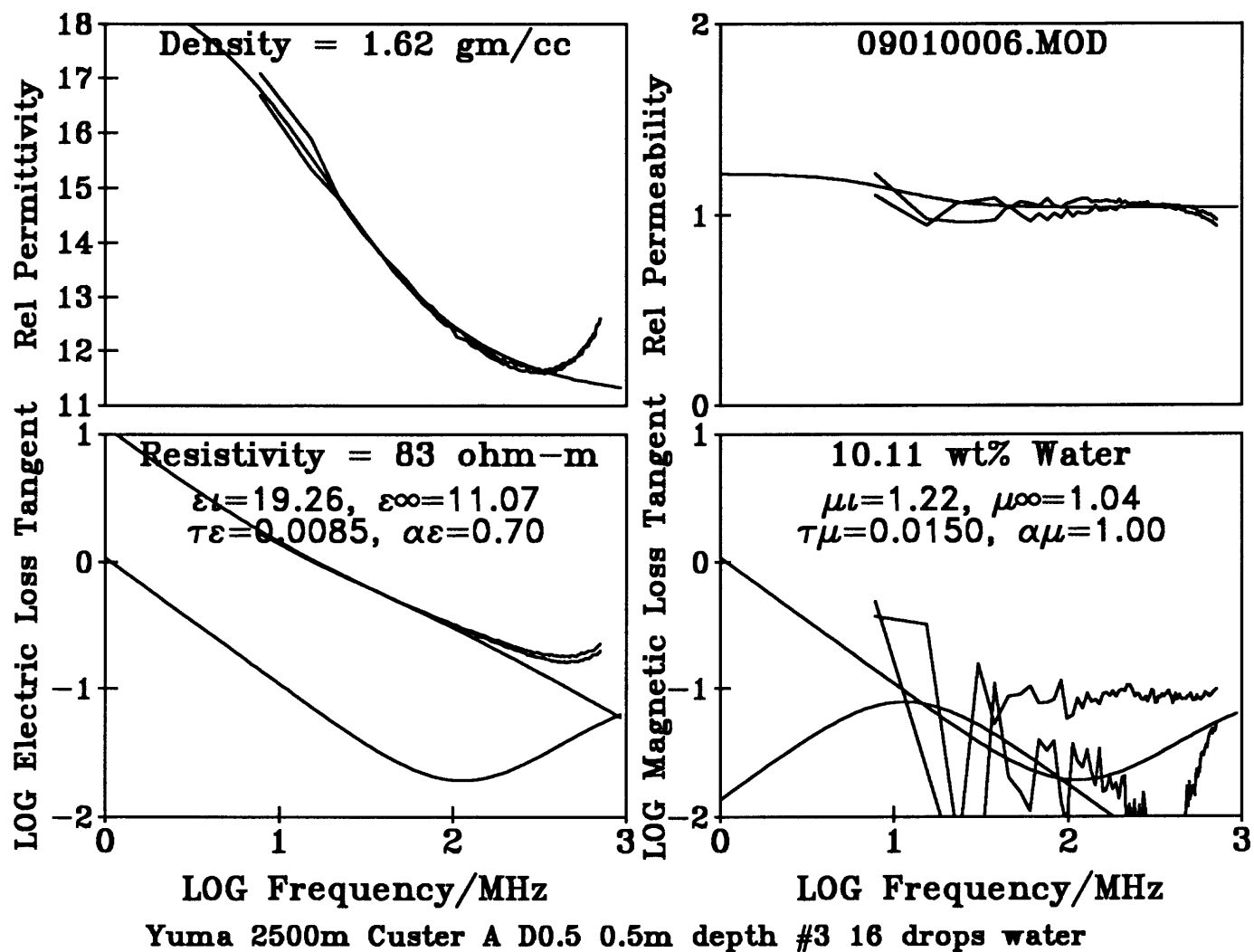


Figure 106 -

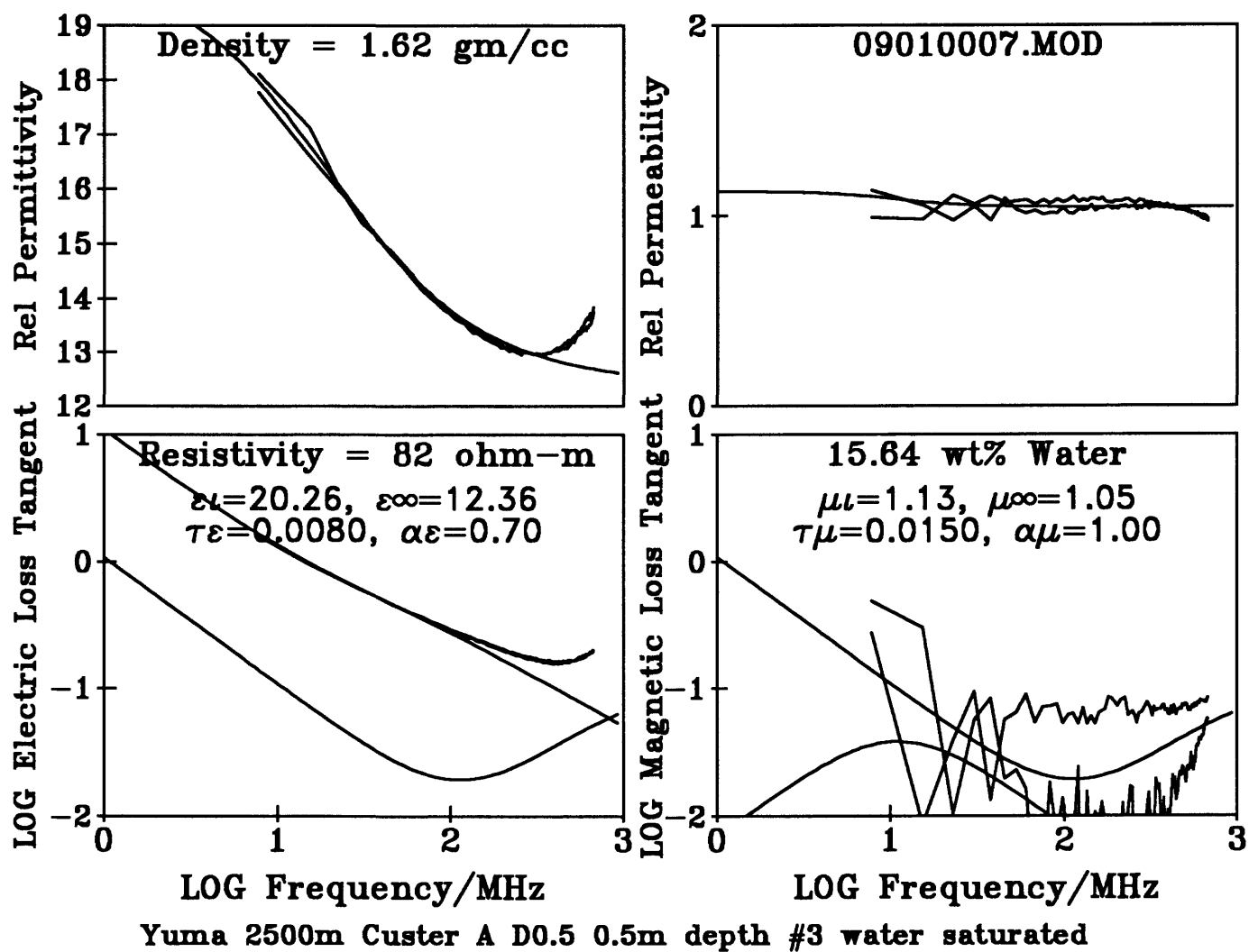


Figure 107 -

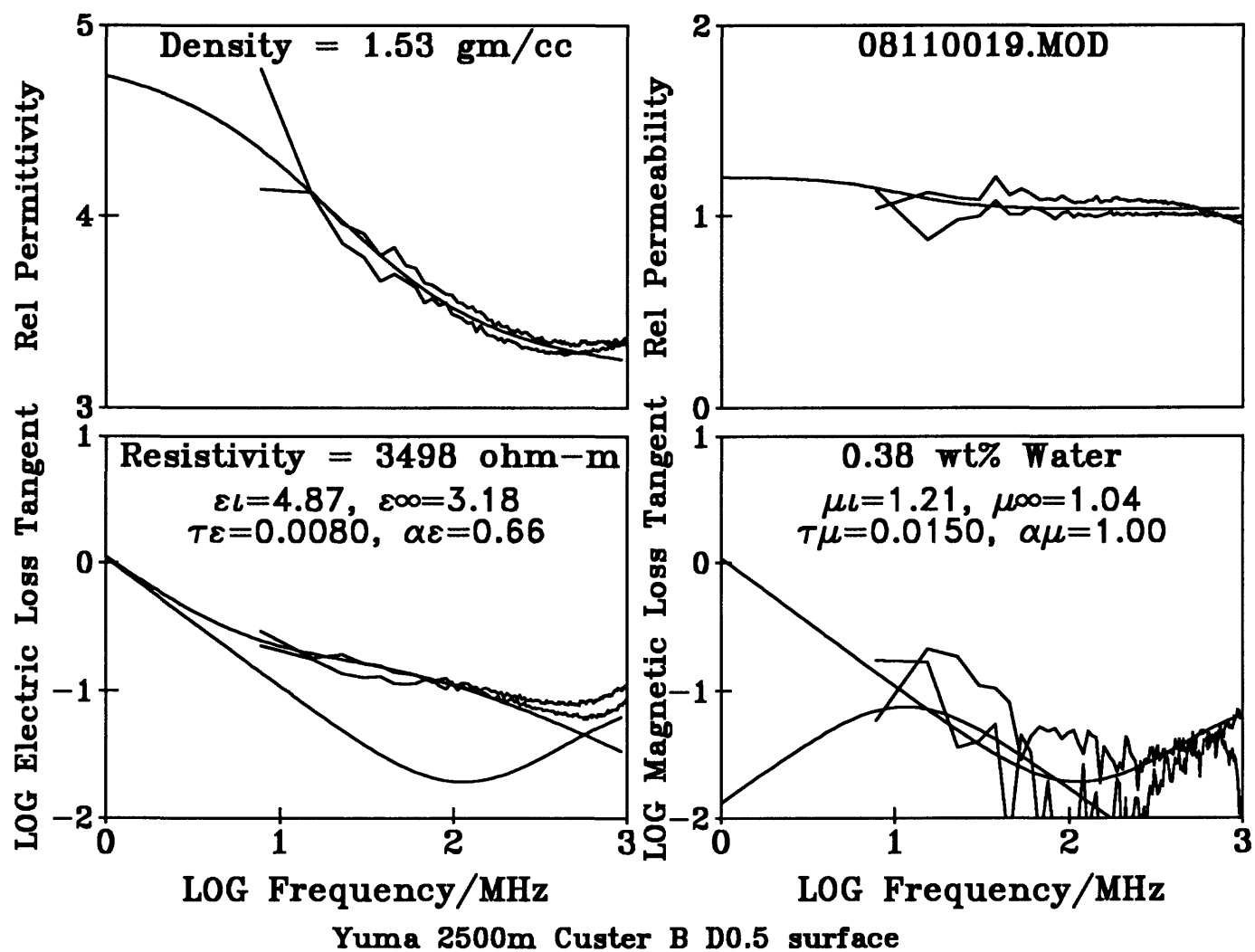


Figure 108 -
Natural state electromagnetic properties with water content preserved in sealed, taped,
sample bottle.

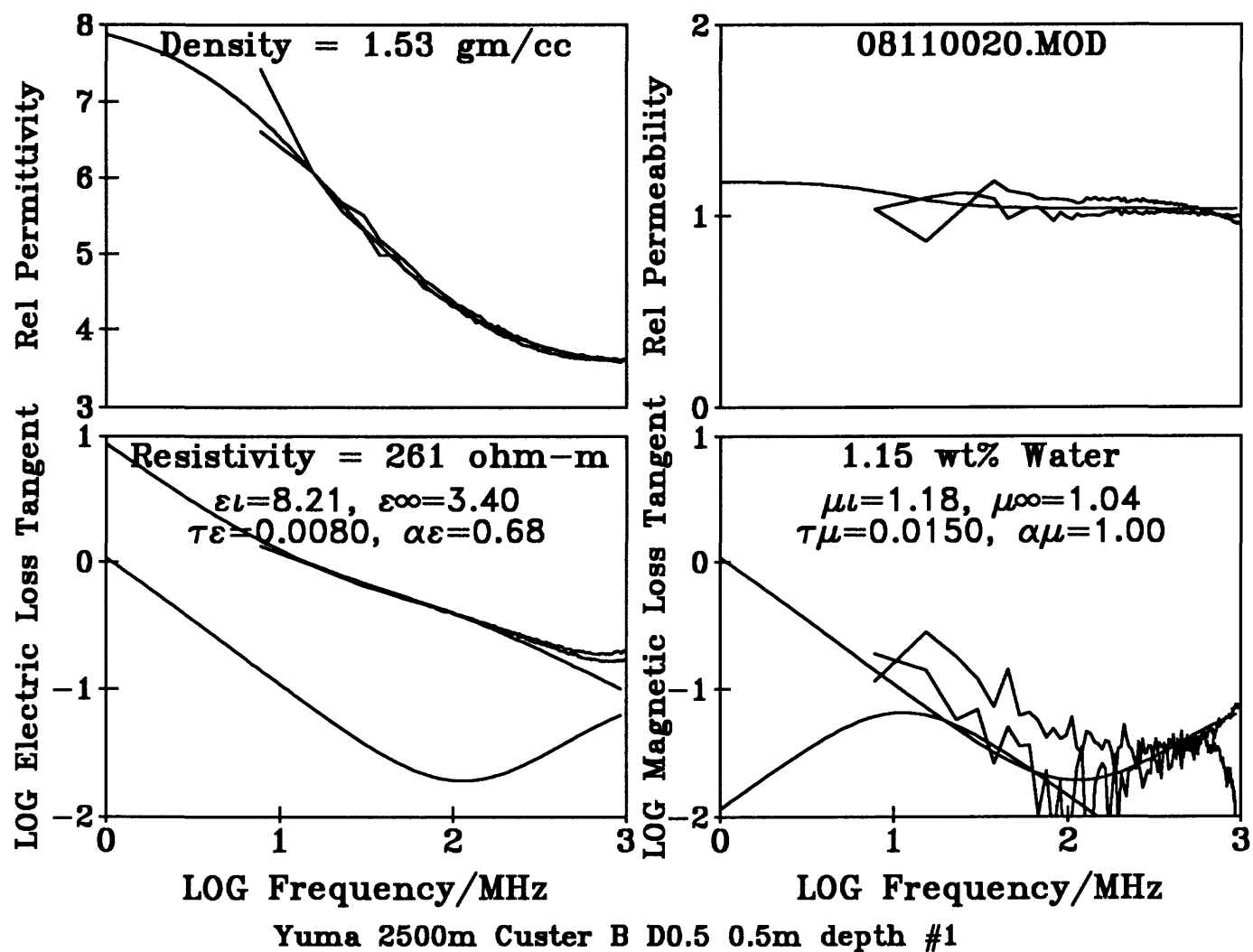


Figure 109 -
Natural state electromagnetic properties with water content preserved in sealed, taped,
sample bottle.

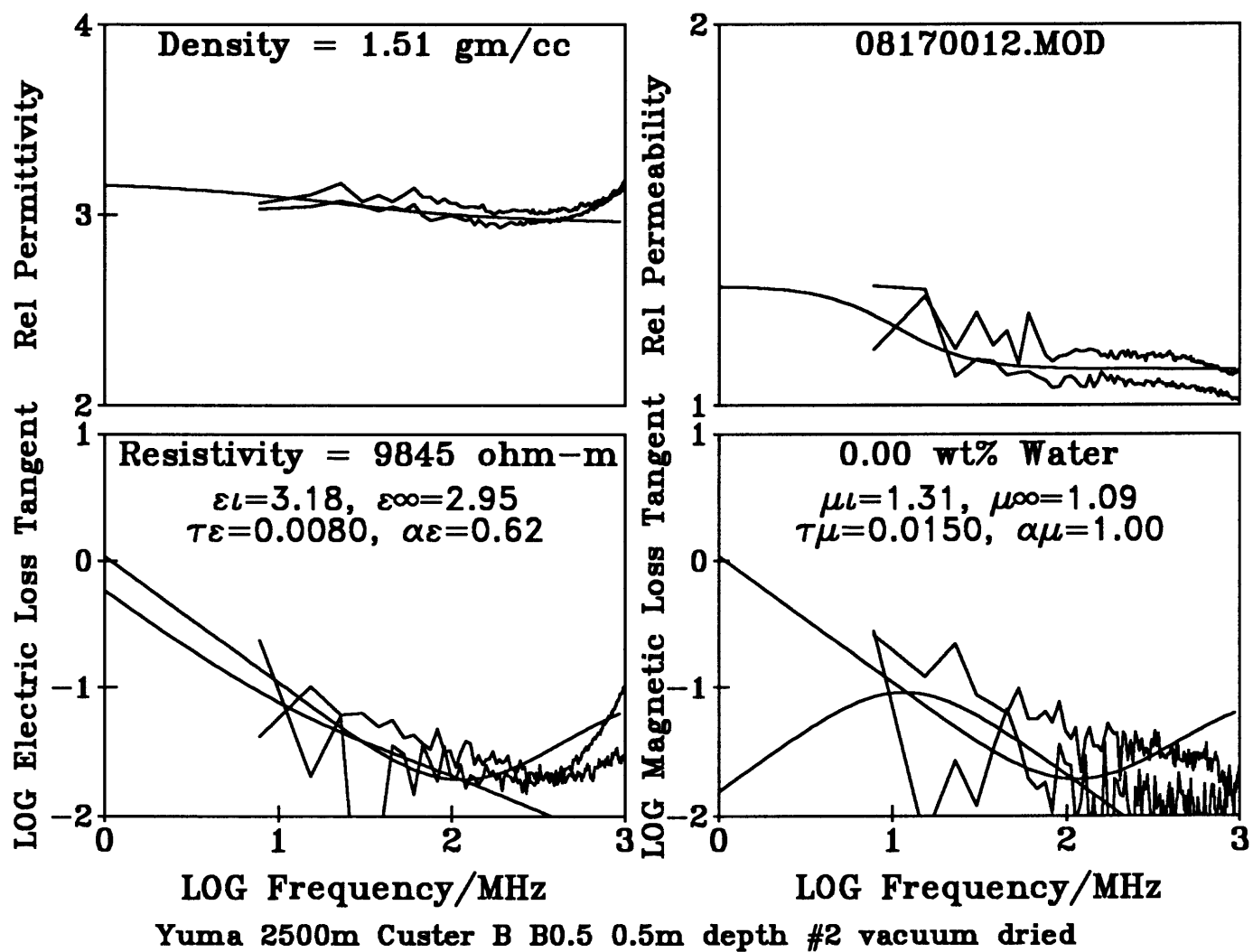


Figure 110 -

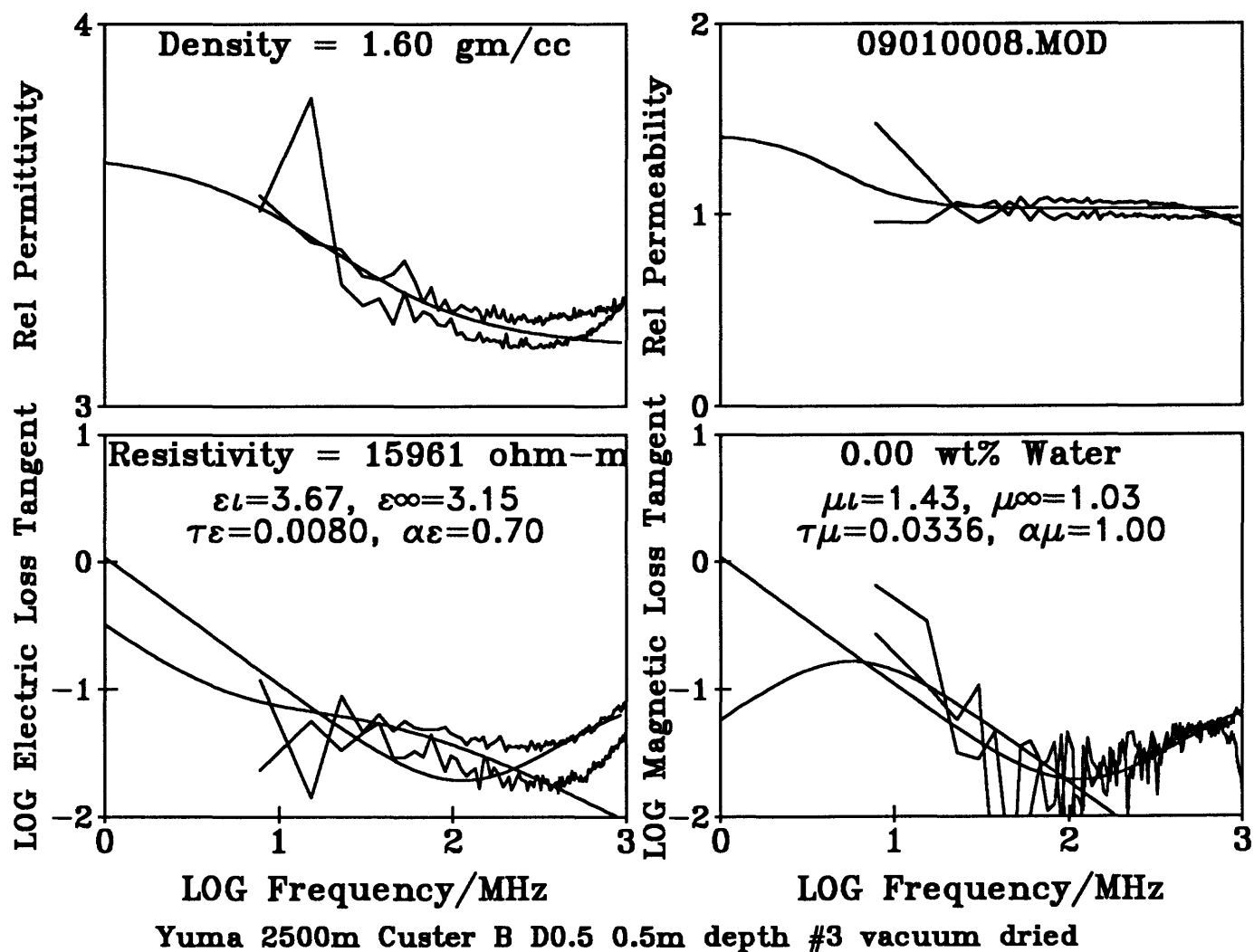


Figure 111 -

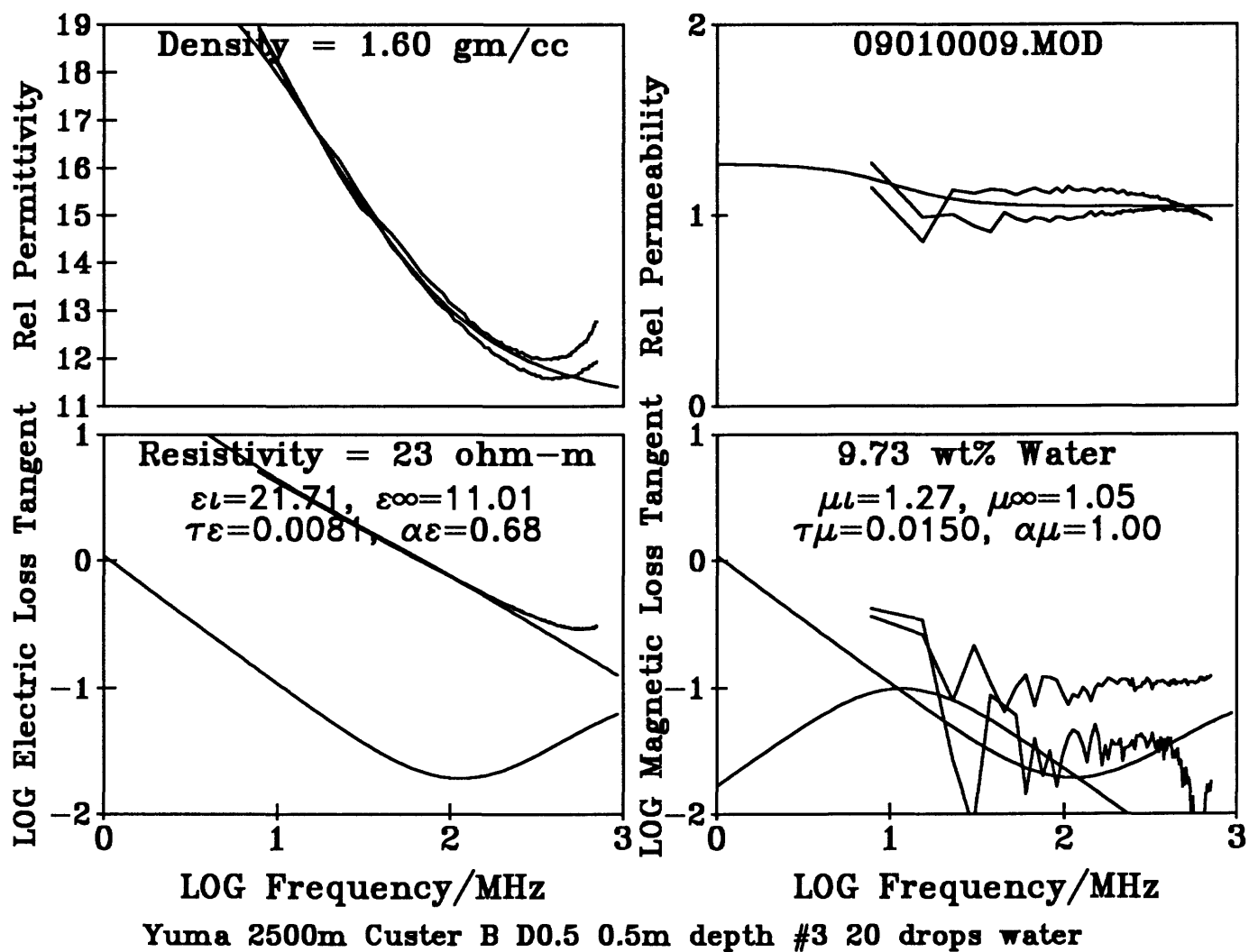


Figure 112 -

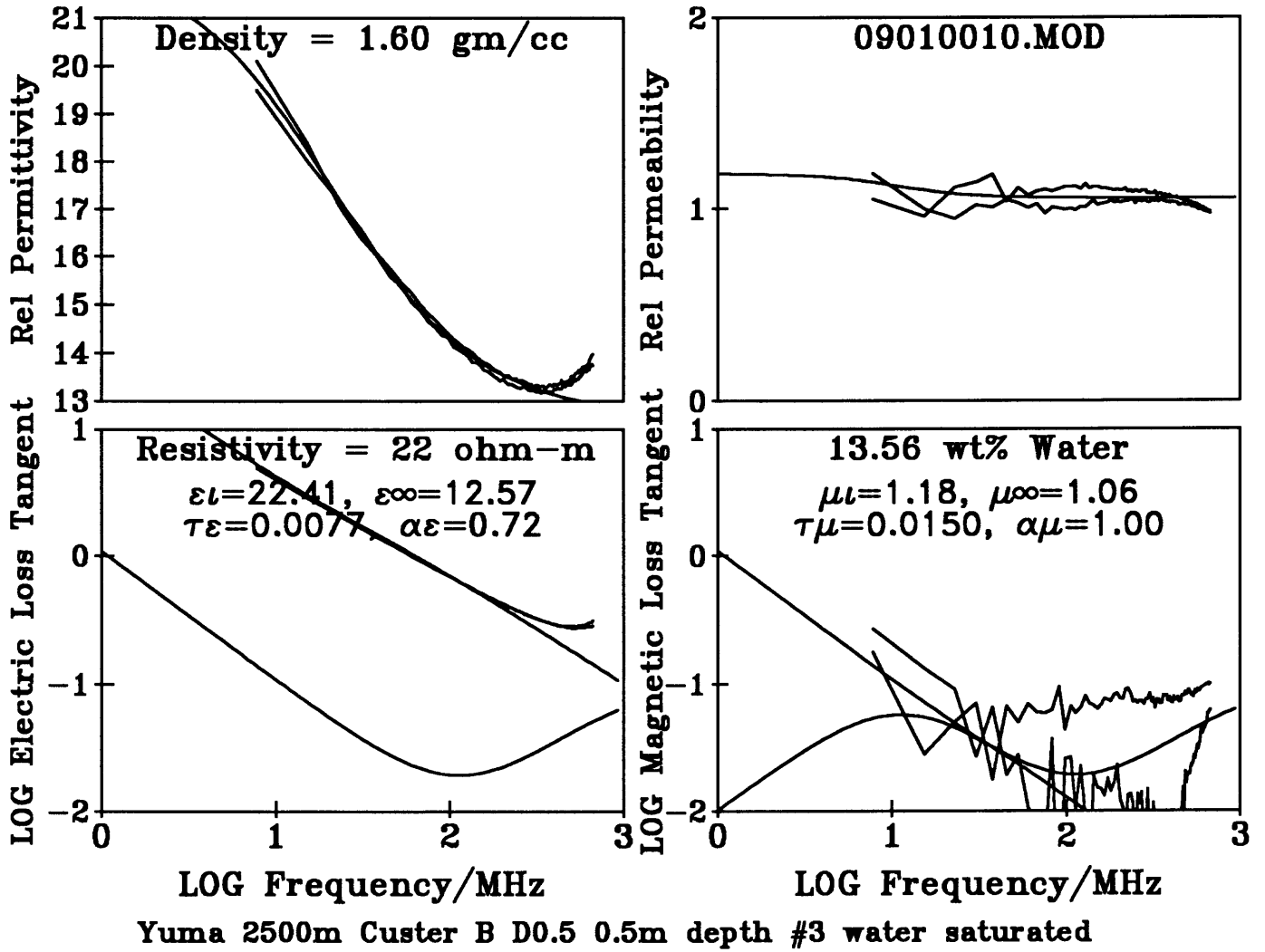


Figure 113 -

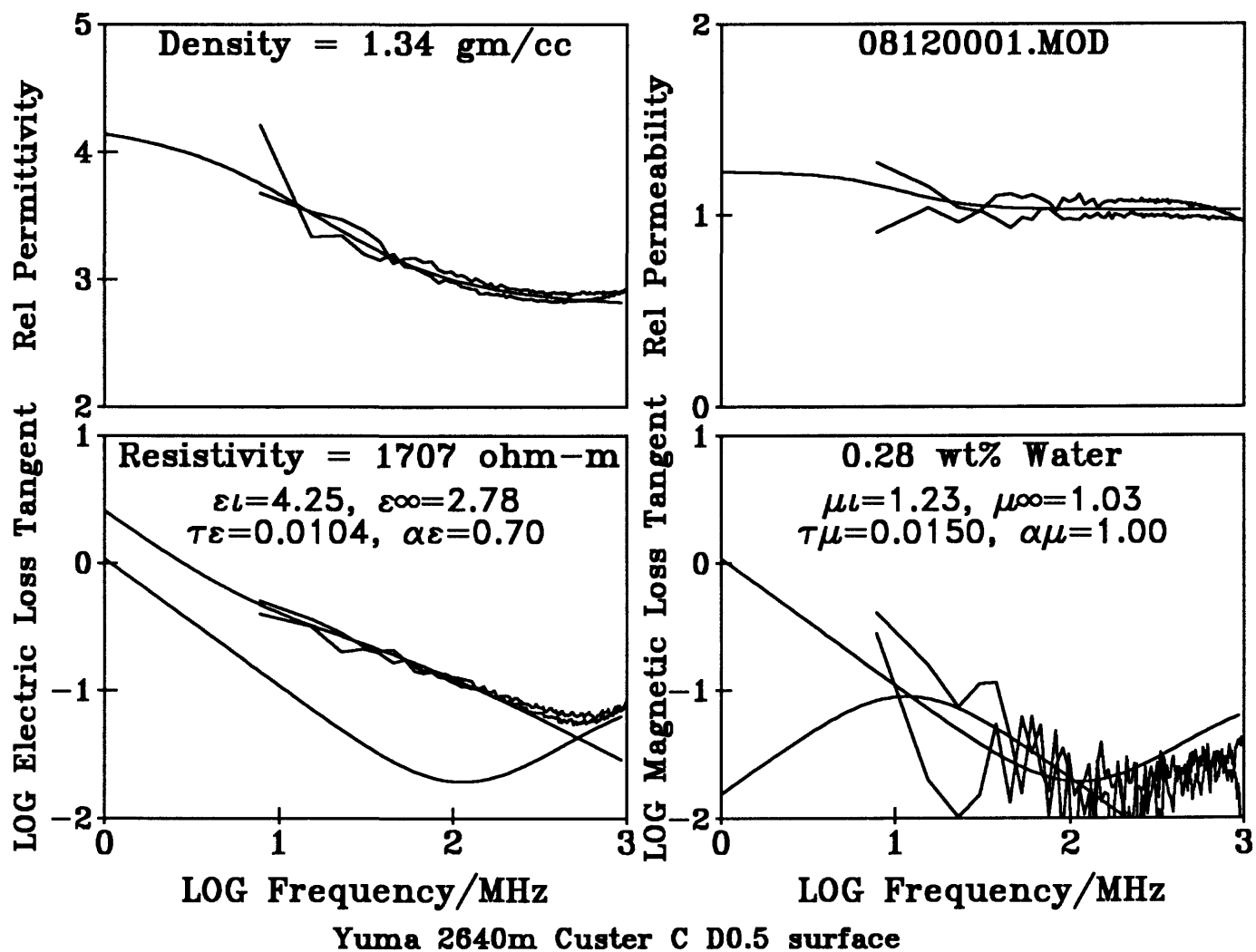


Figure 114 -
 Natural state electromagnetic properties with water content preserved in sealed, taped,
 sample bottle.

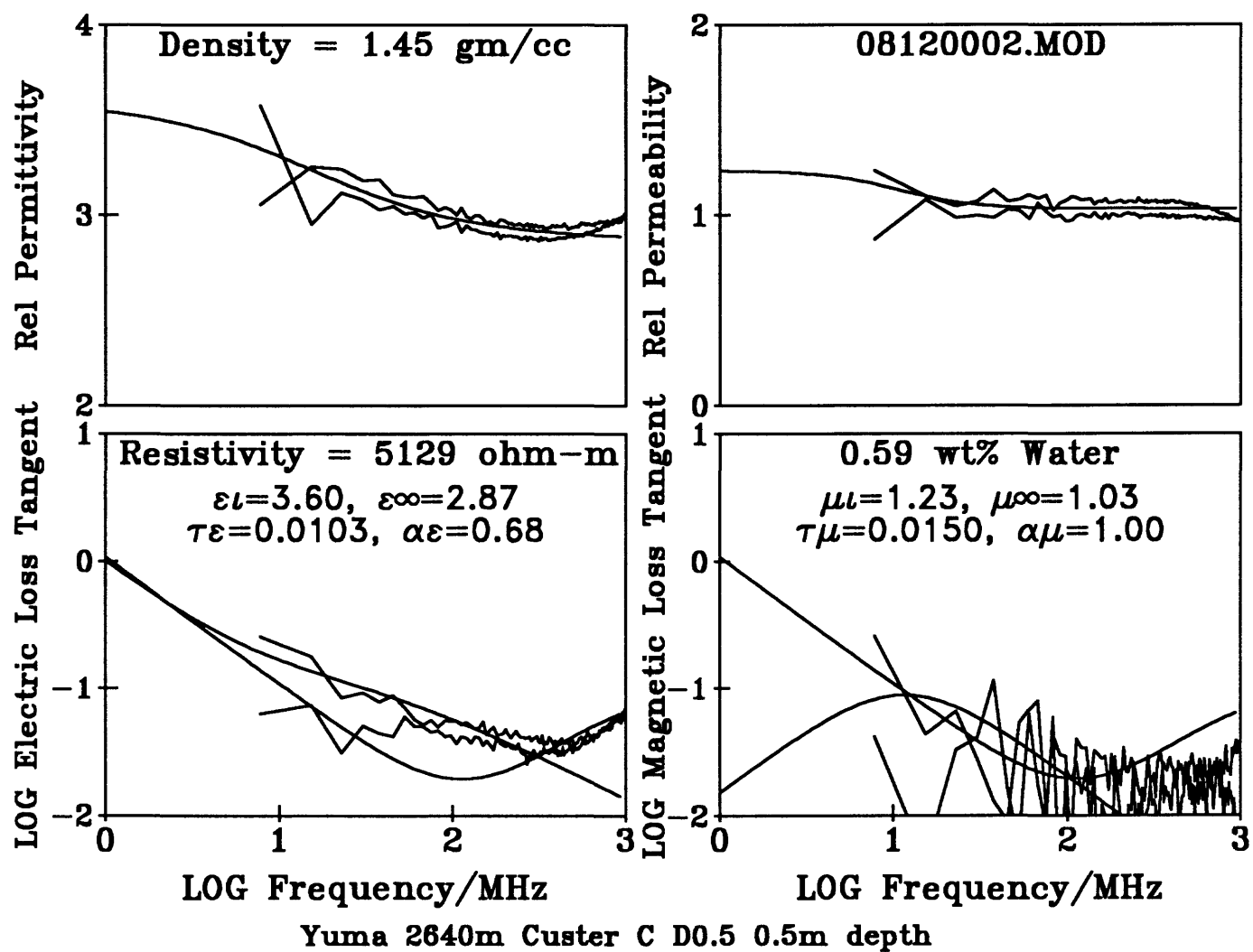


Figure 115 -
Natural state electromagnetic properties with water content preserved in sealed, taped,
sample bottle.

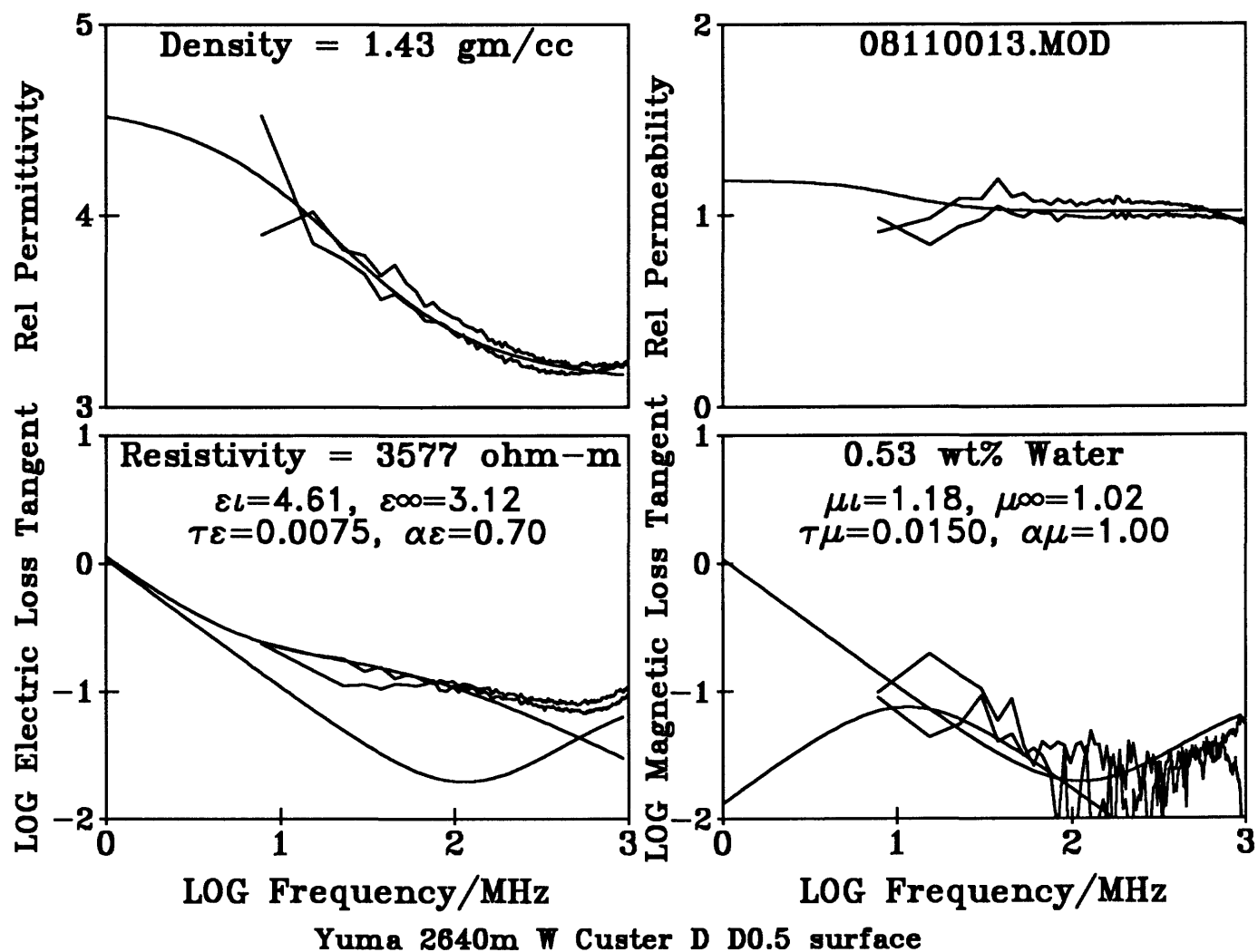


Figure 116 -
Natural state electromagnetic properties with water content preserved in sealed, taped,
sample bottle.

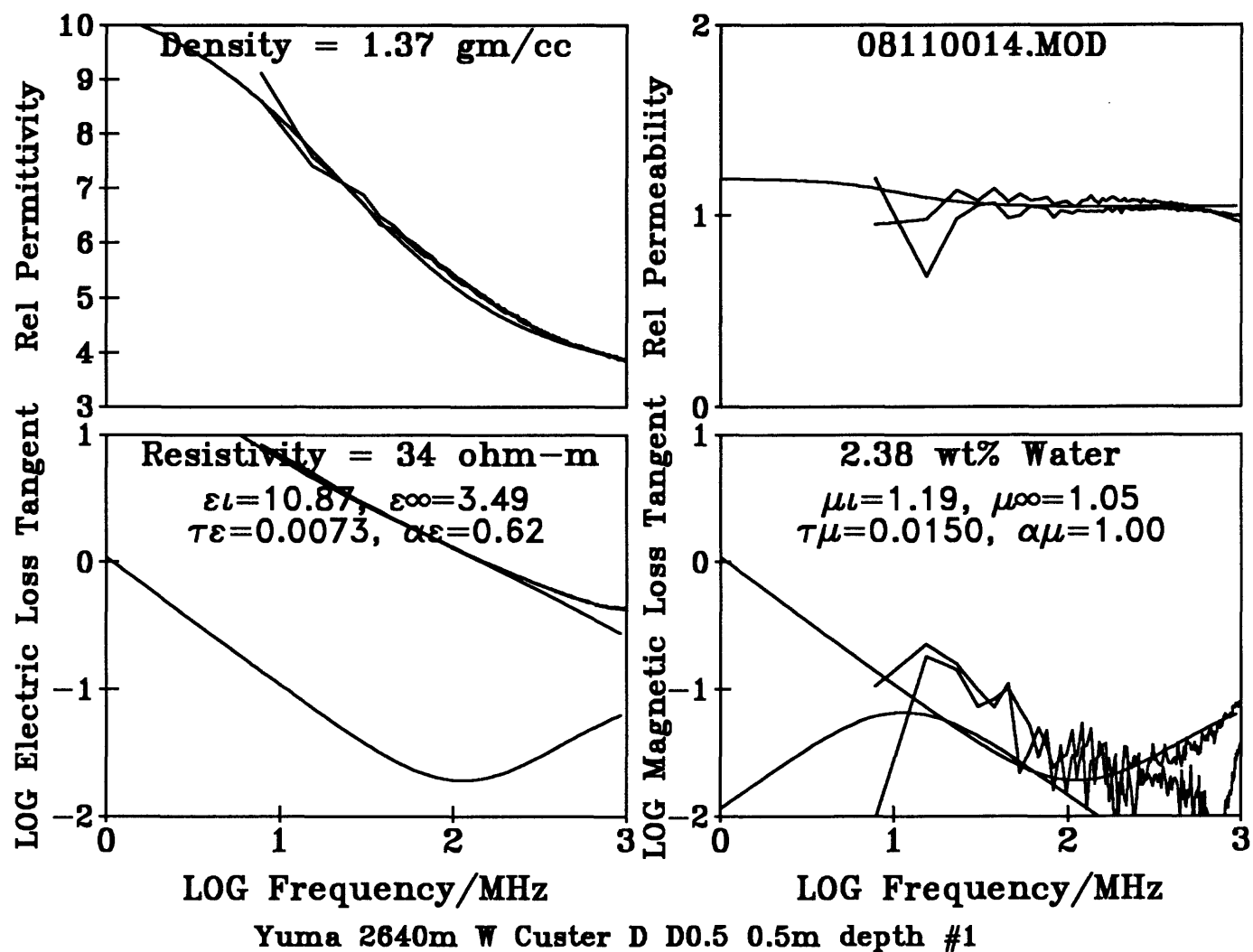


Figure 117 -
Natural state electromagnetic properties with water content preserved in sealed, taped,
sample bottle.

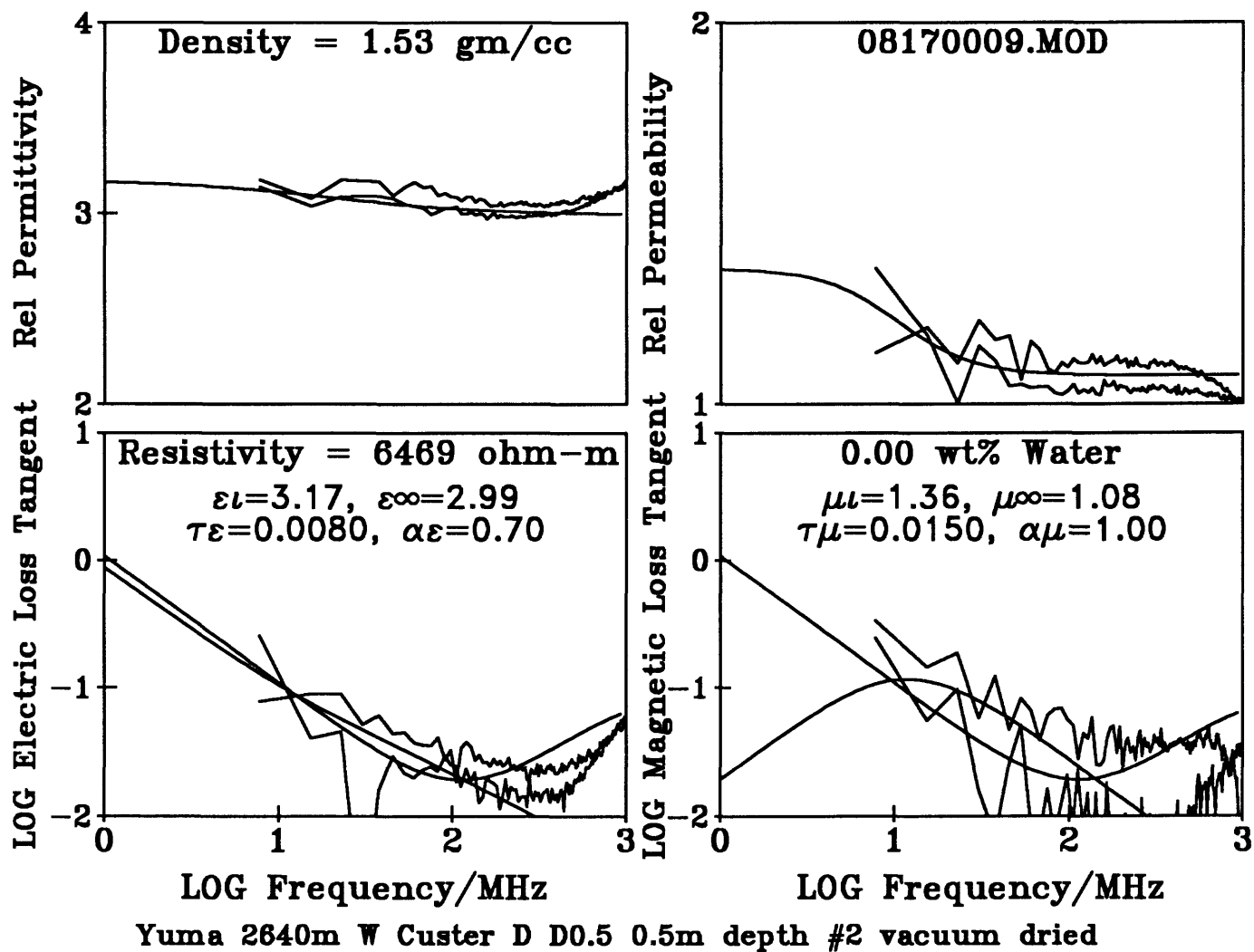


Figure 118 -

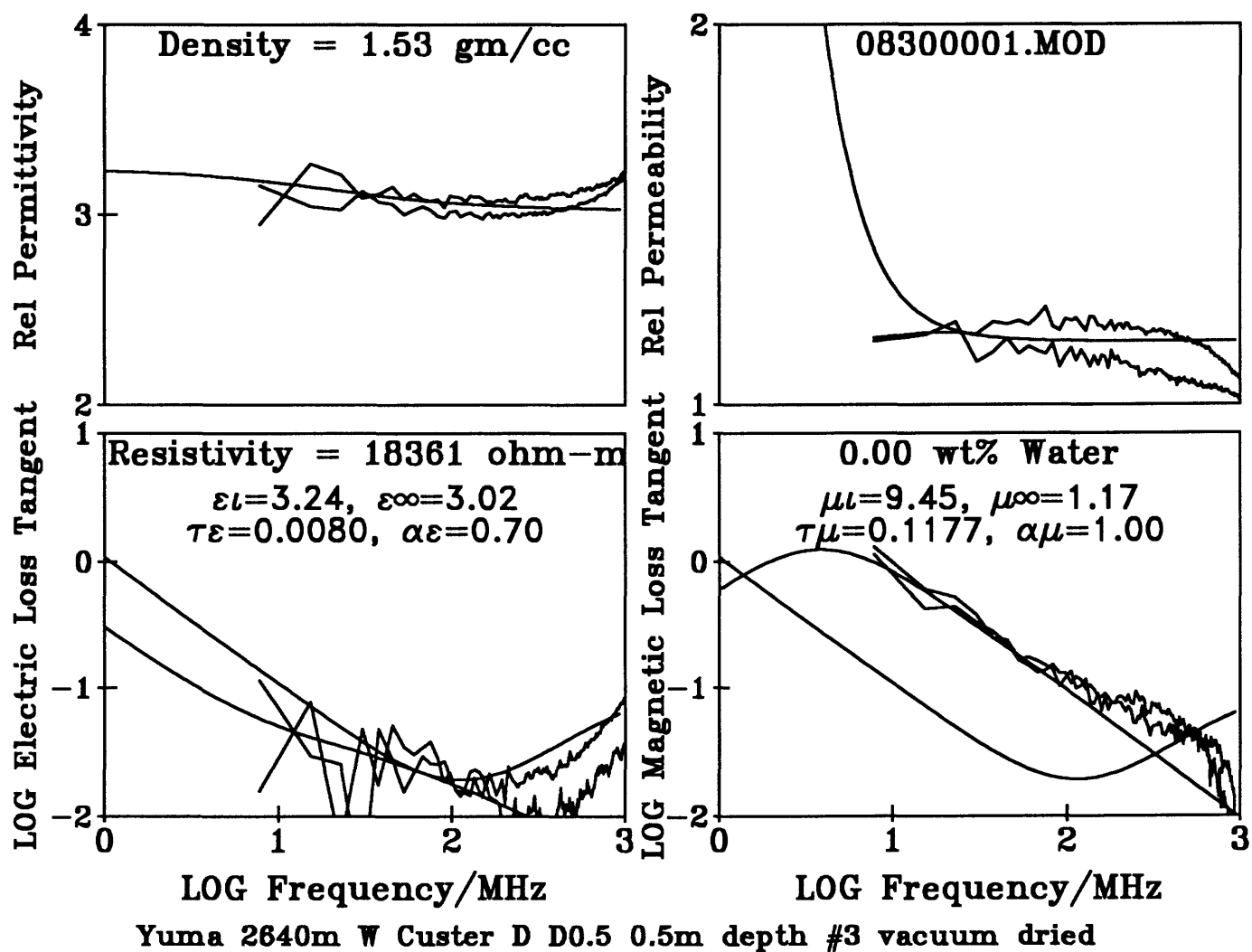


Figure 119 -

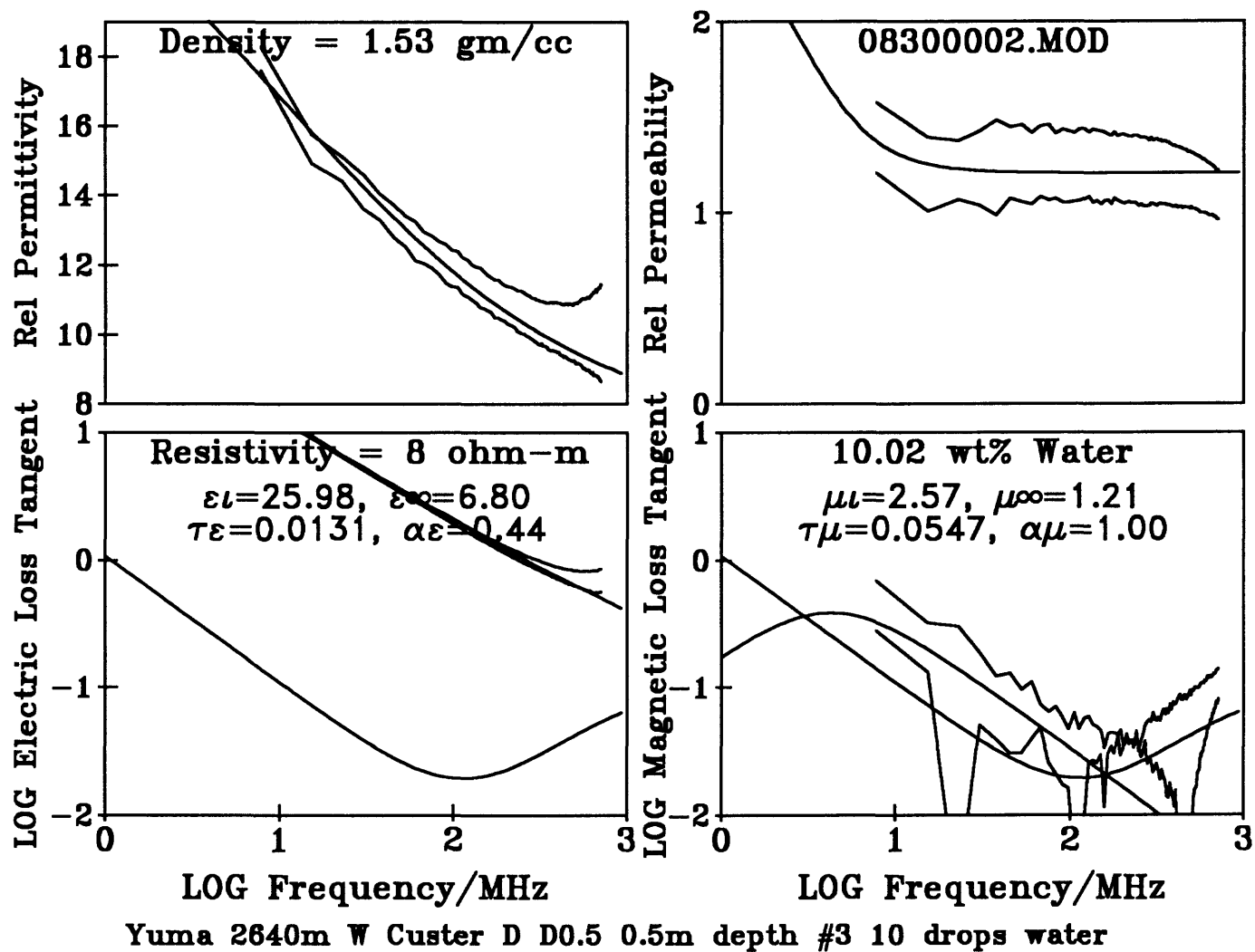


Figure 120 -

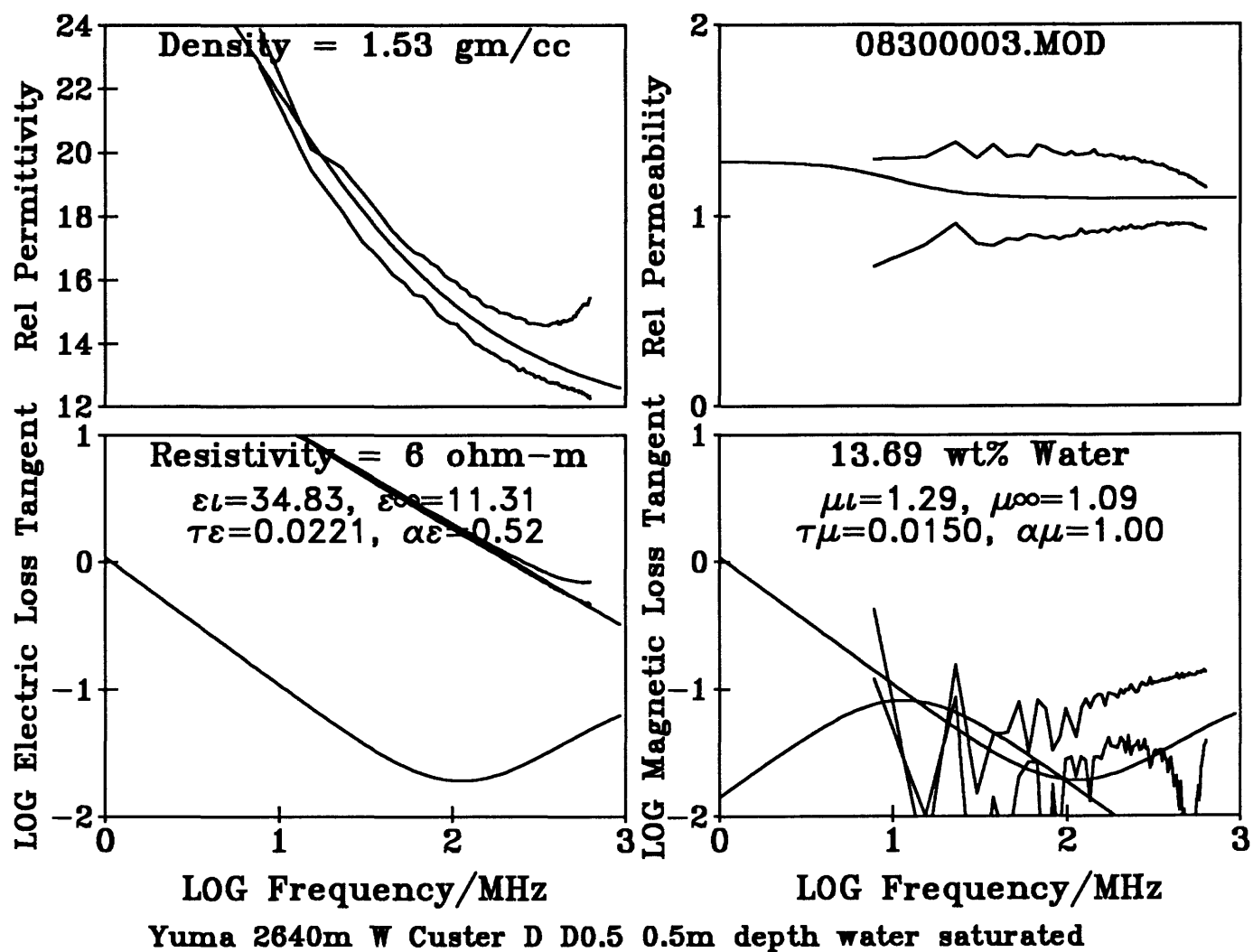


Figure 121 -

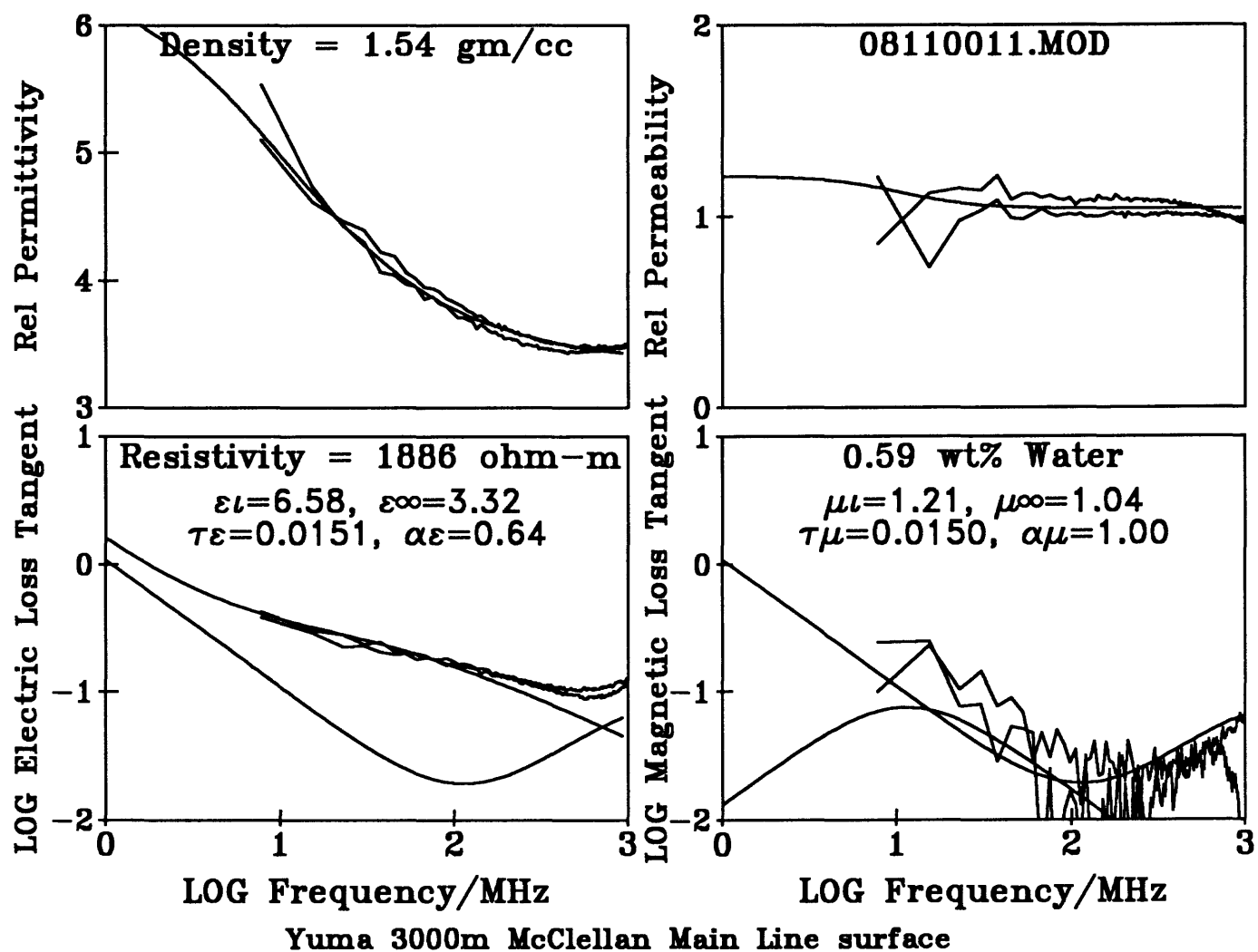


Figure 122 -
Natural state electromagnetic properties with water content preserved in sealed, taped,
sample bottle.

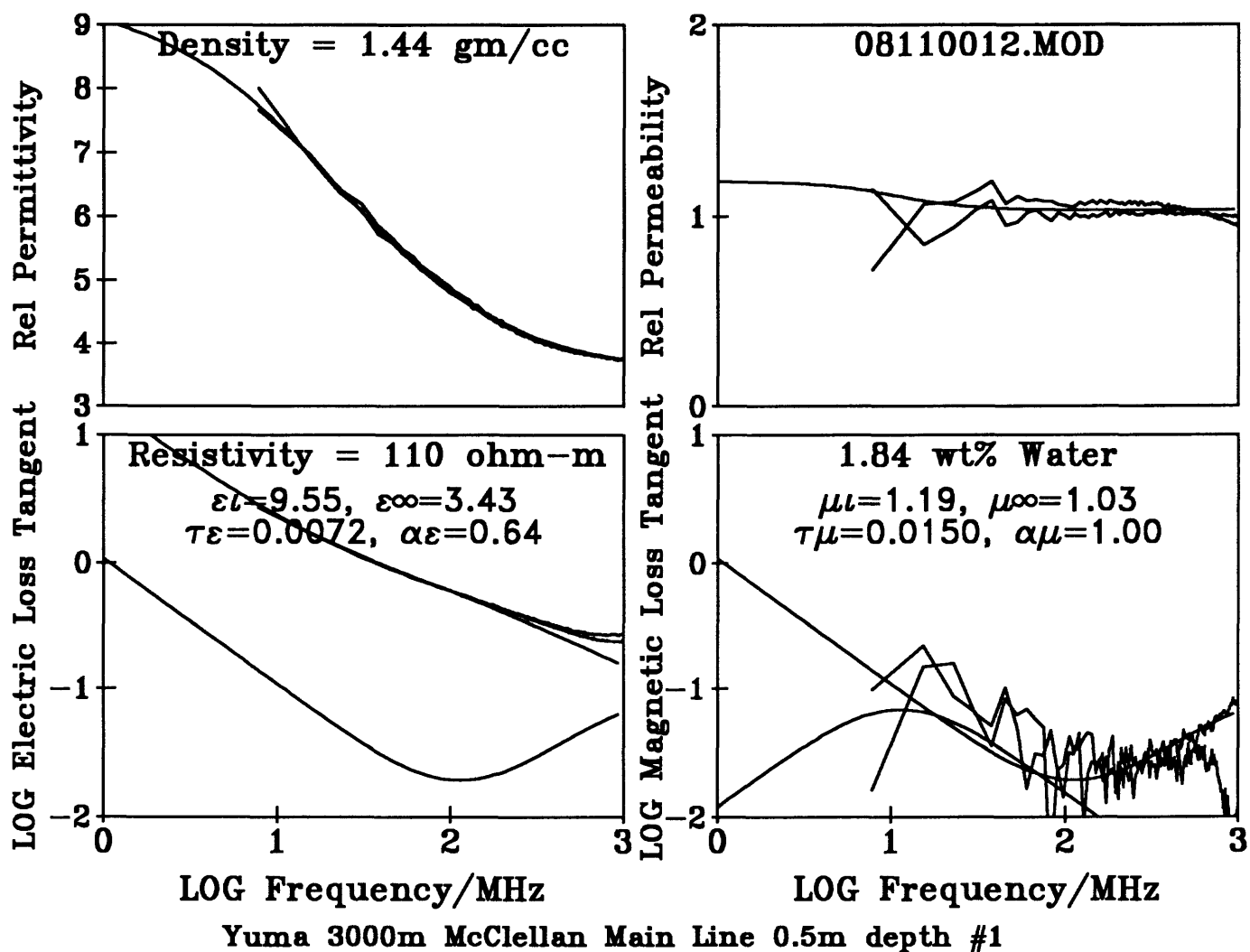


Figure 123 -
Natural state electromagnetic properties with water content preserved in sealed, taped,
sample bottle.

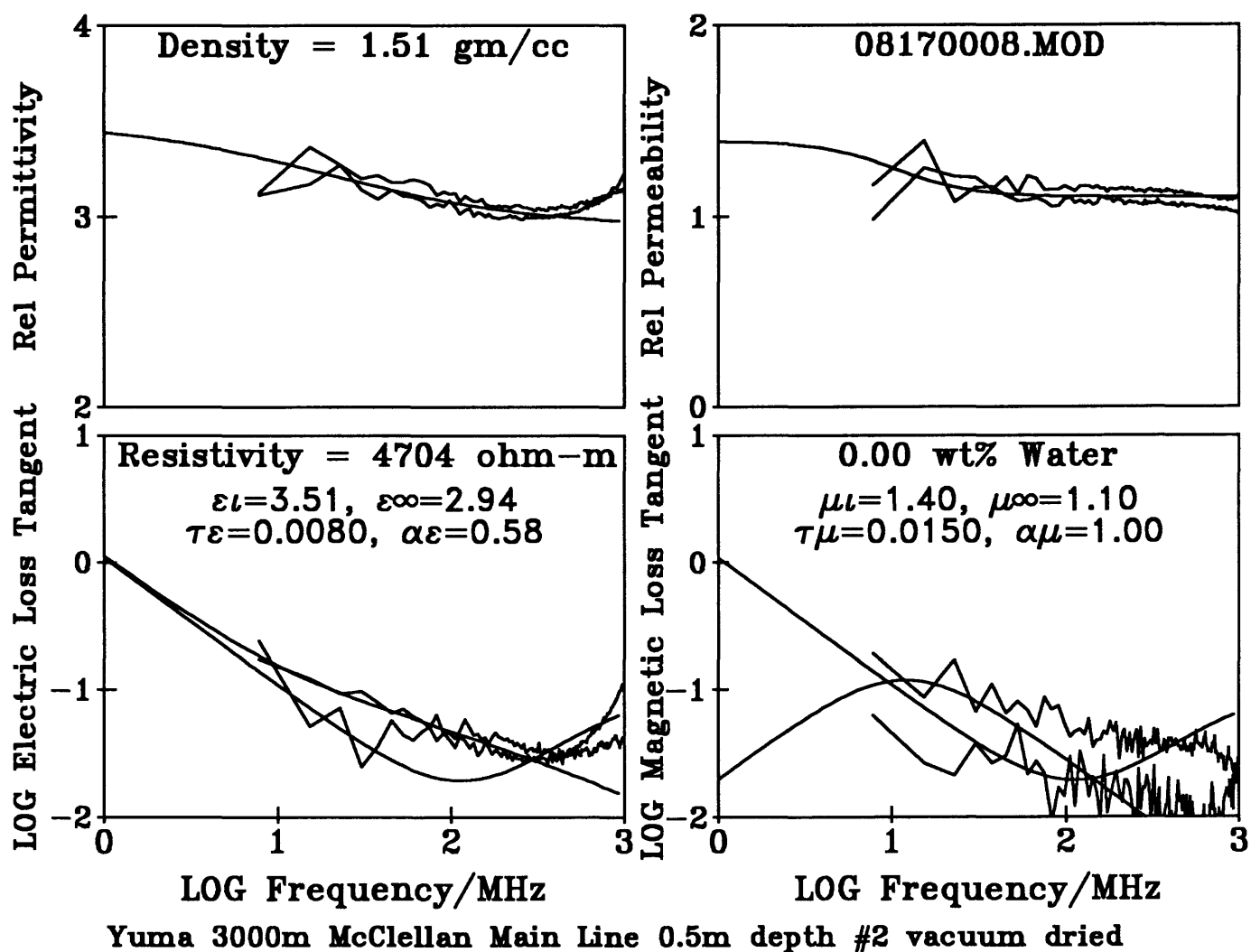


Figure 124 -

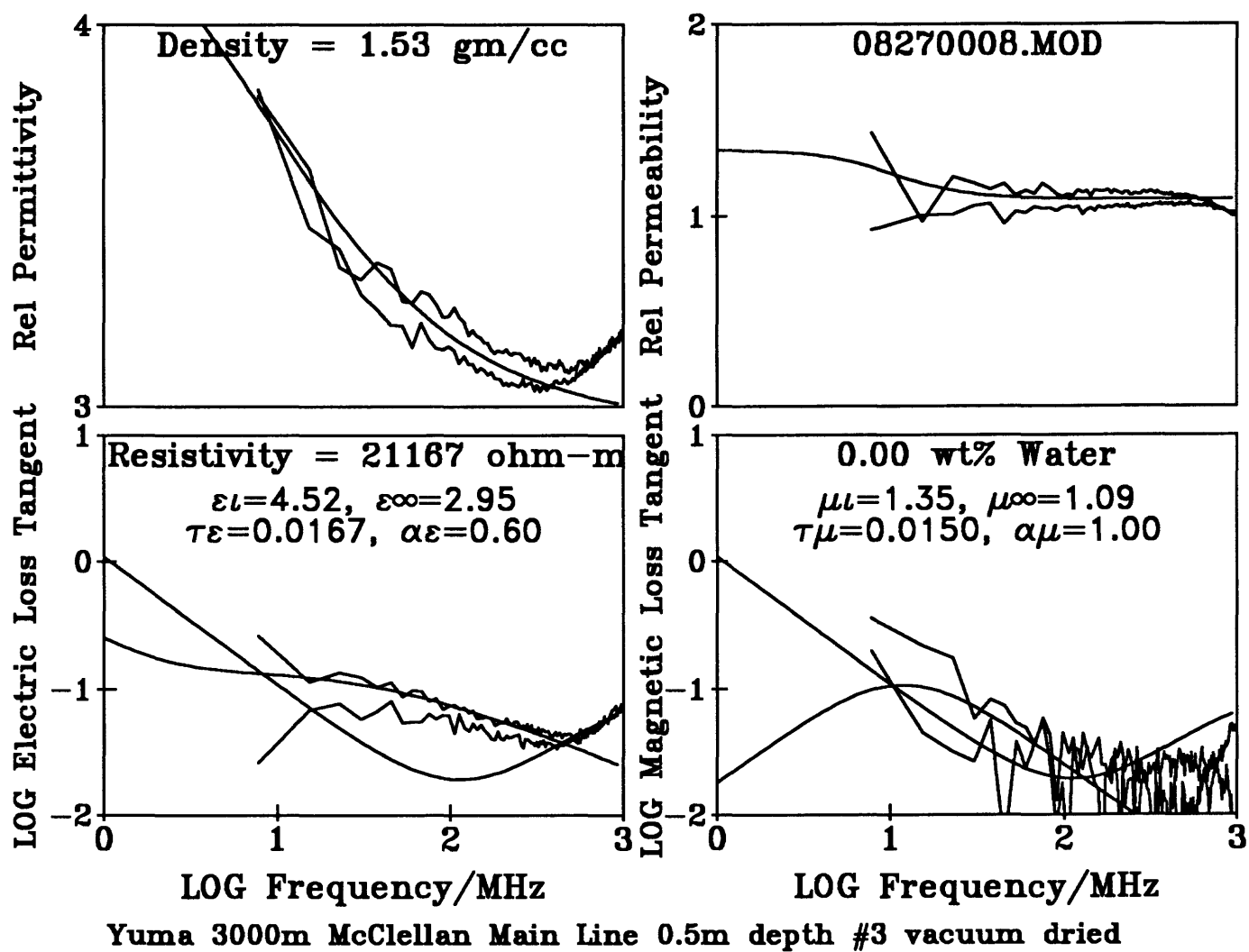
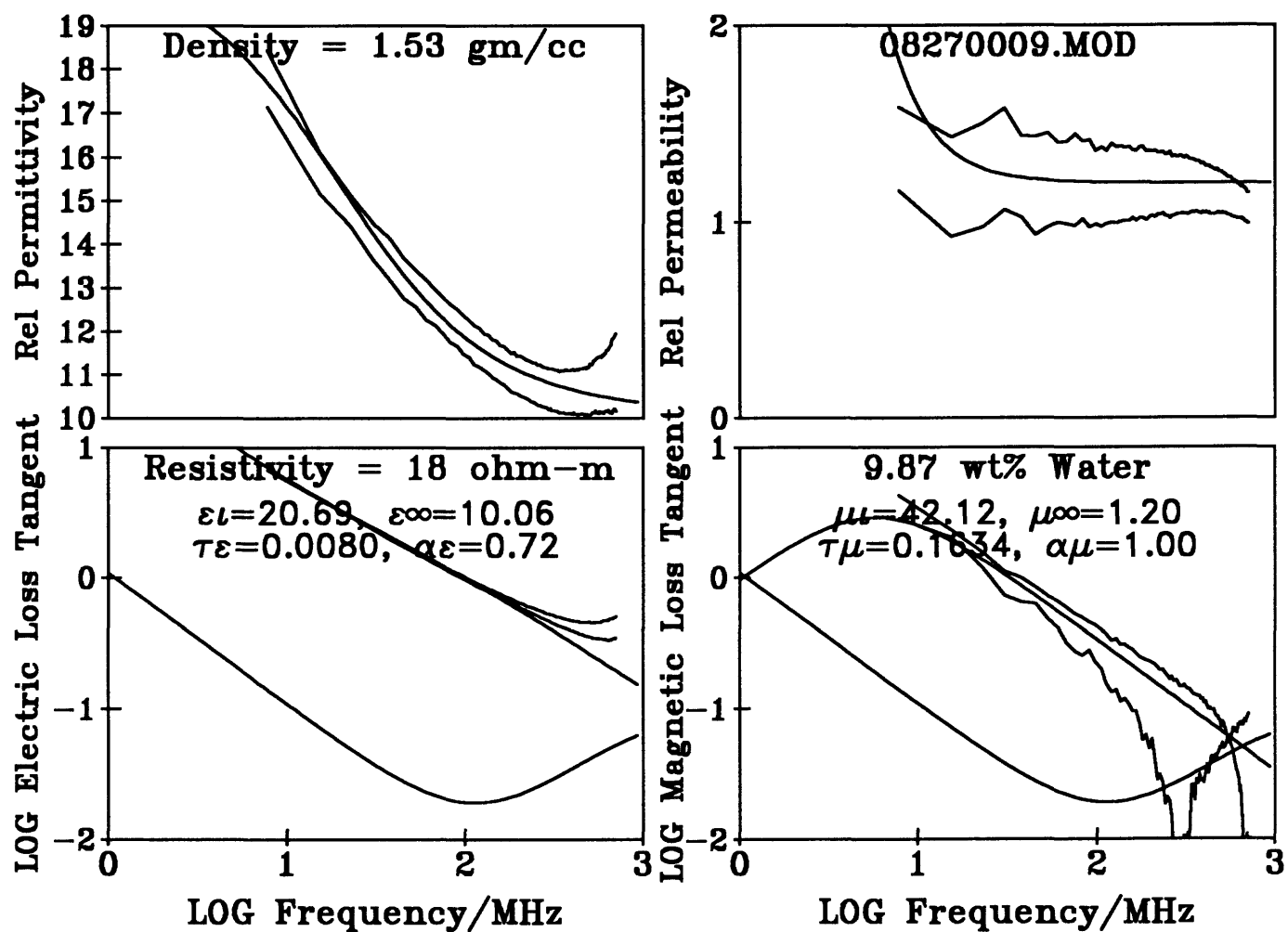
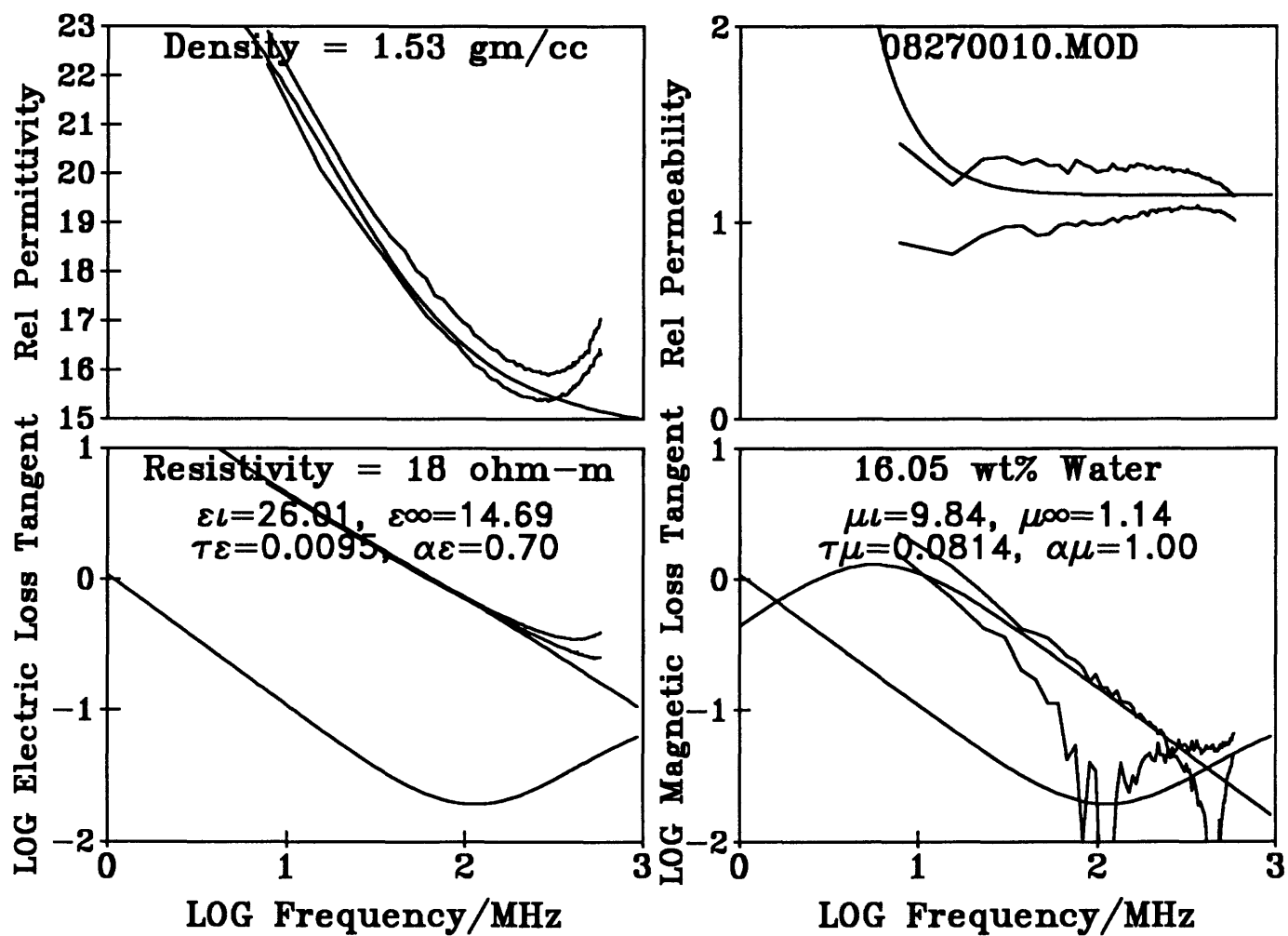


Figure 125 -



Yuma 3000m McClellan Main Line 0.5m depth #3 14 drops water

Figure 126 -



Yuma 3000m McClellan Main Line 0.5m depth #3 water saturated

Figure 127 -

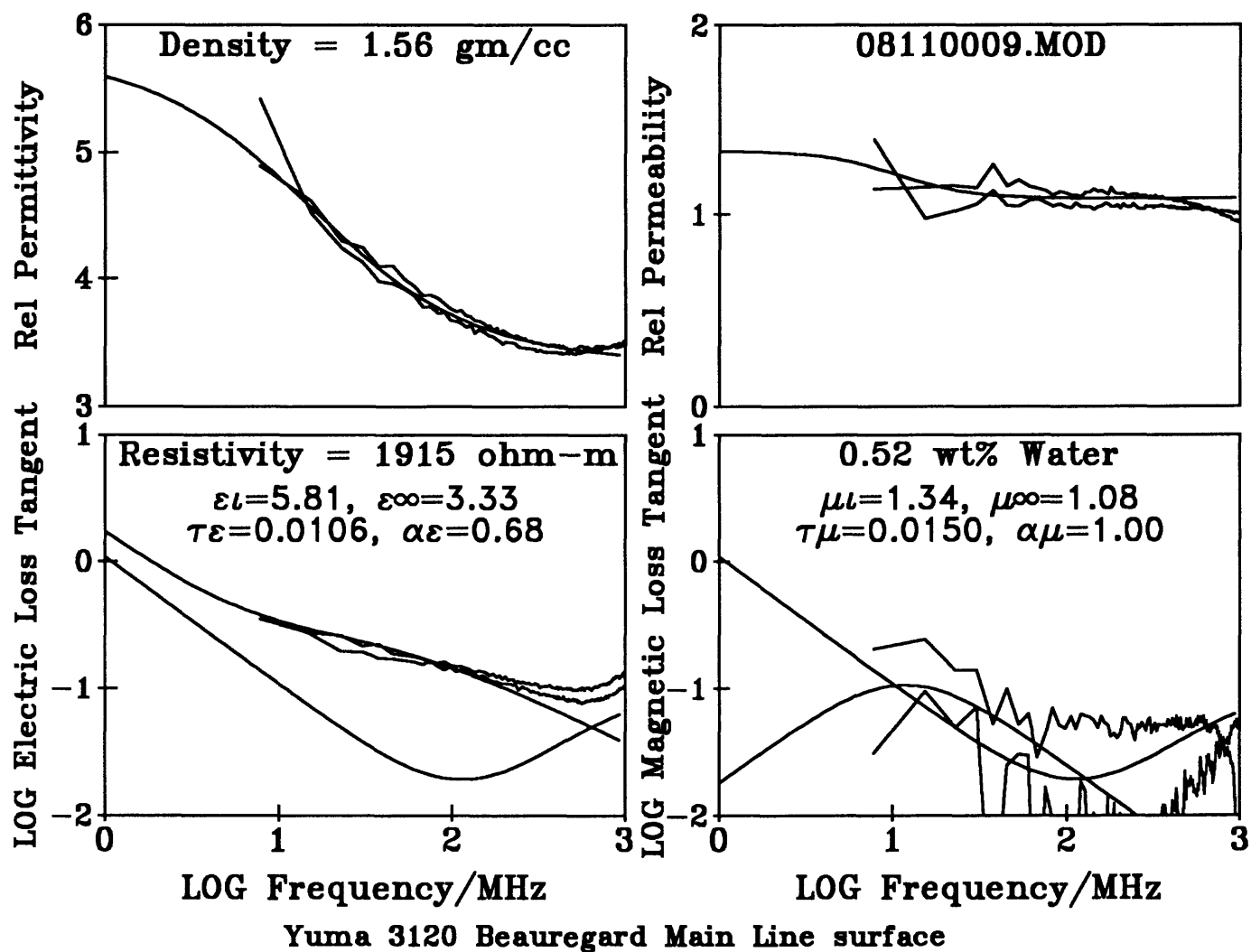


Figure 128 -
Natural state electromagnetic properties with water content preserved in sealed, taped,
sample bottle.

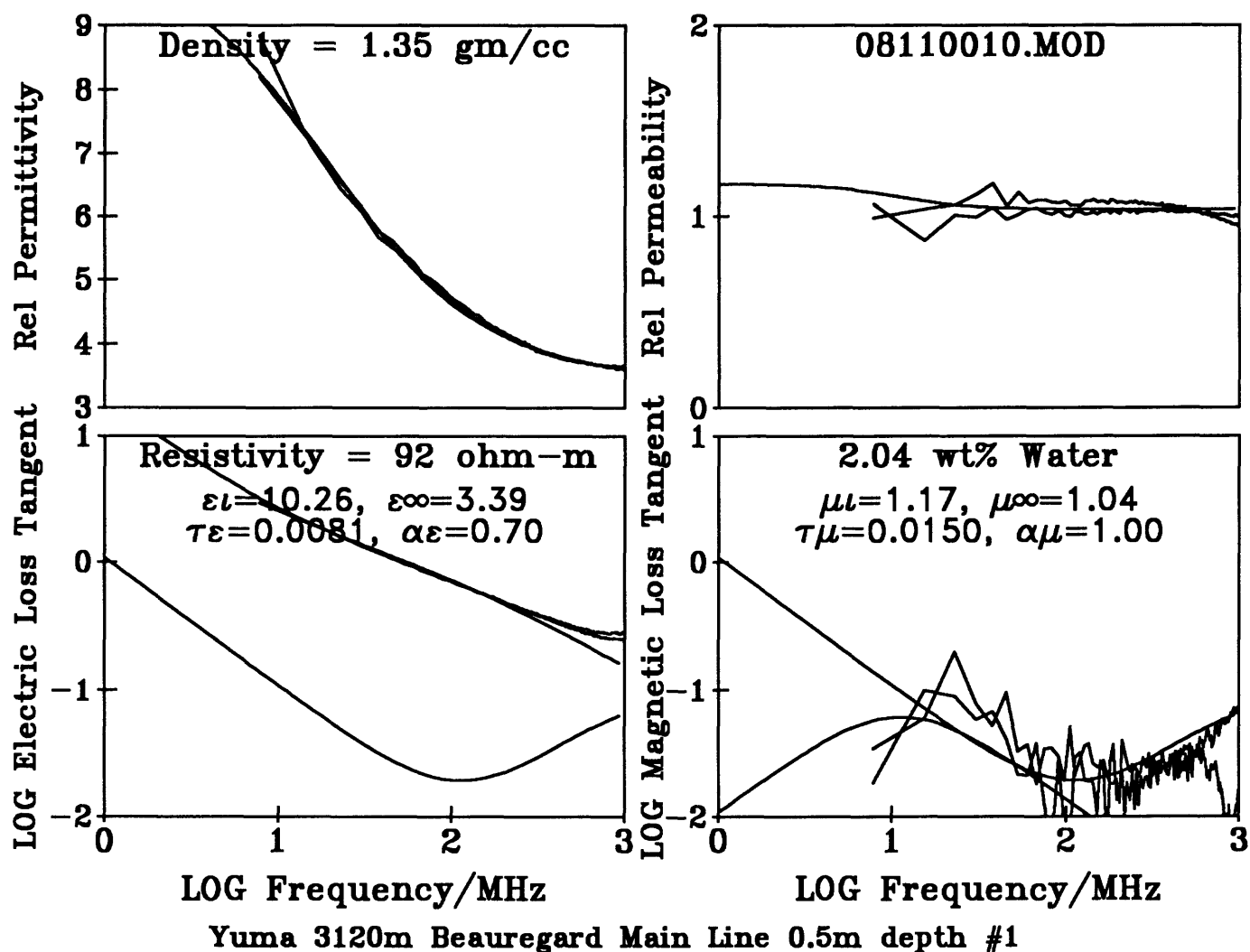
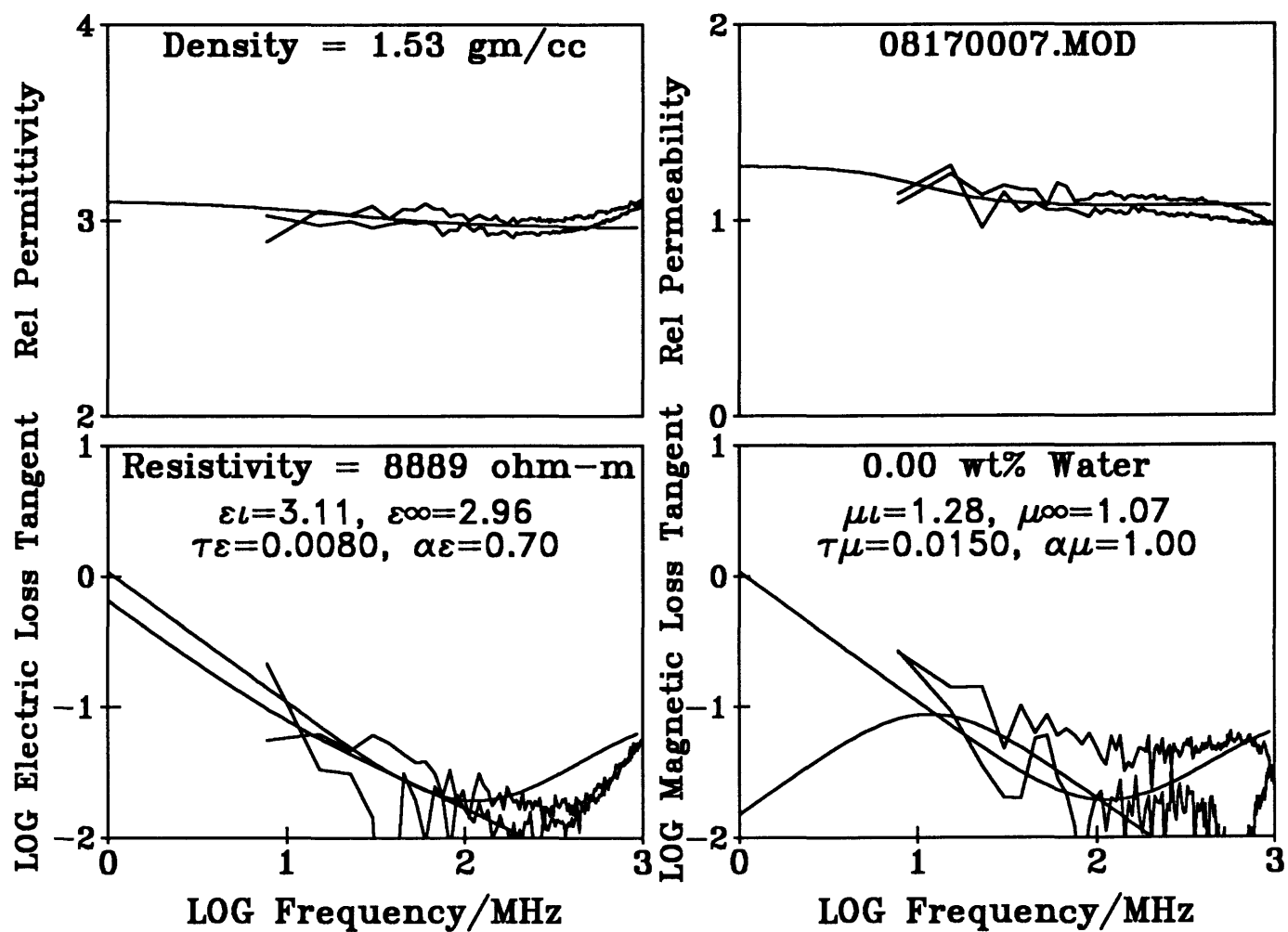
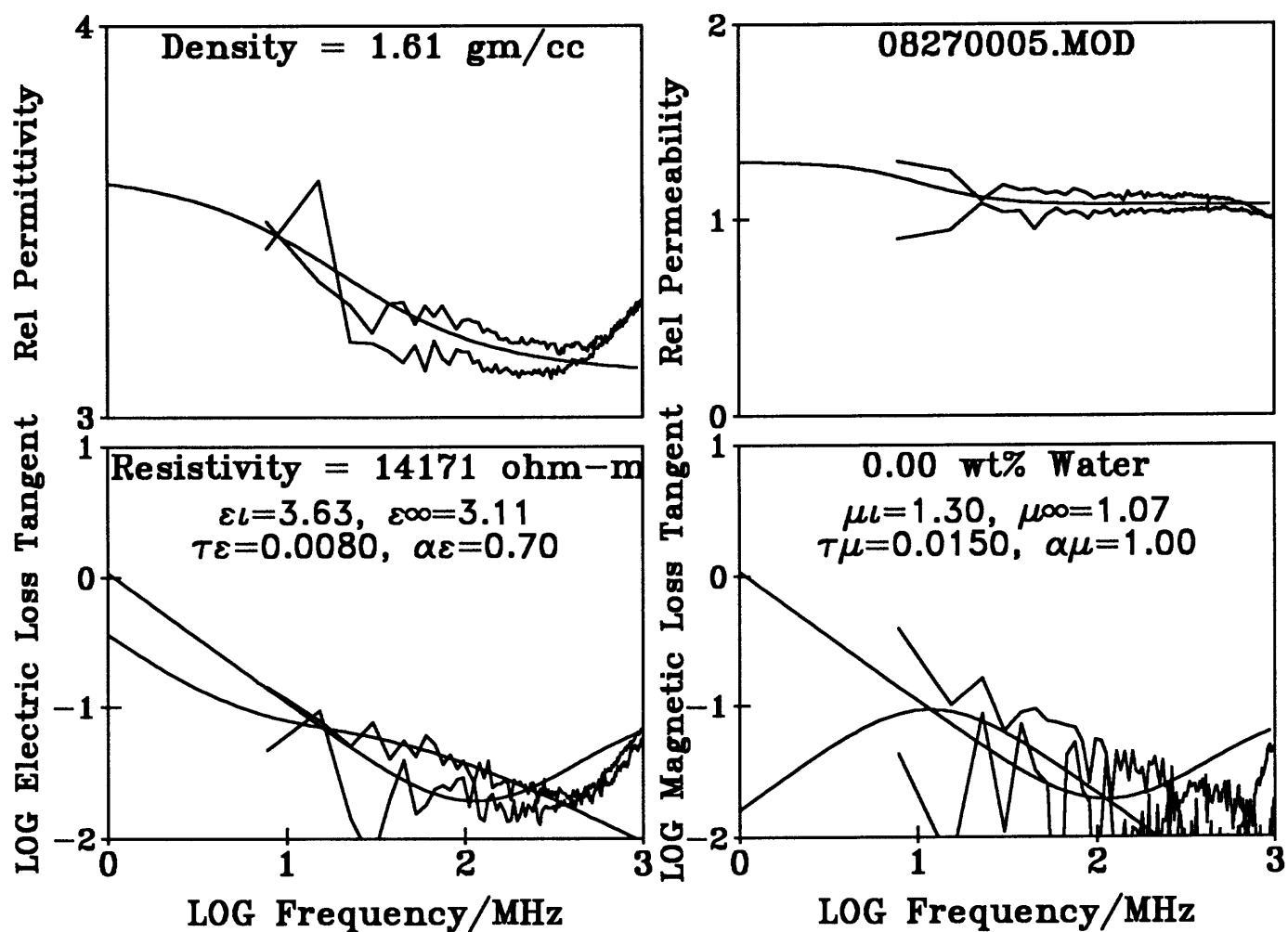


Figure 129 -
 Natural state electromagnetic properties with water content preserved in sealed, taped,
 sample bottle.



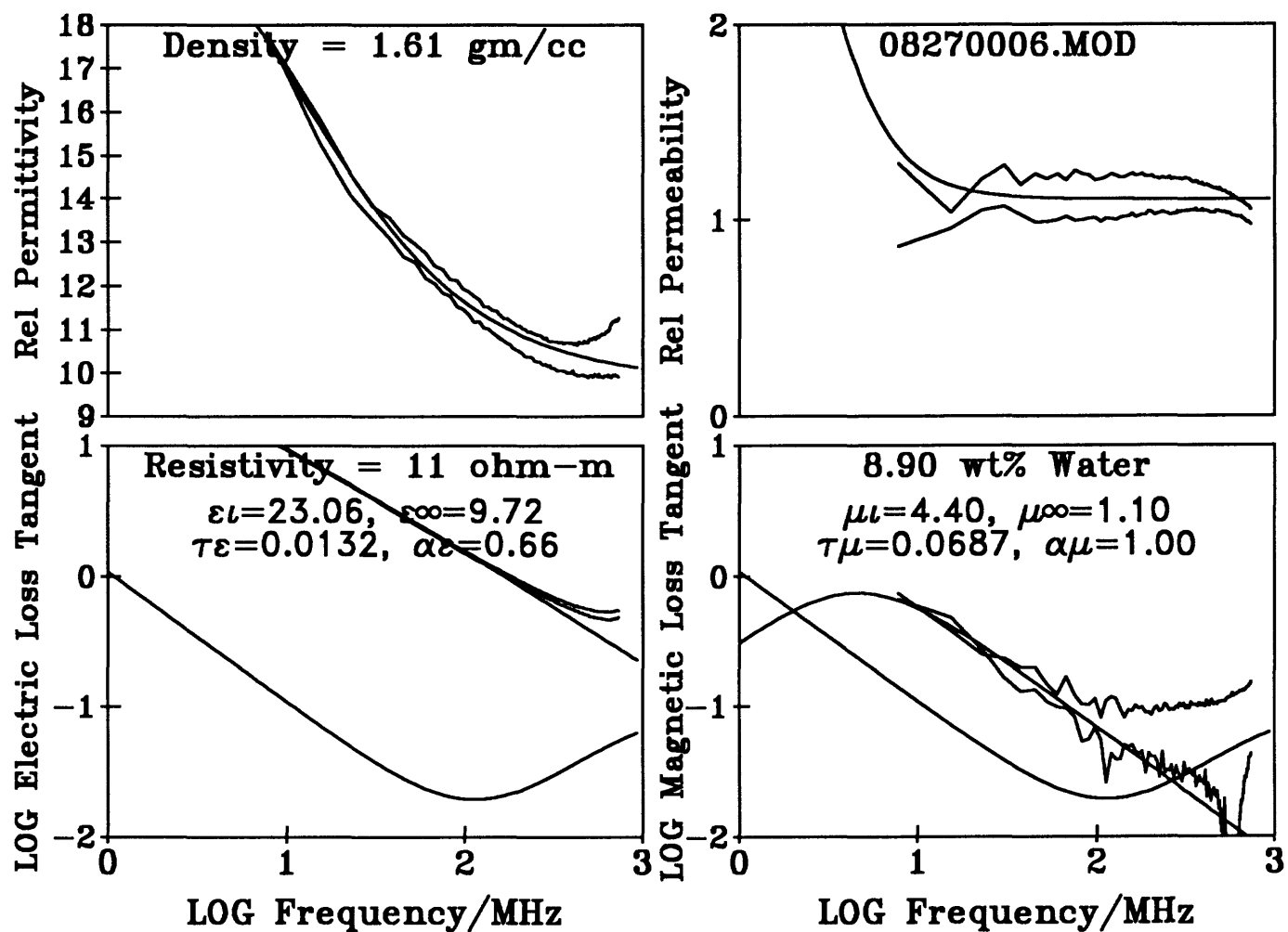
Yuma 3120m Beauregard Main Line 0.5m depth #2 vacuum dried

Figure 130 -



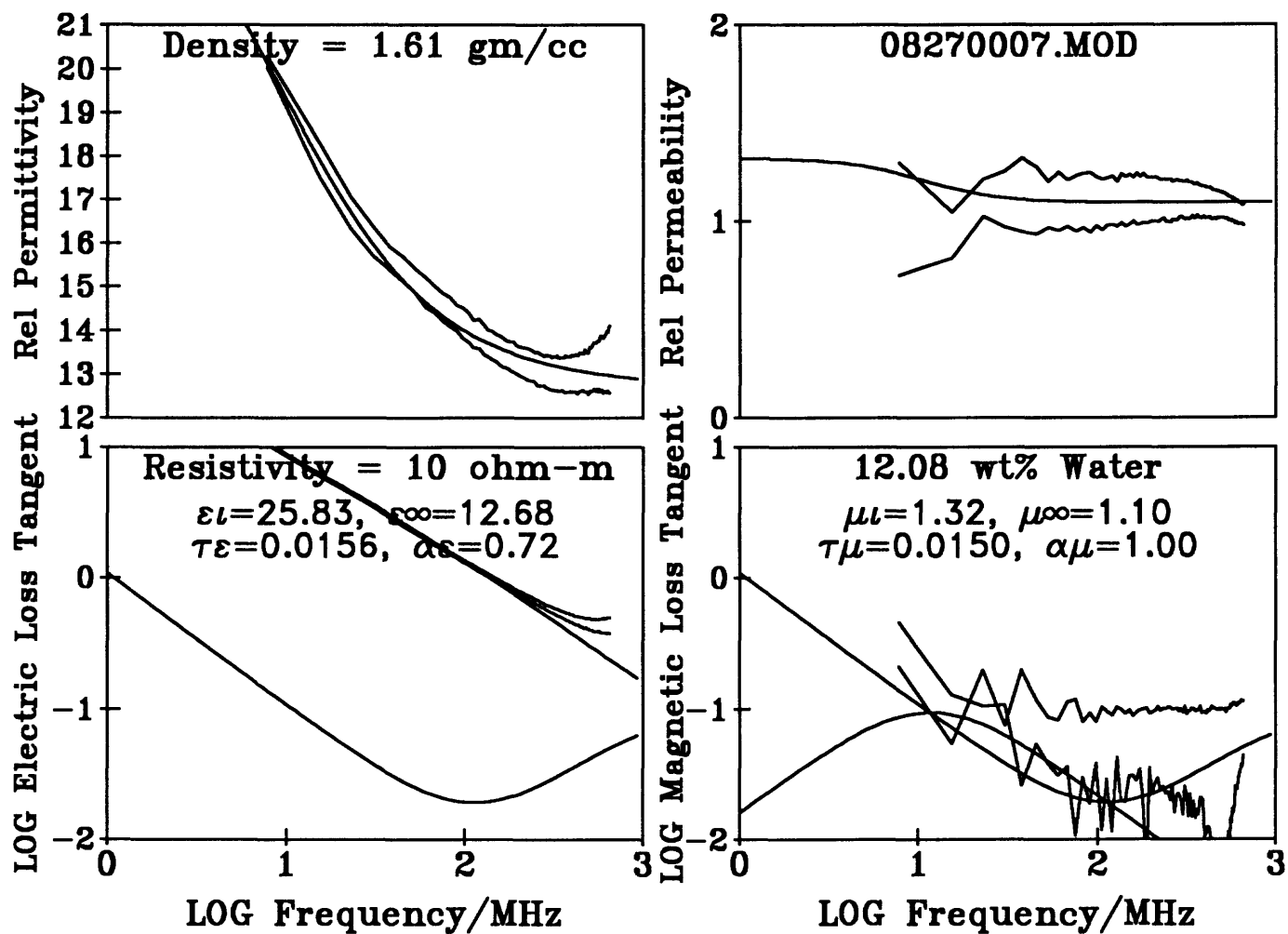
Yuma 3120m Beauregard Main Line 0.5m depth #3 vacuum dried

Figure 131 -



Yuma 3120m Beauregard Main Line 0.5m depth #3 9 drops water

Figure 132 -



Yuma 3120m Beauregard Main Line 0.5m depth #3 water saturated

Figure 133 -

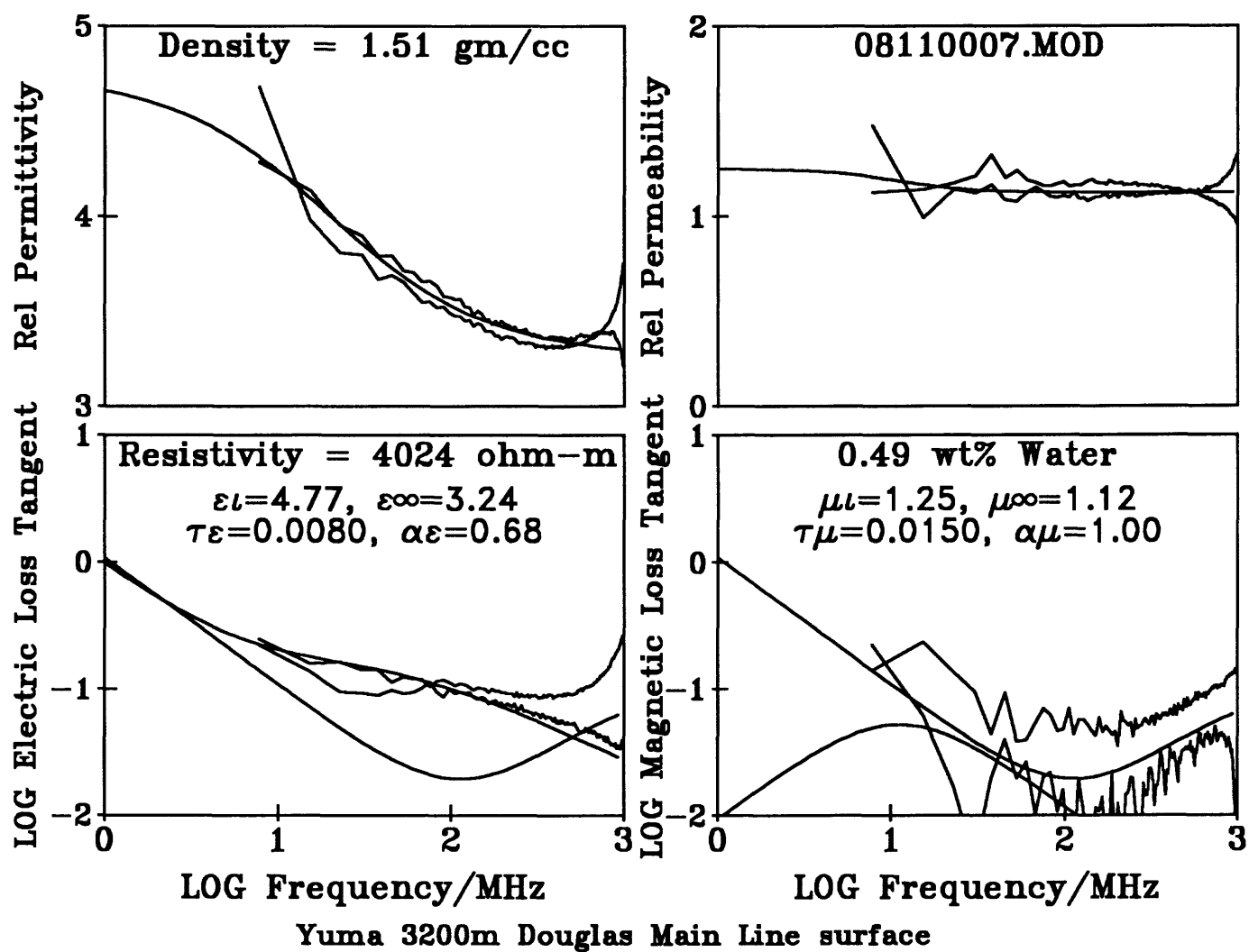


Figure 134 -
Natural state electromagnetic properties with water content preserved in sealed, taped,
sample bottle.

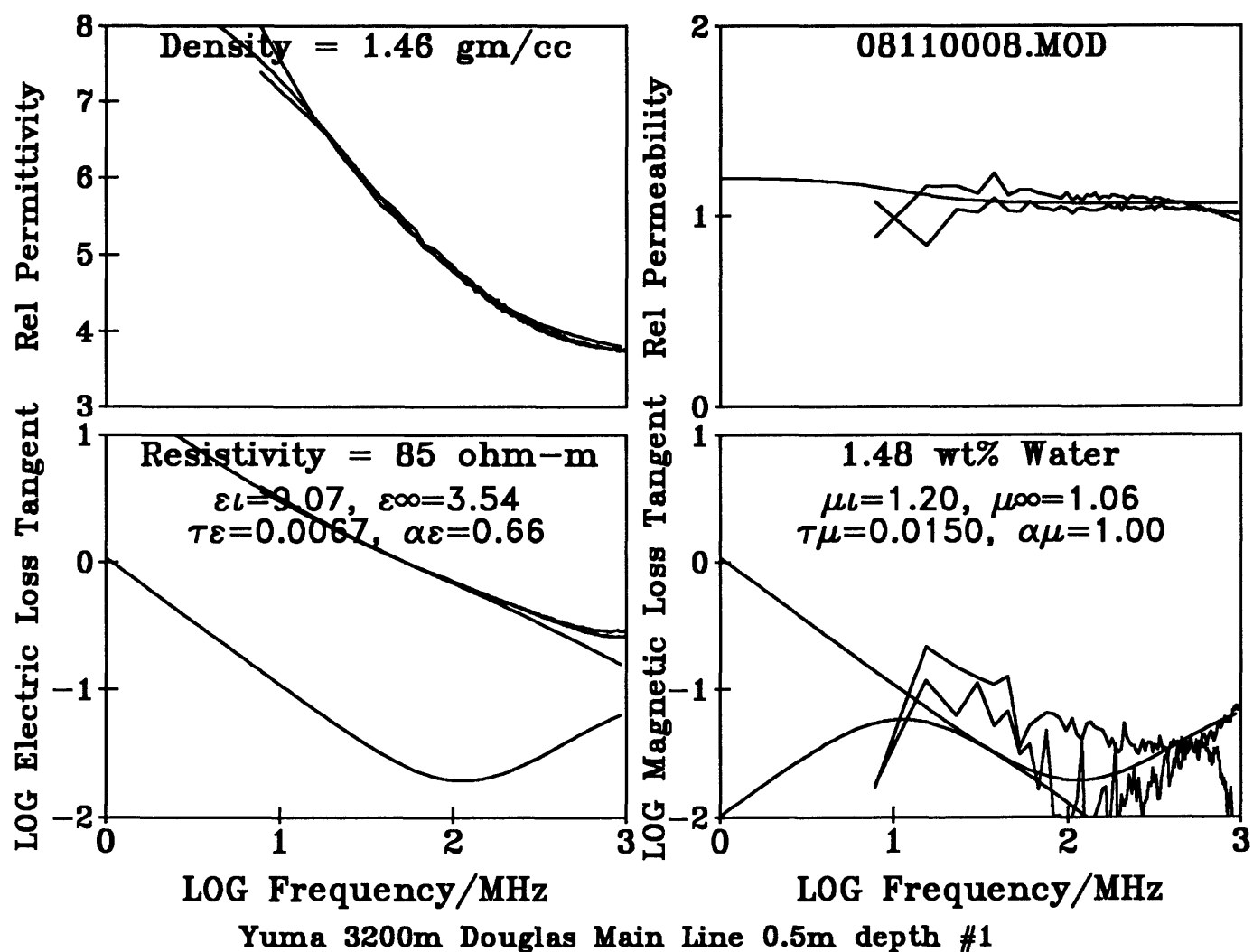


Figure 135 -
Natural state electromagnetic properties with water content preserved in sealed, taped,
sample bottle.

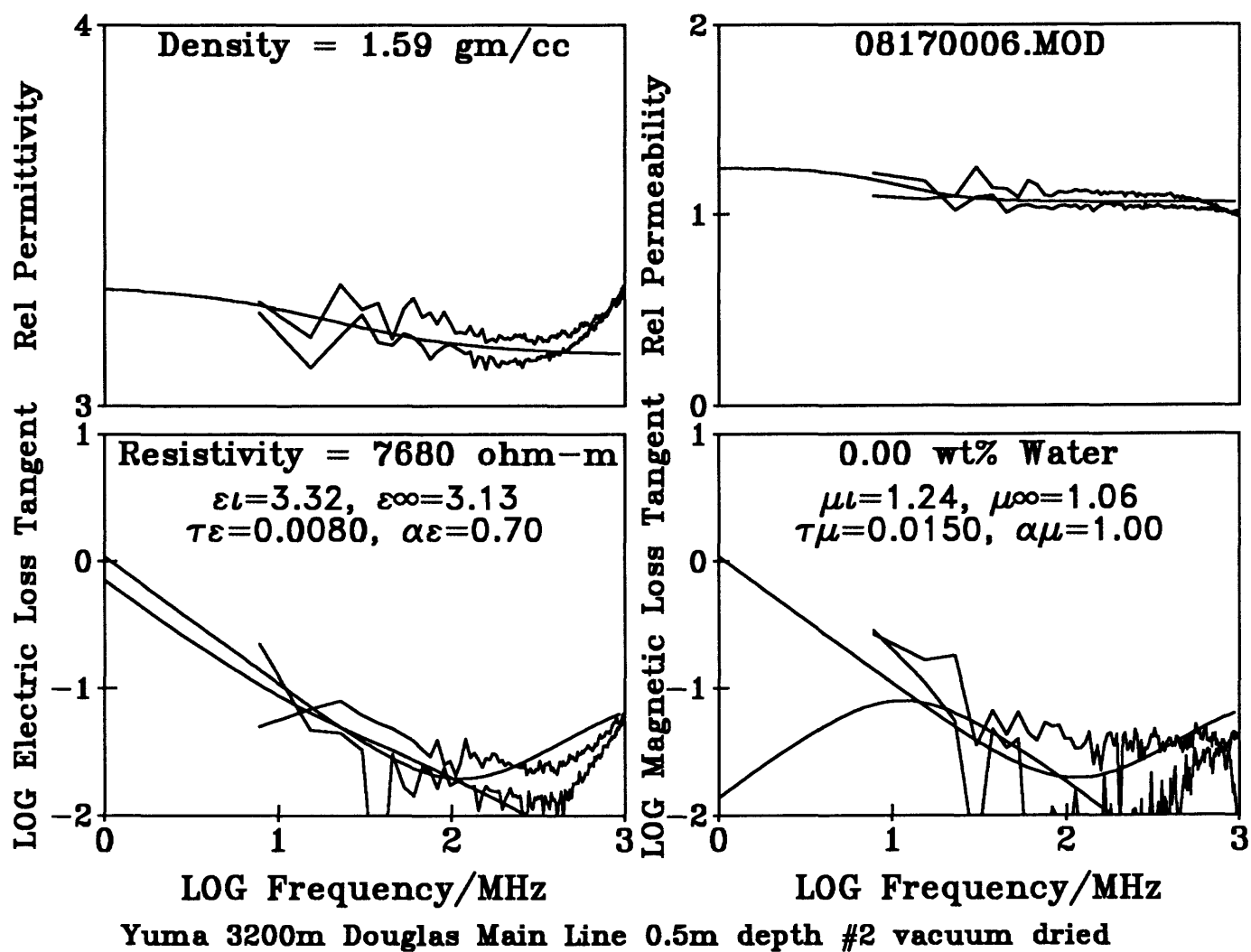


Figure 136 -

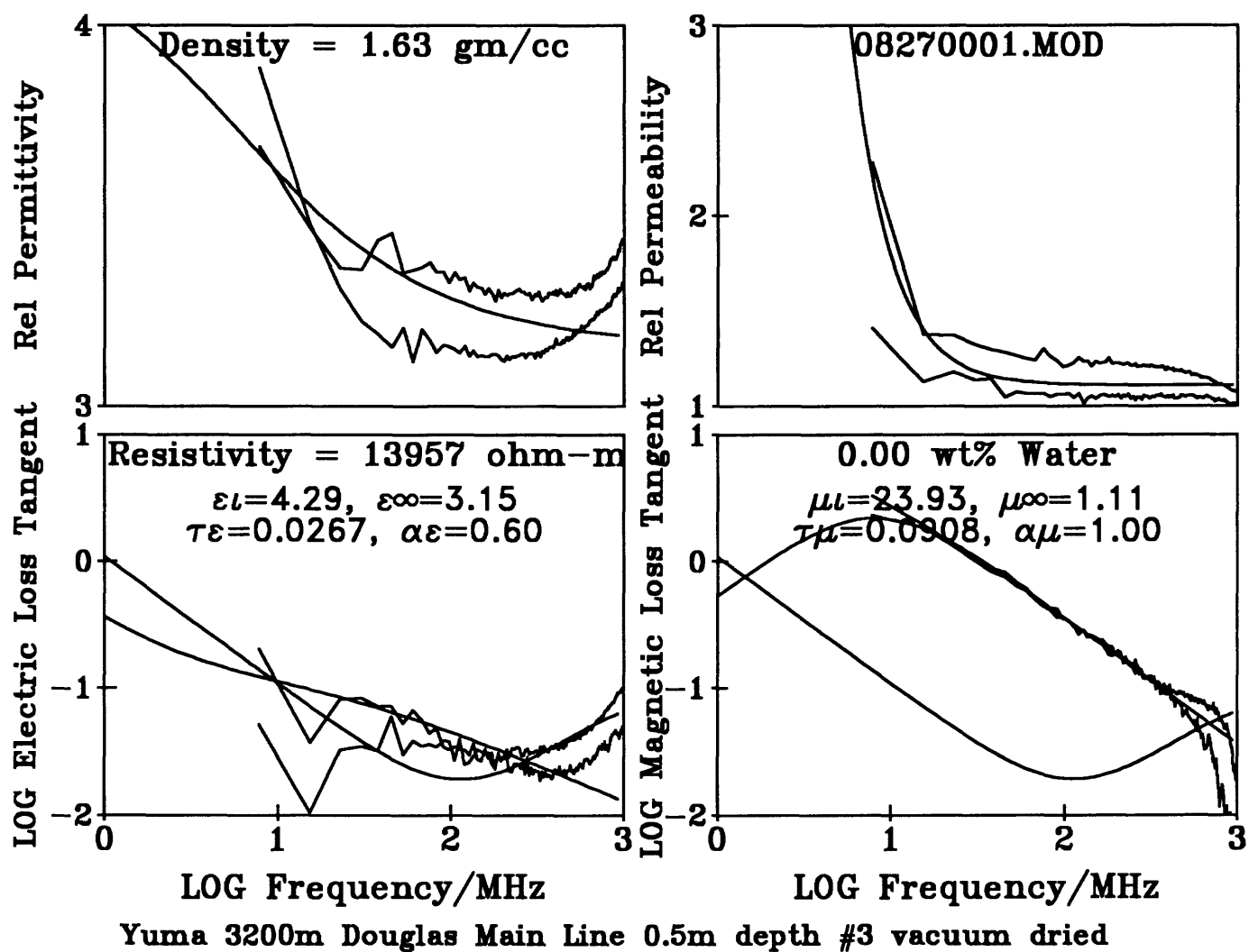


Figure 137 -

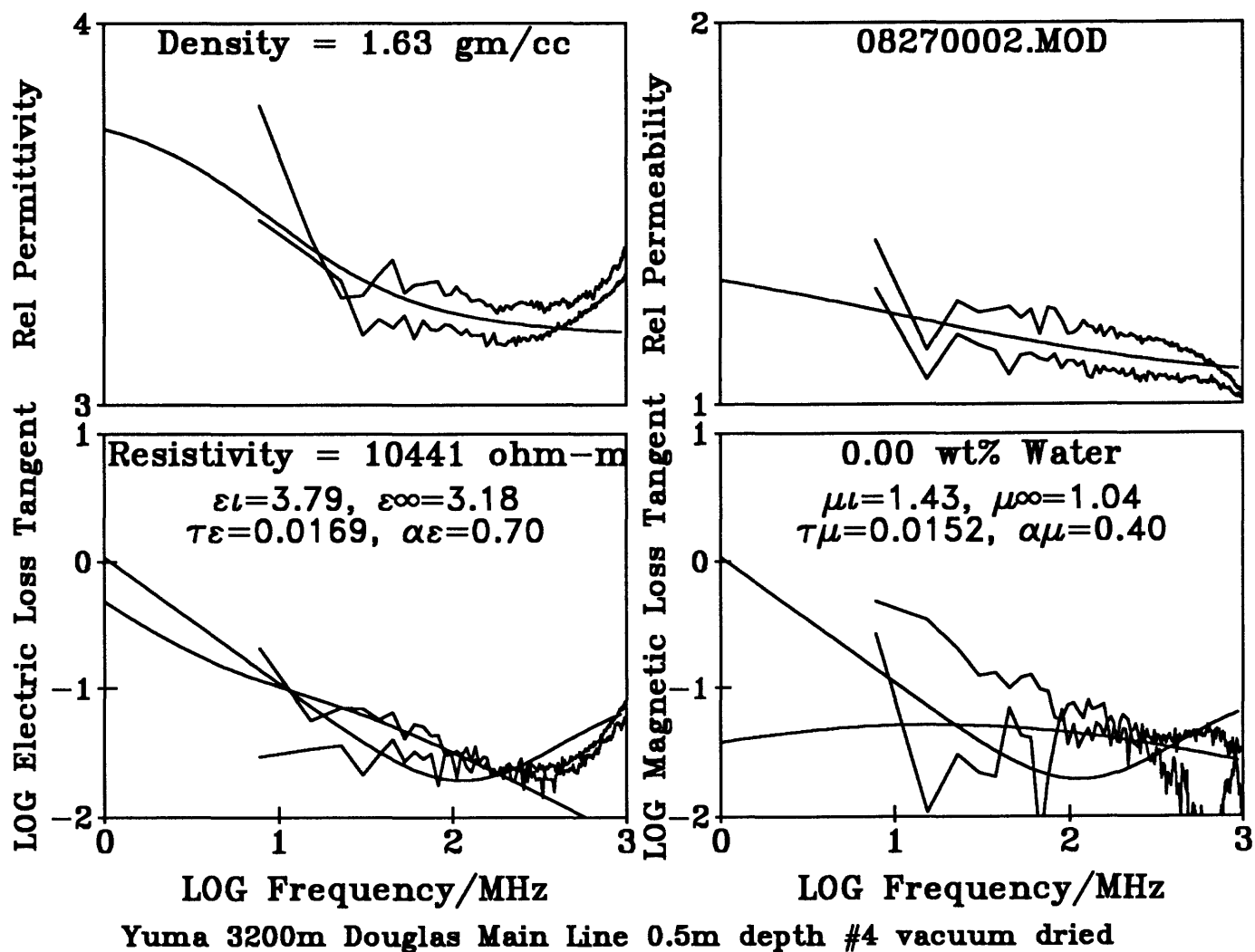


Figure 138 -

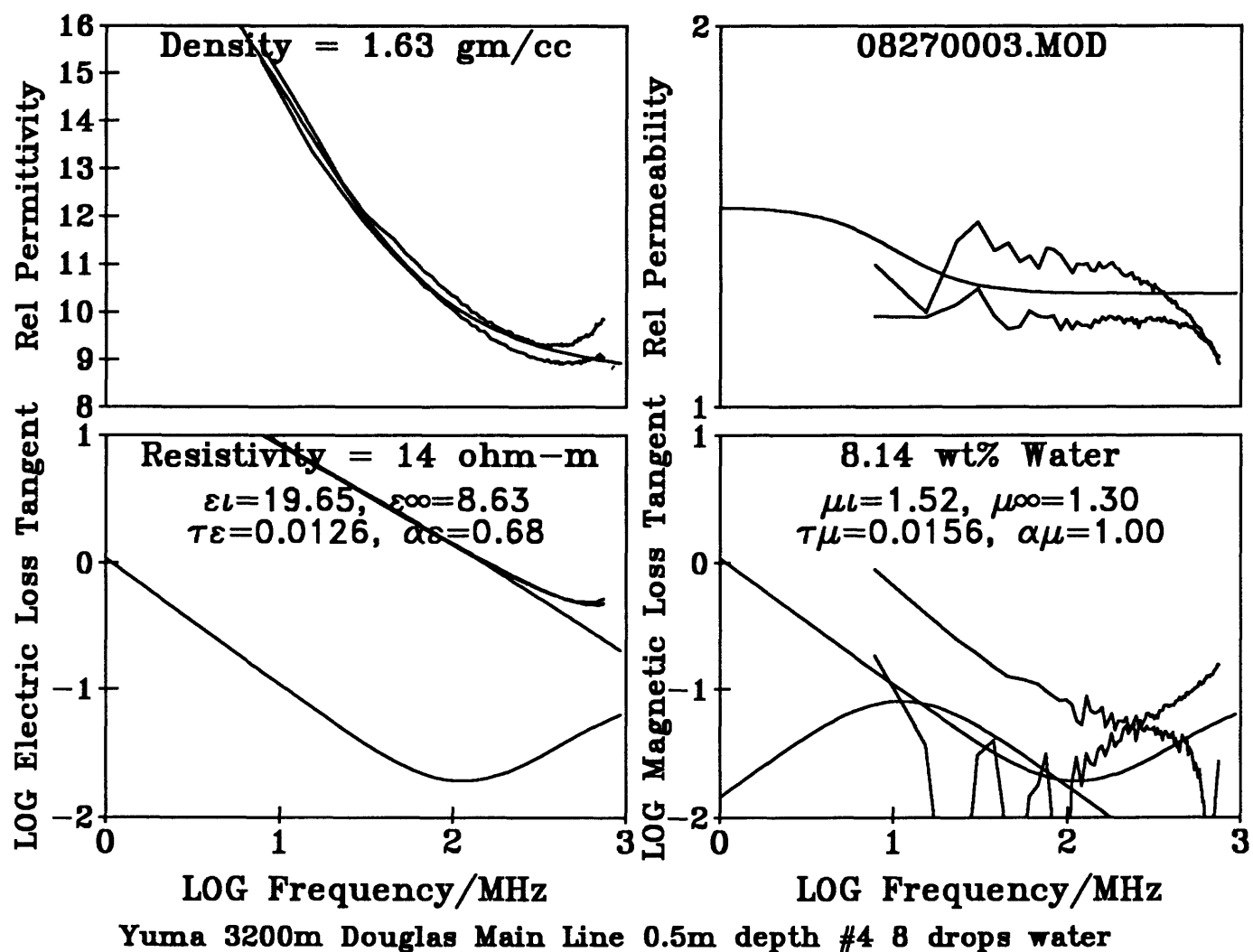


Figure 139 -

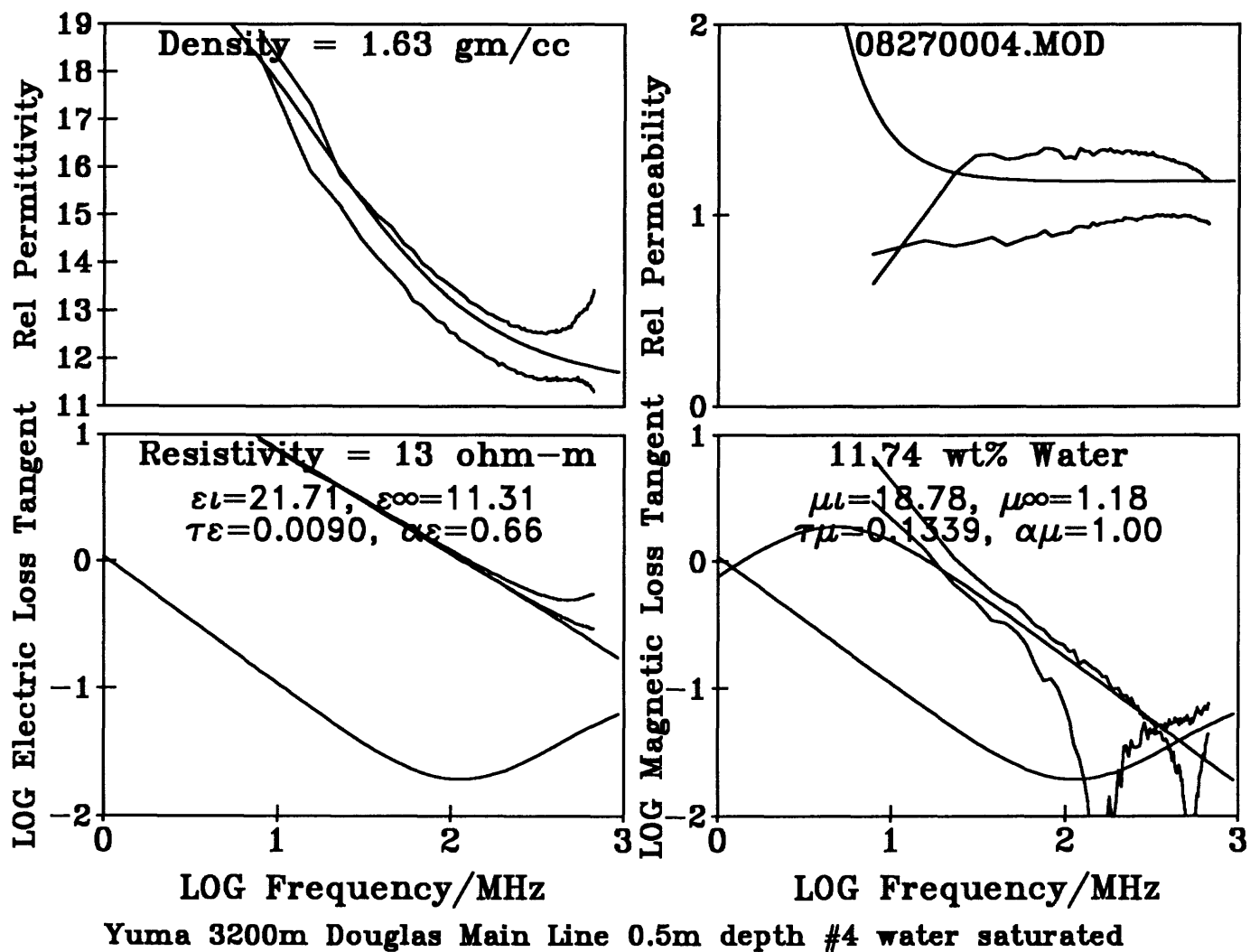


Figure 140 -

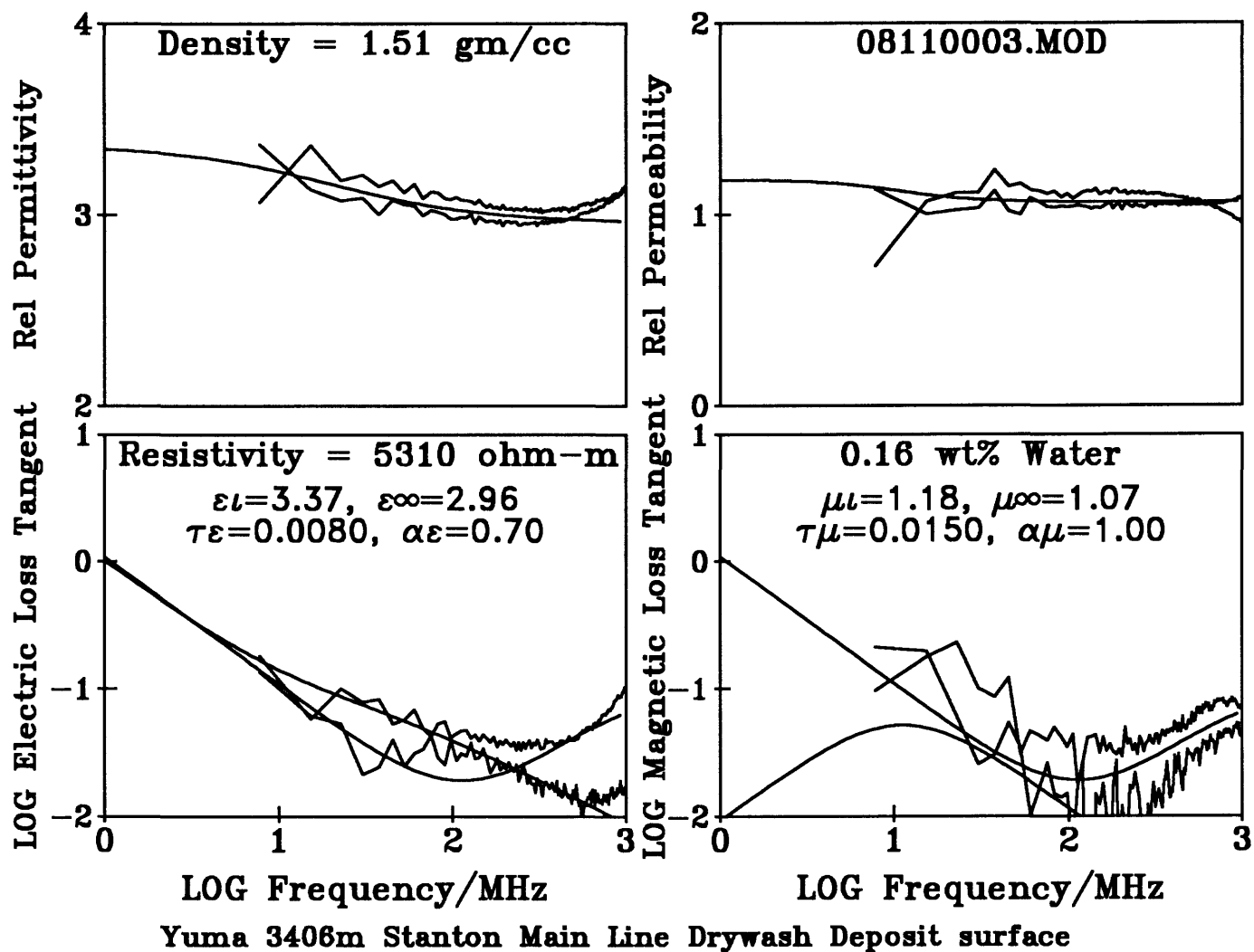
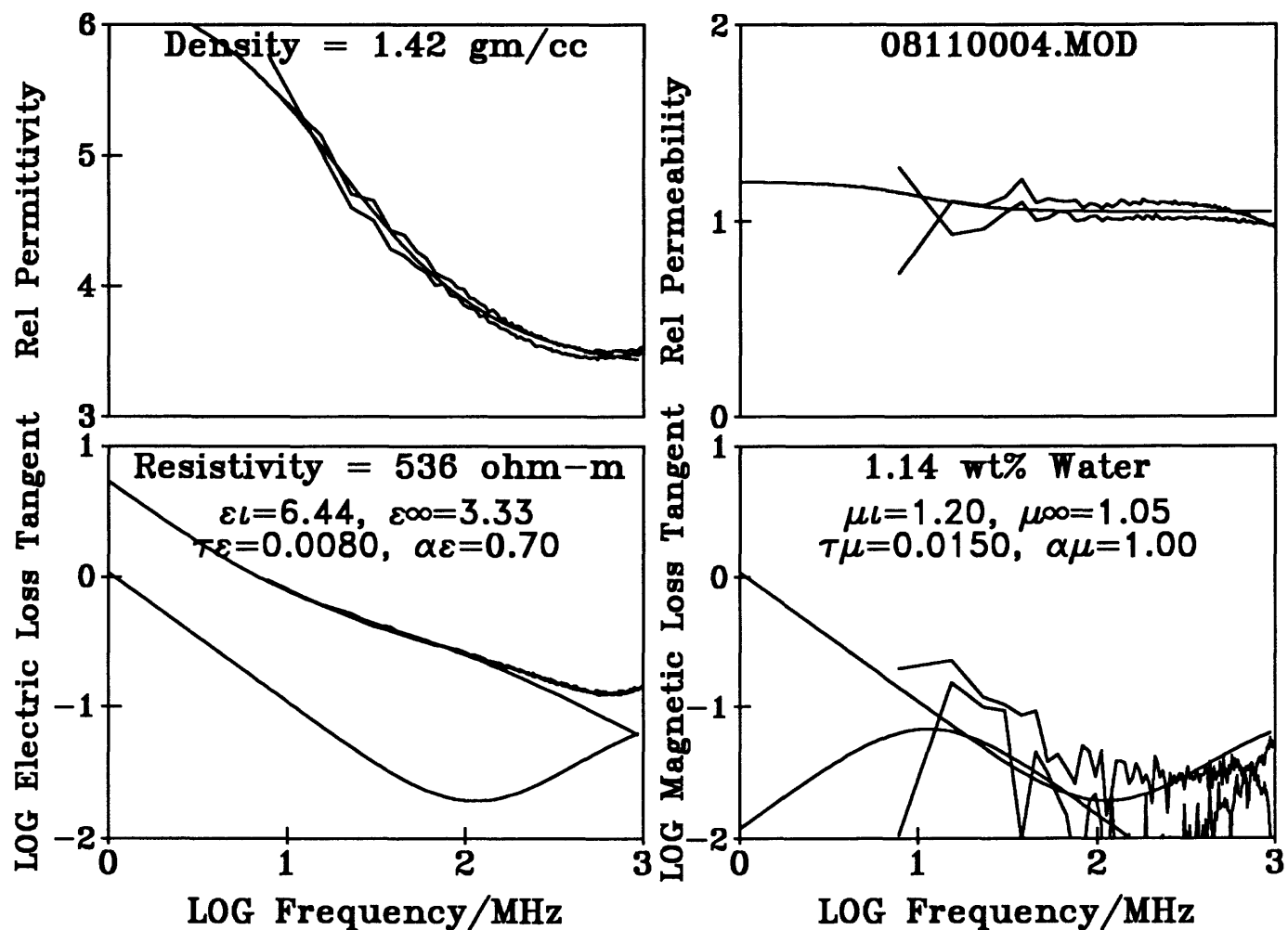
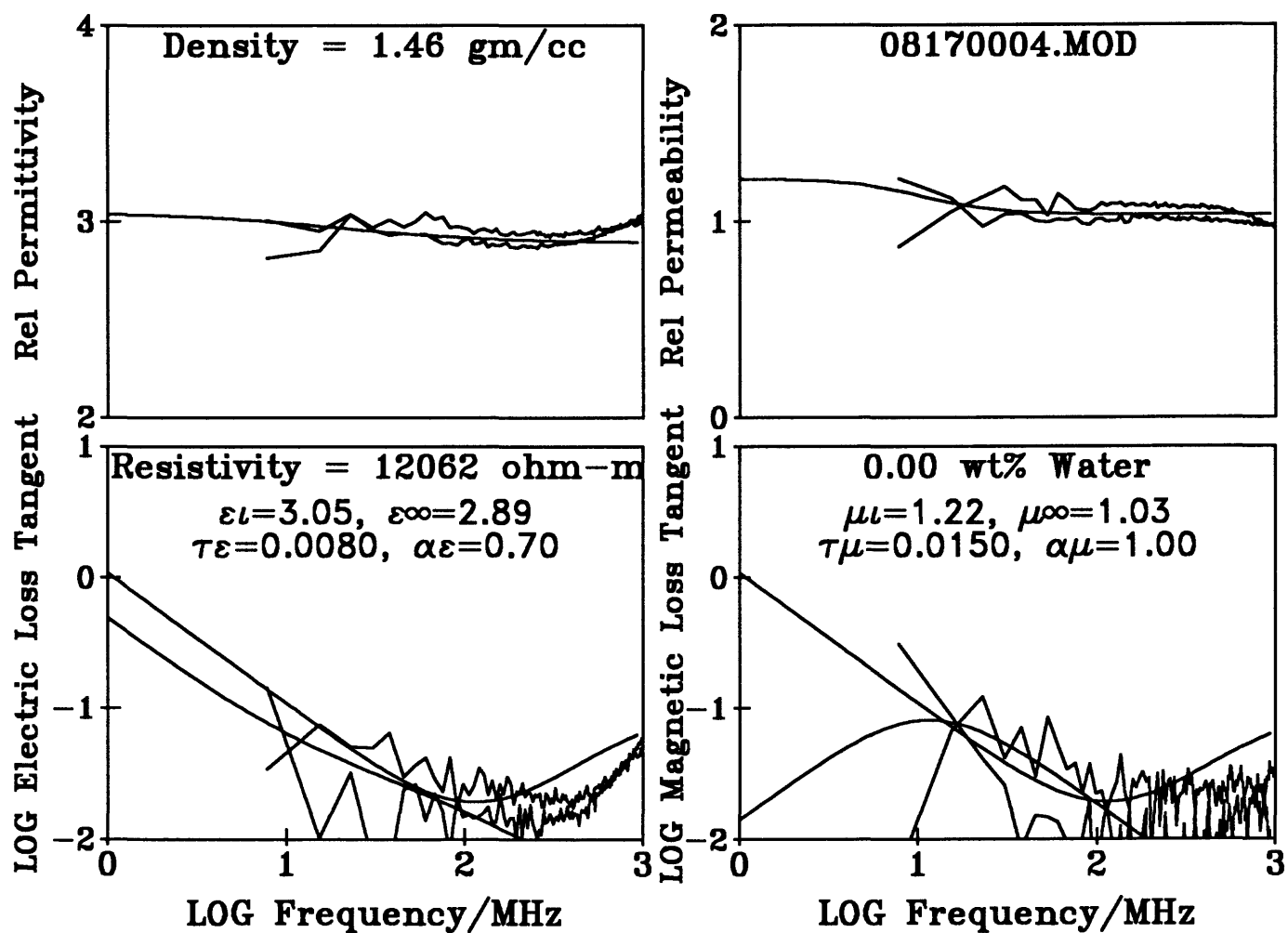


Figure 141 -
Natural state electromagnetic properties with water content preserved in sealed, taped,
sample bottle.



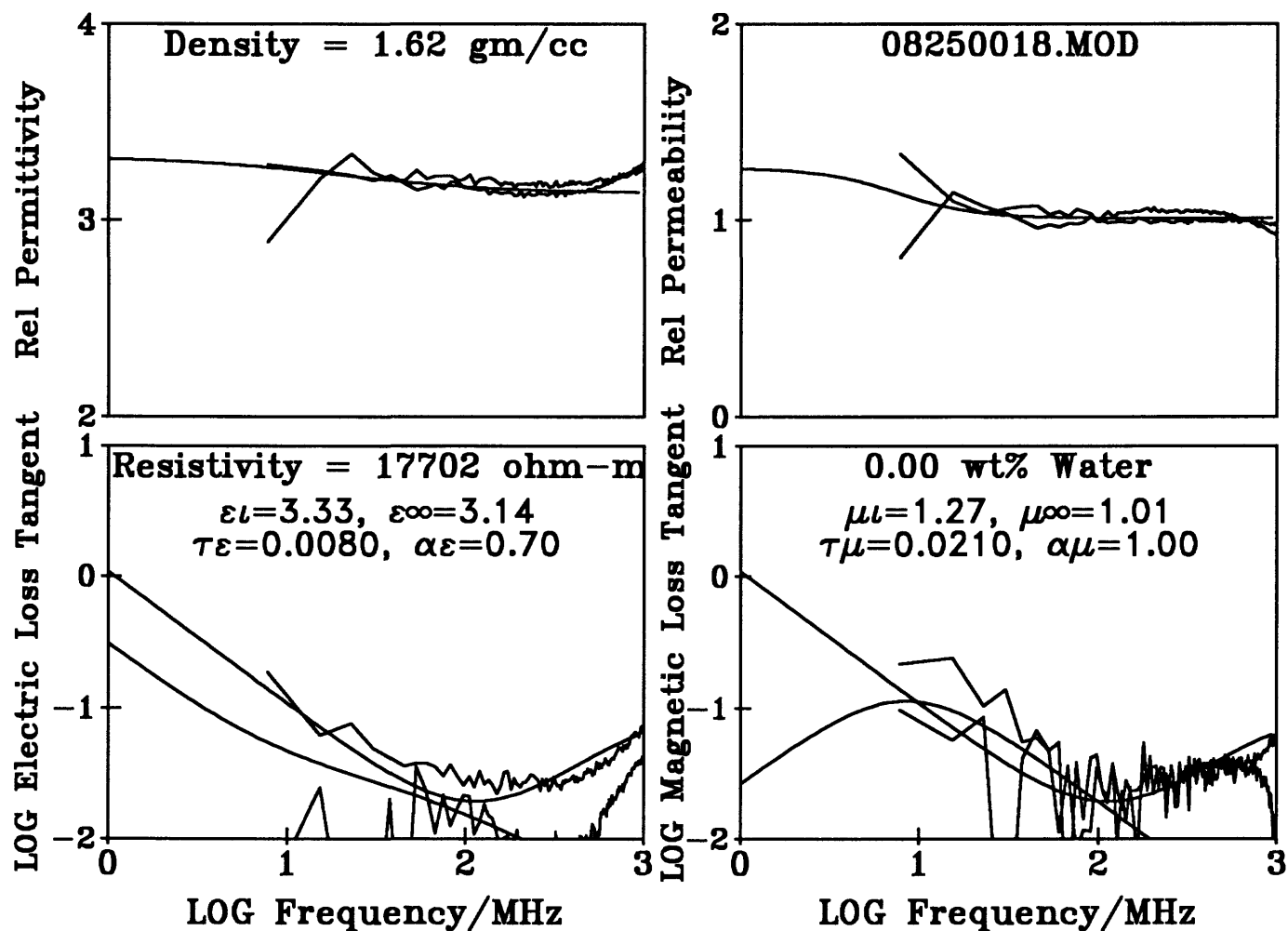
Yuma 3406m Stanton Main Line Drywash Deposit 0.5m depth #1

Figure 142 -
Natural state electromagnetic properties with water content preserved in sealed, taped,
sample bottle.



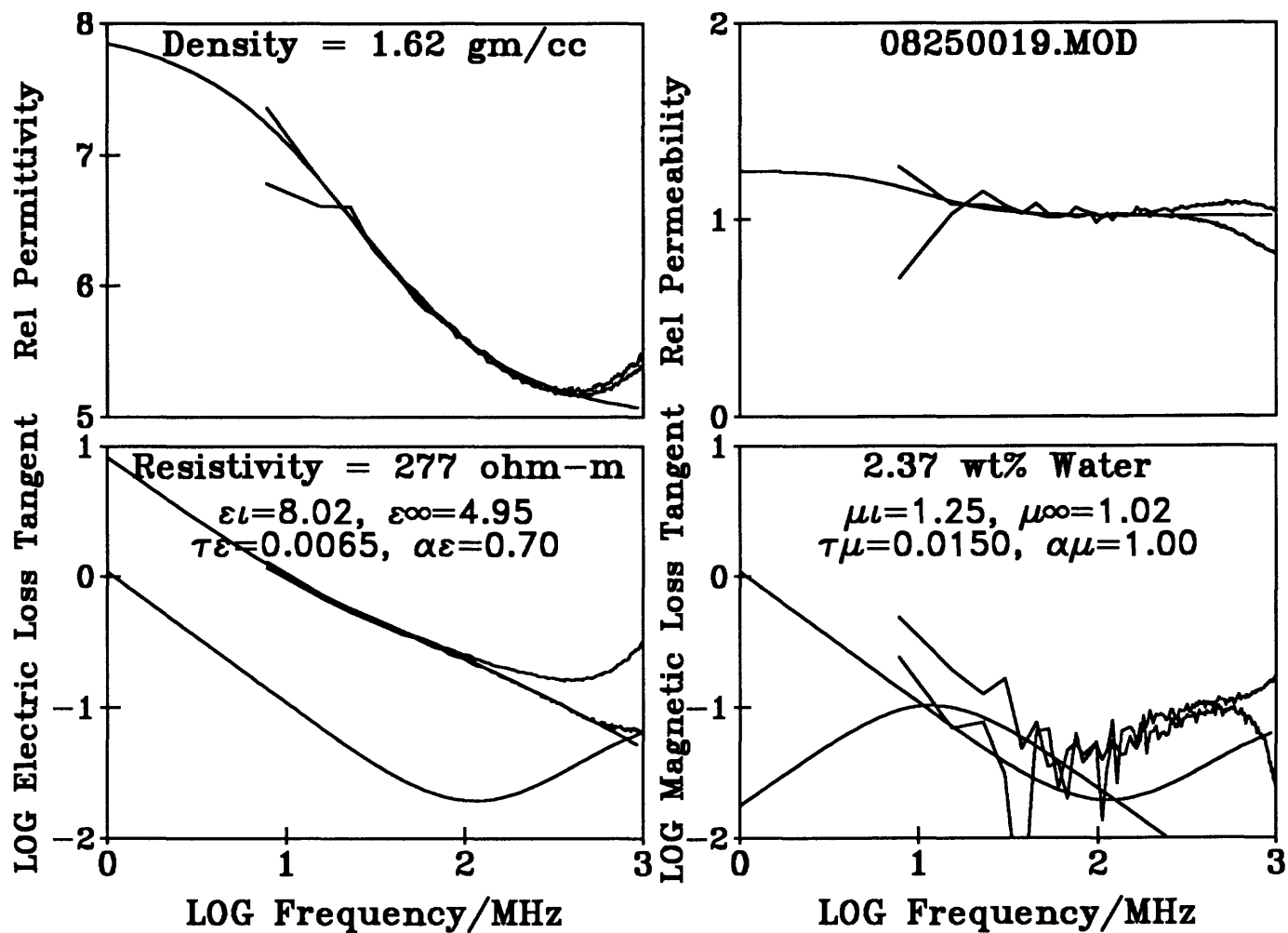
Yuma 3406m Stanton Main Line drywash 0.5m depth #2 vacuum dried

Figure 143 -



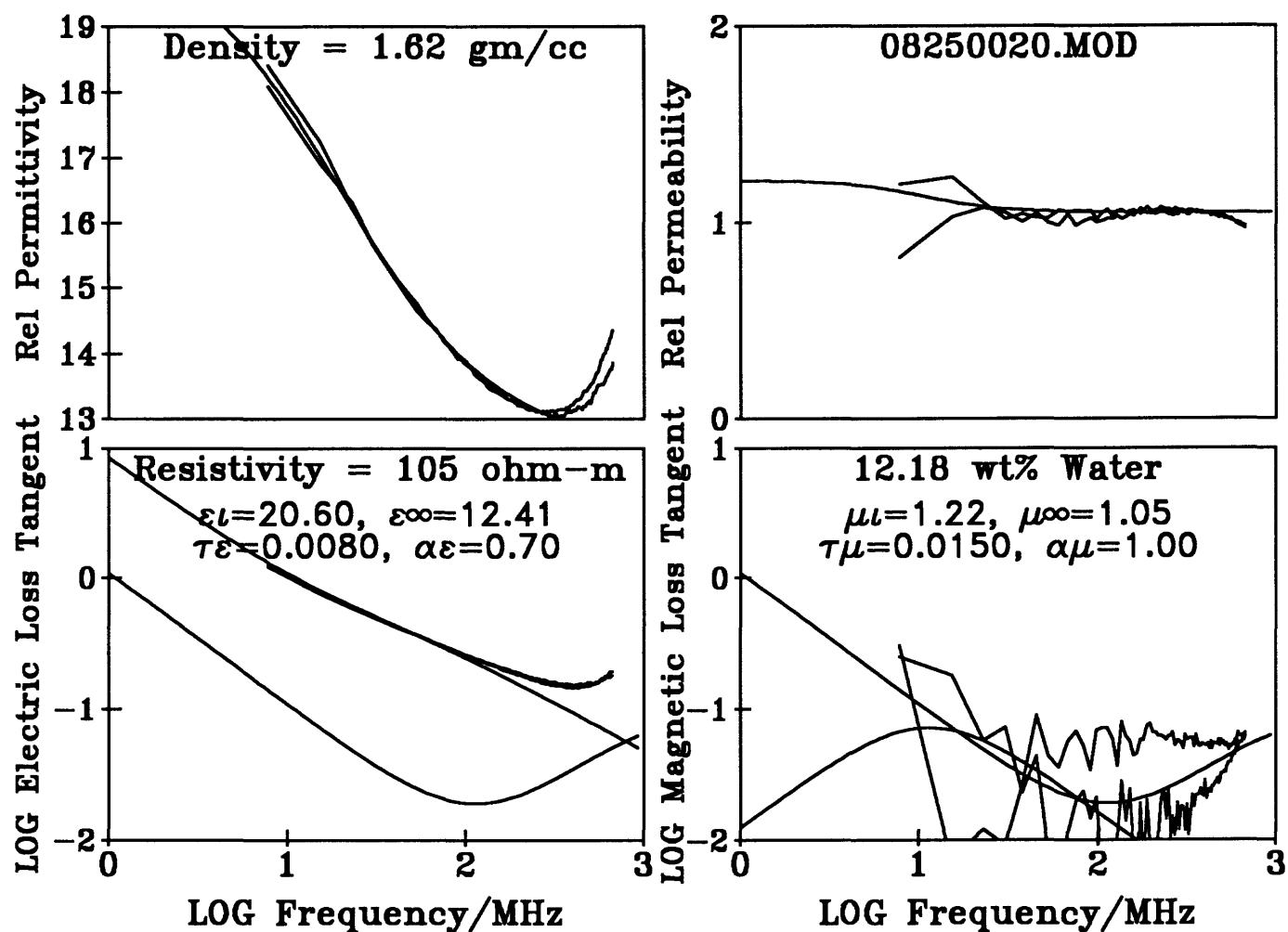
Yuma 3406m Stanton Main Line drywash 0.5m depth #3 vacuum dried

Figure 144 -



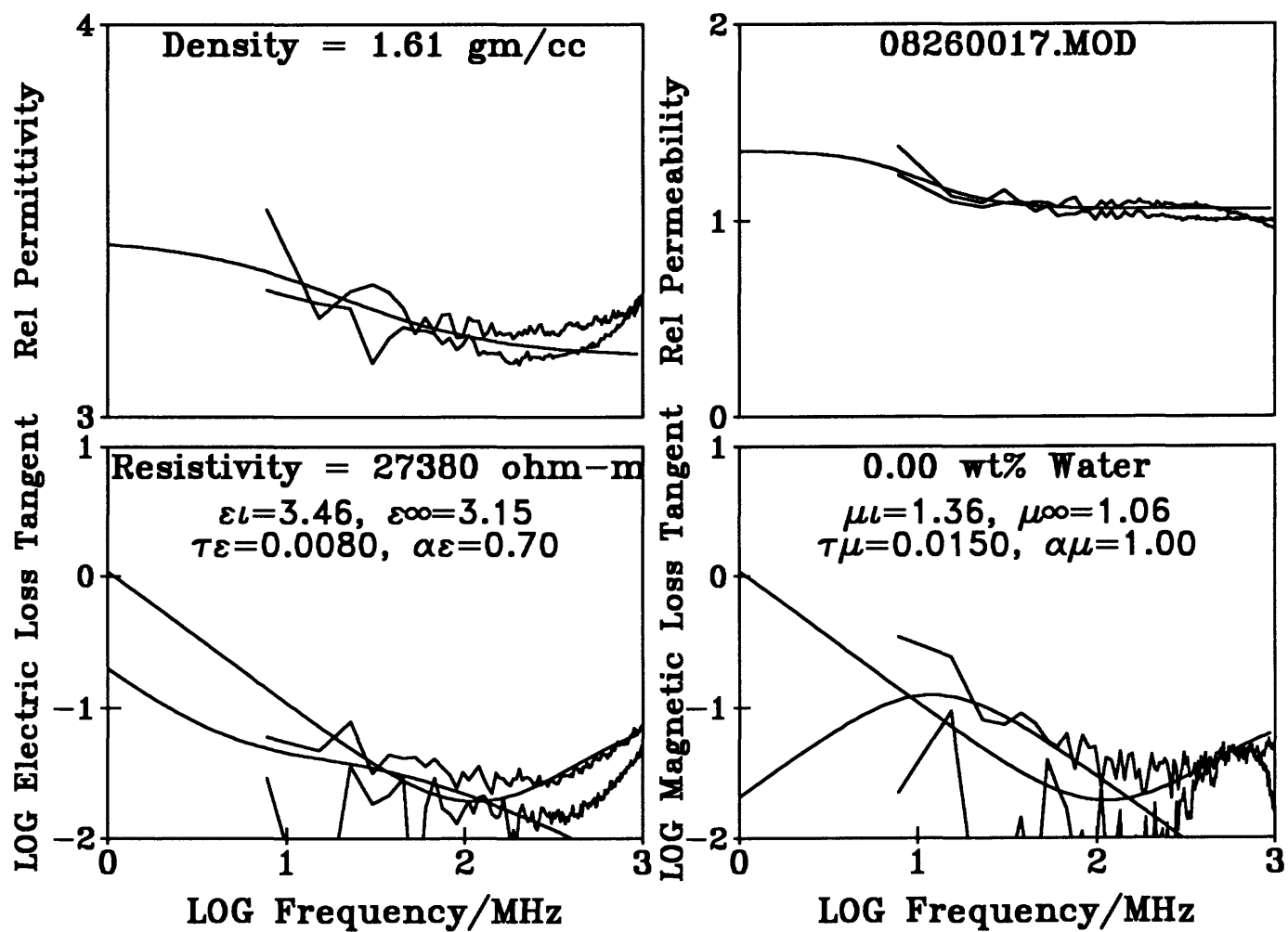
Yuma 3406m Stanton Main Line drywash 0.5m depth #3 4-drops water

Figure 145 -



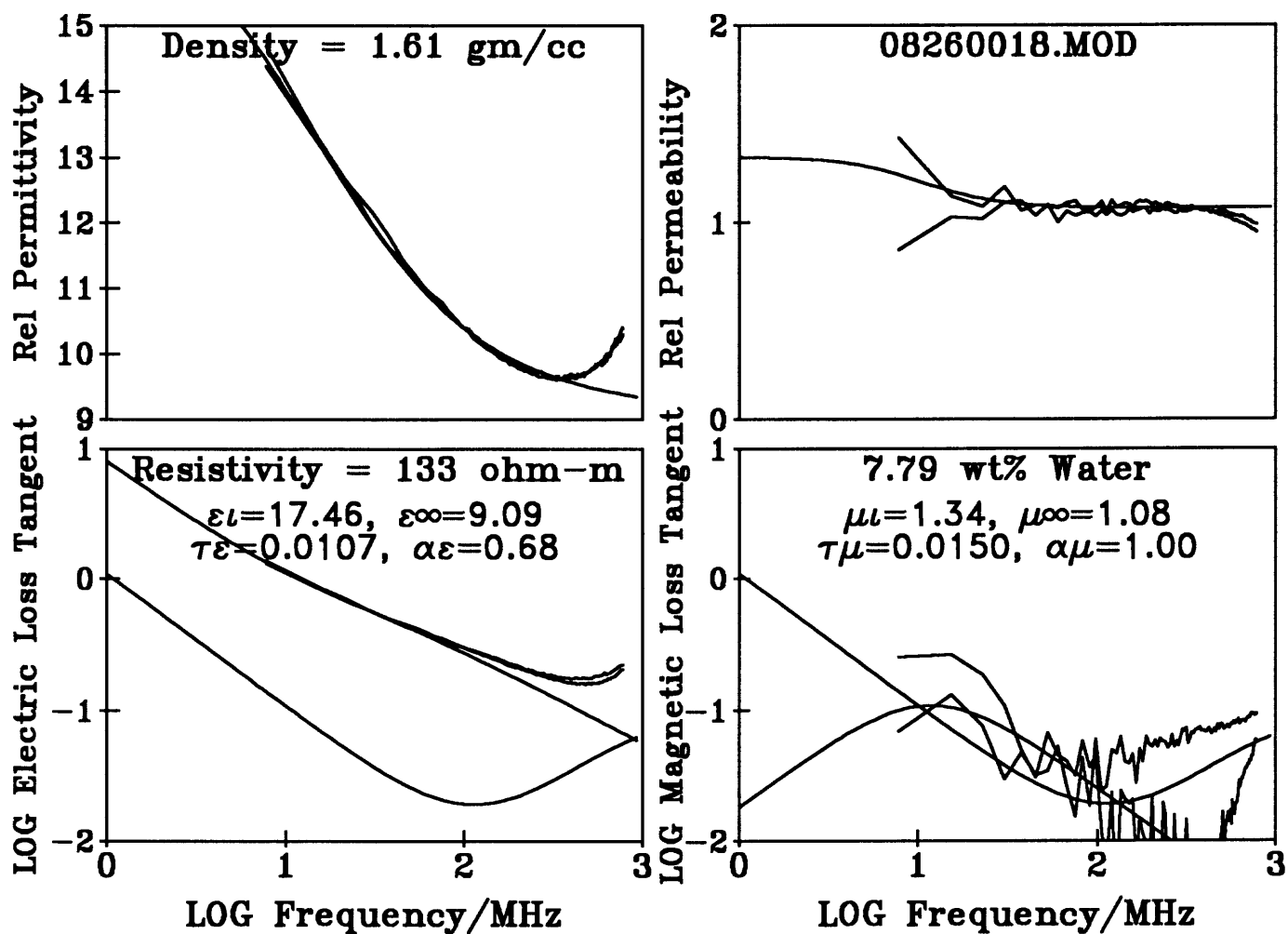
Yuma 3406m Stanton Main Line drywash 0.5m depth #3 water saturated

Figure 146 -



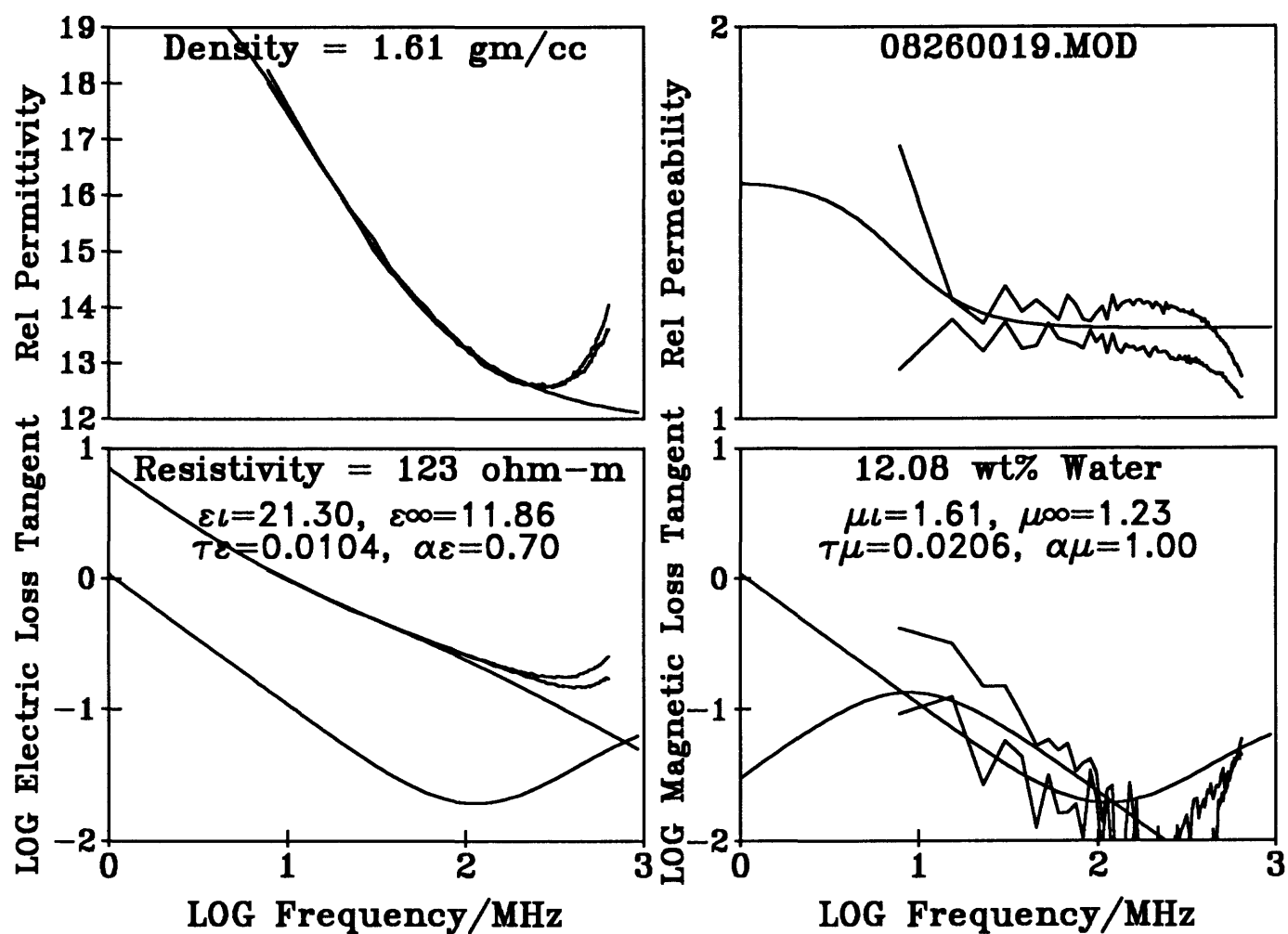
Yuma 3406m Stanton Main Line drywash 0.5m depth #4 vacuum dried

Figure 147 -



Yuma 3406m Stanton Main Line drywash 0.5m depth #4 10-drops water

Figure 148 -



Yuma 3406m Stanton Main Line drywash 0.5m depth #4 water saturated

Figure 149 -

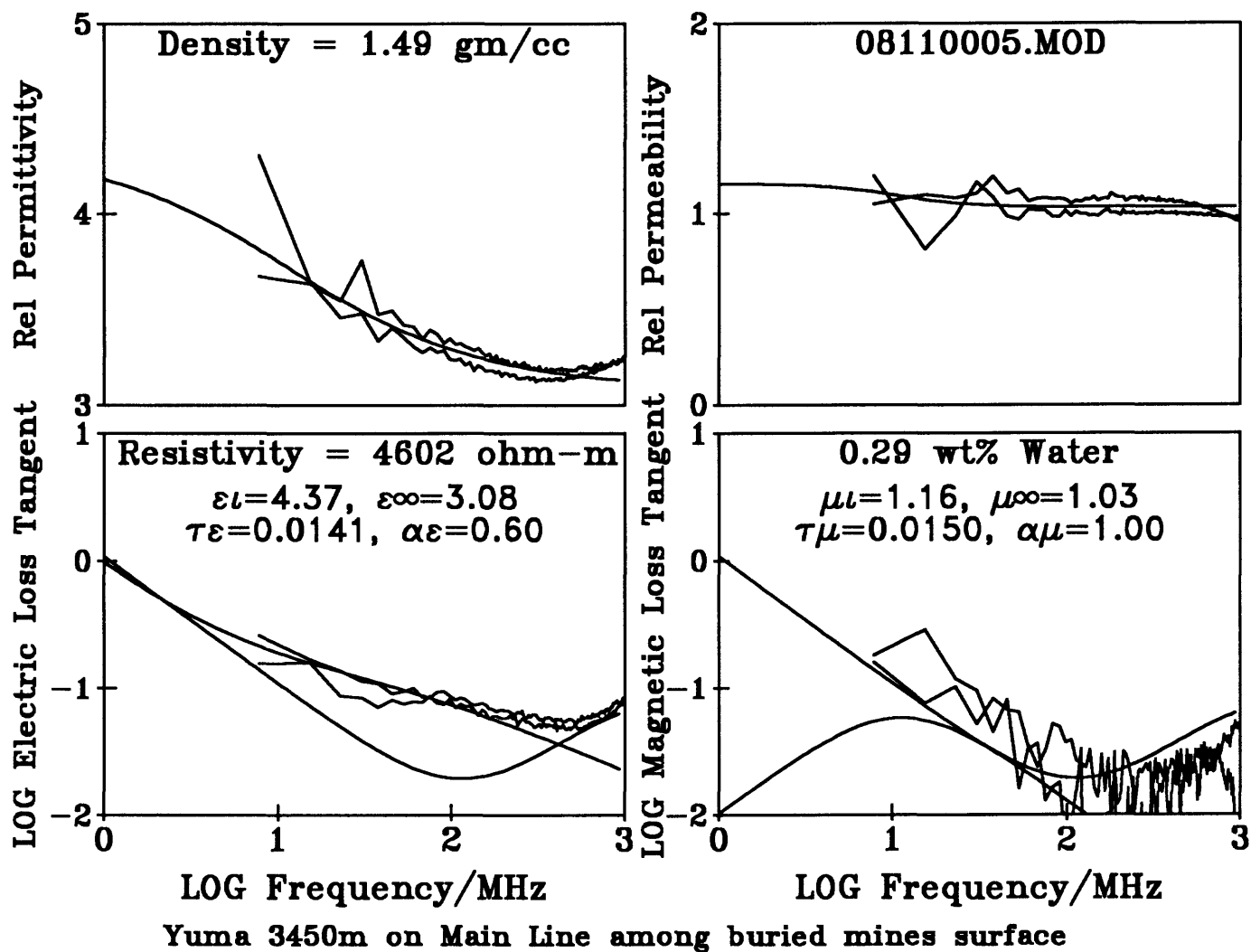
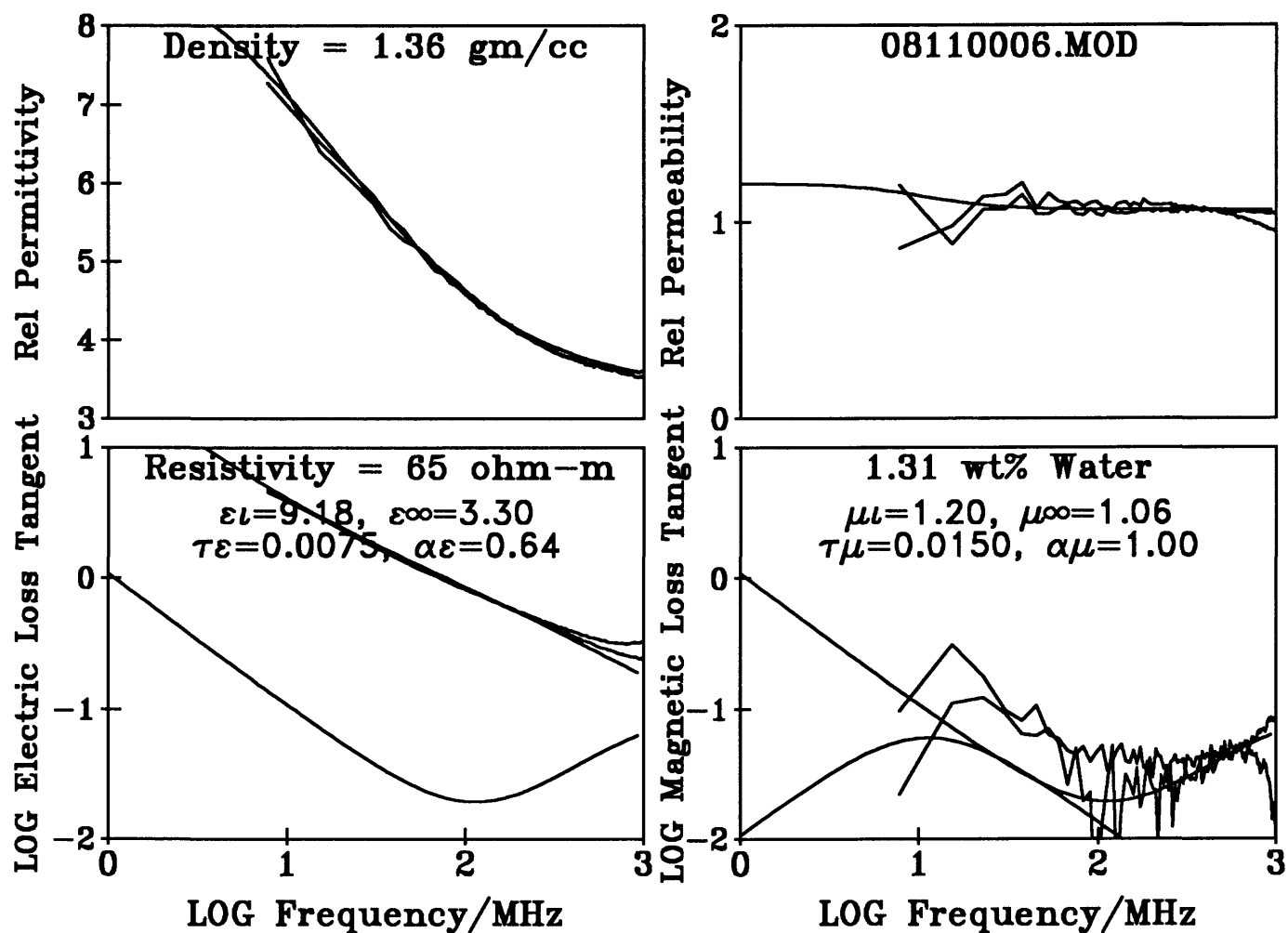
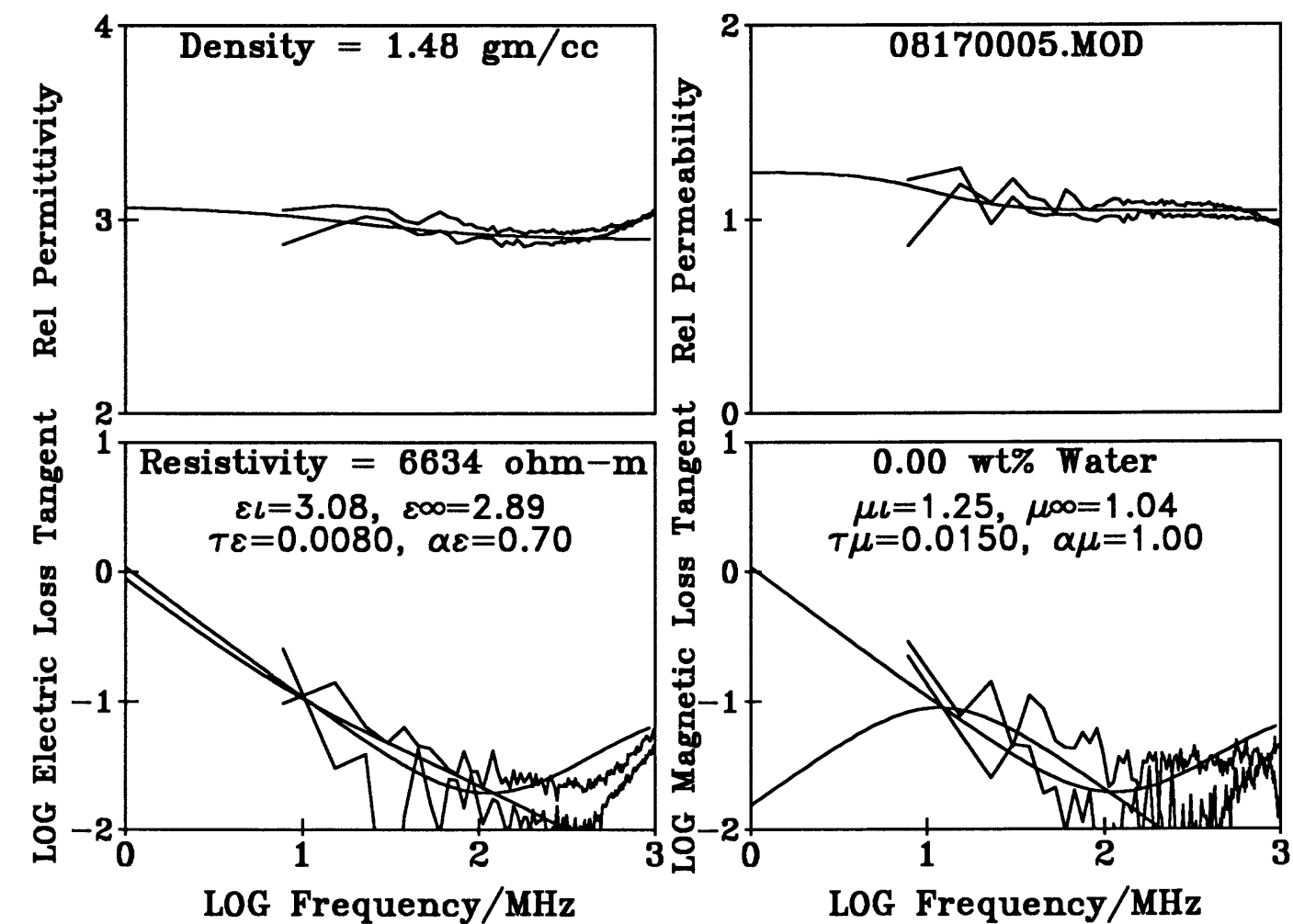


Figure 150 -
Natural state electromagnetic properties with water content preserved in sealed, taped, sample bottle.



Yuma 3450m on Main Line among buried mines 0.5m depth #1

Figure 151 -
Natural state electromagnetic properties with water content preserved in sealed, taped,
sample bottle.



Yuma 3450m on Main Line among buried mines 0.5m depth #2 vacuum dried

Figure 152 -

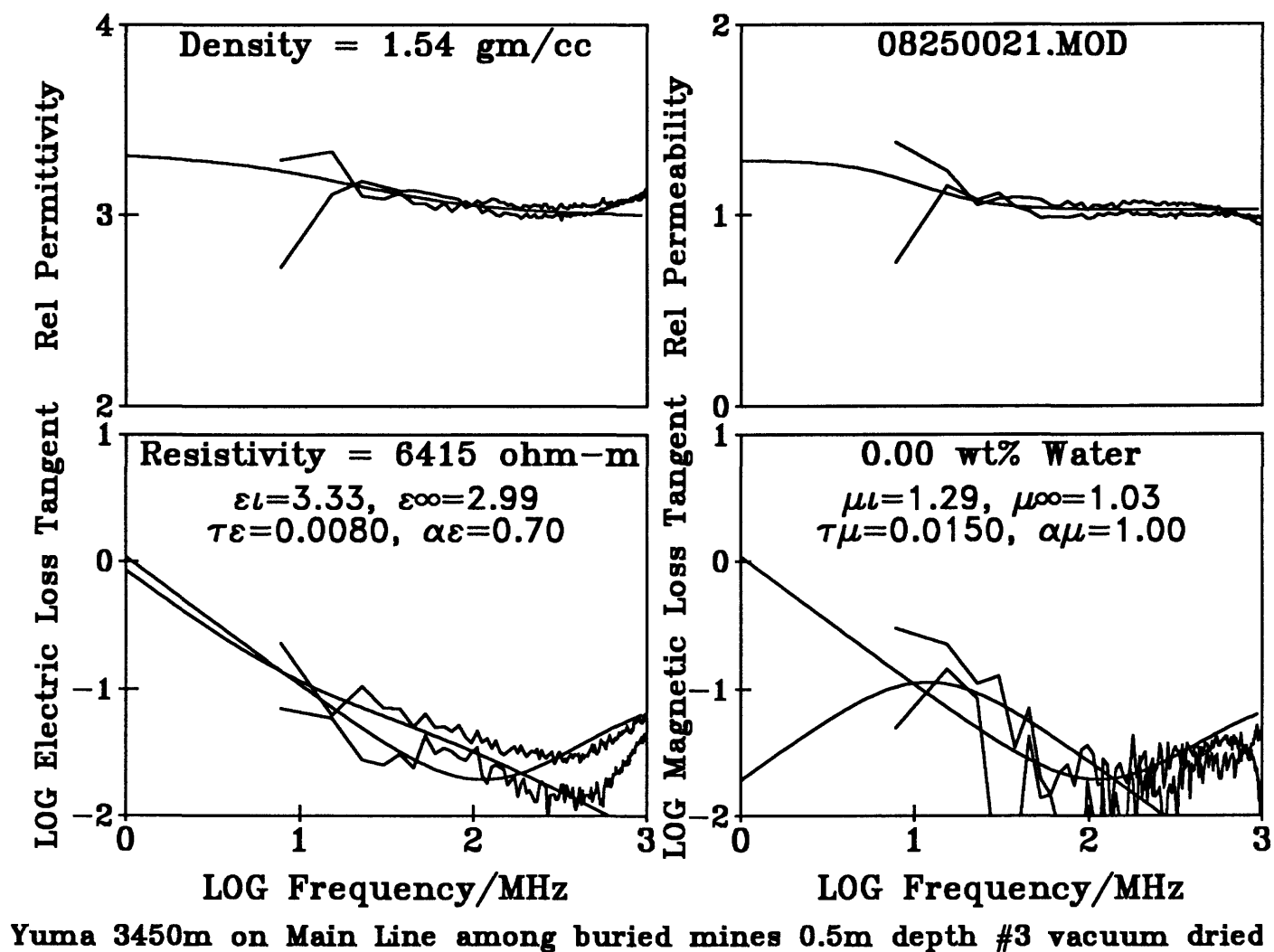
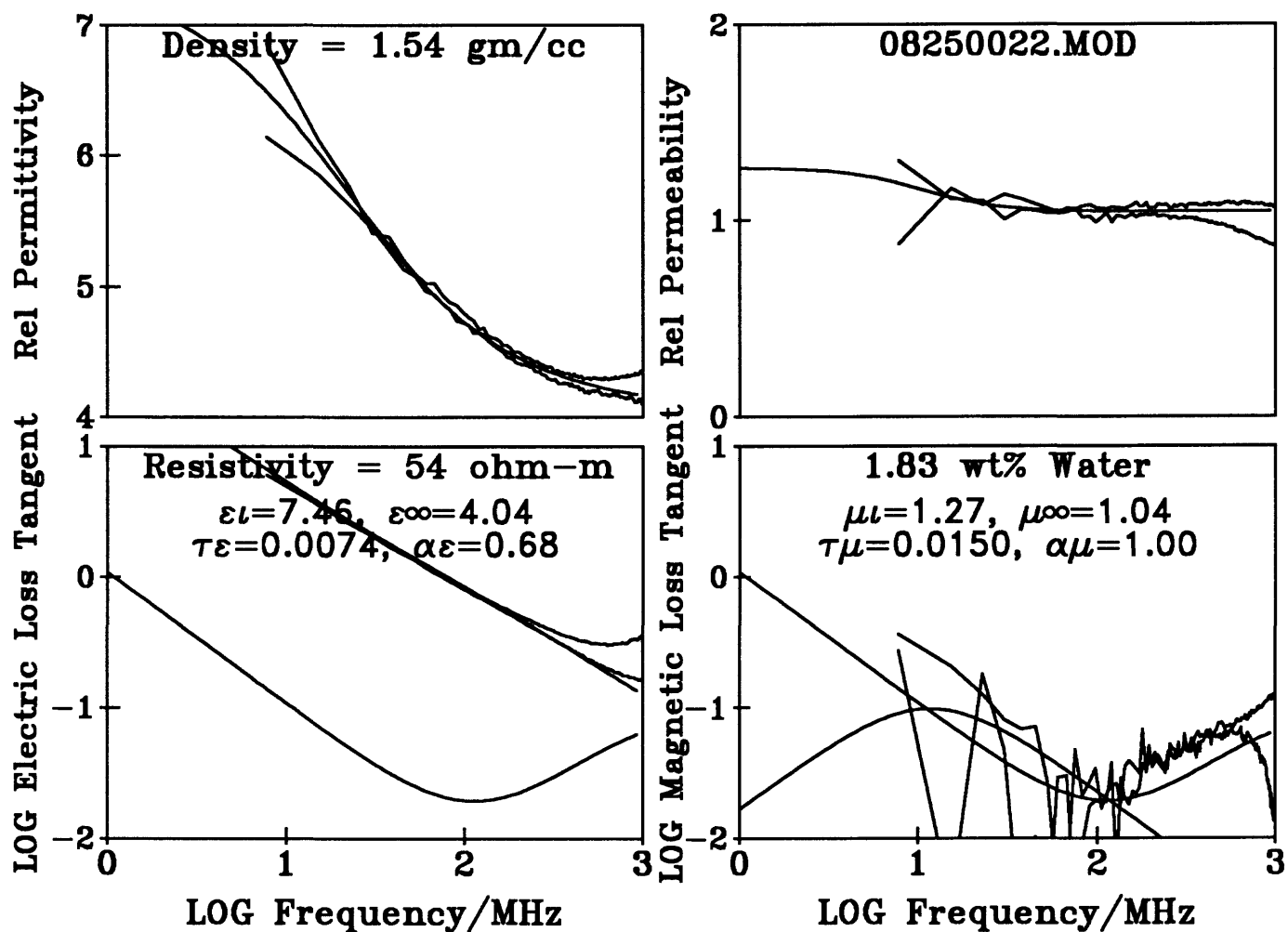
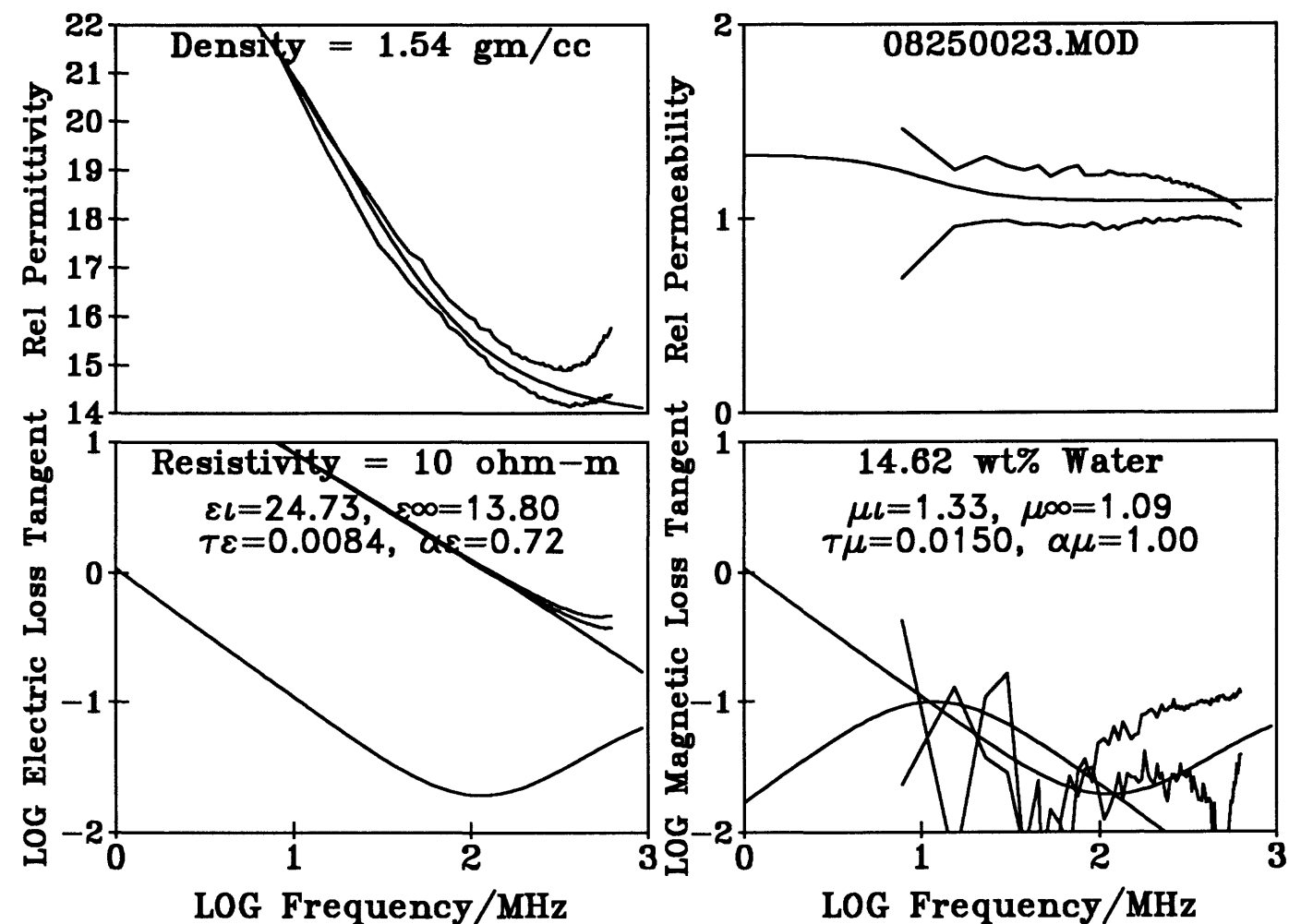


Figure 153 -



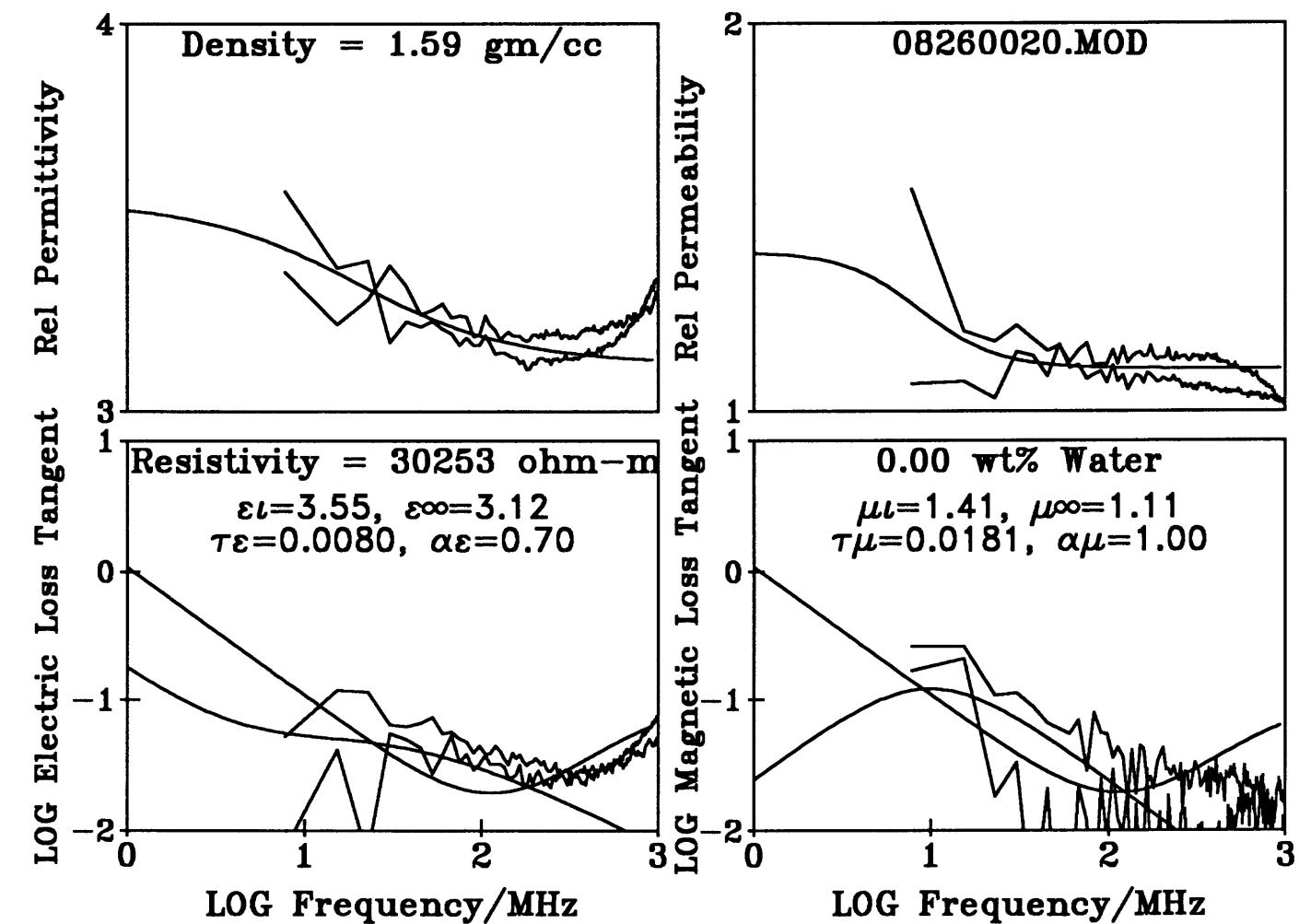
Yuma 3450m Main Line among buried mines 0.5m depth #3 4-drops water

Figure 154 -



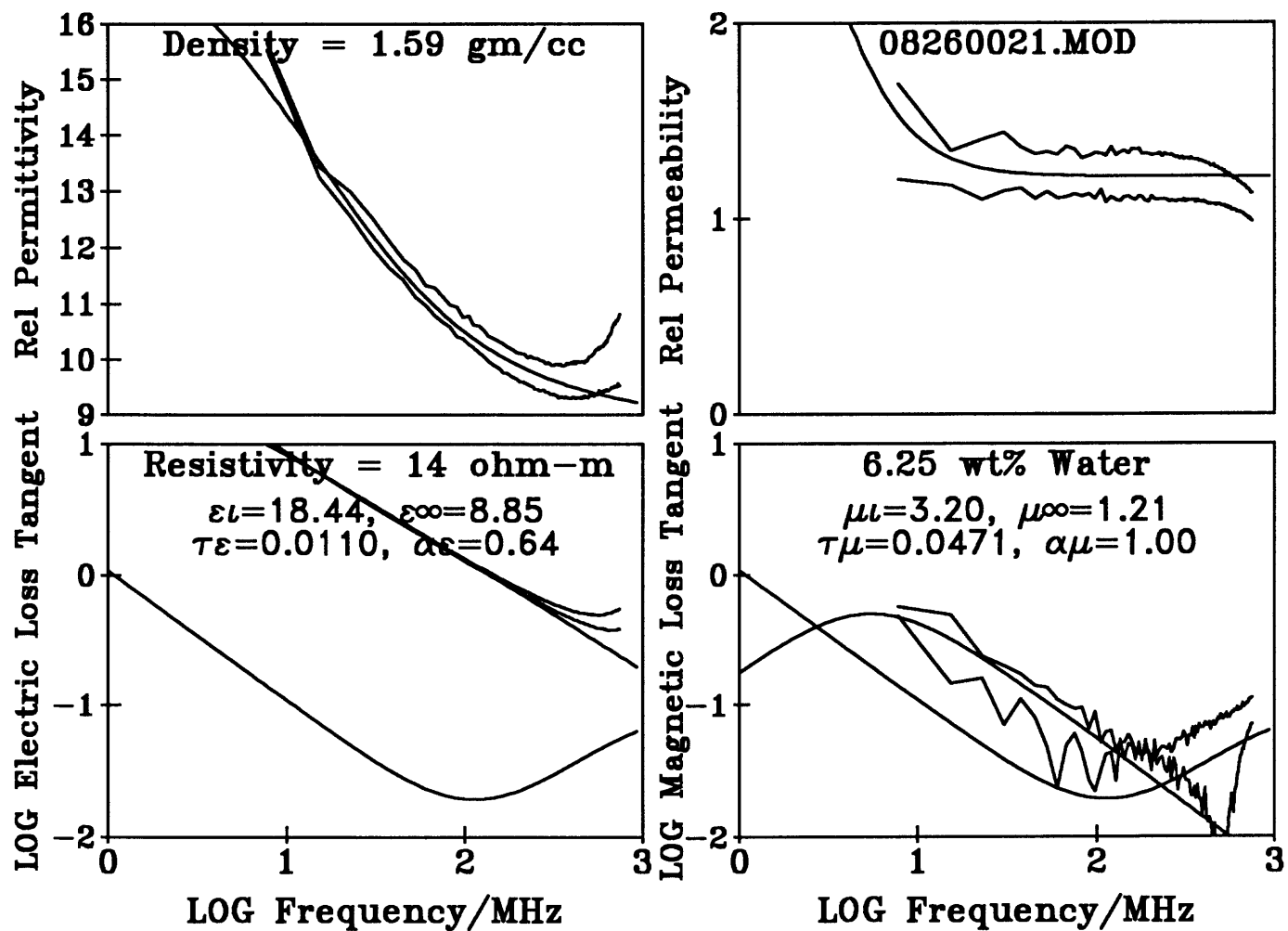
Yuma 3450m Main Line among buried mines 0.5m depth #3 water saturated

Figure 155 -



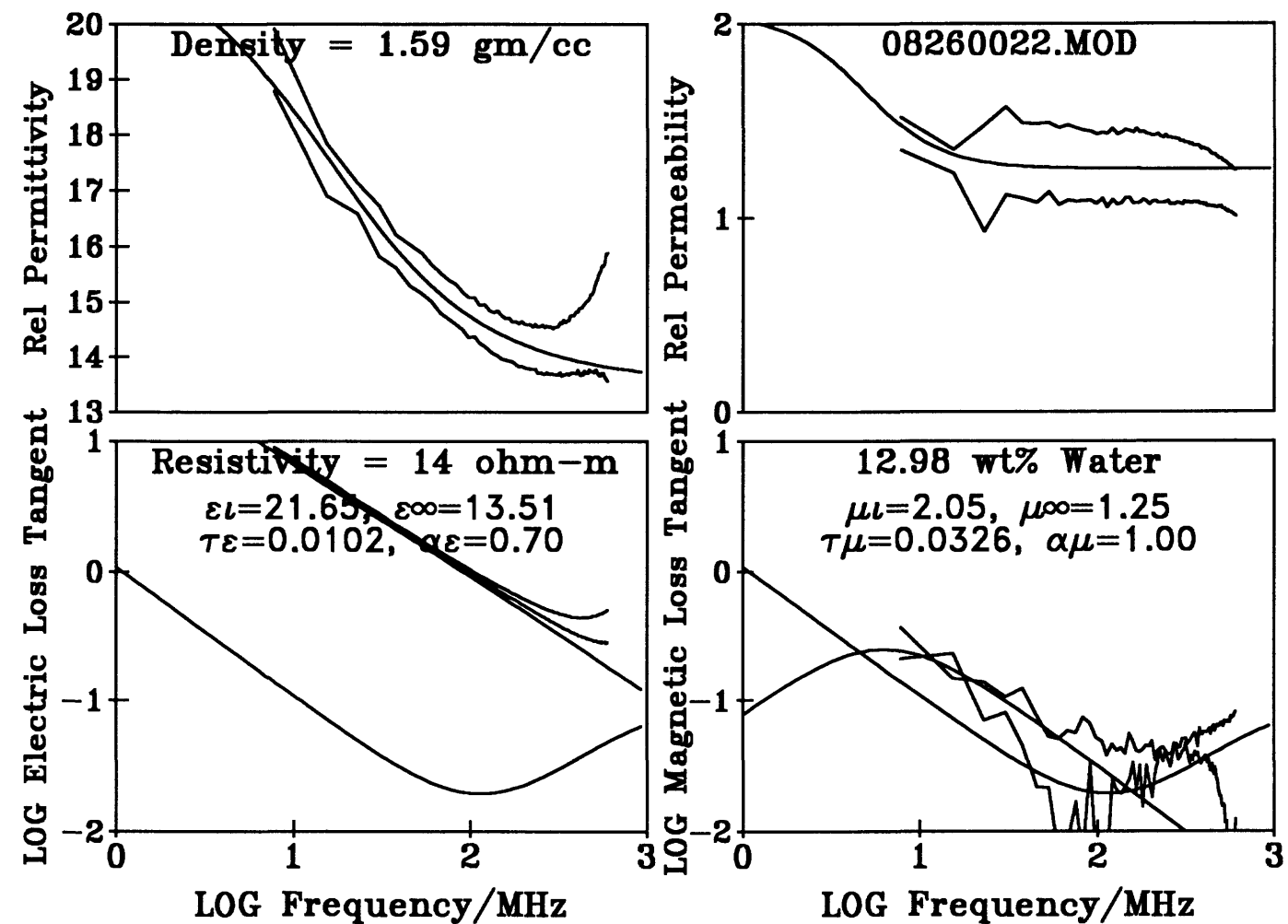
Yuma 3450m on Main Line among buried mines 0.5m depth #4 vacuum dried

Figure 156 -



Yuma 3450m Main Line among buried mines 0.5m depth #4 9-drops water

Figure 157 -



Yuma 3450m Main Line among buried mines 0.5m depth #4 water saturated

Figure 158 -

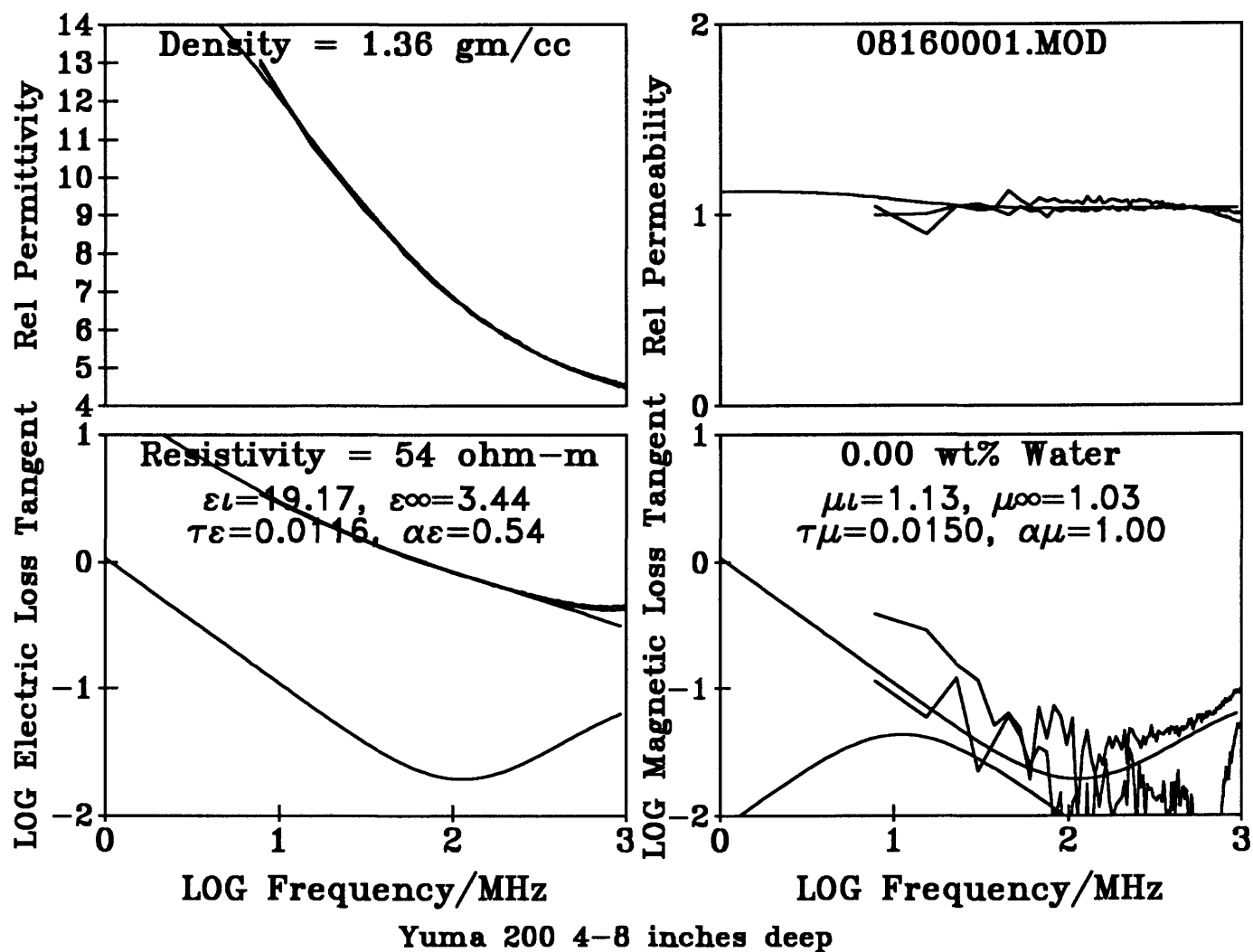


Figure 159 -
 Sample provided by Lincoln Laboratory in a ziplock bag -- water content and location unknown.

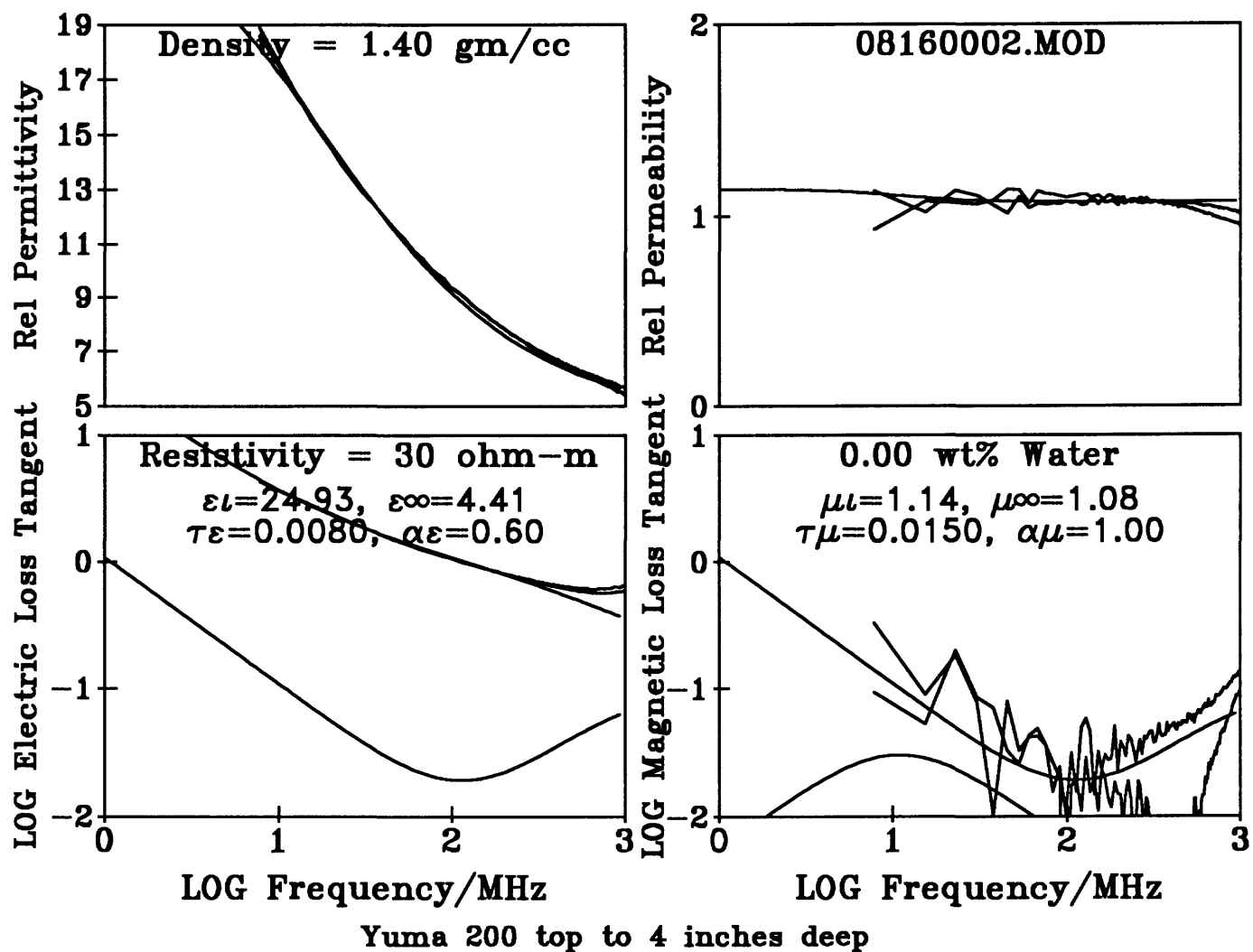


Figure 160 -
Sample provided by Lincoln Laboratory in a ziplock bag -- water content and location unknown.

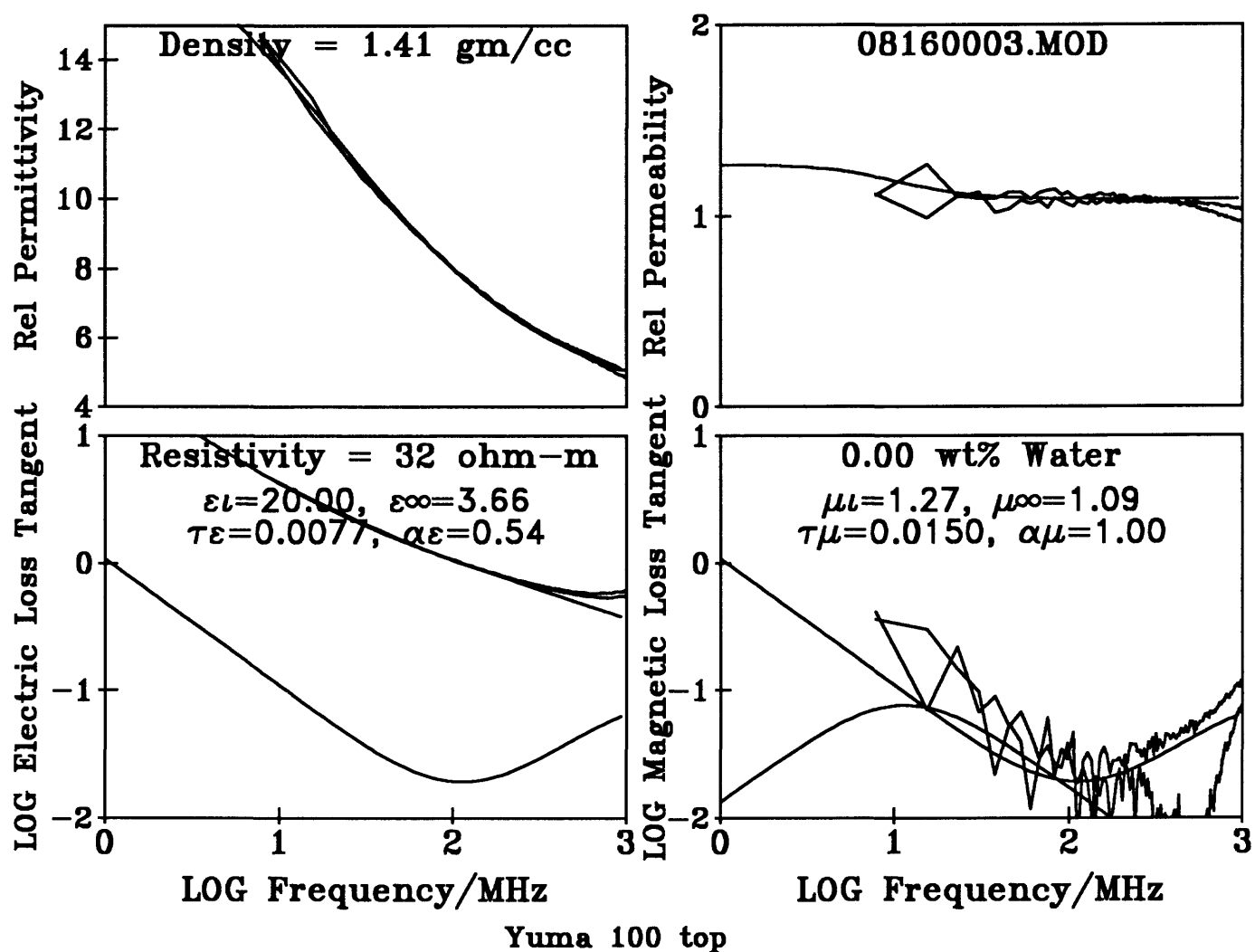


Figure 161 -
 Sample provided by Lincoln Laboratory in a ziplock bag -- water content and location unknown.

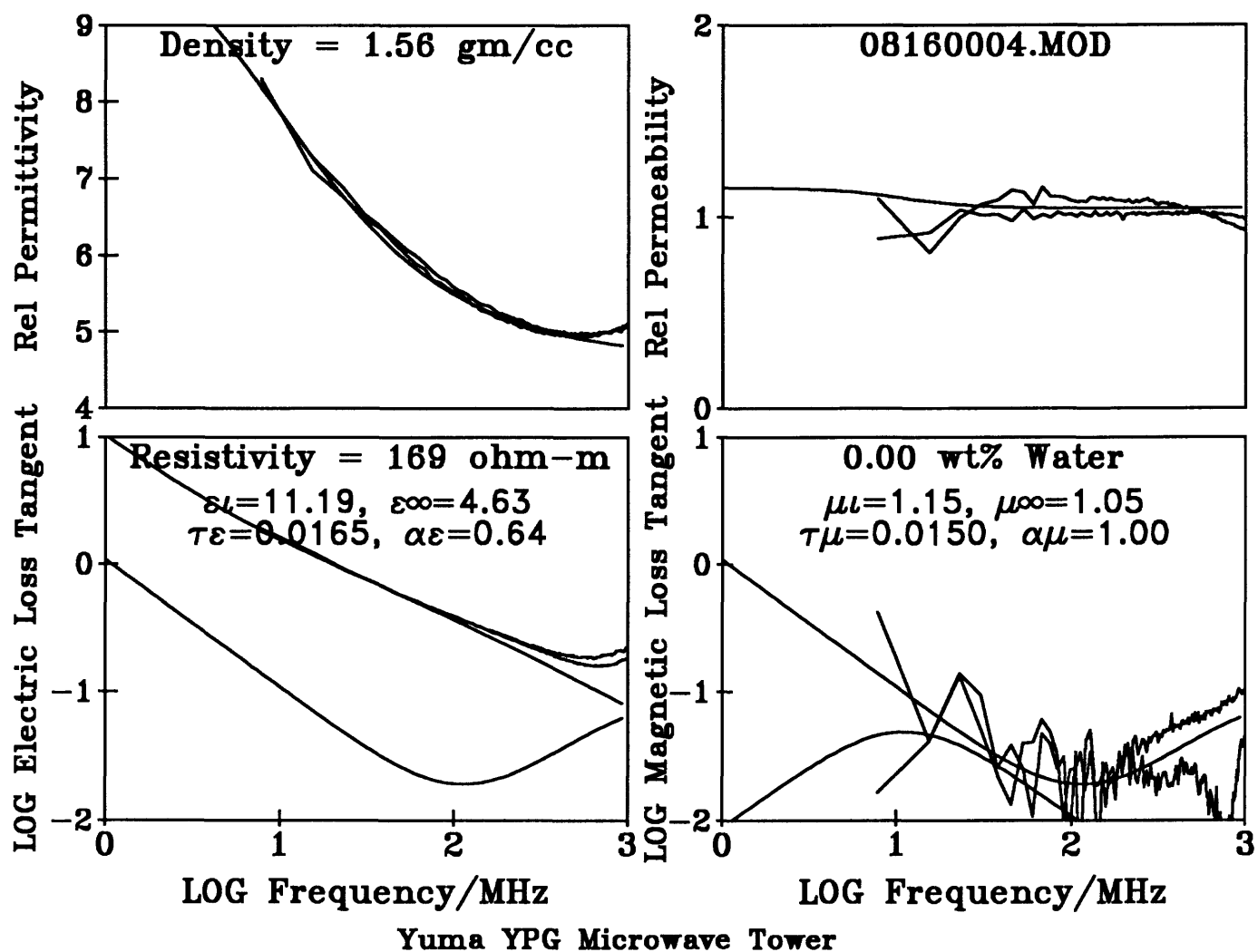


Figure 162 -
Sample provided by Lincoln Laboratory in a ziplock bag -- water content and location unknown.

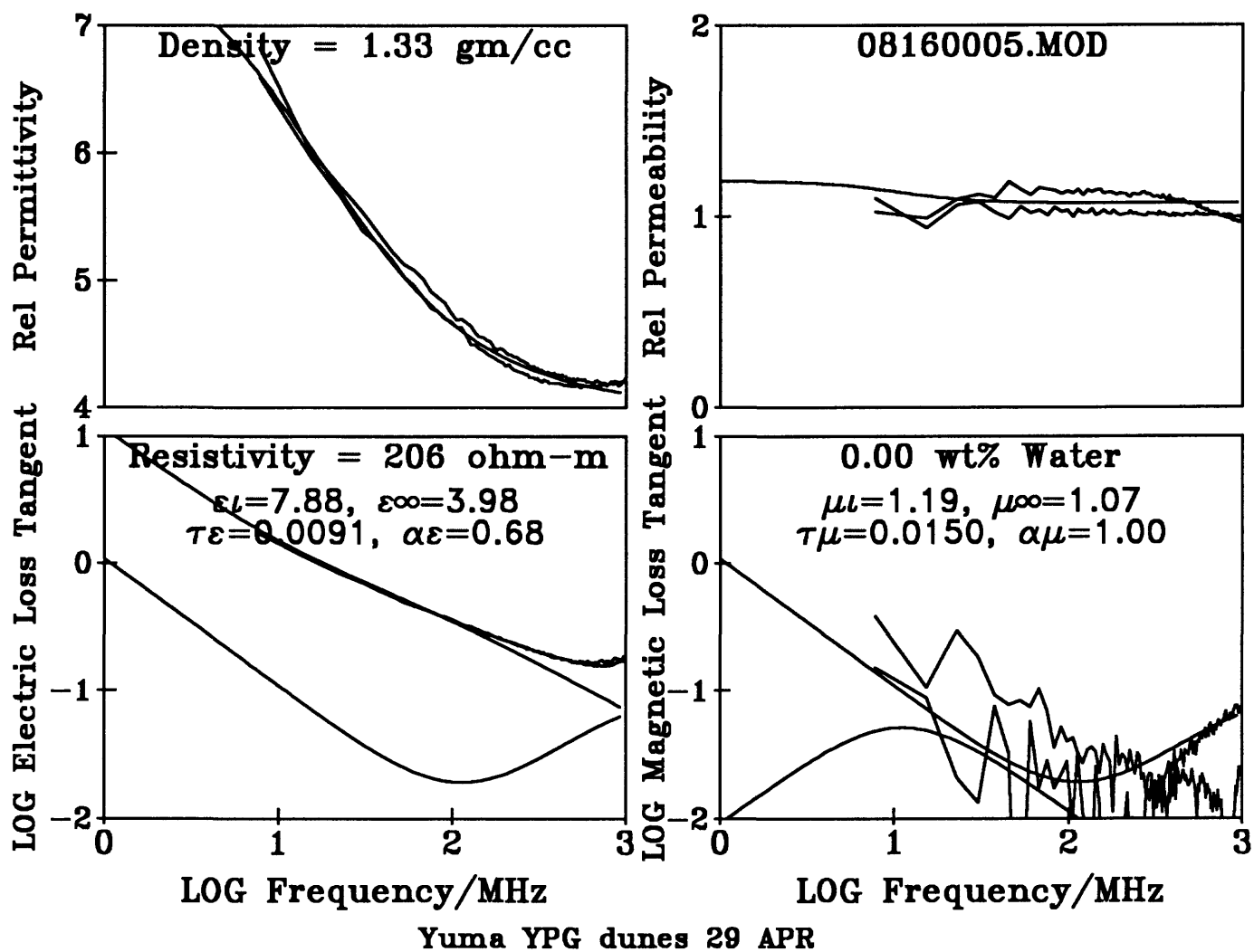


Figure 163 -
Sample provided by Lincoln Laboratory in a ziplock bag -- water content and location unknown.

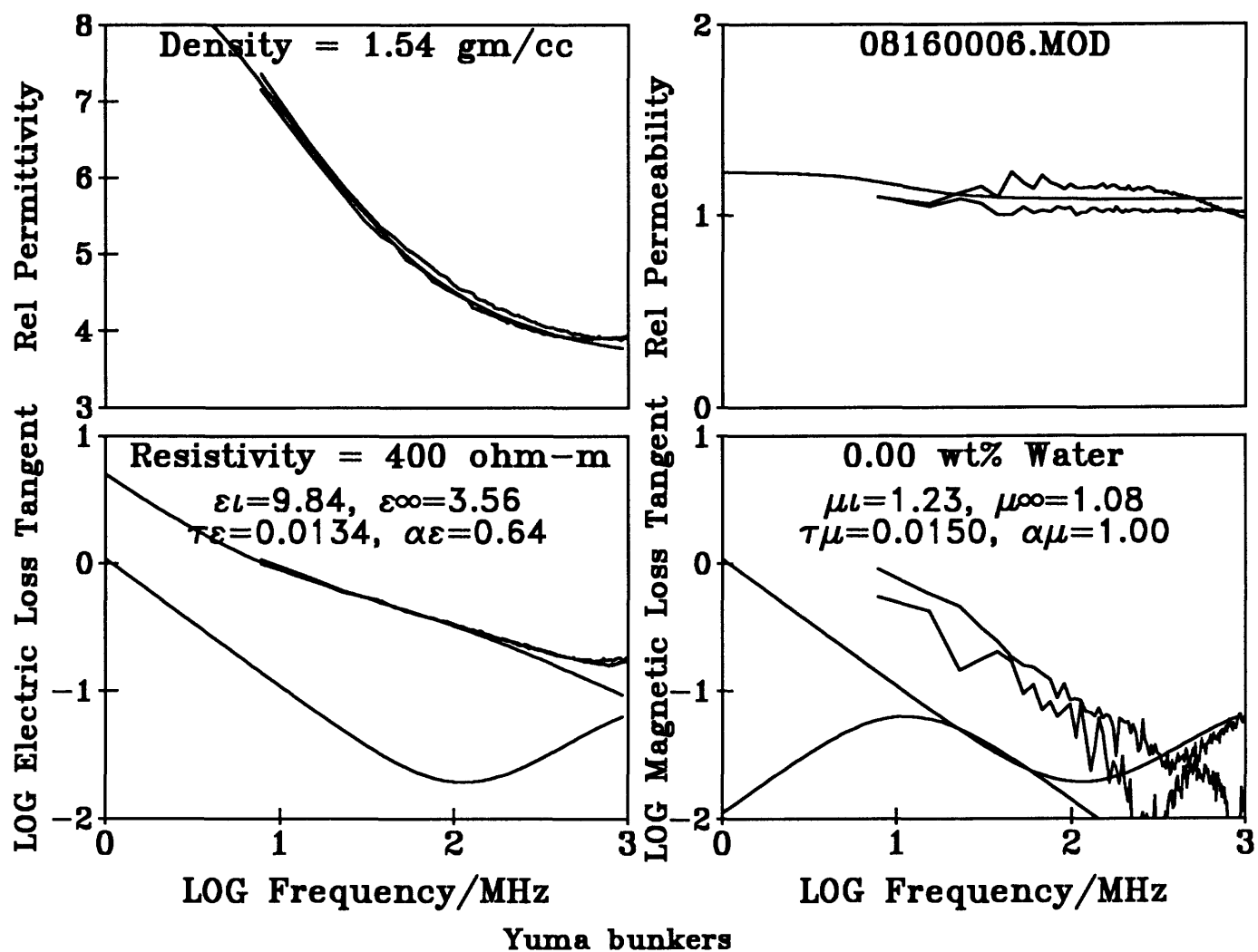


Figure 164 -
Sample provided by Lincoln Laboratory in a ziplock bag -- water content and location unknown.

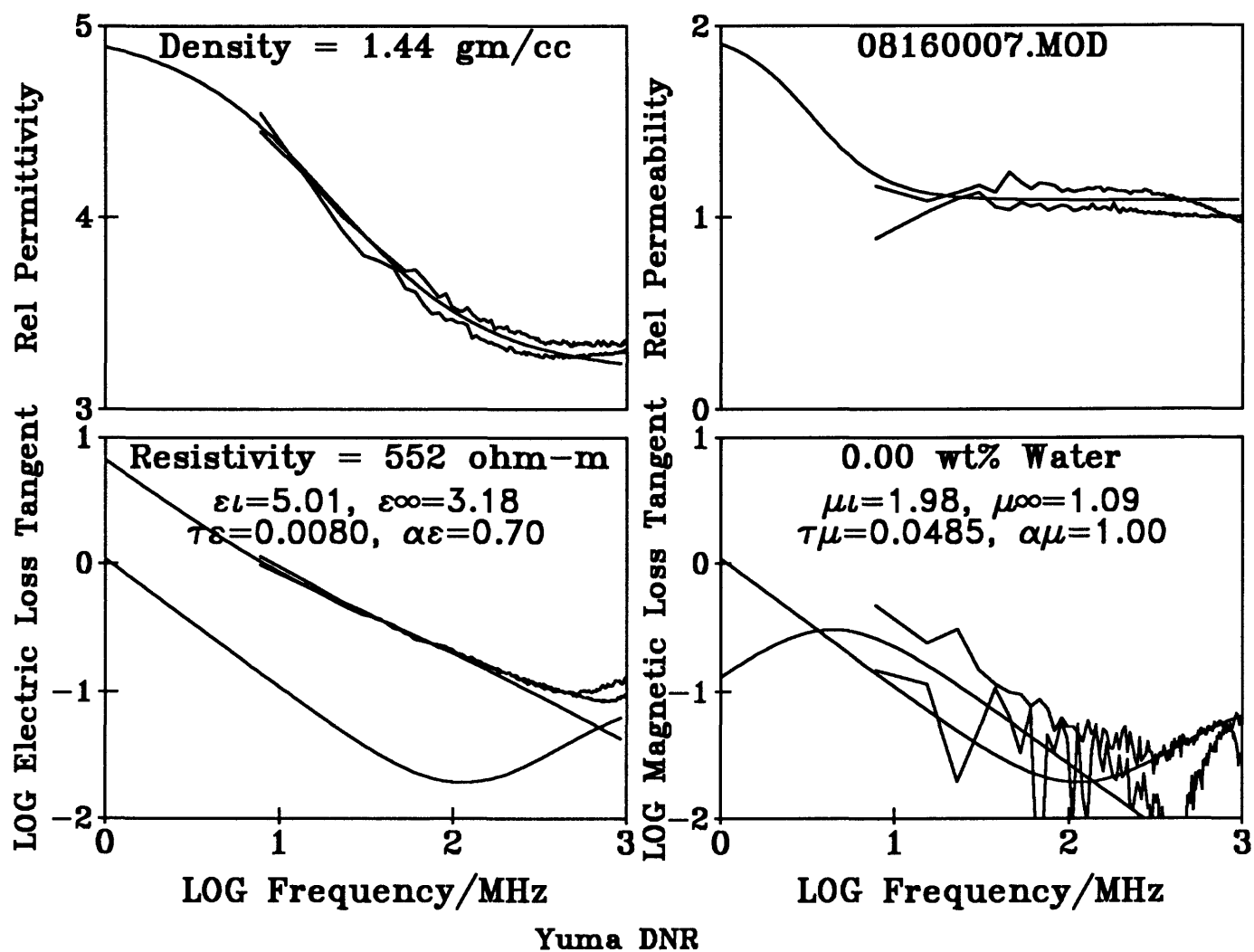


Figure 165 -
Sample provided by Lincoln Laboratory in a ziplock bag -- water content and location unknown.

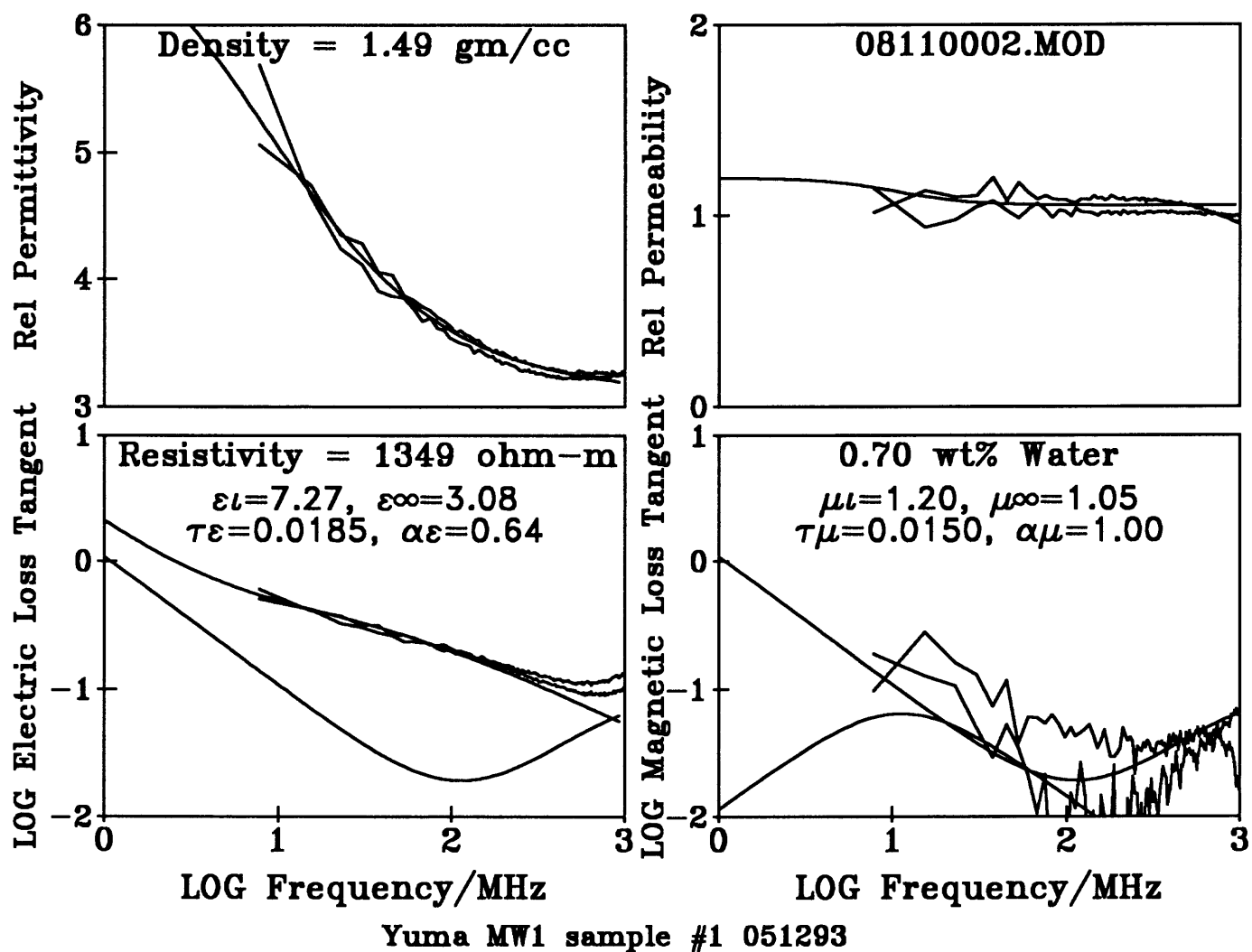


Figure 166 -
Sample provided by Lincoln Laboratory in a sealed bottle -- presumed natural water content -- location unknown.

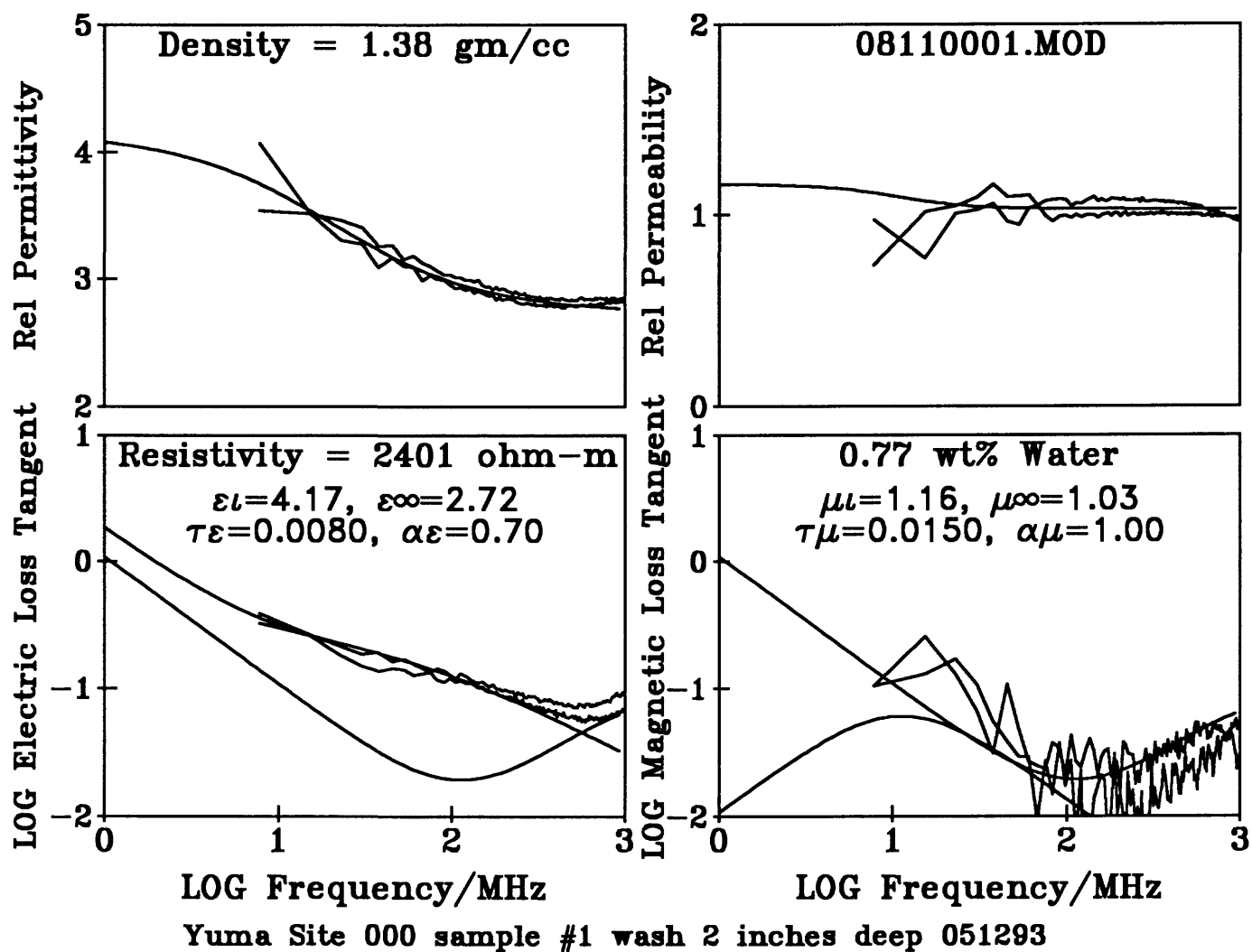
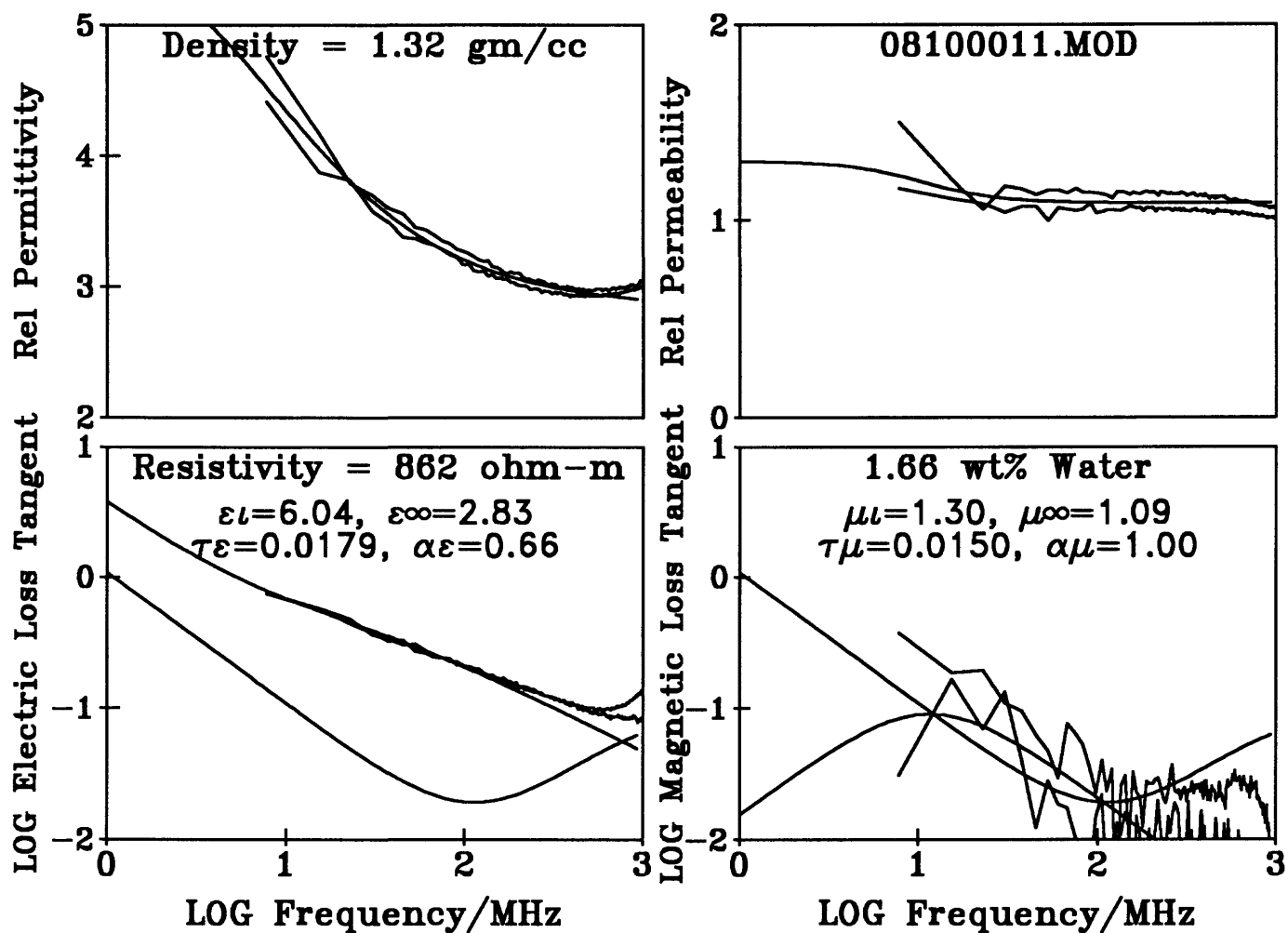


Figure 167 -

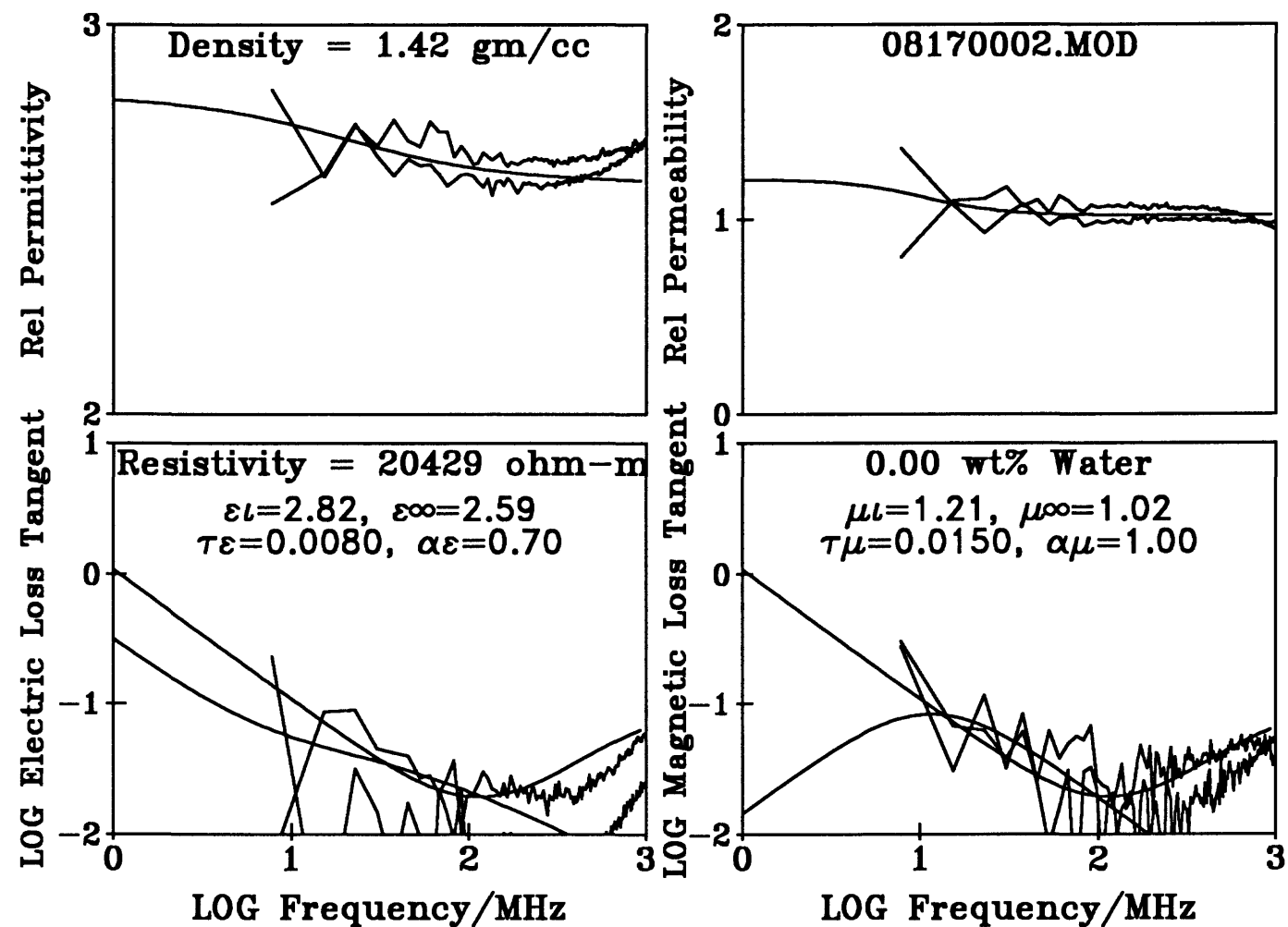
Sample provided by Lincoln Laboratory in a sealed bottle -- presumed natural water content -- location unknown.



Yuma Site 000 sample #2 crest of dune (2nd) 4 inches deep 051293 #1

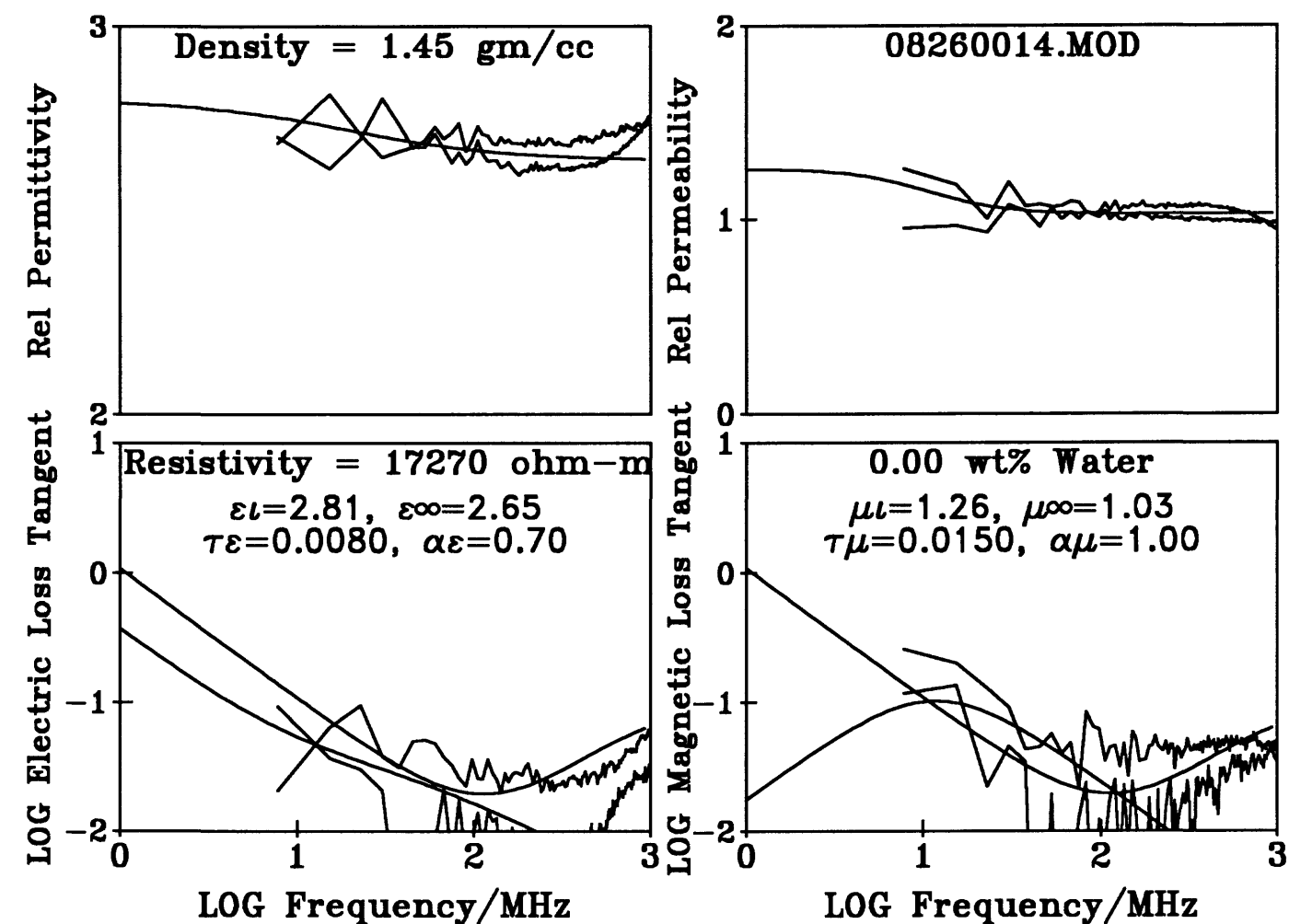
Figure 168 -

Sample provided by Lincoln Laboratory in a sealed bottle -- presumed natural water content -- location unknown.



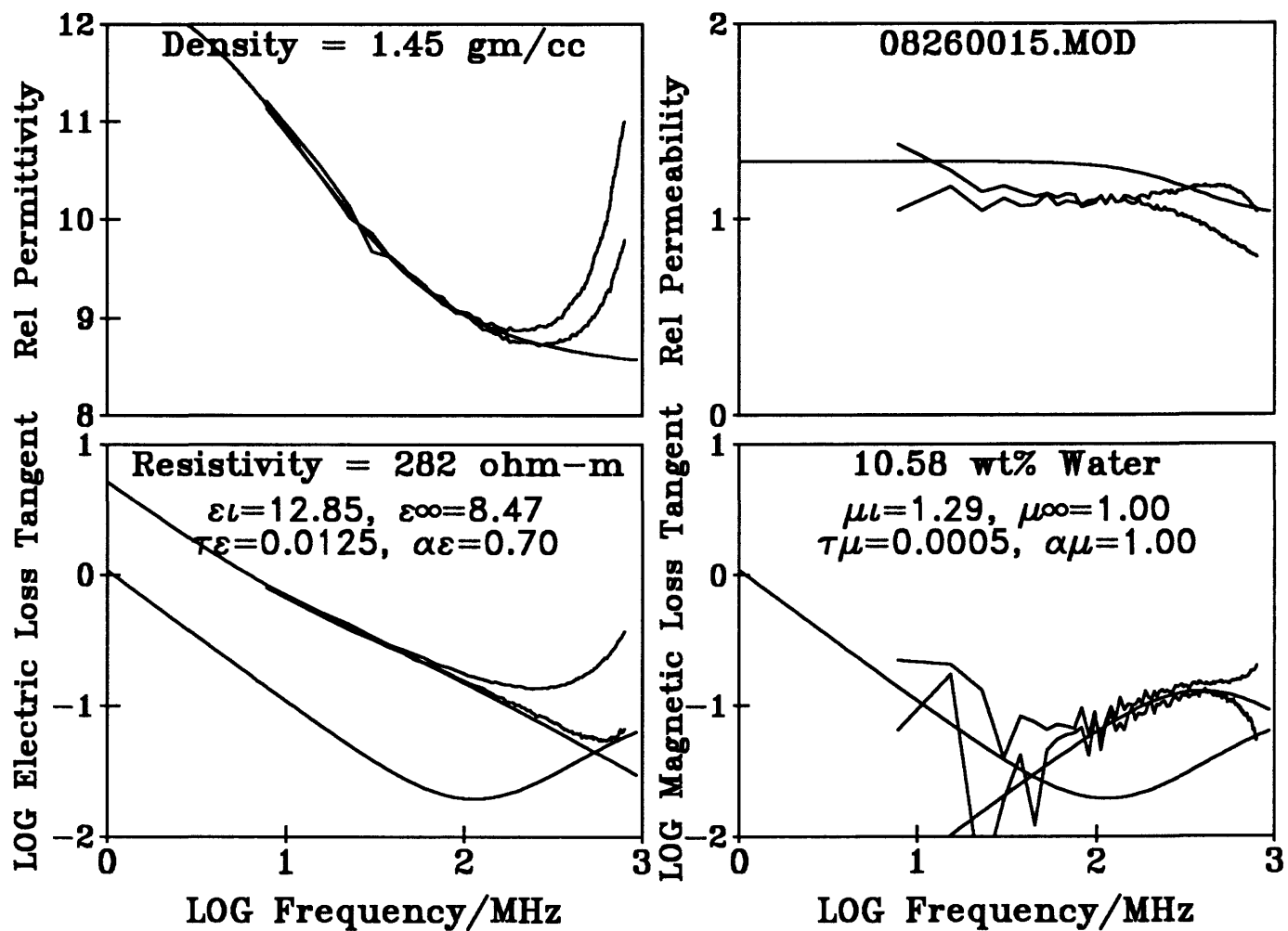
Yuma Site 000 sample #2 crest of dune (2nd) 4-in deep 051293 #2 vac.dry

Figure 169 -



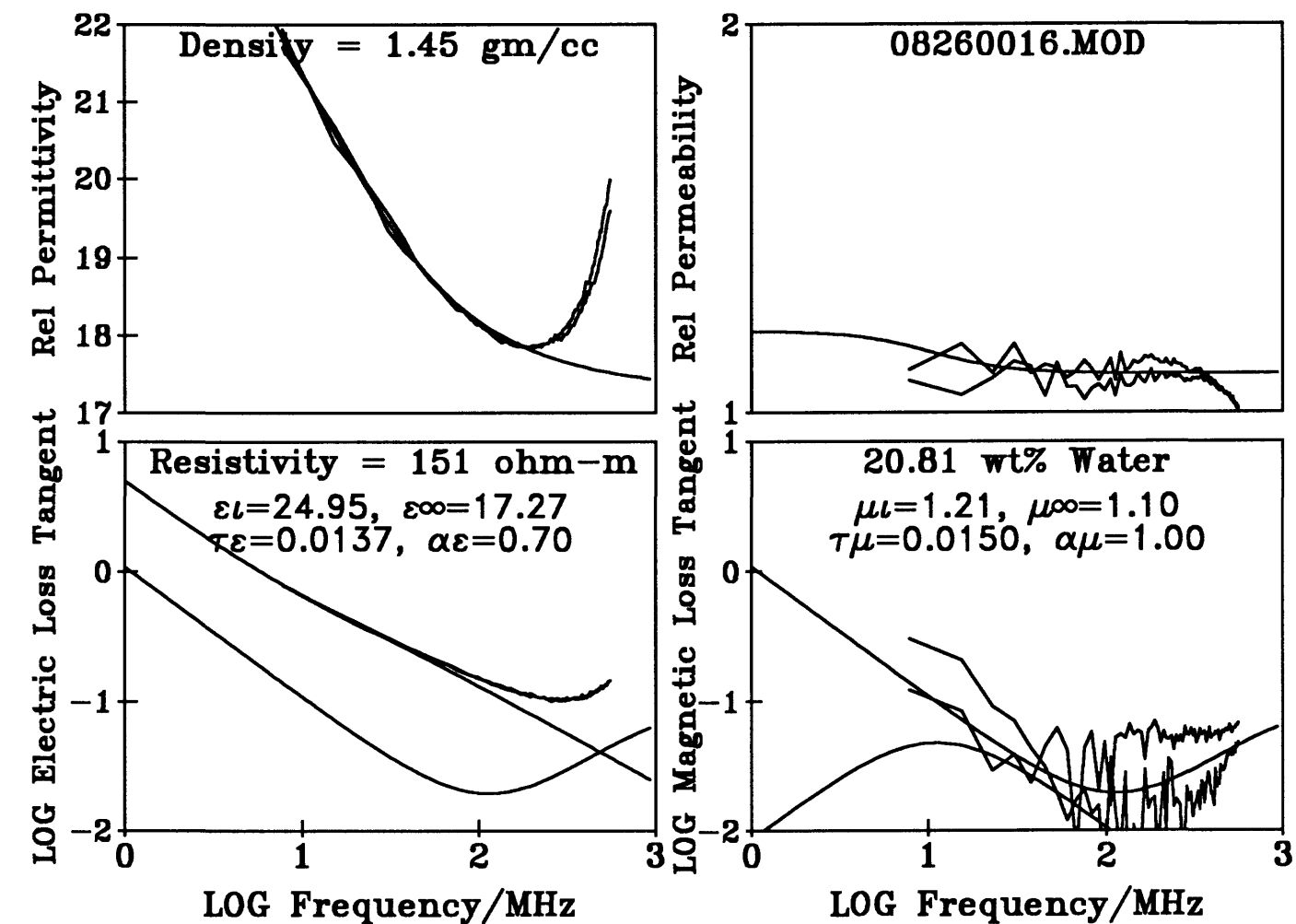
Yuma Site 000 sample #2 crest of dune (2nd) 4-in deep 051293 #3 vac. dry

Figure 170 -



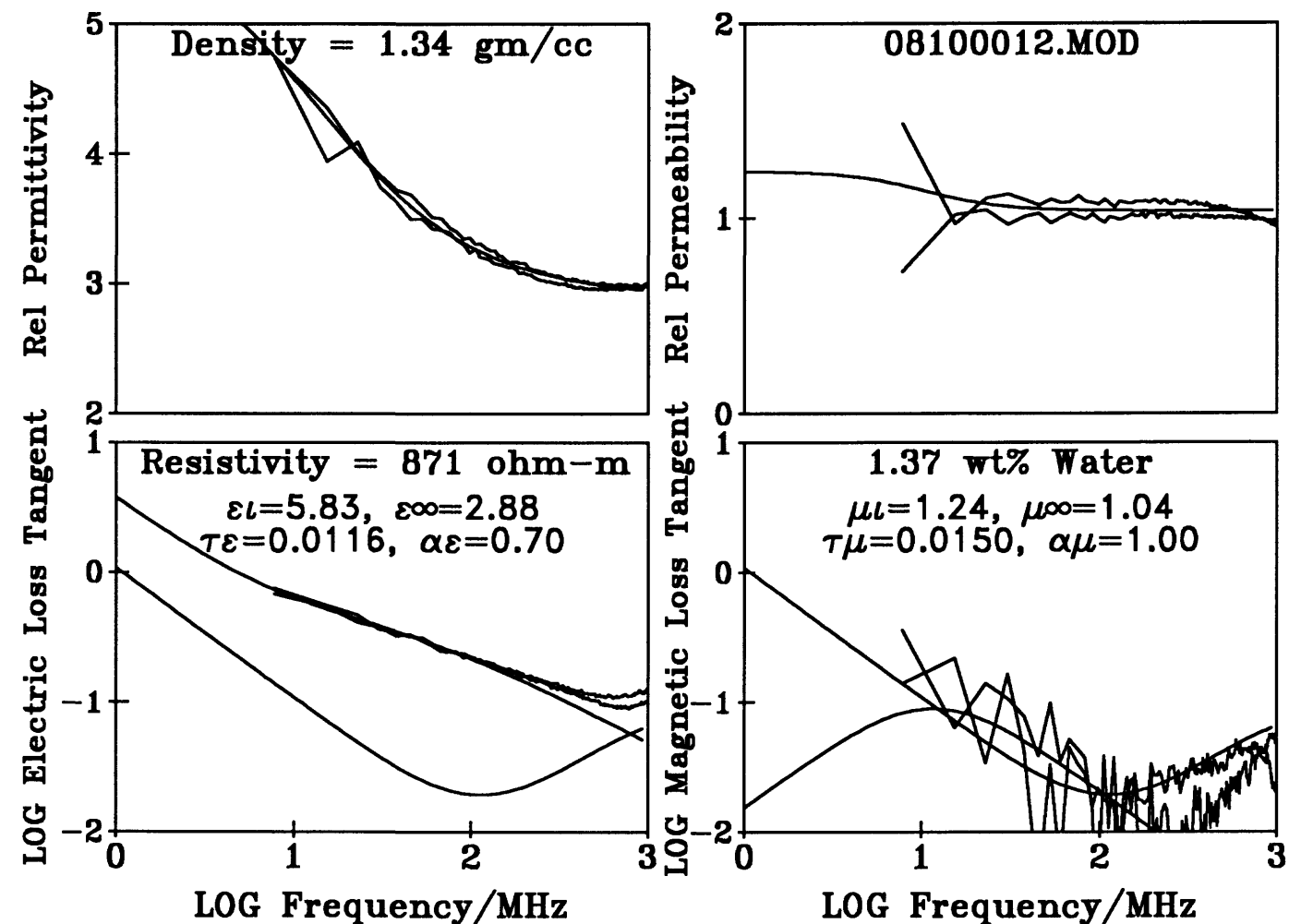
Yuma Site 000 Smpl.#2 crest of dune (2nd) 4-in deep #3 14-drops water

Figure 171 -



Yuma Site 000 smpl. #2 crest of dune (2nd) 4 in. deep 051293 #3 water sat.

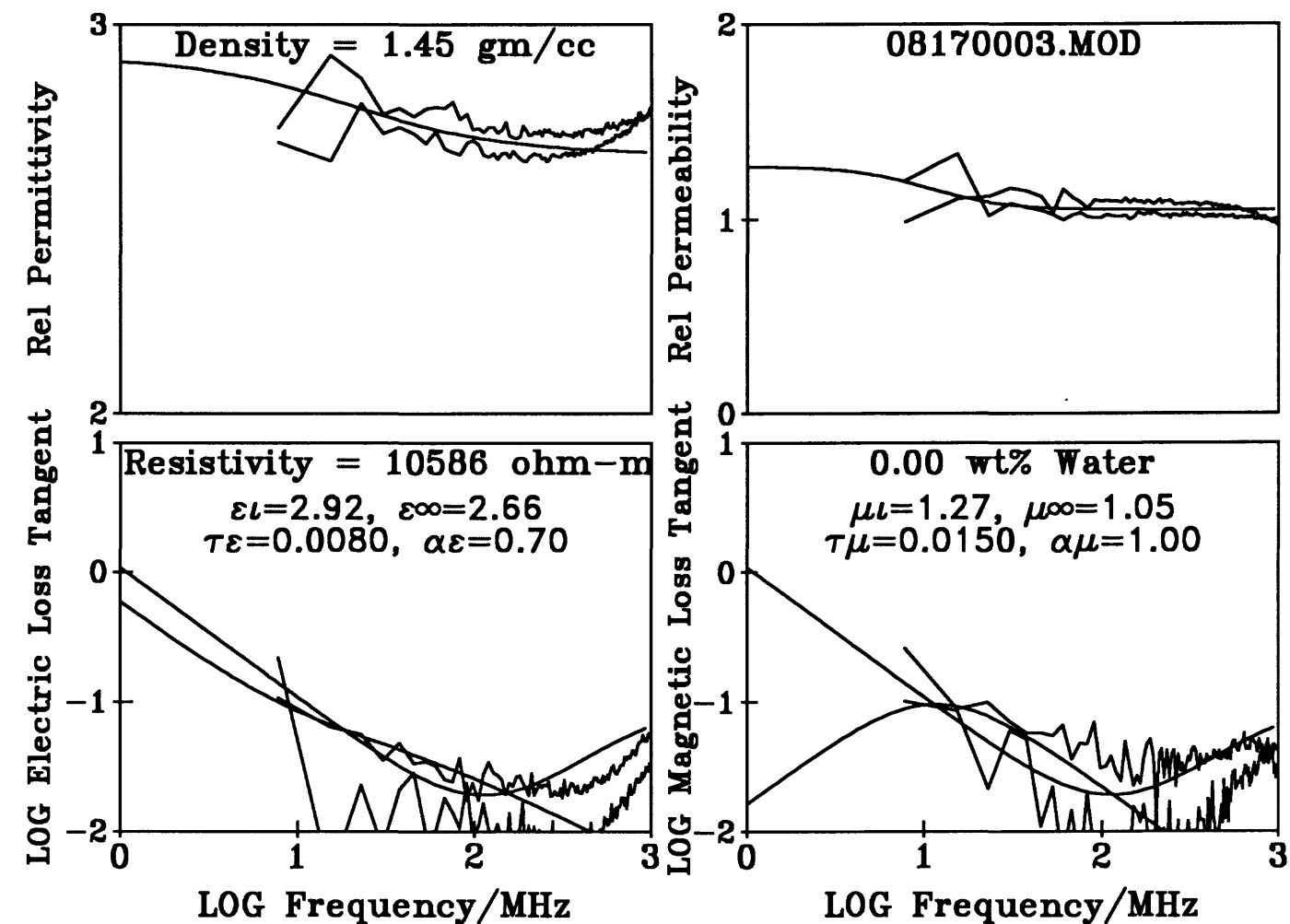
Figure 172 -



Yuma Site 001 Sample #1 (low area) bowl of dune 2 inches deep 051293 #1

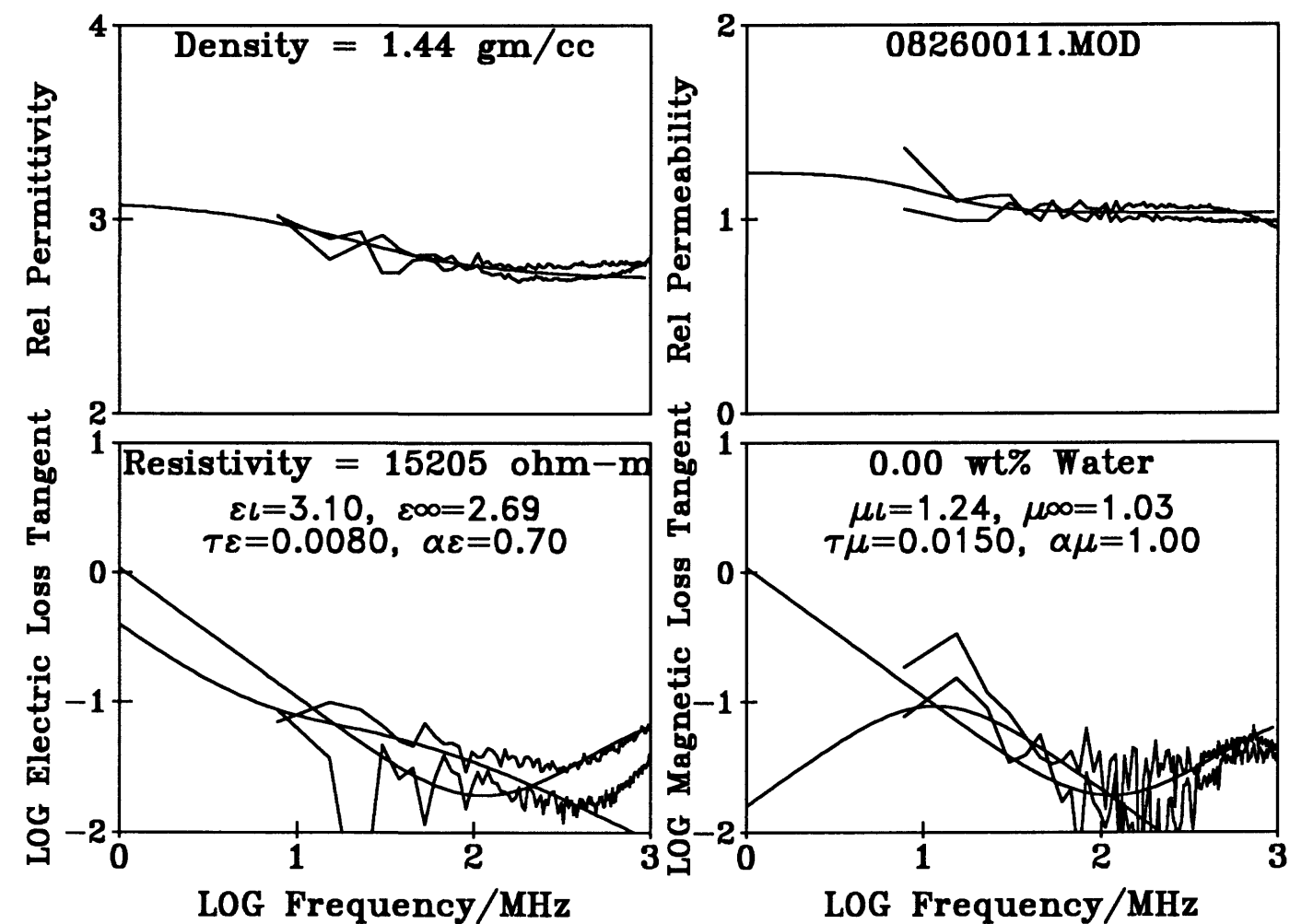
Figure 173 -

Sample provided by Lincoln Laboratory in a sealed bottle -- presumed natural water content -- location unknown.



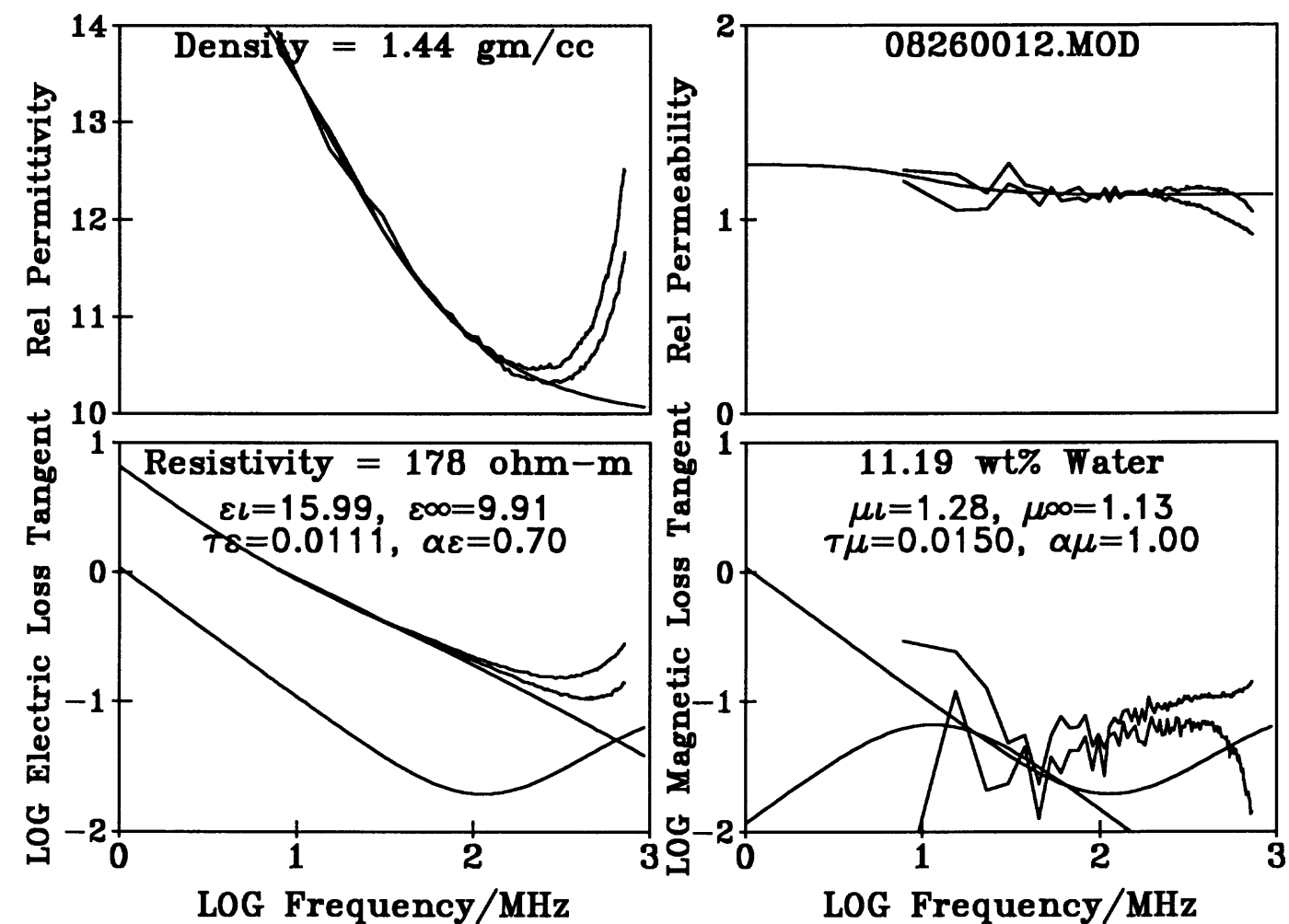
Yuma Site 001 smpl#1 (low area) bowl of dune 2-in deep 051293 #2 vac.dry

Figure 174 -



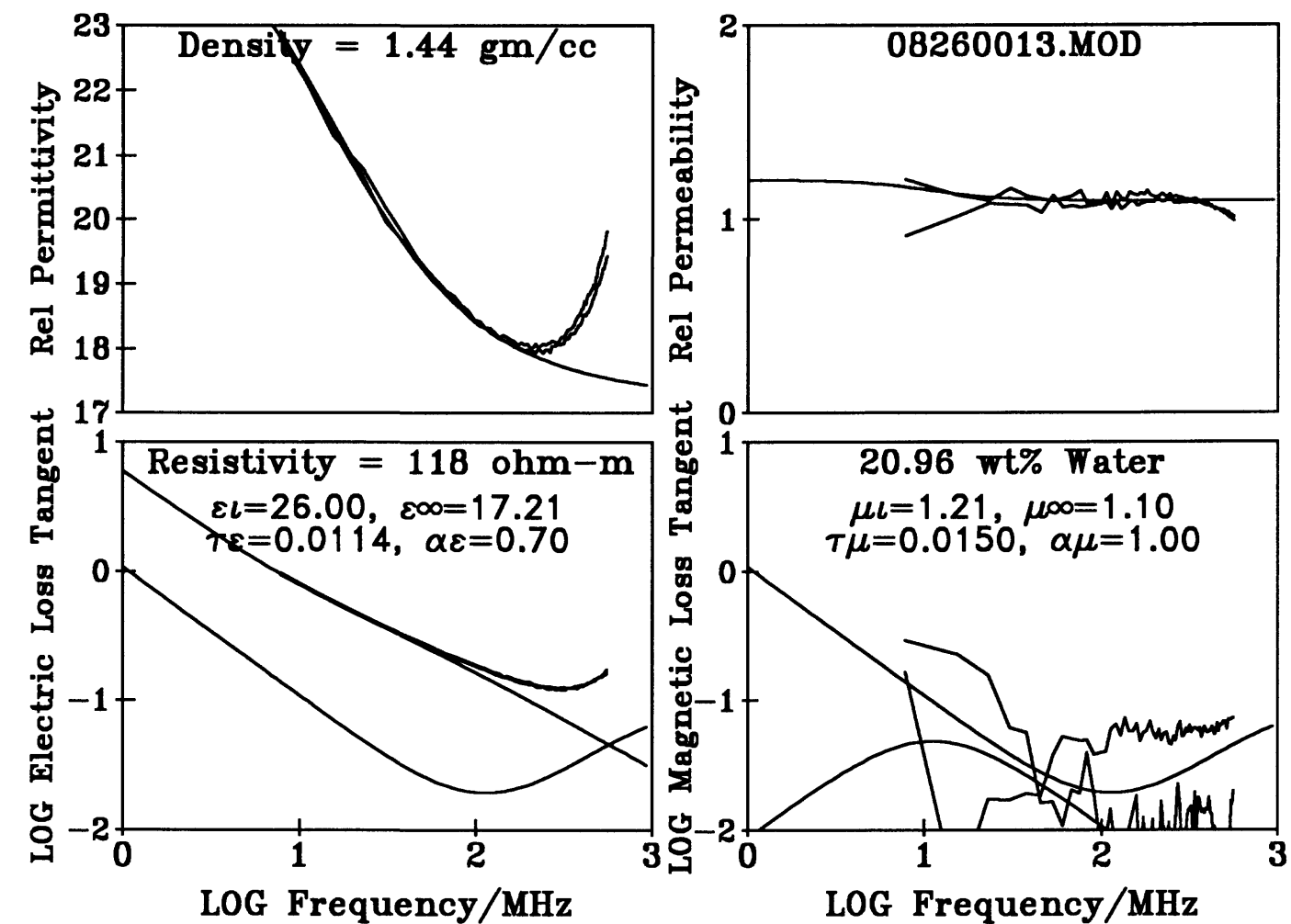
Yuma Site 001 smpl#1 (low area) bowl of dune 2-in deep 051293 #3 vac.dry

Figure 175 -



Yuma Site 001 smpl. #1 (low area) bowl of dune 2in. dp. #3 14 drops water

Figure 176 -



Yuma Site 001 smpl#1 (low area) bowl of dune 2-in deep 051293 #3 wat.sat.

Figure 177 -

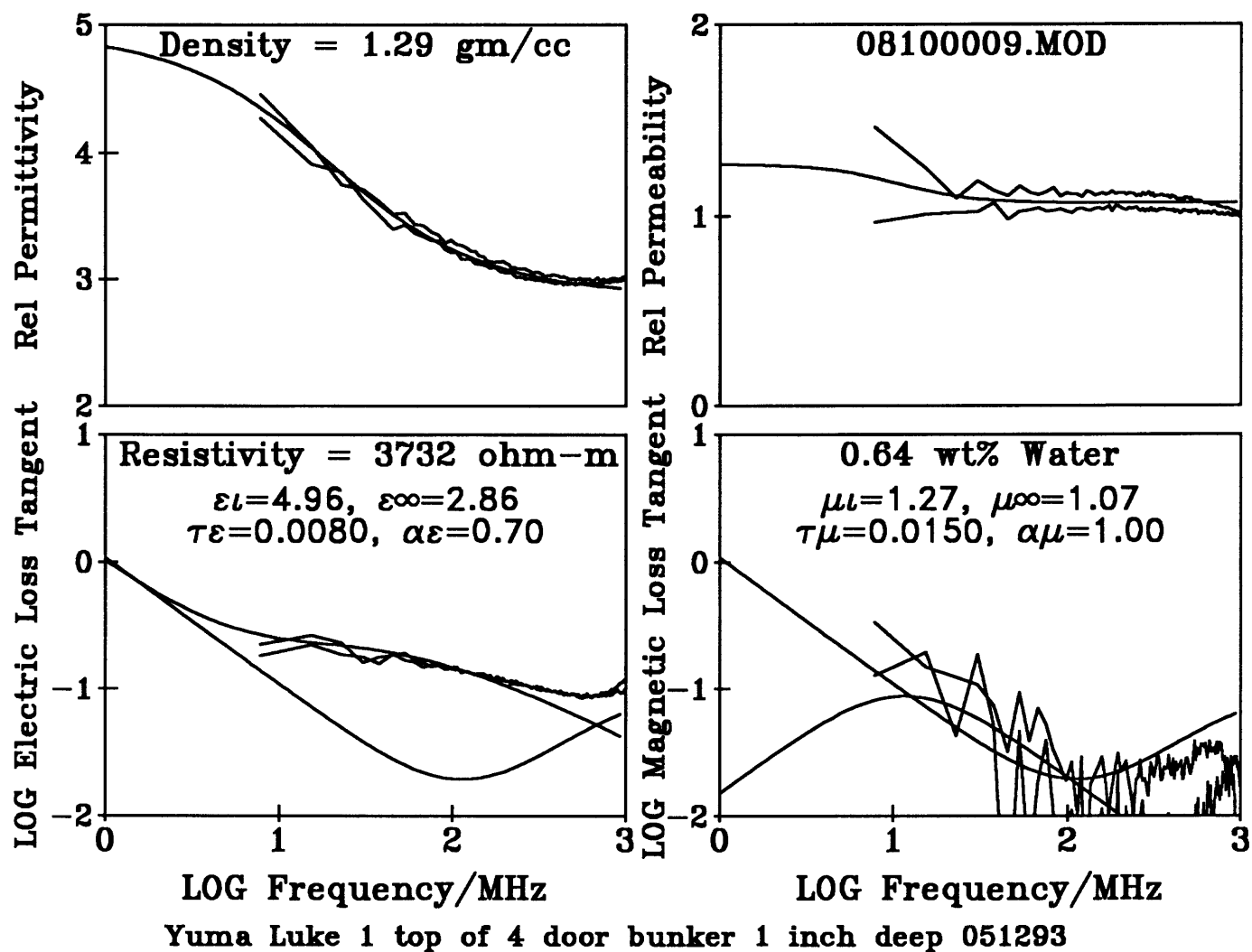


Figure 178 -

Sample provided by Lincoln Laboratory in a sealed bottle -- presumed natural water content -- location unknown.

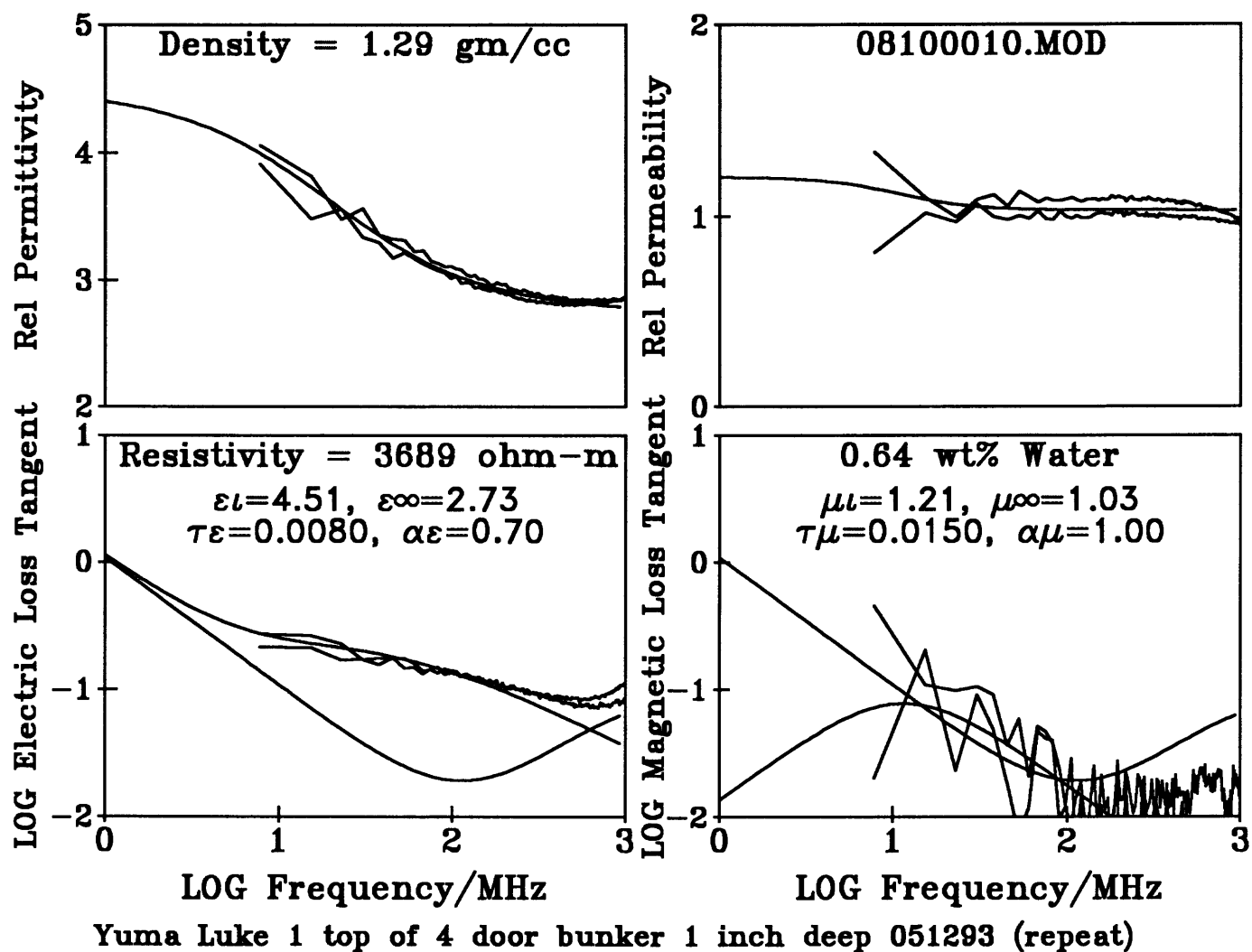


Figure 179 -

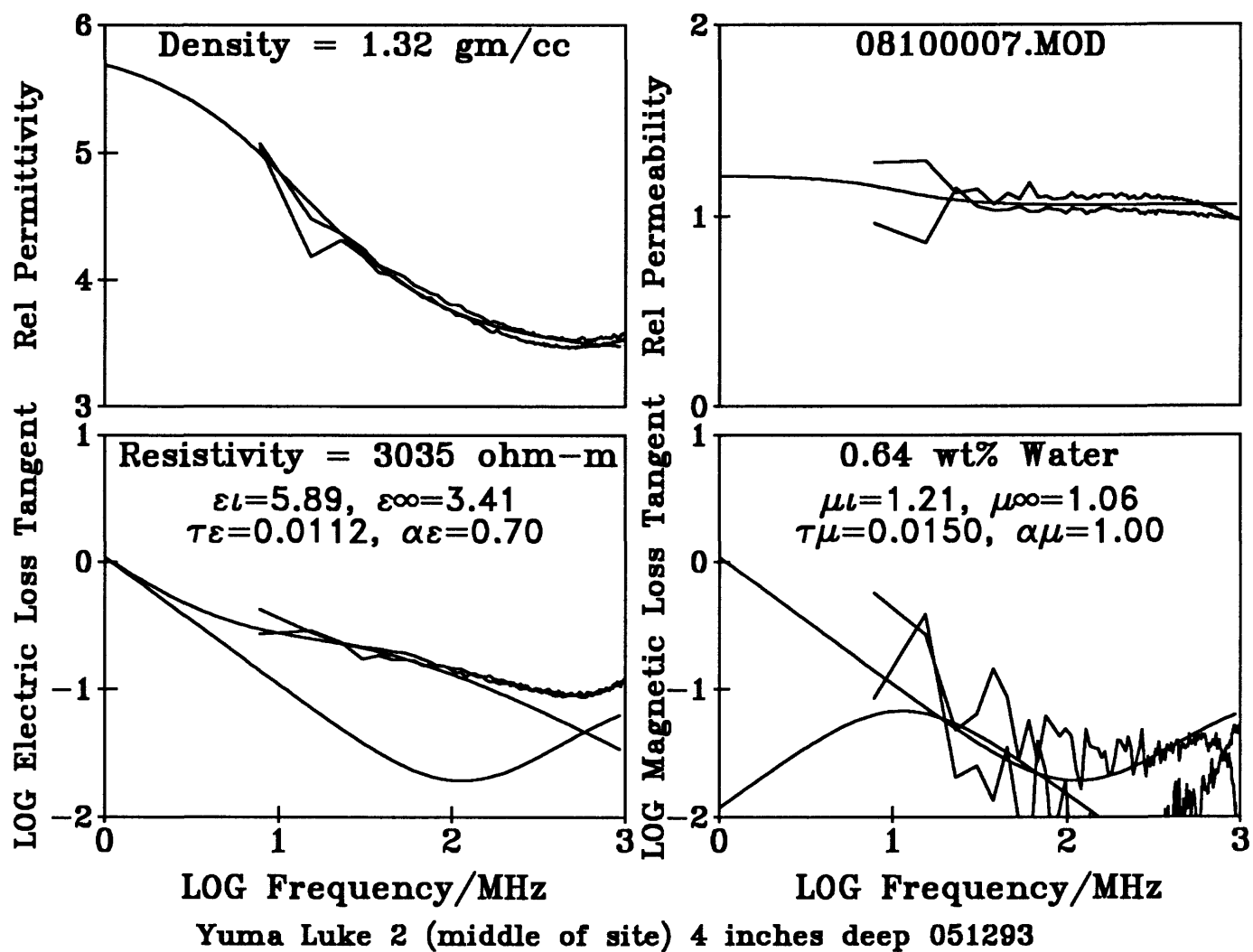


Figure 180 -

Sample provided by Lincoln Laboratory in a sealed bottle -- presumed natural water content -- location unknown.

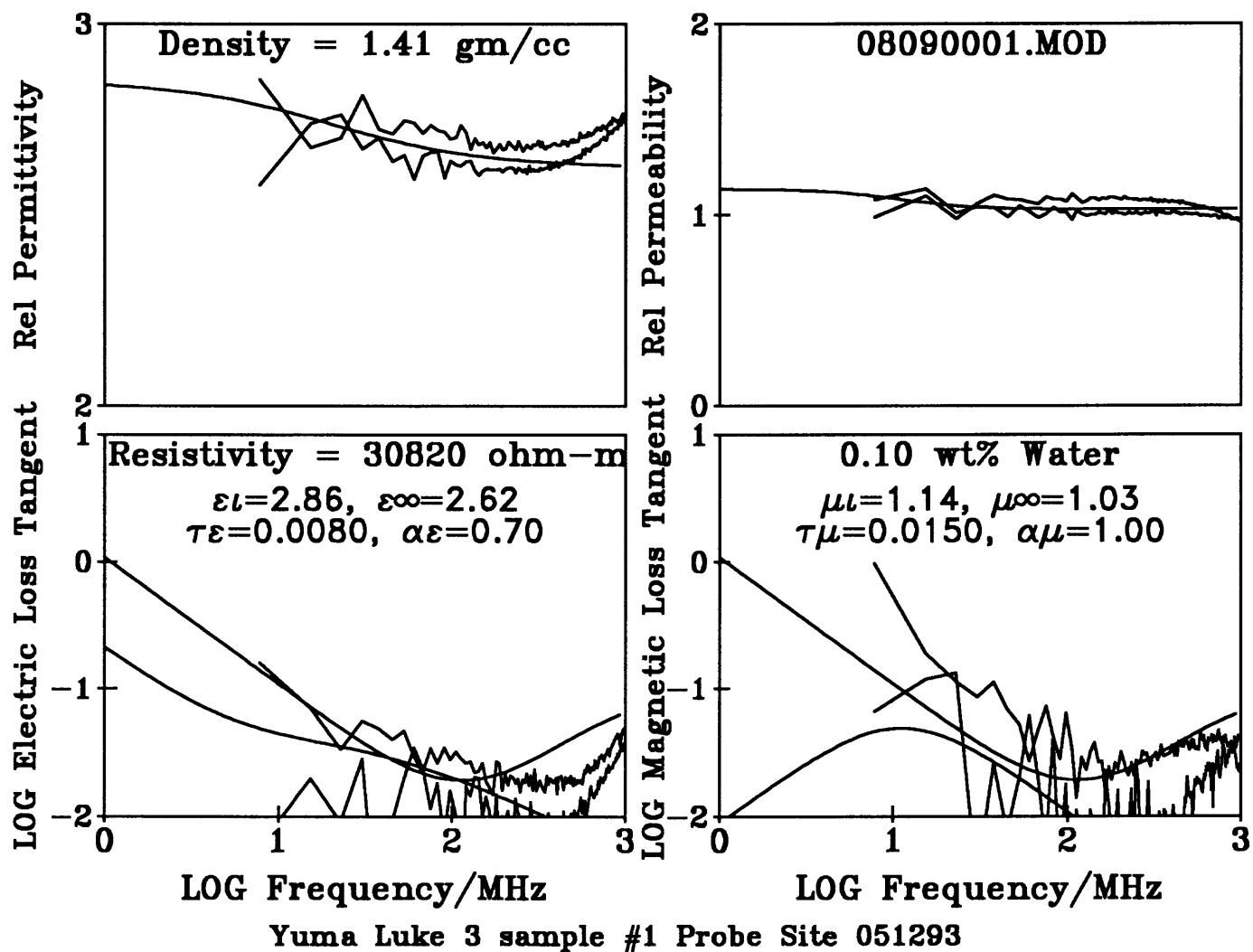


Figure 181 -

Sample provided by Lincoln Laboratory in a sealed bottle -- presumed natural water content -- location unknown.

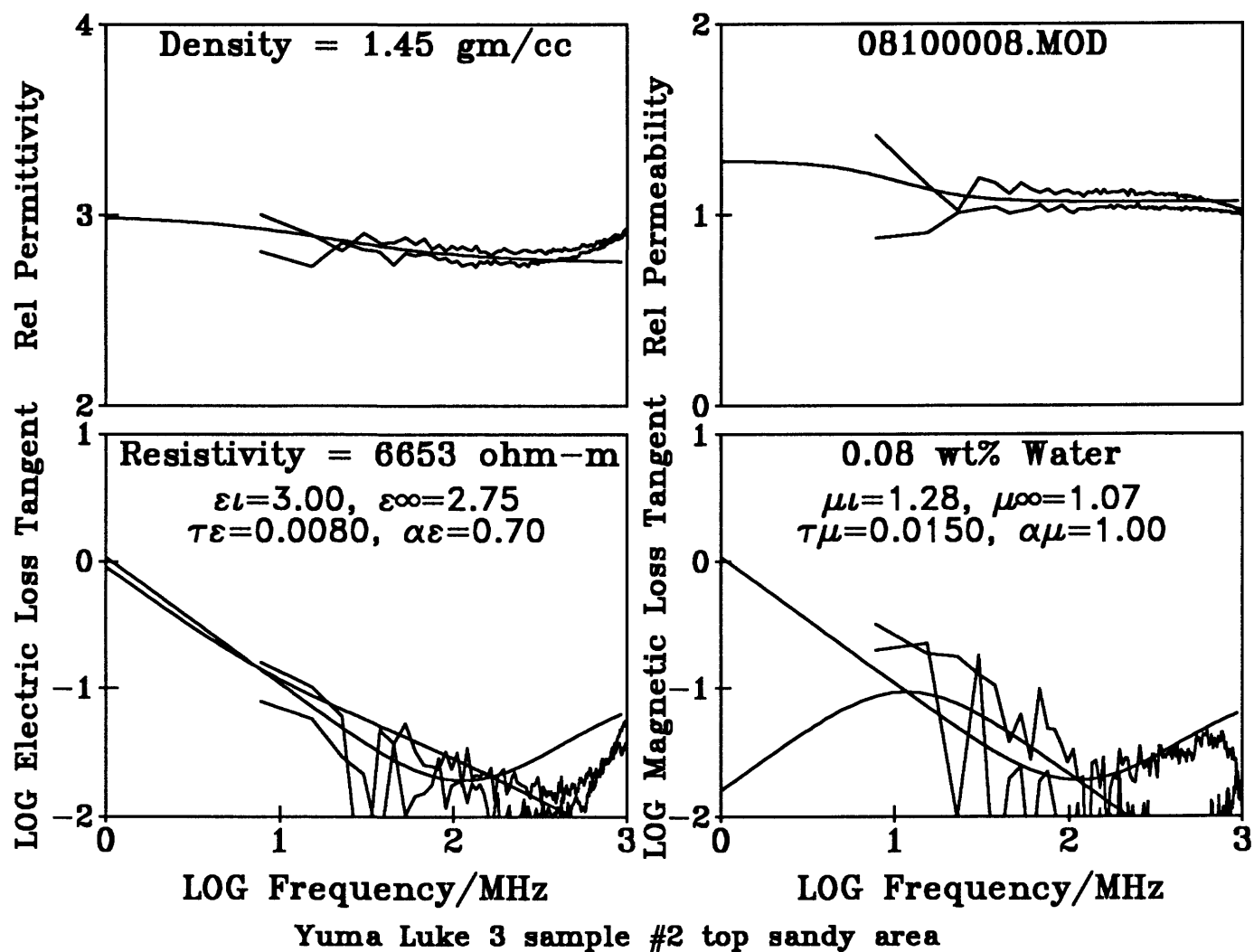


Figure 182 -
Sample provided by Lincoln Laboratory in a sealed bottle -- presumed natural water content -- location unknown.

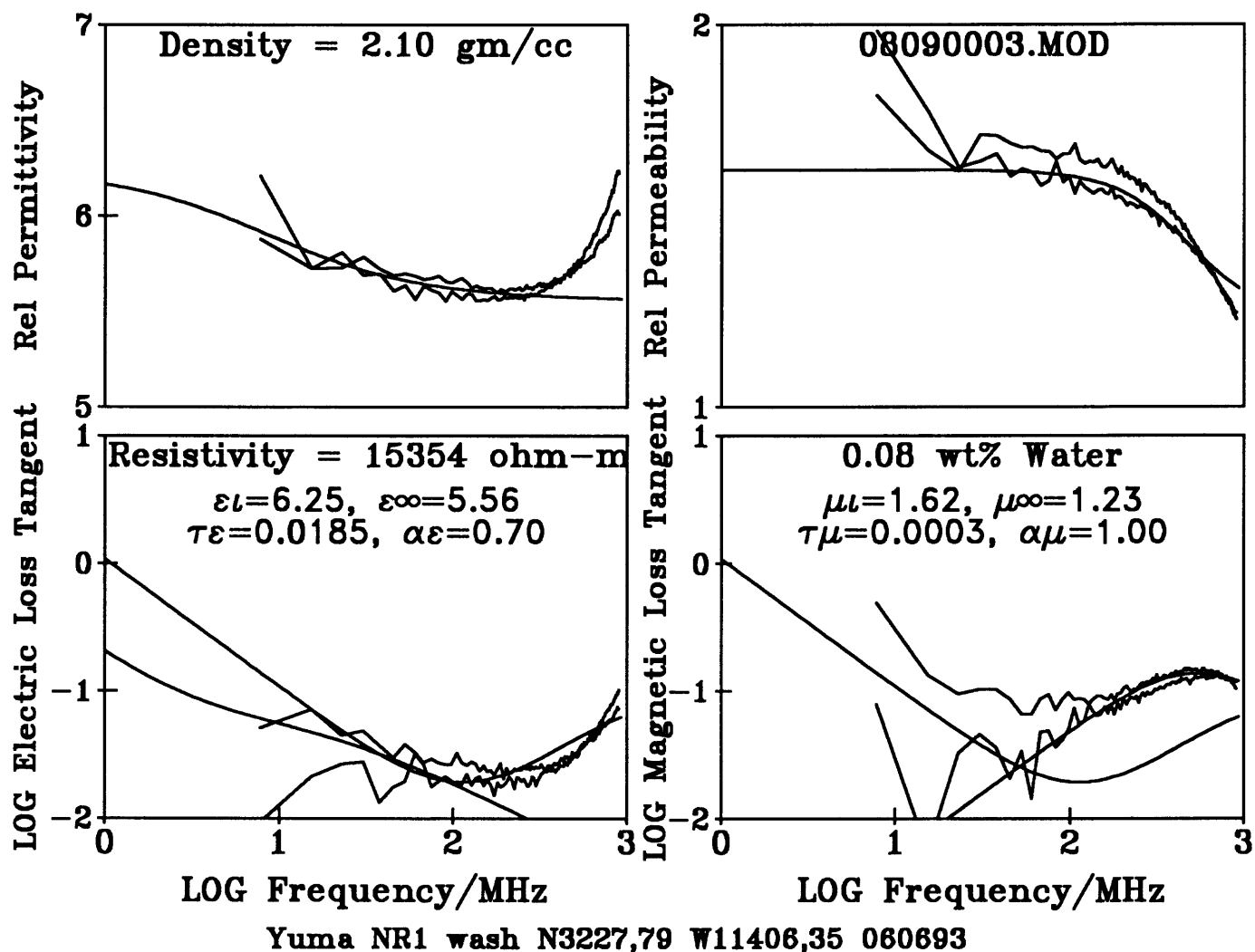


Figure 183 -

Sample provided by Carabas Team in a sealed bottle -- presumed natural water content. Note large magnetic losses compared to electrical losses. Comparing this result to Figures 184 through 194, this sample has the equivalent of 30 percent iron in silica sand.

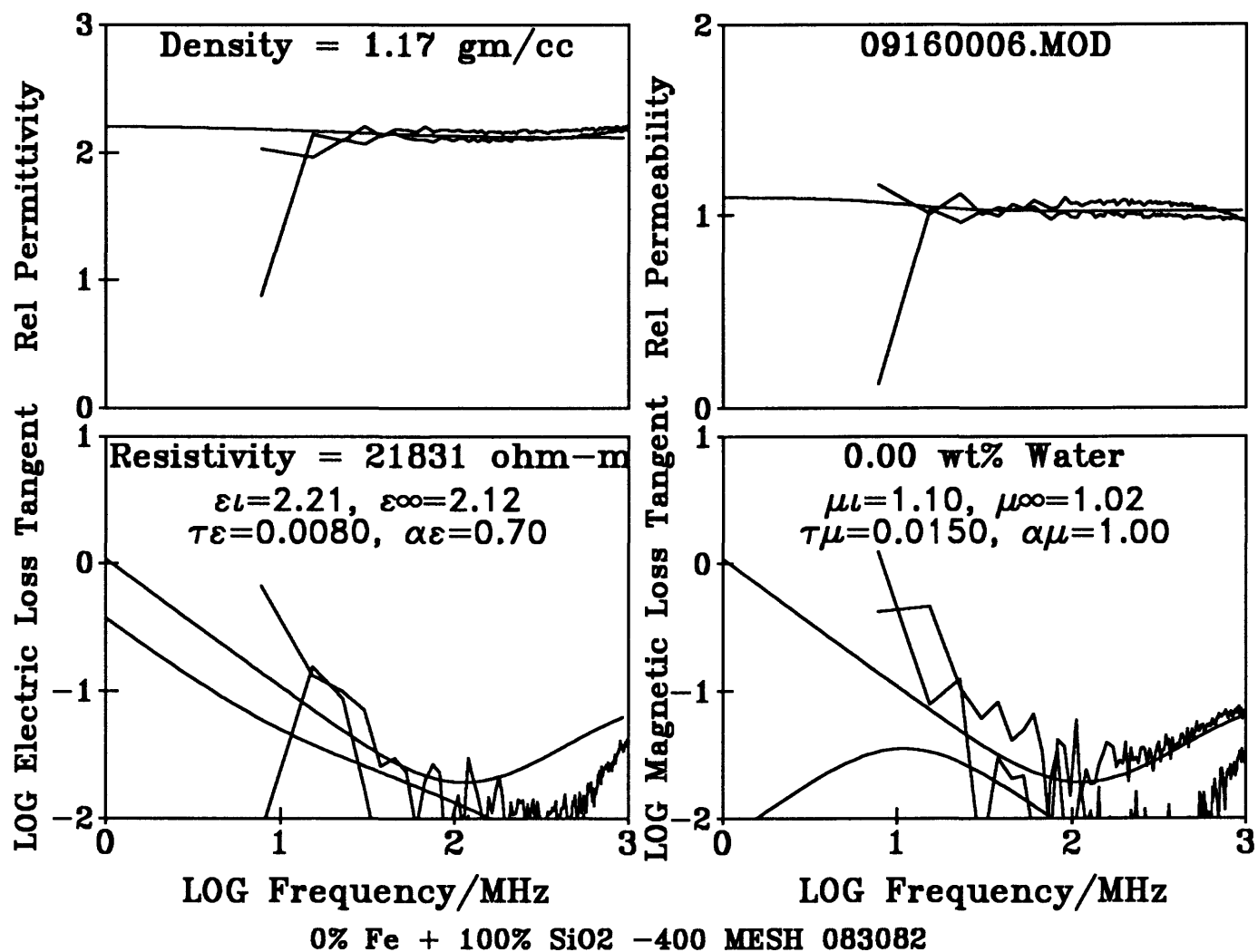


Figure 184 -
Artificial sample composed of a mixture of -400 mesh iron filings in a silica sand matrix.

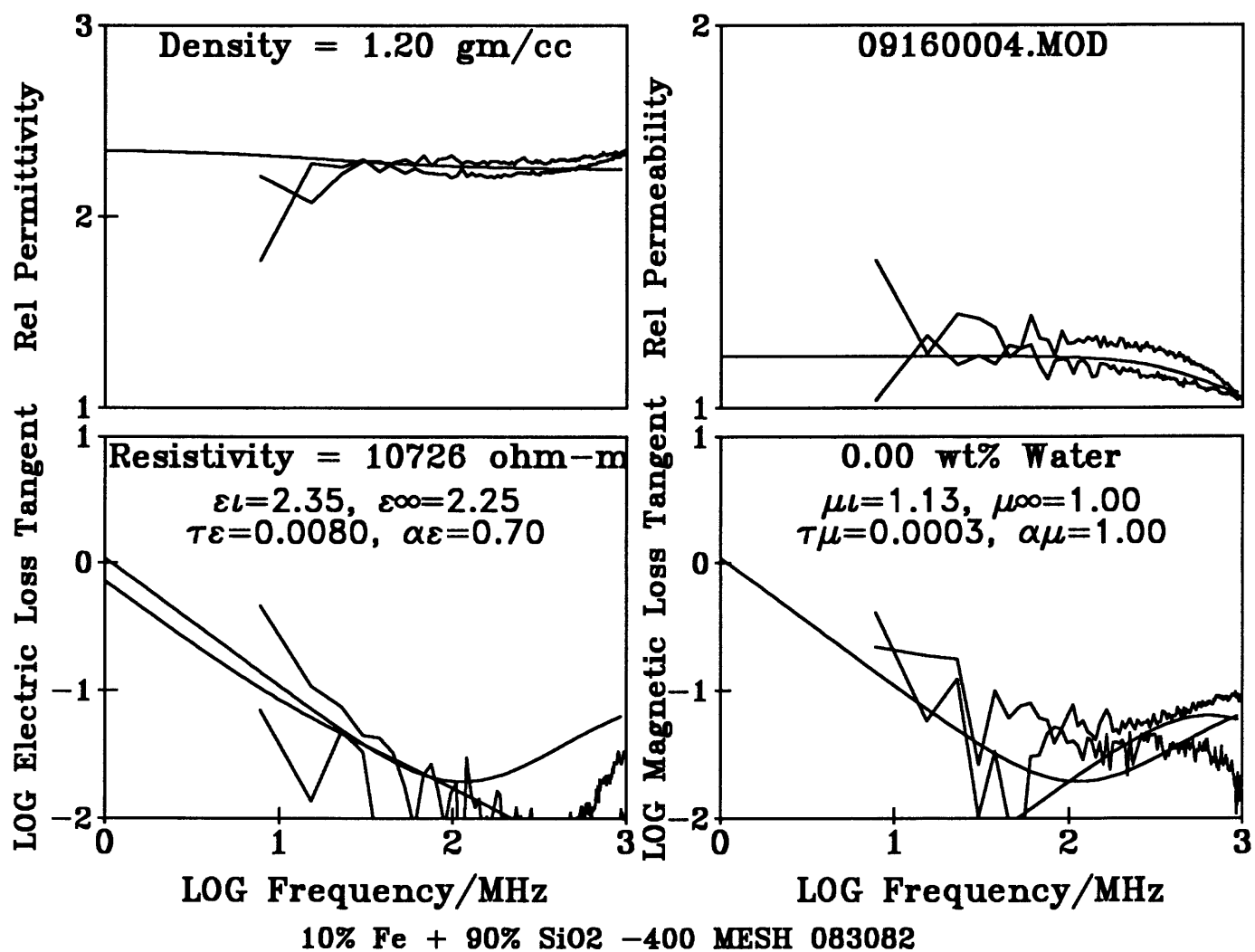


Figure 185 -
Artificial sample composed of a mixture of -400 mesh iron filings in a silica sand matrix.

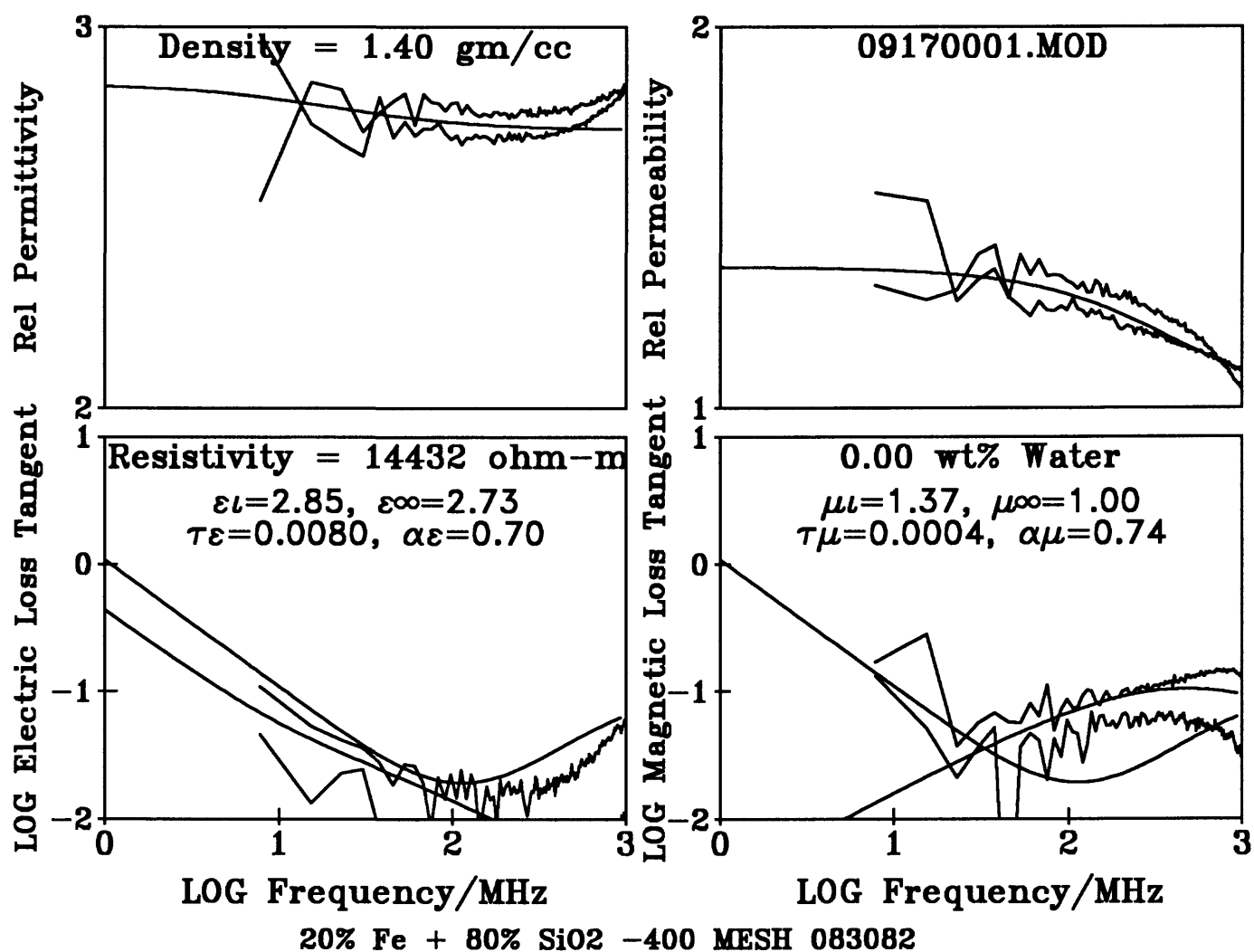


Figure 186 -
Artificial sample composed of a mixture of -400 mesh iron filings in a silica sand matrix.

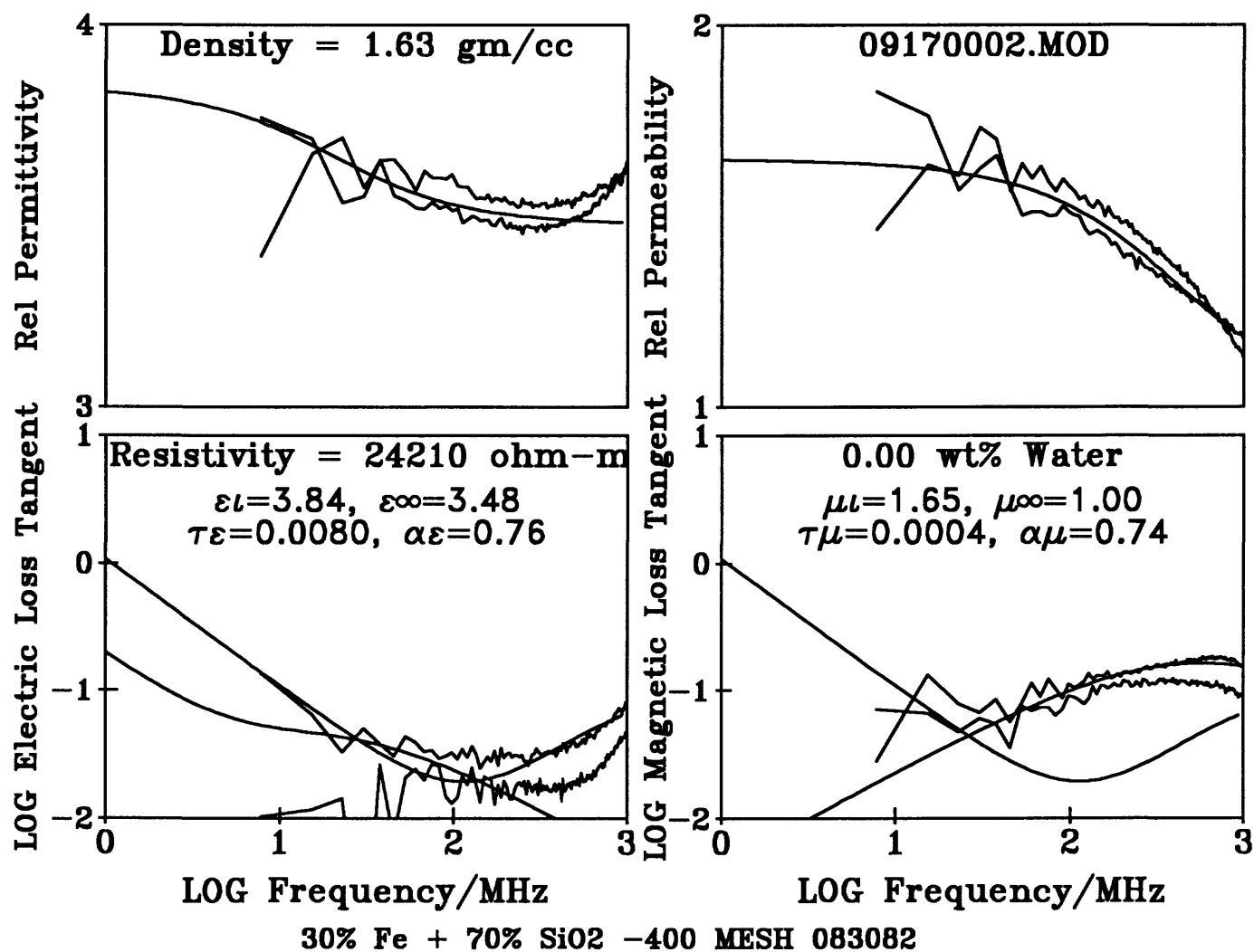


Figure 187 -
Artificial sample composed of a mixture of -400 mesh iron filings in a silica sand matrix.

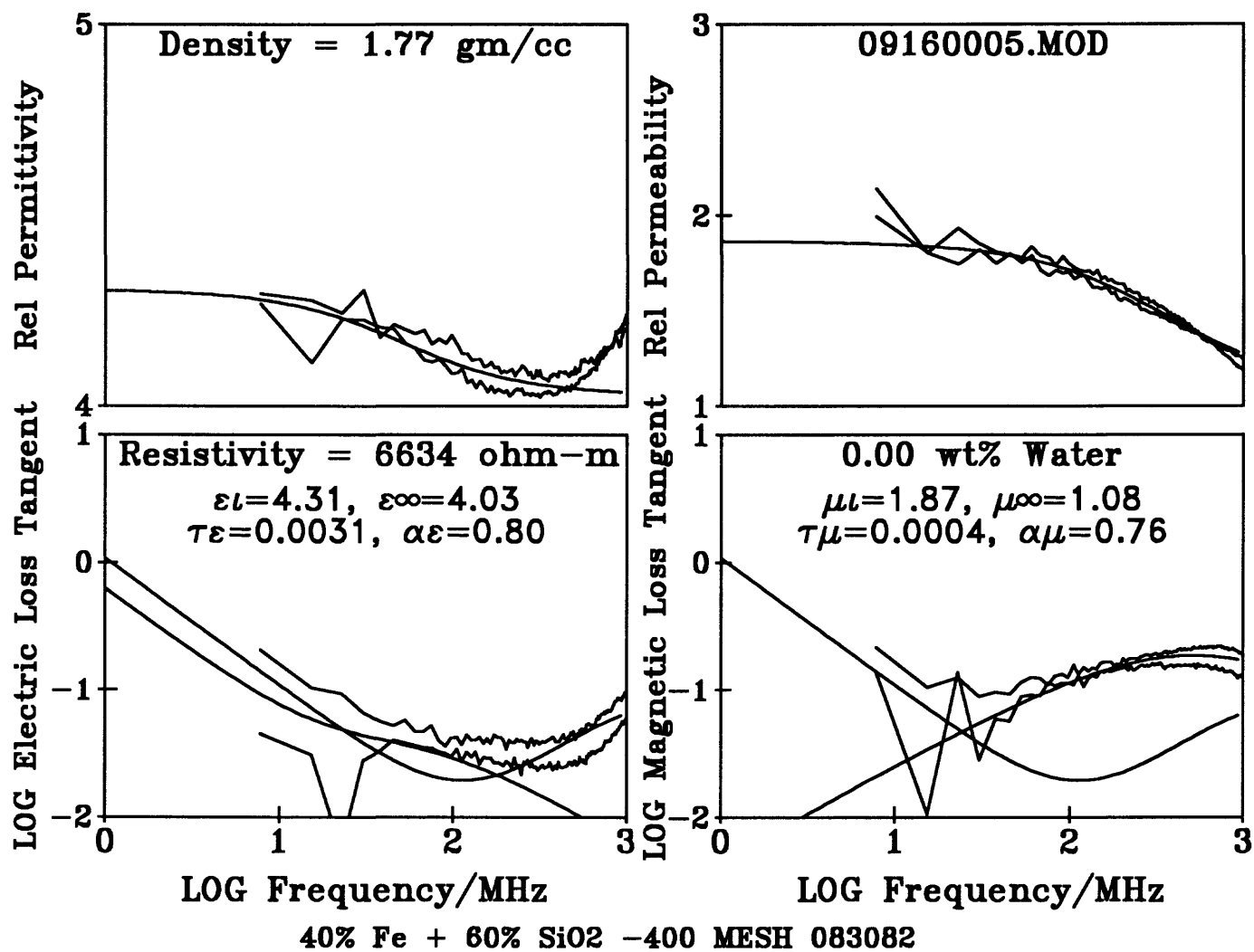


Figure 188 -
 Artificial sample composed of a mixture of -400 mesh iron filings in a silica sand matrix.

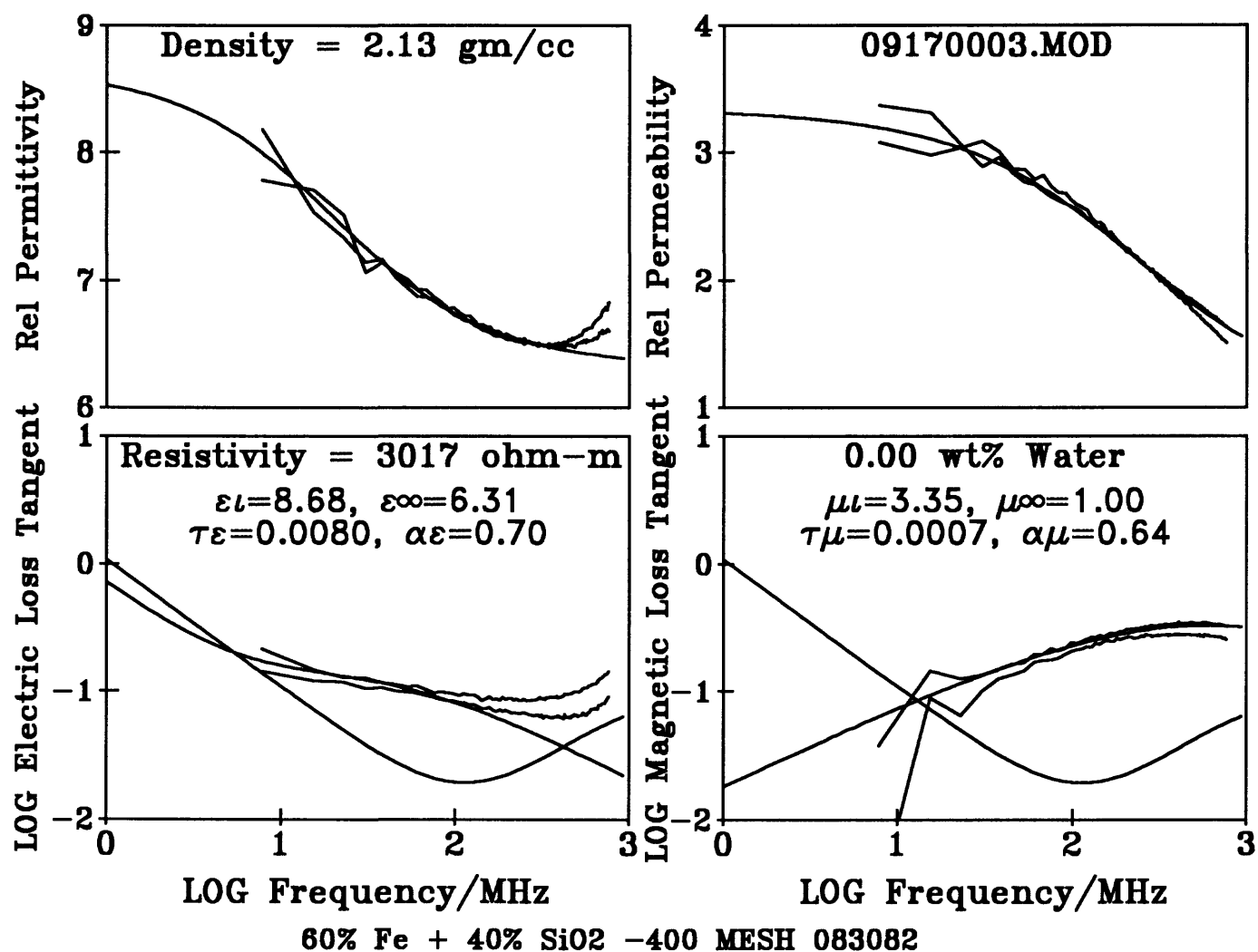


Figure 189 -
Artificial sample composed of a mixture of -400 mesh iron filings in a silica sand matrix.

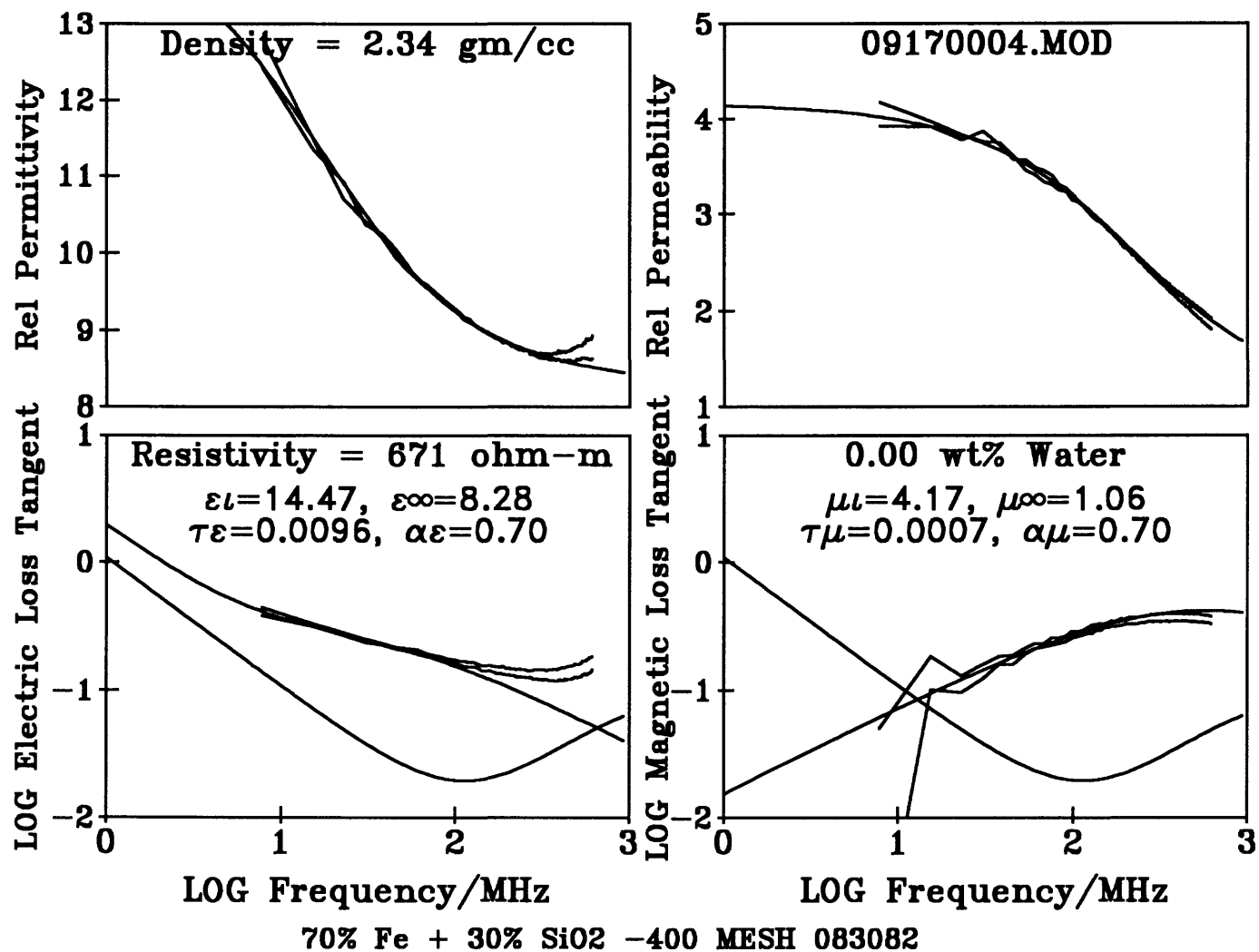


Figure 190 -
 Artificial sample composed of a mixture of -400 mesh iron filings in a silica sand matrix.

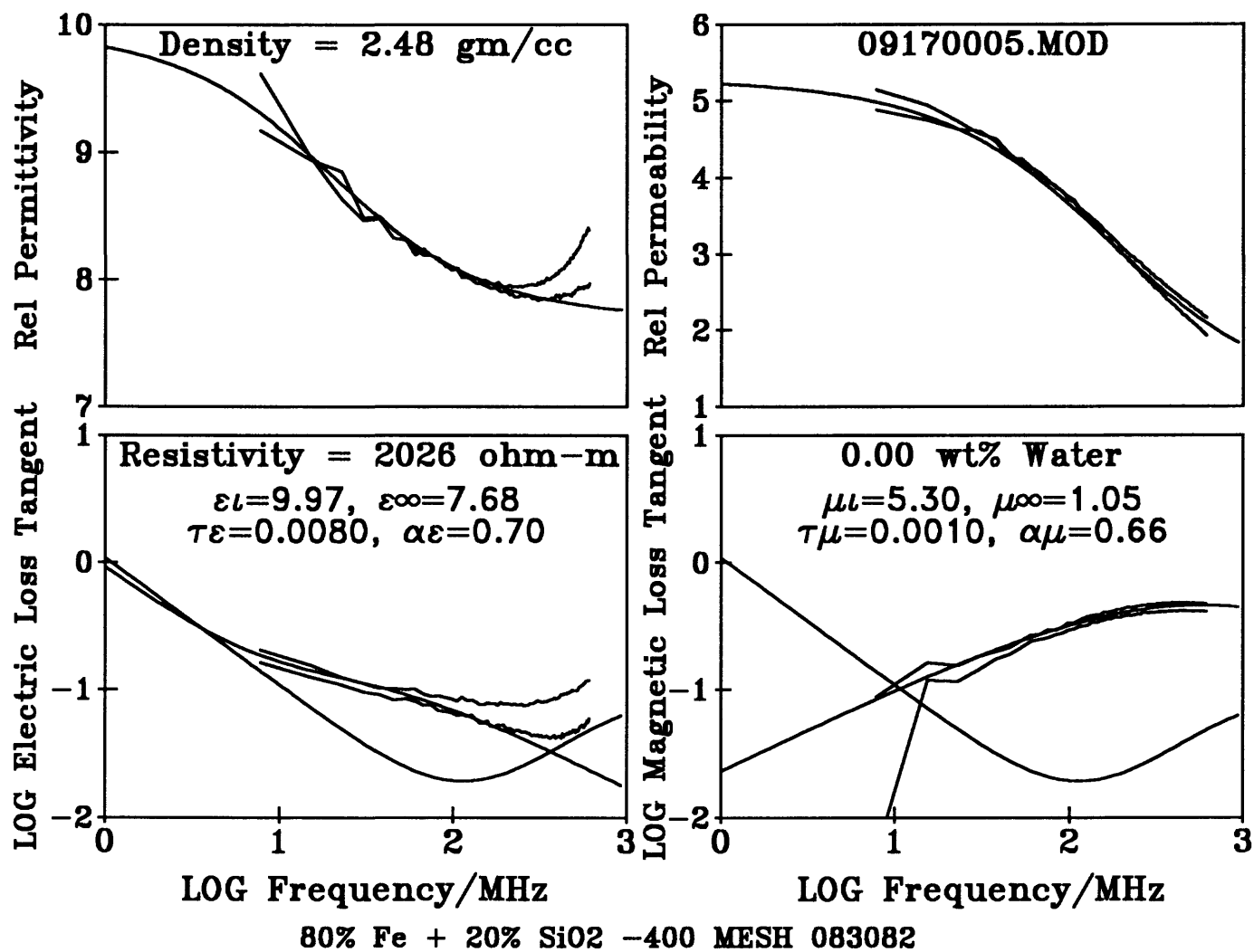


Figure 191 -
 Artificial sample composed of a mixture of -400 mesh iron filings in a silica sand matrix.

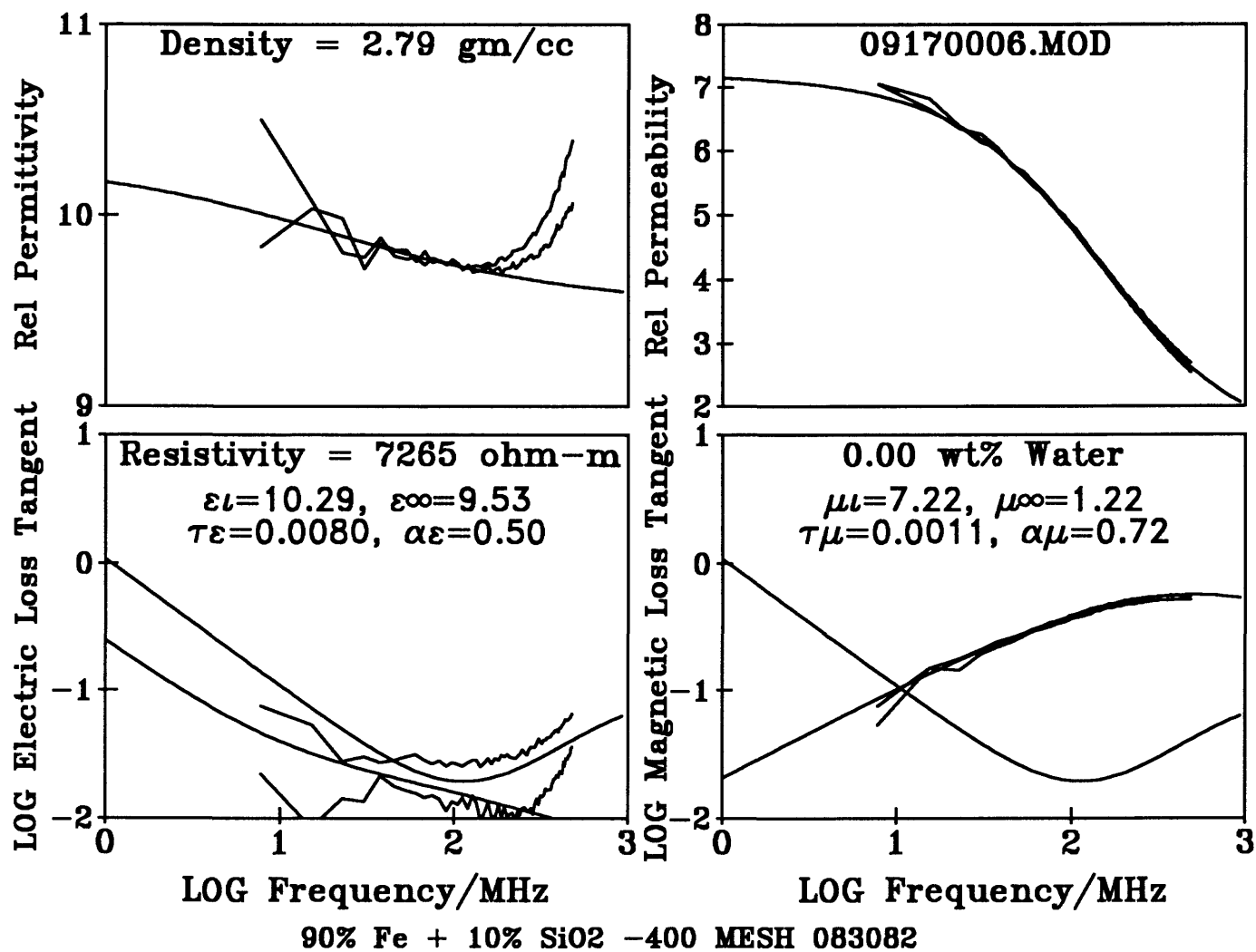


Figure 192 -
 Artificial sample composed of a mixture of -400 mesh iron filings in a silica sand matrix.

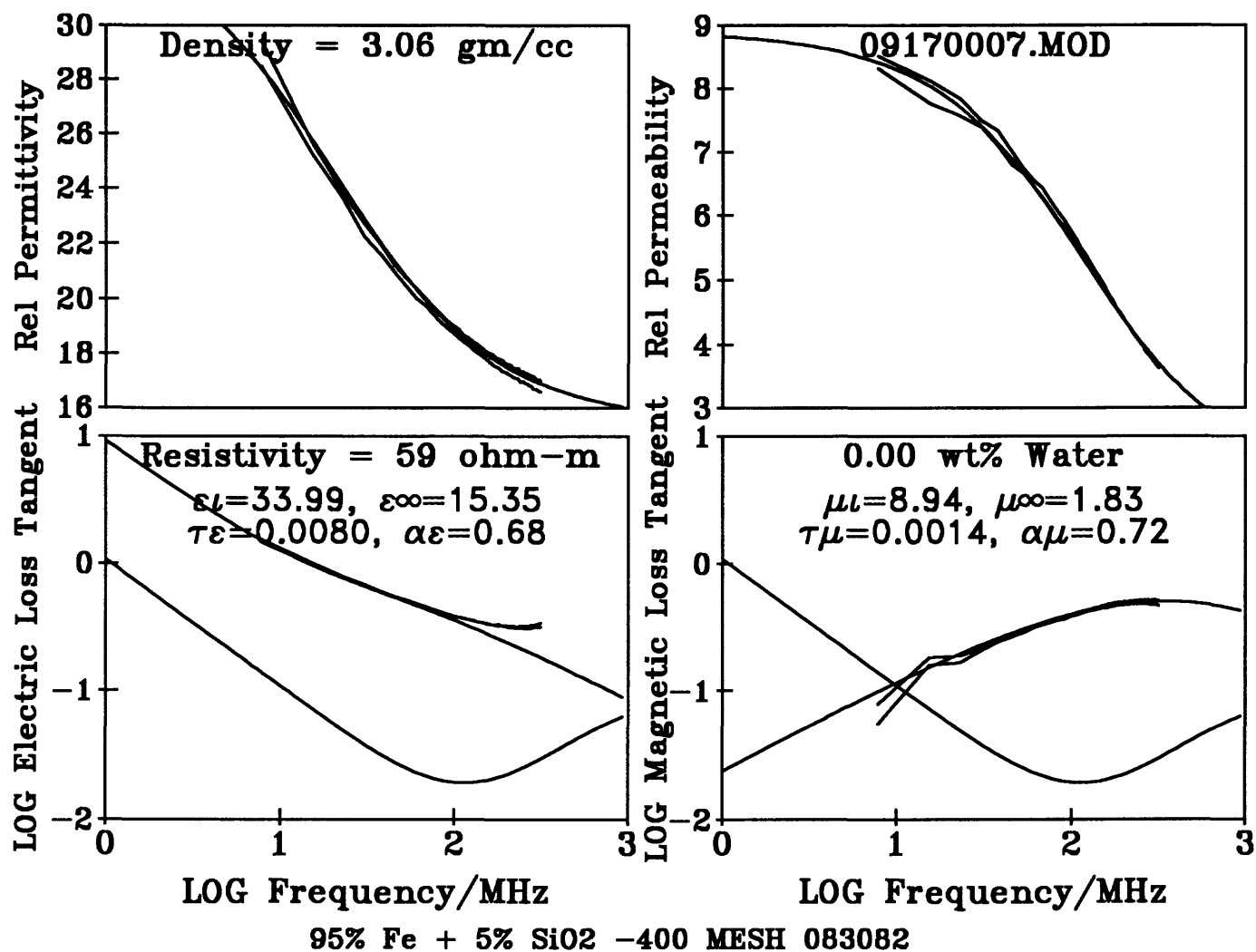


Figure 193 -
 Artificial sample composed of a mixture of -400 mesh iron filings in a silica sand matrix.

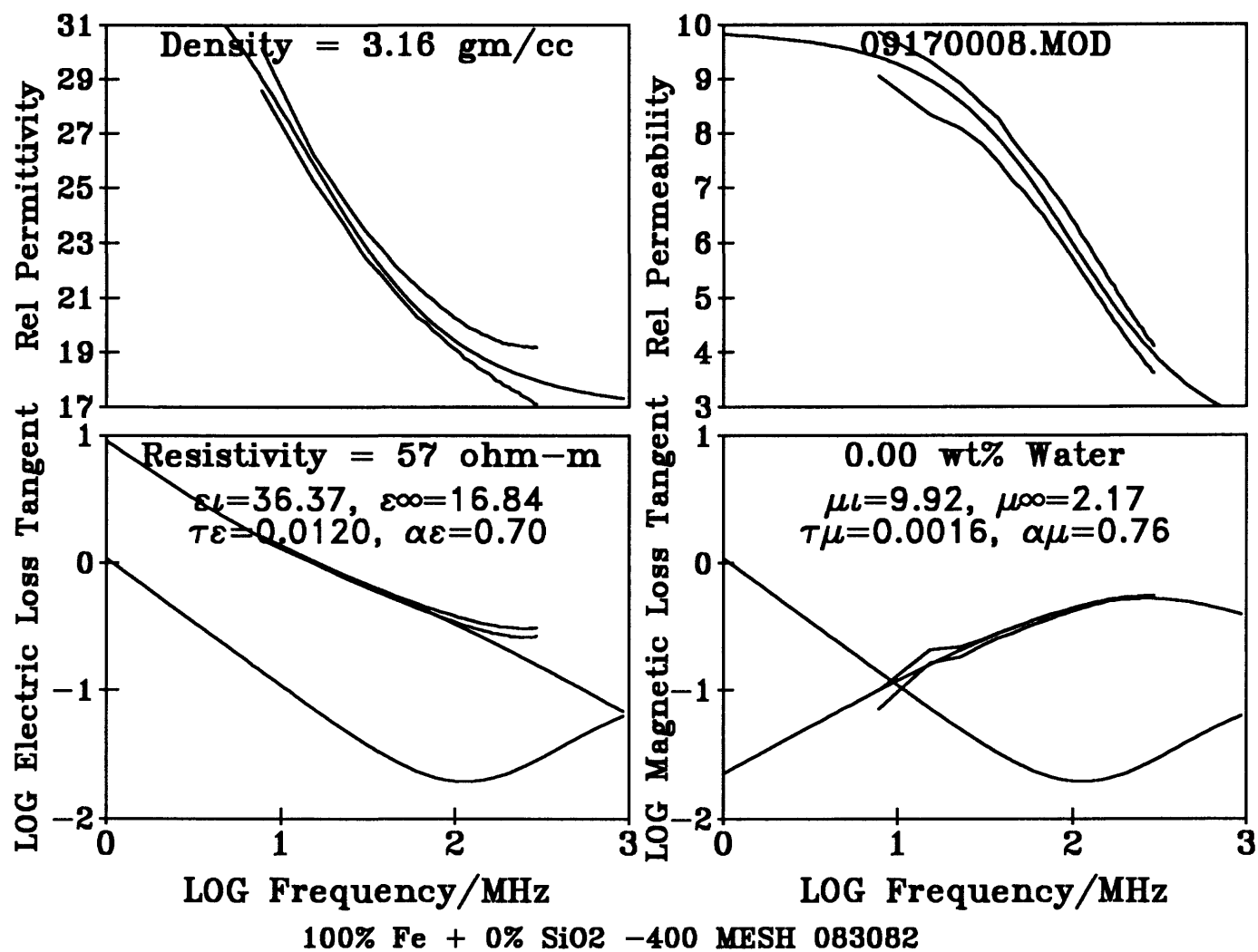


Figure 194 -
 Artificial sample composed of a mixture of -400 mesh iron filings in a silica sand matrix.

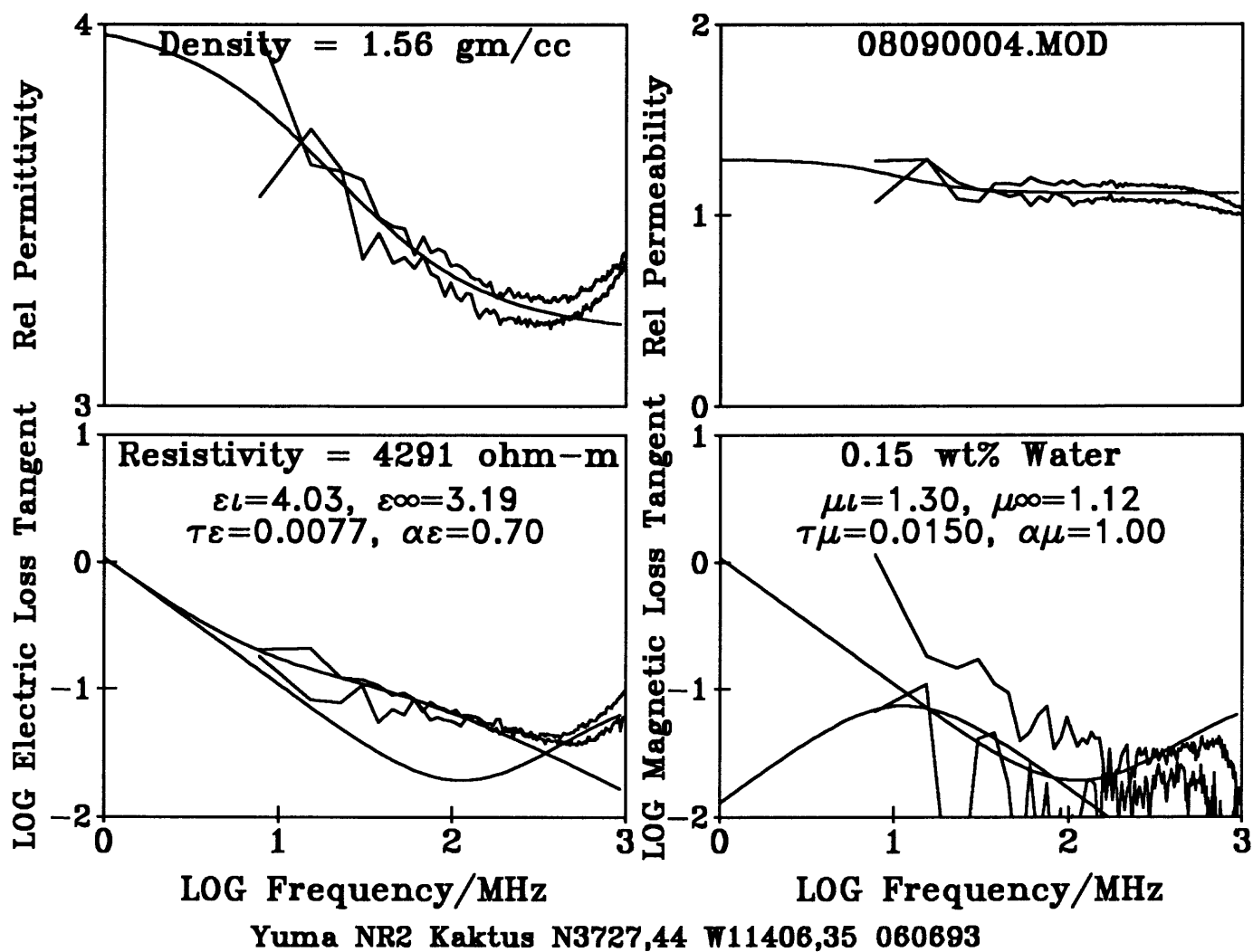


Figure 195 -
Sample provided by Carabas Team in a sealed bottle -- presumed natural water content.

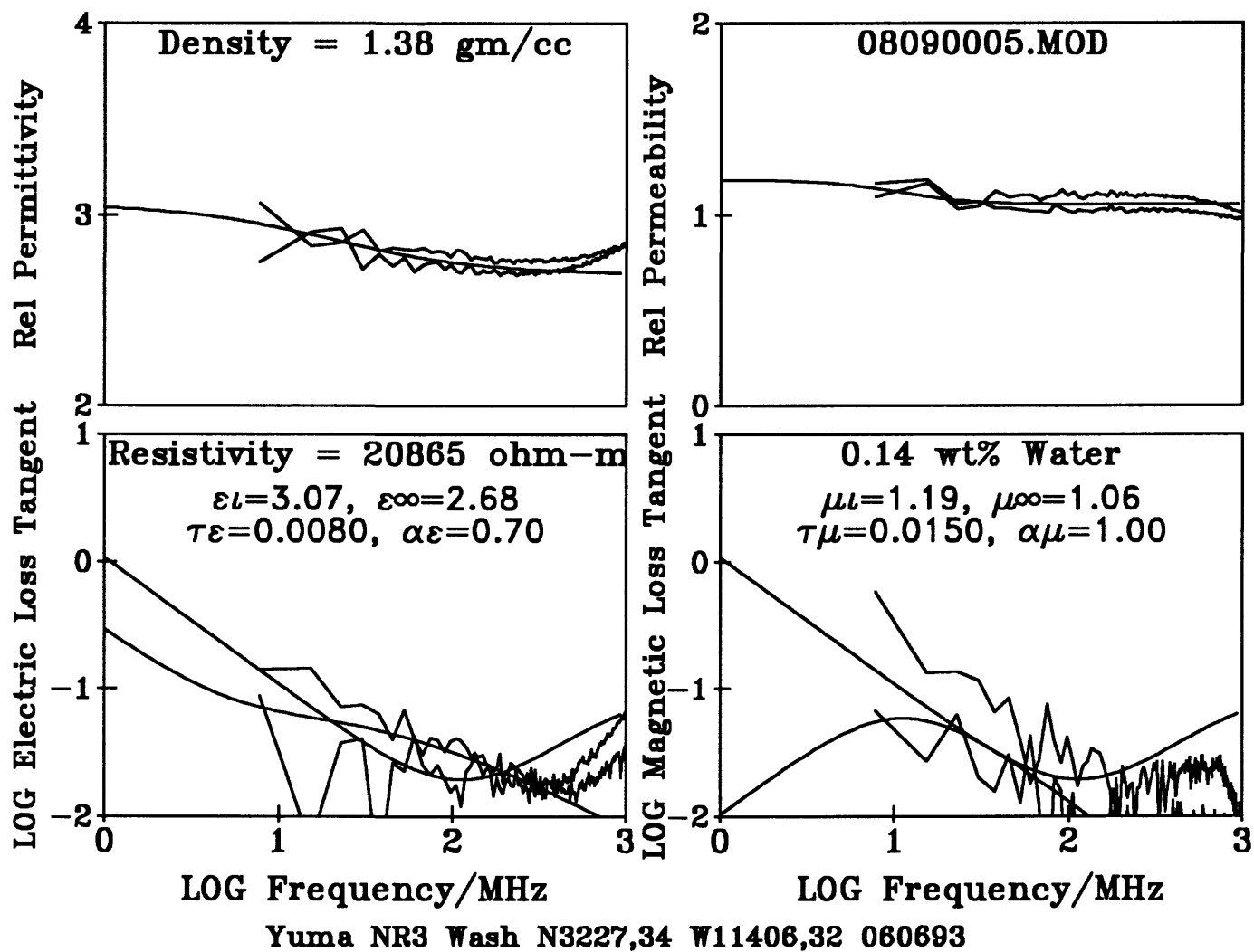


Figure 196 -
Sample provided by Carabas Team in a sealed bottle -- presumed natural water content.

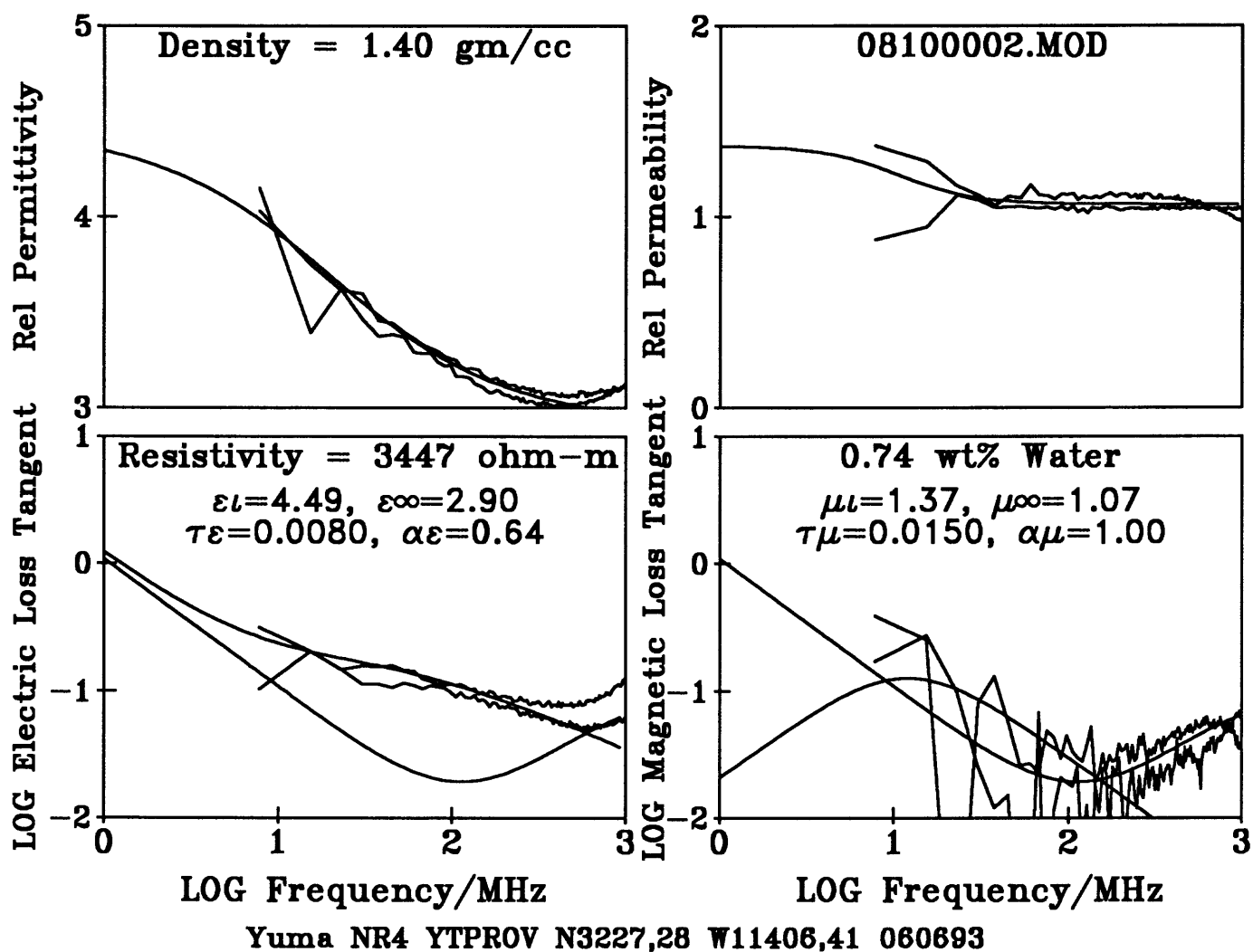
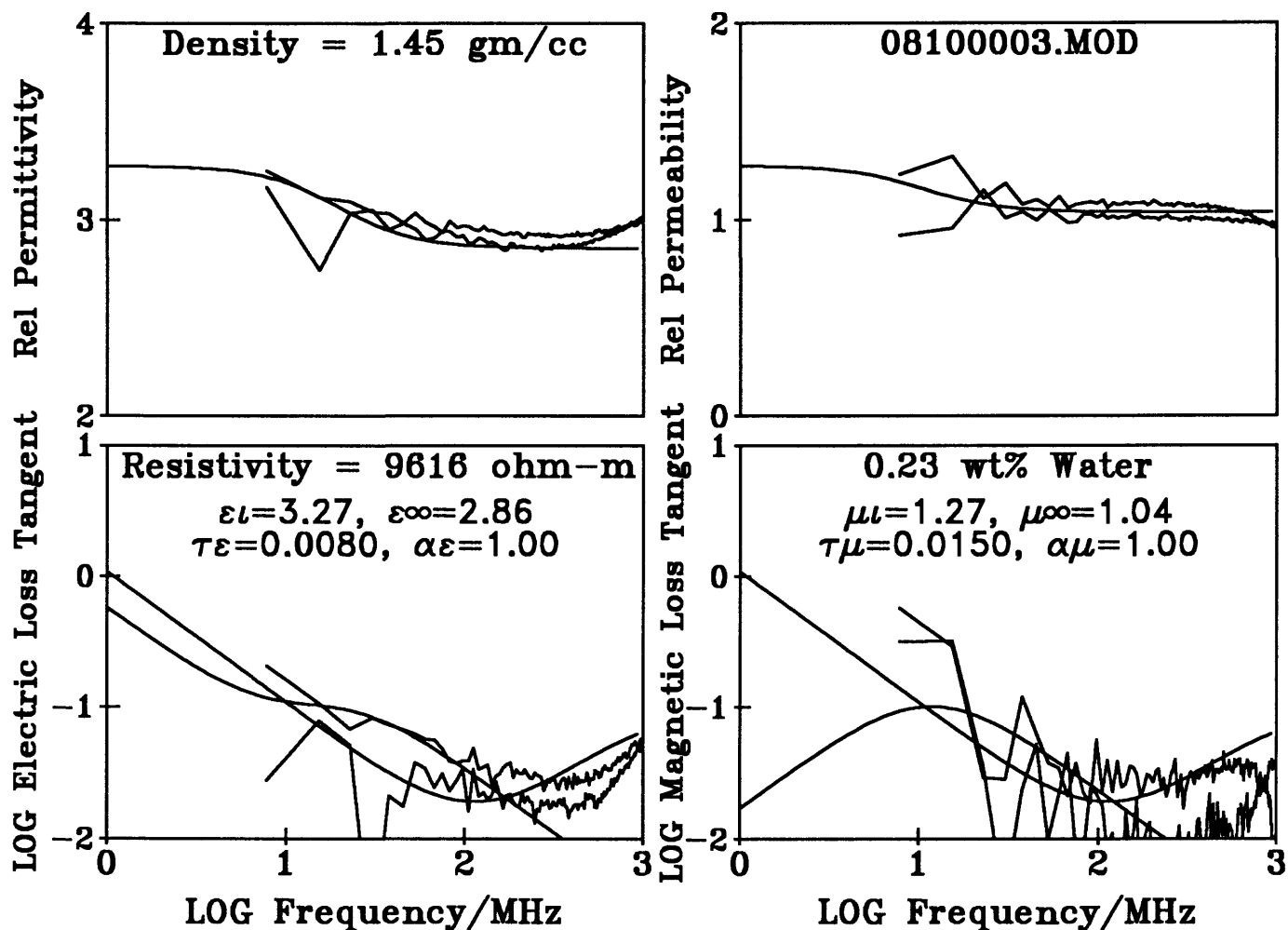
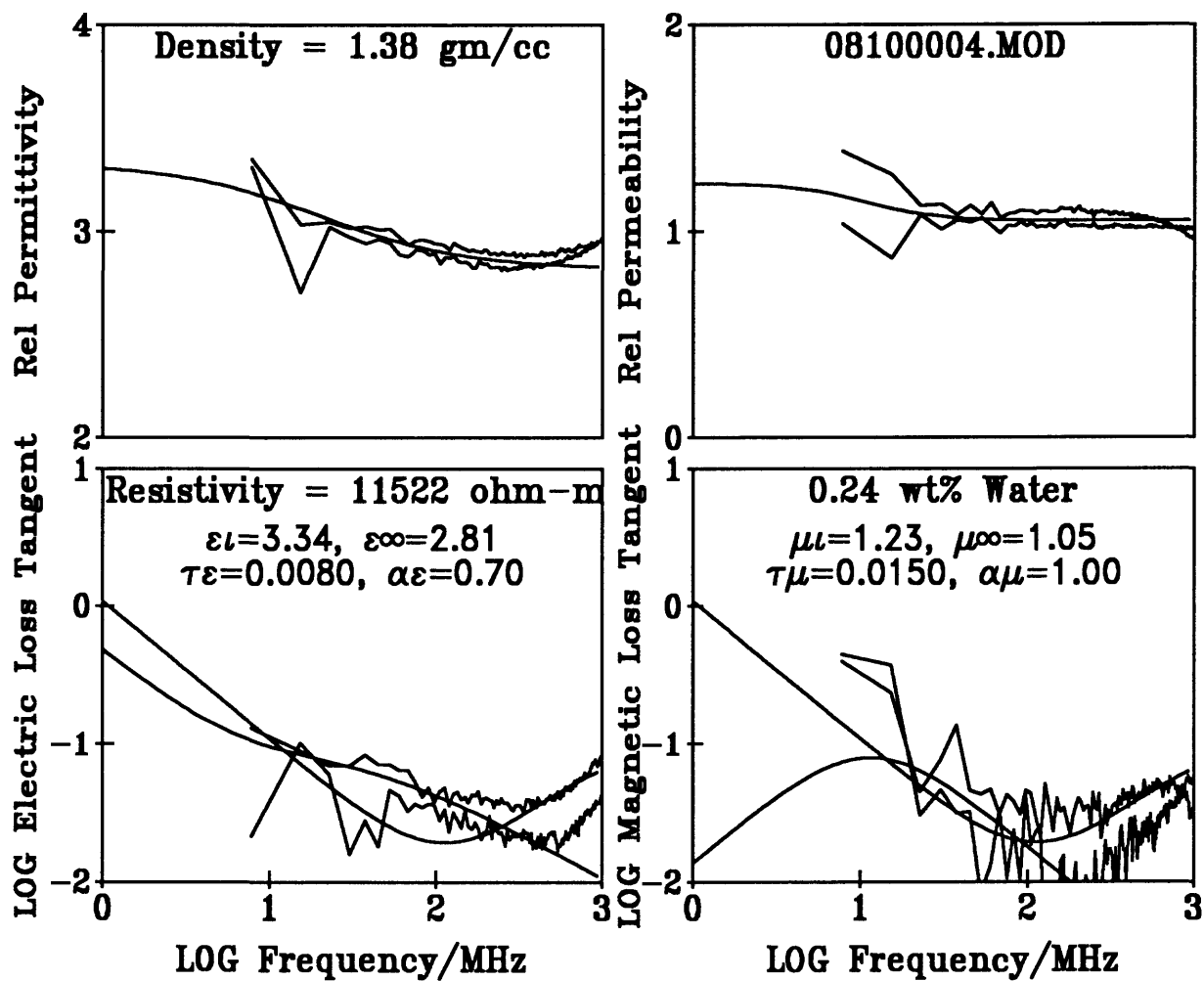


Figure 197 -
Sample provided by Carabas Team in a sealed bottle -- presumed natural water content.



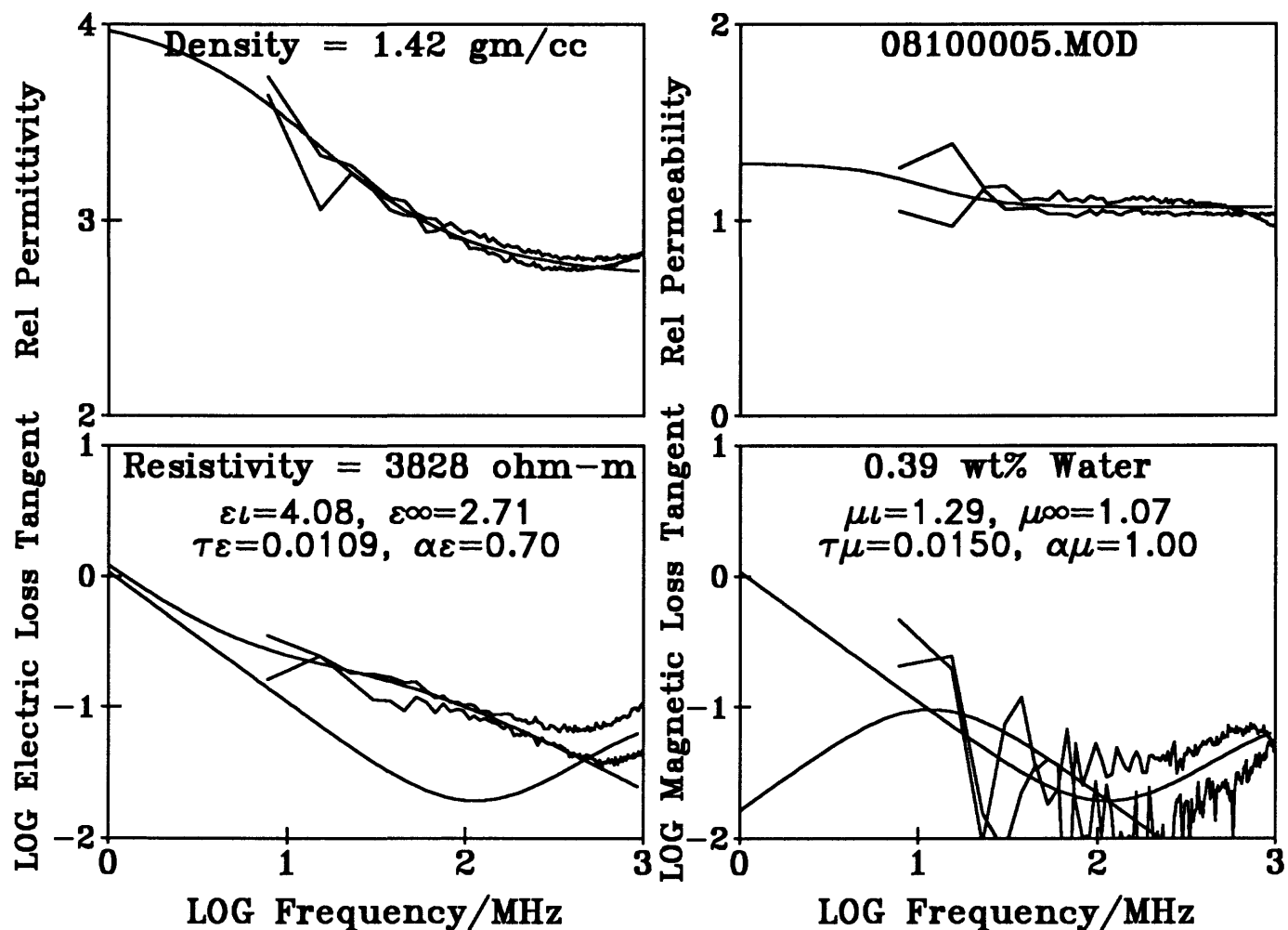
NR5 070693 WASH 600M S. OF TRIHEDRAL ARRAY AND 25 M W. OF RD. 20 CM DP

Figure 198 -
 Sample provided by Carabas Team in a sealed bottle -- presumed natural water content.



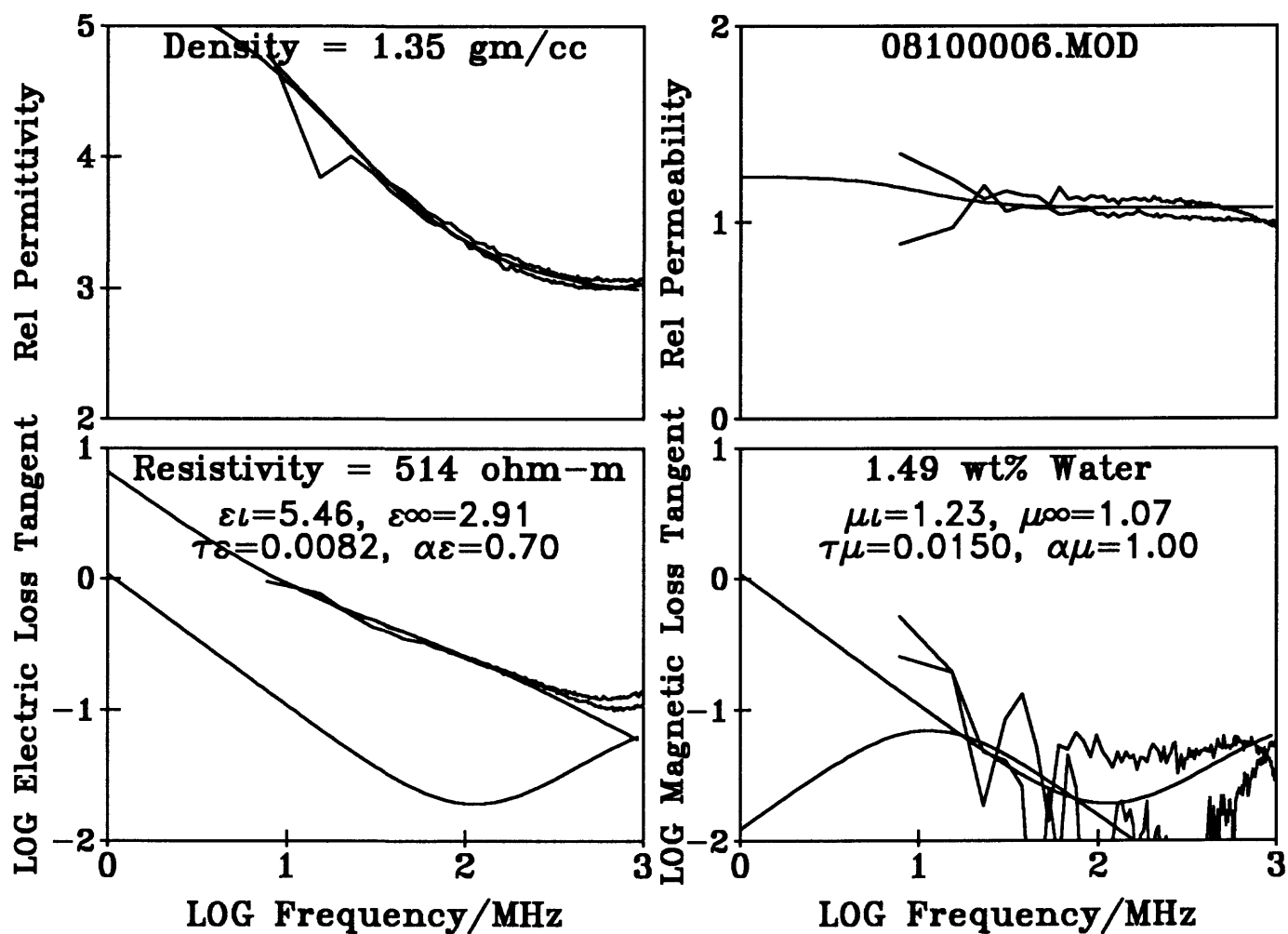
Yuma NR6 575m S of trihedral array 25m W of road on surface 070693

Figure 199 -
Sample provided by Carabas Team in a sealed bottle -- presumed natural water content.



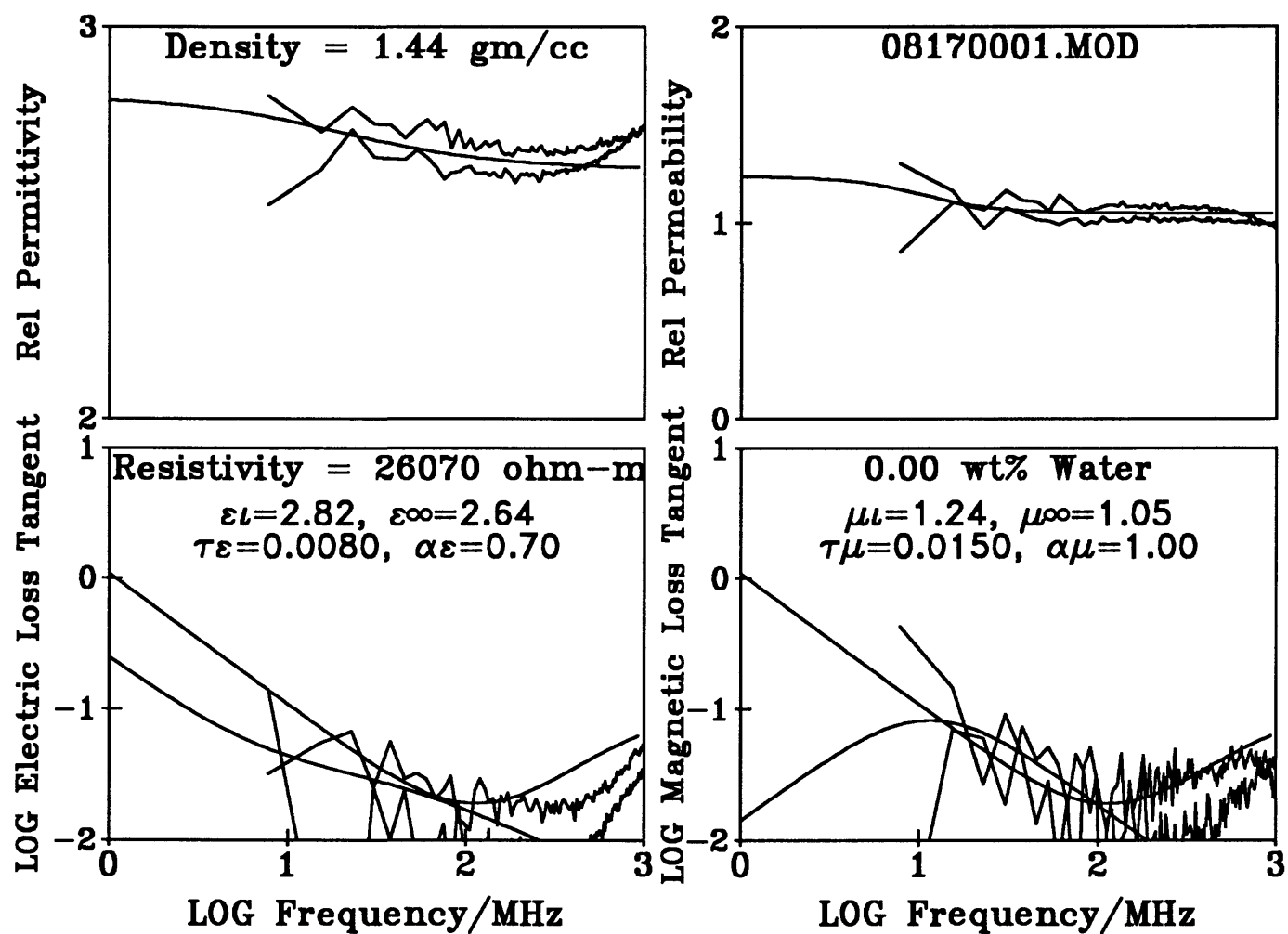
Yuma NR7 dunes sand sample from the surface at the Trihedral 080693

Figure 200 -
 Sample provided by Carabas Team in a sealed bottle -- presumed natural water content.



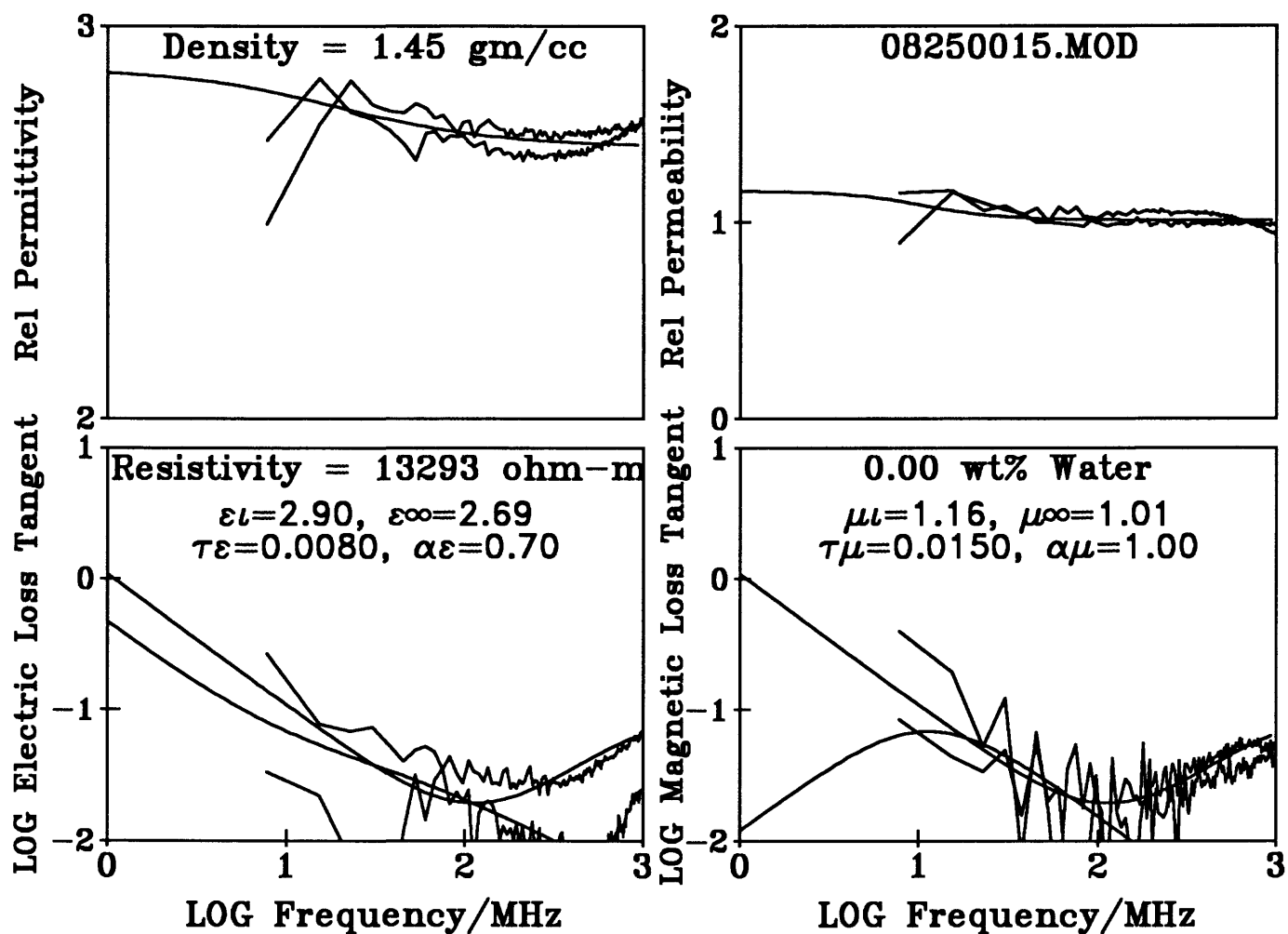
Yuma NR8 at the same spot as sample NR7 but deep (wet sand) 080693 #1

Figure 201 -
Sample provided by Carabas Team in a sealed bottle -- presumed natural water content.



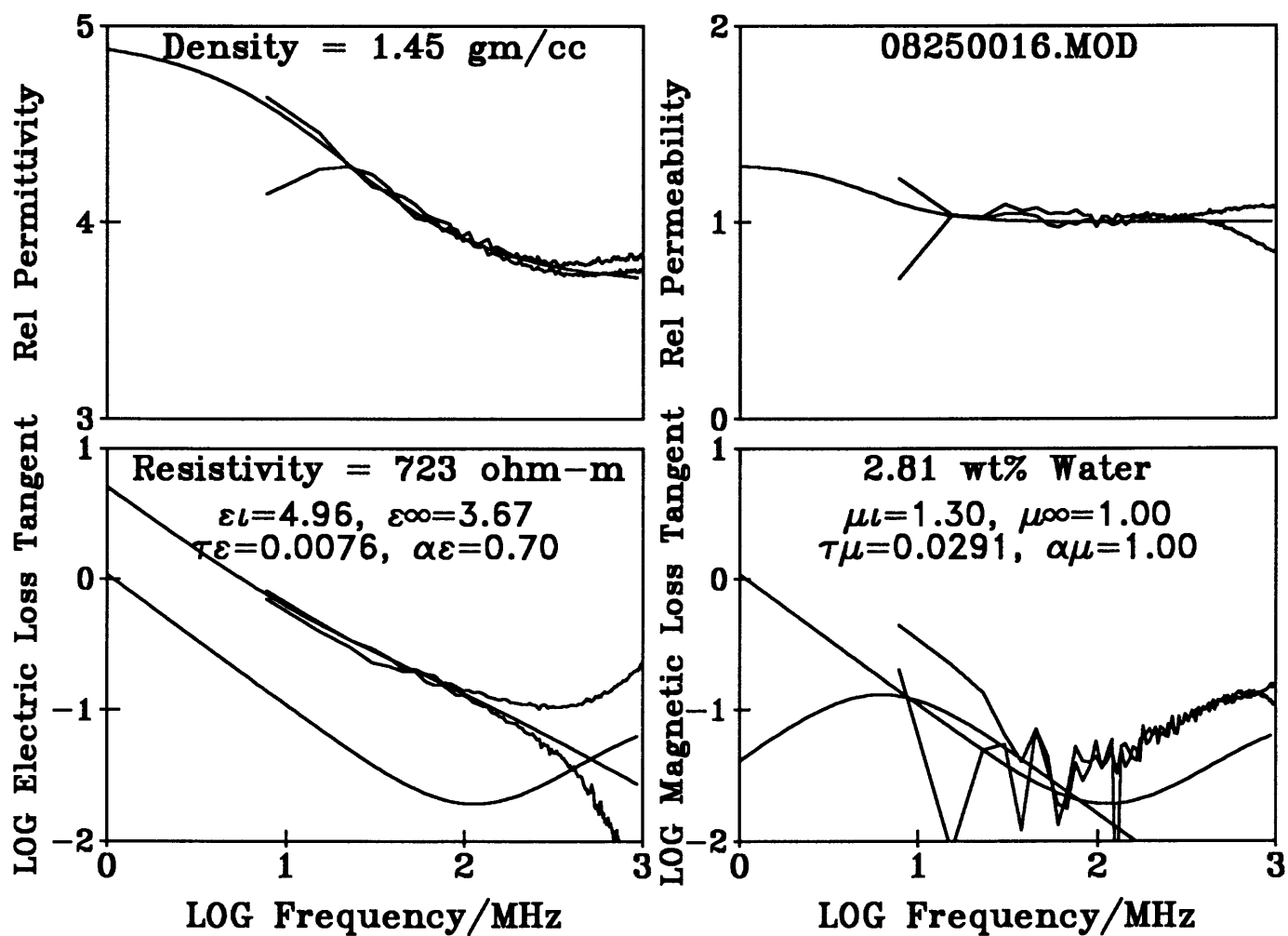
Yuma NR8 same as NR7 but deeper (wet sand) 080693 #2 vac.dry

Figure 202 -



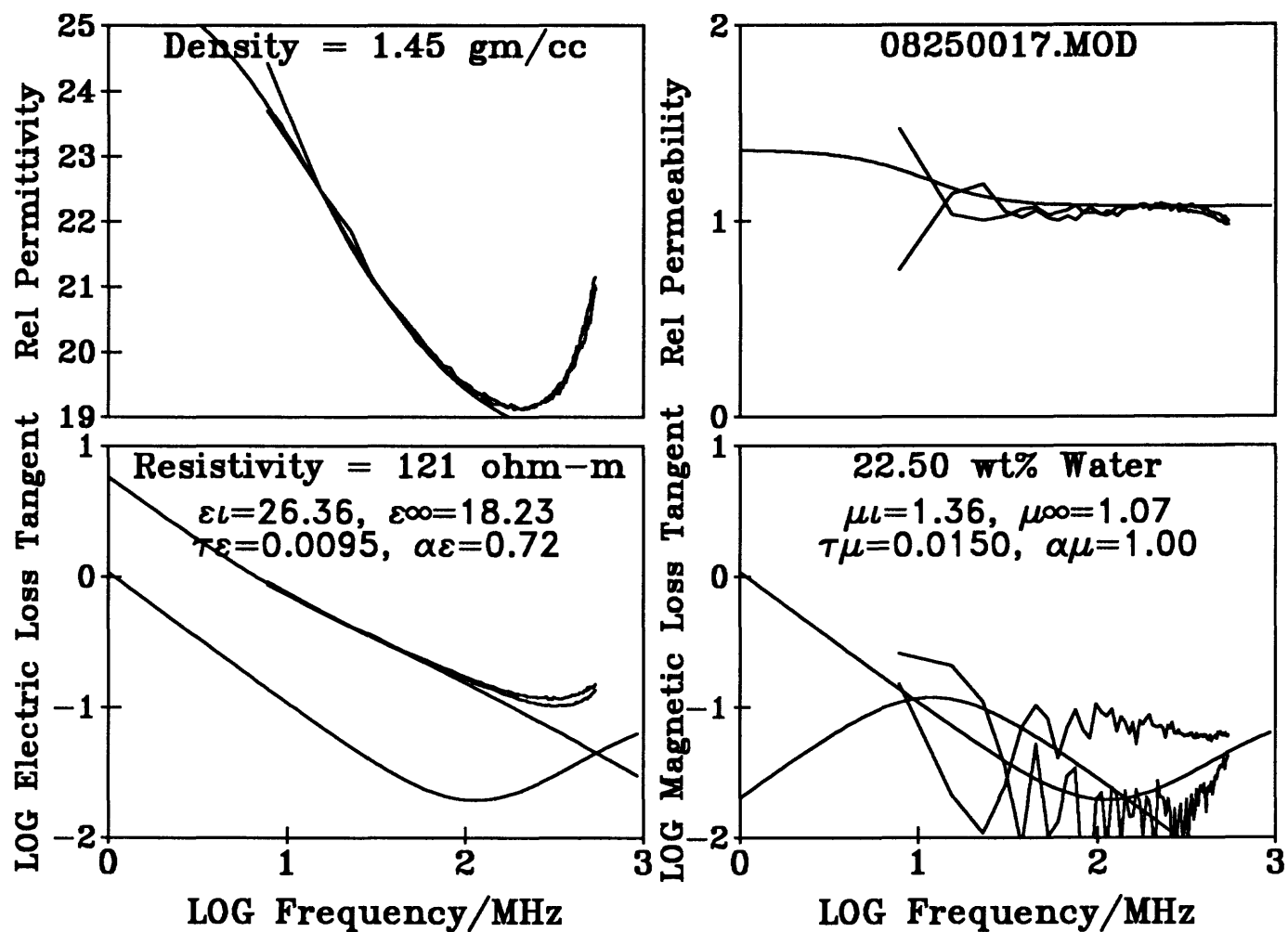
Yuma NR8 same as NR7 but deeper (wet sand) 080693 #3 vac. dry

Figure 203 -



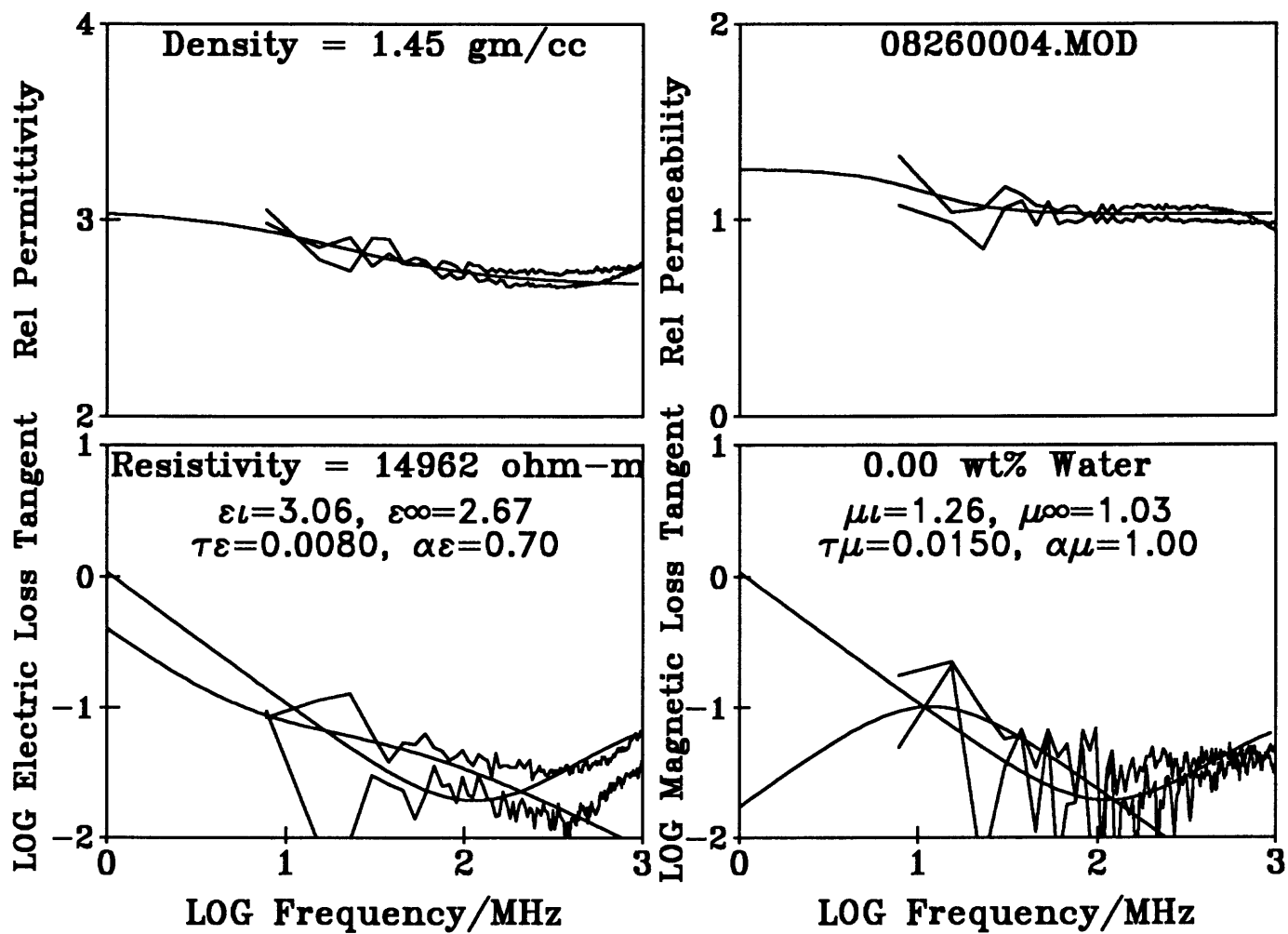
Yuma NR8 same as NR7 but deeper (wet sand) 080693 #3 4-drops water

Figure 204 -



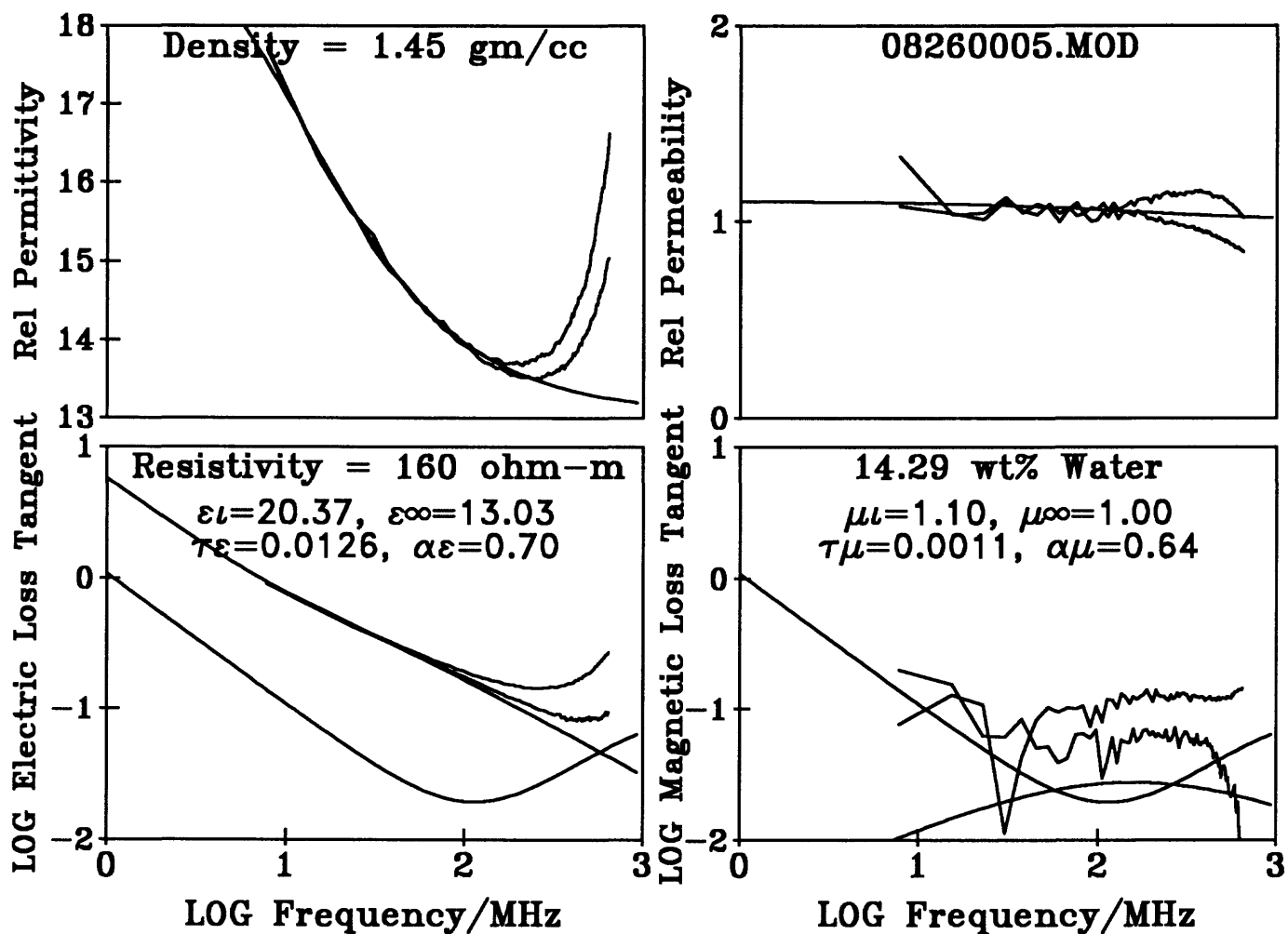
Yuma NR8 same as NR7 but deeper (wet sand) 080693 #3 water saturated

Figure 205 -



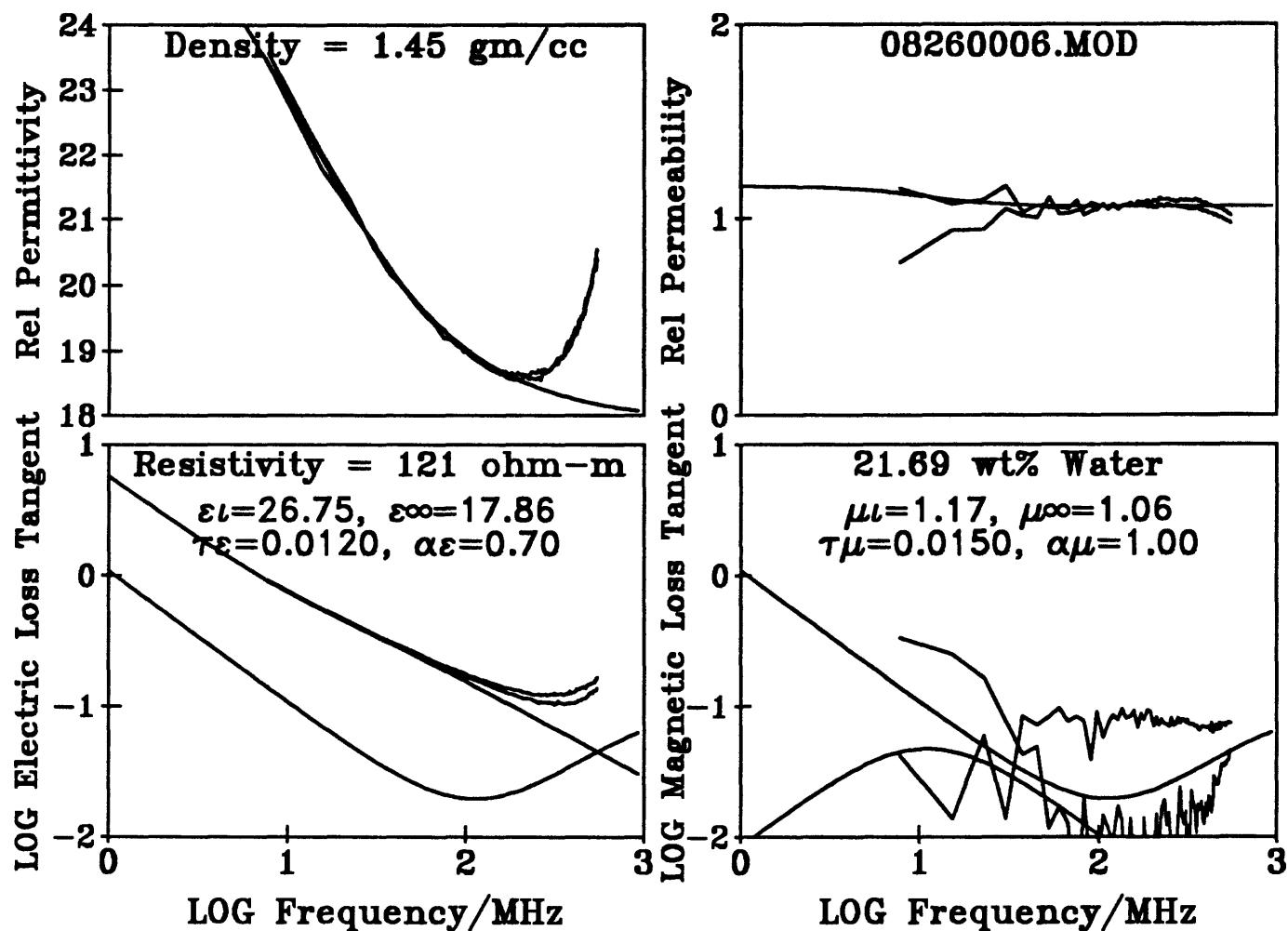
Yuma NR8 same as NR7 but deeper (wet sand) 080693 #4 vac.dry

Figure 206 -



Yuma NR8 same as NR7 but deeper (wet sand) 080693 #4 4-drops water

Figure 207 -



Yuma NR8 same as NR7 but deeper (wet sand) 080693 #4 water saturated

Figure 208 -